FINAL REPORT

Demonstration of a Building Automation System Embedded Performance Degradation Detector Using Virtual Water/Air Flow Meters

ESTCP Project EW-201407

NOVEMBER 2018

Li Song
University of Oklahoma

Distribution Statement A
This document has been cleared for public release

ESTCP

Page Intentionally Left Blank

Page Intentionally Left Blank

REPORT DOCUMENTATION PAGE

Form Approved
OMB No. 0704-0188

1. REPORT DATE *(DD-MM-YYYY)*	**2. REPORT TYPE**	**3. DATES COVERED** *(From - To)*
12-03-2018	ESTCP Final Report	Sep 2014 to Dec 2018

4. TITLE AND SUBTITLE
Demonstration of a Building Automation System-Embedded Performance Degradation Detector Using Virtual

5a. CONTRACT NUMBER
W912HQ-14-C-0050

5b. GRANT NUMBER
EW-201407

5c. PROGRAM ELEMENT NUMBER

6. AUTHOR(S)

Li Song, University of Oklahoma
Gang Wang, University of Miami
Mike Brambley, Pacific Northwest National Laboratory

5d. PROJECT NUMBER
W74RDV40704145

5e. TASK NUMBER

5f. WORK UNIT NUMBER

7. PERFORMING ORGANIZATION NAME(S) AND ADDRESS(ES)

University of Oklahoma — 865 Aps Ave., Norman OK73019;
University of Miami — 1320 S Dixie Hwy, Coral Gables, FL 33146;
Pacific Northwest National Laboratory — 902 Battelle Blvd, Richland, WA 99354;

8. PERFORMING ORGANIZATION REPORT NUMBER
EW-201407

9. SPONSORING / MONITORING AGENCY NAME(S) AND ADDRESS(ES)

Environmental Security Technology Certification Program (ESTCP) — 4800 Mark Center Drive, Suite 16F16, Alexandria, VA 22350-3605

10. SPONSOR/MONITOR'S ACRONYM(S)
ESTCP

11. SPONSOR/MONITOR'S REPORT NUMBER(S)
EW-201407

12. DISTRIBUTION / AVAILABILITY STATEMENT
Approved for public release; distribution is unlimited

13. SUPPLEMENTARY NOTES
none

14. ABSTRACT (200words)

The goal of this demonstration project was to improve the energy efficiency of DoD buildings while maintaining or improving indoor air quality by increasing the intelligence of building energy management using virtual flow meter technologies. Specifically, the technical objectives were to: 1) Validate energy savings, costs and benefits of the proposed technologies; 2) Document findings and guidelines from the demonstration to promote low-cost virtual meter implementation through the existing DoD energy meter policies and encourage widespread adoption of the Building automation system (BAS)-embedded PDD, and 3)Enable technology transfer through the demonstration by showcasing benefits of the technology.

The demonstration involved validation of 43 virtual fan/valve/pump flow meters. Of these, 40 meters (93%) had errors of less than 1.2% at 95% confidence. The average annual total cost savings was $74,629 based on the lumped utility rate of $0.0522/kWh and $4.02/MMBtu, i.e., 15% annual energy cost. It is worth mentioning that the demonstration building is a LEED certified new clinic building.

15. SUBJECT TERMS
Virtual air/water flow meter, performance degradation detection, building automation system

16. SECURITY CLASSIFICATION OF:			**17. LIMITATION OF ABSTRACT**	**18. NUMBER OF PAGES**	**19a. NAME OF RESPONSIBLE PERSON**
U					Li Song
a. PORT	**b. ABSTRACT**	**c. HIS PAGE**	SAR	182	**19b. TELEPHONE NUMBER** *(include area code)*
UNCLASS	UNCLASS	UNCLASS			4053251714

Page Intentionally Left Blank

FINAL REPORT
Project: EW-201407

TABLE OF CONTENTS

Page

TABLE OF CONTENTS (Continued)

Page

LIST OF FIGURES

Page

LIST OF FIGURES

Page

LIST OF FIGURES

Page

LIST OF TABLES

Page

ACRONYMS AND ABBREVIATIONS

ASHRAE	American Society of Heating, Refrigeration, Air-conditioning Engineers
AHU	Air handling unit
BAS	Building automation system
BBtu	Billion British thermal units
BEE	Building Energy Efficiency
CFM	Cubic feet per minute
CUP	Central utility plant
DoD	Department of Defense
DOE	Department of Energy
ESTCP	Environmental Security Technology Certification Program
GPM	gallons per minute
HVAC	Heating, ventilation and air-conditioning
kW	kilowatt
kJ/hr	kilojoule per hour
MMBtu	British thermal unit in million
PDD	Performance degradation detection
OA	Outdoor air
OU	University of Oklahoma
SCC	System coefficient curve
TAFB	Tinker Air Force Base
UM	University of Miami
VFD	Variable frequency drive

ACKNOWLEDGMENTS

The project team would like to acknowledge the financial support of ESTCP office to make the project possible and the facility manager of the demonstration building, Mrs. Deborah Burge, for her support, cooperation and assistance in bringing about the success of the project.

ABSTRACT

Introduction and Objectives: Existing industrial standards, e.g., ASHRAE Standards 62.1 and 90.1, set up detailed *advanced energy efficient operations*. However, some operations cannot readily be implemented because of *the lack of low cost, reliable water and air flow meters. Consequently, the lack of flow measurements leads to inadequate energy performance evaluation for heating, ventilation and air conditioning* (*HVAC) system.* The goal of the proposed demonstration project was to improve the energy efficiency of DoD buildings while maintaining or improving indoor air quality by increasing the intelligence of building energy management using virtual flow meter technologies. Specifically, the technical objectives were to:

1. Validate energy savings, costs and benefits of the proposed technologies, including the virtual flow meters and the performance degradation detection (PDD).
2. Document findings and guidelines from the demonstration to promote low-cost virtual meter implementation through the existing DoD energy meter policies and encourage widespread adoption of the Building automation system (BAS)-embedded PDD.
3. Enable technology transfer through the demonstration by showcasing benefits of the technology to increase DoD and vendor acceptance.

Technology Description: The virtual flow meter technology is a key component of the PDD in the proposed project. Three different types of virtual meters significantly enhance the measurement capacity of the BAS. They are described as follows: In Type 1) meters, the whole building level chilled water flow rate and hot water flow rate are virtually obtained using pump operational characteristics, namely a **pump flow meter**. In Type 2) meters, the airflow rate in each air handling unit (AHU) is virtually obtained using fan operational characteristics, namely a **fan flow meter.** In Type 3) meters, the chilled water flow rate in each AHU is virtually obtained using control valve operational characteristics, namely a **control valve flow meter**. The PDD uses the BAS data plus the measurements from the virtual flow meters at pumps, fans and valves to determine the actual energy use of key building systems and subsystems. The energy use and air/water flow rates of energy efficient operations for those systems, i.e., reference values for practices conforming to standards and guidelines set by ASHRAE and other authorities, can also be obtained through virtual flow measurements based on energy balance and/or mechanisms of subsystems. By comparing the actual energy use/setpoint with the reference energy use/setpoint, the energy degradation or operating system malfunctions can be detected.

Performance and Cost Assessment: The demonstration involved validation of 43 virtual fan/valve/pump flow meters. Of these, 40 meters (93%) had errors of less than 1.2% at 95% confidence. The remaining 3 meters had errors between 2% to 3% at 95% confidence. The average annual total cost savings was $74,629 based on the lumped utility rate of $0.0522/kWh and $4.02/MMBtu, i.e., 15% annual energy cost. It is worth mentioning that the demonstration building is a LEED certified new clinic building. All the savings were obtained through soft corrections on the system operation sequences without hardware replacements. For the demonstration building, the total cost was $110,295 with a simple payback of 1.5 years.

Implementation issues: The implementation issues include obtaining cybersecurity clearances, as well as potential increases in facility operators' workload. Therefore, a more economical implementation approach would be to hire contractors, either BAS service providers or our technology licensee (the PDD installer), by paying a small monthly fee to maintain service to support the technology.

Publications: During the five-year project period, the PIs published 12 technical papers and have presented the technology in eight presentations and workshops.

EXECUTIVE SUMMARY

INTRODUCTION

The *Department of Defense Budget Priorities and Choices – FY 2014*, calls for more effective heating, ventilation and air conditioning (HVAC) metering, which requires precise measurement of HVAC airflow and water flow rates. The building automation system (BAS) embedded performance degradation detector (PDD), with the additional measurements provided by low-cost virtual air/water flow meters, is one of the technologies that has the potential to reduce DoD energy costs by approximately $0.3 Billion per year (relative to the DoD goal of $1.5 Billion annual savings) based on the results in a laboratory environment test.

Existing industrial standards, e.g., ASHRAE Standards 62.1 and 90.1, set up detailed *advanced energy efficient operations*. However, some approaches cannot readily be implemented in HVAC systems because of *the lack of low cost, reliable water and air flow meters.* Airflow and water flow rates are key controlled variables of HVAC systems, which impact indoor environmental quality, equipment safety, and system energy performance. For example, a lower supply airflow rate may cause poor indoor ventilation, while a higher supply airflow rate may cause excessive use of fan power and reheat energy. For a variable chilled water loop, a lower water flow rate may damage chillers while a higher water flow rate may cause an excessive use of pump power. Airflow and water flow rates are also essential indices to evaluate energy performance of HVAC systems. Flow rates can be used to simultaneously measure *actual* energy use and project the *reference* (fault-free) energy usage based on energy balance and/or mechanism of subsystems. For example, the actual energy usage of cooling coils can be measured by water flow rates. At the same time, the reference value (fault-free) of energy usage can be also projected by air flow rates based on energy balance. Deviations between actual and reference energy usage and air/water flow rates are always indicators of faults and inefficient operations. *Consequently, the lack of flow measurements leads to inadequate energy performance evaluation indices for HVAC system operations.* Efforts to commission buildings and improve energy performance are similarly limited without BAS-embedded metering capacities. Today, energy efficiency measurements require professionals to travel to each facility with portable meters. Embedded metering within BAS will save labor-related costs while providing more accurate and timely data.

OBJECTIVES

The goal of the proposed PDD demonstration project was to improve the energy efficiency of DoD buildings while maintaining or improving indoor air quality by increasing building energy management intelligence using low cost and reliable virtual flow meter technologies. Specifically, the technical objectives were to:

1. Validate energy savings, costs and benefits of the proposed technologies, including the virtual flow meters and the PDD.
2. Document findings and guidelines from the demonstration to promote low-cost virtual meter implementation through existing DoD energy meter policies and encourage widespread adoption of the BAS-embedded PDD in DoD buildings.
3. Enable technology transfer through the demonstration by showcasing benefits of the technology to increase DoD and vendor acceptance, making the technology available across DoD agencies and facilities.

TECHNOLOGY DESCRIPTION

The demonstrated technology includes two major elements: virtual meter technology and performance degradation detection algorithms.

Virtual meter technology:

The virtual flow meter technology is a key component of the PDD in the proposed project. Three different types of virtual meters significantly enhance the measurement capacity of the BAS. In Type 1 meters, the whole building level chilled water flow rate and hot water flow rate are virtually obtained using pump operational characteristics, namely a **pump flow meter.** In Type 2 meters, the airflow rate in each AHU is virtually obtained using fan operational characteristics, namely a **fan flow meter.** The chilled water flow rate in each AHU is virtually obtained in Type 3 meters using control valve operational characteristics, namely a **control valve flow meter**. The water flow rate through the cooling coil, airflow rate, and chilled/hot water flow rate through each main duct or pipe are regulated by the valve movement and the fan and pump speed adjustment. As a result, the virtual meters installed in this project used both available or inexpensive/easy methods to obtain measurements of operational variables, such as valve position, differential pressure across the valve, fan/pump head and motor input power and frequency, and device characteristic curves that relate the behavior of these devices to the desired virtual values and commonly measurable variables. Device characteristic curves can be determined empirically using measurements or analytically from first principles. The desired virtual values can then be calculated using measured values of variables for which meters are commonly installed.

- **Pump/fan flow meter**

Both the virtual pump and fan flow meters work under the same principle. Motor input power (*W*) is determined by useful mechanical work imparted into fluid, the product of head (*H*) and flow rate (*Q*), fan/pump efficiency and motor efficiency. Theoretically, the fan/pump efficiency ($\eta_{f/p}$) is a function of the ratio of head (*H*) to flow rate (*Q*) squared, while motor efficiency (η_{motor}) is theoretically a function of power (*W*), frequency (*f*), and voltage (*V*). Practically, head can be measured by a pressure differential sensor while voltage, power and frequency can be obtained through the existing variable frequency drive (VFD). Meanwhile, the fan/pump efficiency curve can be calibrated through experiments on each system. Using calibrated motor and fan/pump efficiencies (η_{motor} and $\eta_{f/p}$), the flow rate (Q) can be obtained numerically based on the fan/pump head (H) and VFD output power (W), as well as the VFD output frequency (f) and voltage (V), shown in Equation (E-1) below.

$$Q = \frac{W \cdot \eta_{motor}(W,f,V) \cdot \eta_{f/p}(\frac{H}{Q^2})}{H} \quad \text{(E-1)}$$

- **Virtual valve flow meter**

A cooling or heating energy meter is typically not installed in an AHU because of high installation and maintenance costs and increased water loop pressure drop. It is often impossible to install one in existing AHUs due to space and system dimension limitations. The virtual valve flow meter

uses existing coil control valve operational variables to indirectly obtain the water flow rates. Theoretically, the pressure drop through a valve is determined by valve position and flow rate for a given valve, which has a fixed valve characteristic curve. The pressure drop can be measured by a water pressure differential sensor, and the valve position can be obtained by either valve command through a BAS or valve position feedback from the valve actuator. The valve characteristic curve needs to be obtained through a calibration process. Therefore, the flow rate (Q) can be obtained based on the pressure drop ($\Delta P_{L,x}$) and valve position (x) as well as calibrated valve curve ($F_{L.x}$), as described in Equation (E-2).

$$Q = F_{L.x}(x)\sqrt{\Delta P_{L,x}} \qquad \text{(E-2)}$$

Performance degradation detection (PDD):

The PDD uses the available BAS data plus the measurements from the proposed virtual flow meters at pumps, fans, and valves to determine actual energy usage of key building systems and subsystems. The energy usage and air/water flow rates of energy efficient operations for those systems, i.e., reference values for practices conforming to standards and guidelines set by ASHRAE and other authorities, can also be obtained through virtual flow measurements based on energy balance and/or mechanisms of subsystems. As a result, the actual energy usage and reference energy uses for fans, reheats, and cooling coils in AHUs and pumps, as well as chillers and boilers in chilled and hot water systems, can be automatically obtained in Phase I, Data Collection. Besides the energy comparison, the duct and water loop pressure setpoints for fan and pump speed can be calculated based on the virtual flow measurements. *The variation between the measured and simulated setpoints indicates a faulty setpoint or the incorrect damper or valve position.* By comparing the actual energy use/setpoint with the reference energy uses/setpoint, the energy degradation or system malfunction operations can be determined in Phase II, Online Diagnosis. The severity of the performance degradation or faults will trigger alarms and motivate facility operators for quick corrections and is shown by the empty box to the right of the detector module. The mechanism of the detector is shown in Figure E-1. The shaded box bordered by the dashed line represents an add-in PDD (a set of function modules) in a BAS. The two boxes on the left represent available sensor and command information in a BAS.

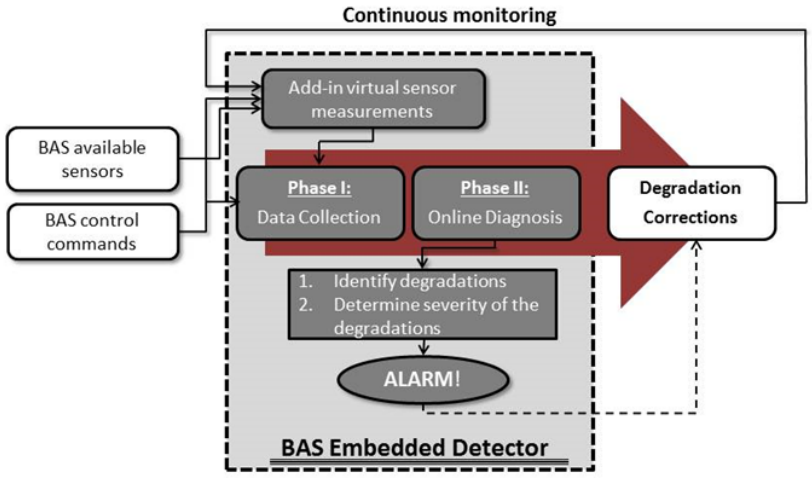

Figure E.1 Flow Chart of the Embedded PDD.

PERFORMANCE ASSESSMENT

The newly constructed clinic building at the Tinker Air Force Base (TAFB) in Oklahoma City, OK, was chosen as the demonstration site. The building, with a floor area of 162,000ft^2, has standard building operating hours from 8:00am to 5:00pm. The building consists of two (300 tons each) chillers along with three primary chilled water pumps at 7.5 HP each, three secondary chilled water pumps at 20HP each, and three condensing water pumps at 20 HP each. The heating system is served by two (3,348MBH each) boilers with three primary hot water pumps at 3HP each and two secondary pumps at 25HP each. The central plant is located on the ground floor. Both chilled water and hot water loops are formed as primary and secondary water loop systems. A total of 13 AHUs serve in the entire building. Of these, 11 AHUs have both supply air return air fans and two AHUs have supply air fans only.

The project team installed virtual flow meters for the technology demonstration on all supply and return air fans, the cooling coil control valves, all secondary pumps including hot water and chilled water pumps, primary chilled water pumps, and condensing water pumps. The hardware installations included 24 air differential pressure transducers, 24 water differential pressure transducers and 6 variable frequency drives on the 3 primary chilled water pumps and 3 condensing water pumps. However, because the building was operational, the facility was not ready to shift the current constant flow primary loop and condensing loop to variable flow systems due to constant unreliable chiller operations. We did not make any operational changes to the pumps on the primary and condensing loops. Additionally, we programmed the corresponding virtual flow rate calculation algorithms and PDD algorithms in the BAS.

Performance assessment for virtual meter technology:

The virtual flow meter demonstration encompassed two phases. The first phase was to use our original proposed flow rate calculation algorithms to calculate the flow rate, and the second phase used the improved algorithms built on the lessons that we learned through this demonstration project. The results of the first phase virtual flow meter demonstration were submitted for mid-progress report review in November 2015 (in Appendices E, F and G). At that time, we had documented that 85% of the virtual fan flow meters, 30% of the valve flow meters and 75% of the virtual pump flow meters passed the success criterion, which is less than 2% error at 95% confidence. Over 90% of the virtual meters passed 3% error at 95% confidence. We had since concluded that the sacrificed error is due to the following reasons:

1. The motor harmonic loss increases as the VFD frequency decreases. The motor efficiency variations under different frequencies were not reflected in flow rate calculation algorithms that we originally proposed.
2. Dynamic control valve behavior has a significant impact on valve flow rate calculation, especially when a valve experiences slow position change. The steady-state model we adopted in our original virtual valve flow meter calculations did not consider this impact.
3. A loose belt was another factor that caused virtual fan flow sensor errors.
4. We selected a 25PSI measurement range of differential pressure (DP) transducers for virtual valve flow meters according to the design information. However, we observed that the dynamic feature of the operational system can easily exceed this threshold. There were several periods during which the DP transducers reached maximum capacity because the range of the DP was not large enough.

5. The return fan is interactive with the supply fan. As a result, the return fan operated with a negative fan head when the return fan speed was low and the supply fan speed was high. The virtual fan airflow calculation algorithms do not apply to this abnormal fan operation.

The mid-progress report was approved by the ESTCP office in March 2016. Since that time, we have continued our efforts to improve the accuracy of the virtual flow meters, especially for the errors caused by the first two reasons listed above, by revising our flow calculation algorithms to consider motor efficiency loss due to the harmonics by low VFD frequencies and the valve dynamic behavior. We have also added a new PDD algorithm to detect the loose fan belt problem for the facility to resolve the third reason listed above. Items 4 and 5 above required hardware replacements to address these issues, which were prohibited by budget constraints.

Due to time constraints, we could not implement the new algorithm in all units. The improved virtual flow meter models were implemented in the secondary chilled water and hot water pumps and the supply air fans in AHU 2 and AHU 13. The results of the four test units showed that the accuracy of the virtual flow meter was improved by 15% to 20% compared with the calculated flow rate using our originally proposed algorithm. The accuracy improvement also depends on how frequent the evaluated points fall under low motor frequency operations. Meanwhile, to describe the valve dynamic behavior, a BAS-programmable algorithm was developed to convert the valve commands to the true valve position by factoring in the impacts of resolution errors, valve stiction, and deadband. The correction algorithm was implemented in the virtual valve flow meters in AHU2 and AHU13 for test purposes. The results showed that valve flow meter accuracy was improved by 40% to 45% compared with the valve flow rate calculated using the original algorithm without the corrections. As a result, with the improvements we have made in the flow rate calculation algorithms, the virtual flow rate errors were reduced significantly compared with the results in the mid-term report. If a 15% to 20% improvement was applied to the errors of the fan/pump flow meters summarized in the mid-progress report, the uncertainty of all the fan/pump flow meters would be less than 1.2% at 95% confidence. If the 40% to 45% improvement was applied to the errors of all valve low meters summarized in the mid-progress report, the uncertainty of 10 out of 13 valve flow meters would be less than 1.1% error at 95% confidence; three would be between 2% and 3% error at 95% confidence.

<u>Performance assessment for PDD technology:</u>

The goal of the PDD was to identify energy saving opportunities in the demonstration building through the PDD. Our performance assessment approach was to commission the building first to make sure the building was in a fault-free condition, i.e., used as the equipment performance baseline in the PDD algorithms, and then manually generate faults to validate the effectiveness of the PDD responses and correct the problems that the PDD identified to validate the savings that otherwise would be lost if the PDD was not in place. The operation parameters and/or energy usage before and after corrections at the system level and for the whole building were both collected to validate the system performance improvement and the energy savings. The implemented PDD included detection of excessive outdoor air intake using the cooling energy calculated by the virtual valve flow rate in each AHU, simultaneous heating and cooling detection using the virtual fan flow meter, fan operation-related faults and pump operation-related faults using the virtual fan/pump flow meter, and accessory signals such as fan/pump head and fan/pump motor power.

Through the demonstration, the installed PDD was found to be effective in detecting the proposed faults. When the cooling energy in an AHU was used as an energy index to detect the excessive outdoor air intake faults, an outdoor air humidity sensor was necessary to increase the sensitivity of this fault detection method. Due to the lack of an outdoor air humidity sensor, the installed PDD for outdoor air detection can only detect the outdoor air faults that result in more than 15% cooling energy loss.

To validate the whole building level energy performance and savings, we collected monthly utility bills from January 2014 through December 2017, a total of four years of data. The improvements by the project team were primarily made from January 2016 to May 2016. The facility operators overrode all the AHUs to 24-hour operations in mid-July 2016 with 5°F lower supply air temperature to correct an observed mold risk. The overrides significantly altered the energy performance of the building. Therefore, we selected the energy usage data in Year 2015 as a baseline and the energy usage data in Year 2017 for after the improvements. Although the supply air temperature overrides were released in late 2016, the schedule overrides were still not completely released, i.e., there were still several AHUs running 24x7 at the present time. The savings were compromised by this operational change.

The energy savings was the difference between the baseline energy (2015) and the energy after the PDD implementation (2017). However, weather impacts need to be considered. We have utilized a scatter chart to regress the energy usage versus average outdoor air temperature before and after the corrections to eliminate weather impacts. Figure E-2 shows the monthly electricity usage versus average outdoor air temperature in each month, while Figure E-3 shows the monthly natural gas usage before and after the correction versus the monthly average outdoor air temperature. The red triangles denote the months before the correction and the green dots denote the months after the correction. By using the linear regression of the red triangles and green dots respectively, shown by the solid lines in both figures, the average electricity and natural gas usage versus average outdoor air temperature values are obtained. The difference between the two solid lines in Figure E-2 was the electricity savings, equivalent to 14.7% of the electricity usage baseline. The difference between the two solid lines in Figure E-3 was the natural gas savings, equivalent to 16.9% of the natural gas usage baseline. For Year 2017 weather conditions, the average annual total cost savings was $74,629 for the whole building level energy usage based on the lumped utility rate of $0.0522/kWh for electricity and $4.02/MMbtu (the utility rates were calculated using the average rates from 2014 to 2017 due to the rate changes over time), equivalent to 15% annual energy cost savings overall.

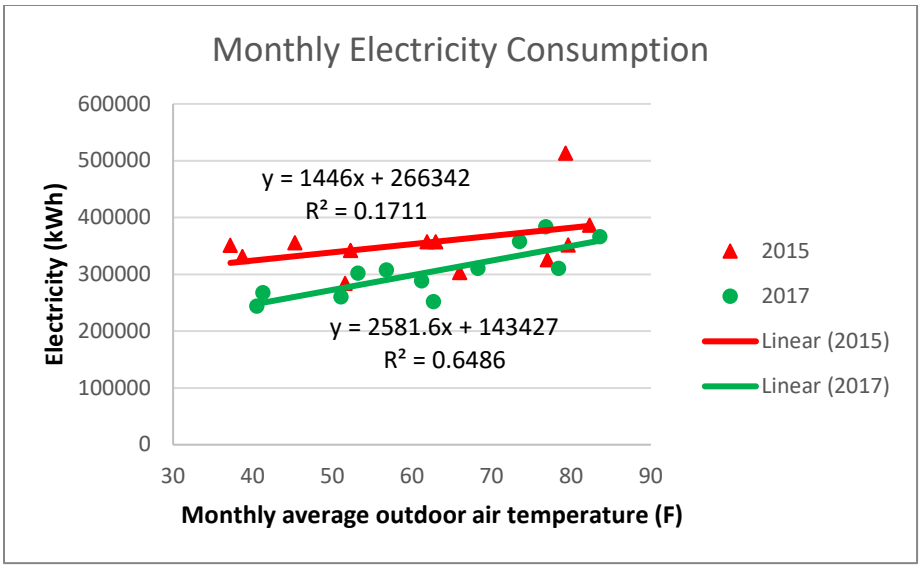

Figure E.2 Monthly Electricity Use vs. Monthly Average Outdoor Air Temperature.

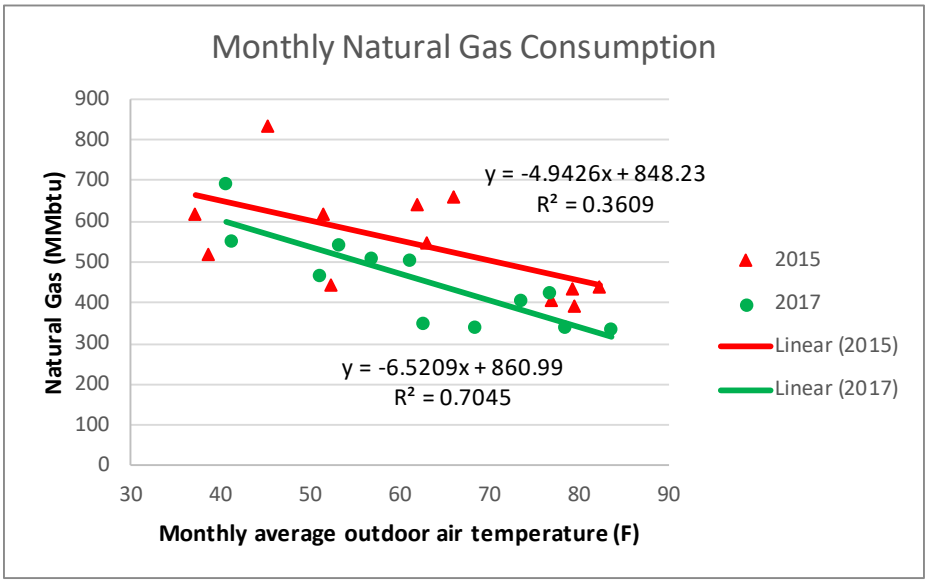

Figure E.3 Monthly Natural Gas Usage vs. Monthly Average Outdoor Air Temperature.

COST ASSESSMENT

The cost of the installations of virtual meters and the PDD was estimated in Table E-1. The hardware costs were estimated using the actual subcontractor's invoice in the demonstration project and the programming costs were estimated based on actual engineering effort needed to implement the algorithms in the BAS. For the demonstration building, the total construction cost of PDD was $97,170 and total cost including soft corrections of the faults and deficiencies identified through PDD was $110,295. The measured savings of the building was $74,629. Therefore, the simple payment was 1.5 years.

Table E.1. Cost Assessment.

Cost Element	Data Tracked During the Demonstration	Estimated Costs
Hardware capital costs	Subcontractor's invoice	$62,705 (the costs of six VFDs was deducted because they did not contribute to the savings we obtained)
Installation costs	Subcontractor's invoice	$19,465 (the costs of six VFDs was deducted because they did not contribute to the savings we obtained)
Programming and PDD implementation costs	Estimates based on the engineering programming effort by the project team	$15,000 (estimated by assuming 200 engineering hours were needed at a rate of $75 per hour)
Facility operational costs	Reduction in energy required vs. baseline data	$74,629 (The savings was obtained by correcting the faults/deficiencies identified through PDD.)
Maintenance	• Frequency of required maintenance • Labor and material per maintenance action	$0 (not beyond routine maintenance costs. Particularly for this project, no equipment replacement was needed for the 15% savings we obtained. . However, our team made soft corrections on fan and pump operation set points, outdoor air intake and VAV box minimum airflow setting, estimated at $13,125 one-time engineering cost for the correction at $75 per hour for a total of 175 hours.)
Hardware lifetime	Estimate based on components degradation during demonstration	50 years
Annual service costs	Based on 50 engineering hours annually	$3,750 ($4^{+}$ hours per month)

IMPLEMENTATION ISSUES

The project was successfully demonstrated with measurable savings and an attractive payback. More importantly, we have learned a lot through the process that not only help us enhance the technology, but also prepare us for a better understanding of future technology commercialization. We have summarized three possible implementation issues below that can help us facilitate a realistic commercialization plan to promote the virtual flow meters and PDD technology across the DoD installations.

- Potential regulation issues: the major regulation issue is cybersecurity clearance. Although we did not have this trouble during this project, because the BAS we needed to access is a standalone system, i.e., it is not on the Tinker network system, it can potentially increase the project cost through the extra time and effort required to obtain the necessary cybersecurity clearance.

- End-user concerns: It is not realistic to train facility operators to use the PDD technology, including reading the alarms and making necessary corrections for energy savings. This approach would potentially increase the workload of the staff and potentially could increase the need for additional staffing. Instead, we have learned through the demonstration that a more economical and practical approach would be to hire contractors who can be either BAS service providers or our technology licensees (the PDD technology installers) by paying a small amount monthly fee to receive the alarms and make necessary soft changes in programs if needed and/or suggest hardware replacements to the facility operators.
- Procurement issues: There are two approaches to implement the technology. One is the same as we did in the demonstration project, i.e., implement the calculation algorithms into the existing BAS, and the other is to install our mini-converter, which includes flow rate calculations and then outputs the signal directly to the BAS. The first approach has no procurement issues, as all accessories to be installed are off-the-shelf. The second approach may need special procurement procedures because our mini-converter is currently a custom-built prototype.

Page Intentionally Left Blank

1.0 INTRODUCTION

The *Department of Defense Budget Priorities and Choices – FY 2014* (DoD 2013a), calls for more effective heating, ventilation and air conditioning (HVAC) metering, which requires precise measurement of HVAC airflow and water flow rates. The building automation systems (BAS) embedded performance degradation detector (PDD), with the additional measurements provided by low-cost virtual air/water flow meters, has the potential to reduce DoD energy costs by approximately $0.3 Billion per year (relative to the DoD goal of $1.5 Billion annual savings) based on the results in a laboratory environment test. The PDD needs to be tested in a DoD facility to validate its efficacy, cost-effectiveness, and interoperability across multiple BASs. If proven, these cost savings results will enable the University of Oklahoma (OU) to commercialize the PDD through licensing agreements with BAS manufacturers, service providers and other companies, which will then make the PDD available throughout the DoD as well as other public and private sector facilities.

1.1 BACKGROUND

Existing industrial standards, e.g., ASHRAE Standards 62.1 (ASHRAE 2010a) and 90.1(ASHRAE 2010b), set up detailed *advanced energy efficient operations*. However, some approaches cannot readily be implemented in HVAC systems because of *the lack of low cost, reliable water and air flow meters.* Airflow and water flow rates are key controlled variables of HVAC systems, which impact indoor environmental quality, equipment safety and system energy performance. For example, a lower supply airflow rate may cause poor indoor ventilation, while a higher supply airflow rate may cause excessive use of fan power and reheat energy. For a variable chilled water loop, a lower water flow rate may damage chillers while a higher water flow rate may cause an excessive use of pump power. Airflow and water flow rates are also essential indices to evaluate energy performance of HVAC systems. Flow rates can be used to simultaneously measure *actual* energy use and project the *reference* (fault-free) energy use based on energy balance and/or mechanism of subsystems. For example, actual energy uses of cooling coils can be measured by water flow rate and, at the same time, the reference value (fault-free) of energy usage can also be projected by air flow rates based on energy balance. Deviations between actual and reference energy use are always indicators of faults and inefficient operations.

Consequently, the lack of flow measurements leads to inadequate energy performance evaluation indices for HVAC system operations. Efforts to commission buildings and improve energy performance are similarly limited without BAS-embedded metering capacities. Today, energy efficiency measurements require professionals to travel to each facility with portable meters. Embedded metering within BAS will save labor-related costs while providing more accurate and timely data.

1.2 OBJECTIVE OF THE DEMONSTRATION

The goal of proposed PDD demonstration project was to improve the energy efficiency of DoD buildings while maintaining or improving indoor air quality by increasing the intelligence of building energy management using low cost and reliable virtual flow meter technologies. Specifically, the technical objectives were to:

- Validate energy savings, costs and benefits of the proposed technologies including the virtual flow meters and the PDD.
- Document findings and guidelines from the demonstration to promote low-cost virtual meter implementation through the existing DoD energy meter policy and encourage widespread adoption of the BAS-embedded PDD in DoD buildings.
- Enable technology transfer through the demonstration by showcasing benefits of the technology to increase DoD and vendor acceptance, making the technology available across the DoD.

1.3 REGULATORY DRIVERS

- Executive Orders: Executive Order 13514 (DOE 2014) clearly states that it is the policy of the United States Federal agencies to increase energy efficiency; measure, report and reduce their greenhouse gas emissions from direct and indirect activities. The demonstrated technology will contribute significantly to the DoD's stated goal of saving $1.5 Billion per year claimed in Defense Budget Priorities and Choices – FY 2014 (DoD 2013a) and metering solution in DoD buildings, which also aligns with this Order.
- Metering: In addition to energy reduction, the proposed virtual meters also contribute to the following objectives of the DoD Utilities Meter Policy (the Policy)(DoD 2013b), which was designed with the intent that energy monitoring will contribute to the energy efficiency goals of DoD.
  - The Policy requires capturing 60% of energy use at a whole-building level. Many buildings on military bases are served by either a centralized or decentralized central utility plant (CUP). If a centralized CUP is used, a building receives chilled water and steam (or hot water) from an outside centralized CUP, and the building level energy use is monitored by a power meter plus whole-building thermal energy meters, where *the proposed virtual meters can provide a low-cost alternative*. If a decentralized CUP is used, a building has its own chillers and boilers and building level energy use can be monitored by a power meter and a natural gas meter. However, *the proposed virtual meters provide a low-cost thermal energy metering of HVAC systems, which is essential to gain an in-depth understanding of how energy is distributed.* This understanding is an important objective described in the Policy and will be discussed in the next bullet.
  - The Policy states that "Where practical, energy-intensive buildings should be sub-metered to identify electricity use by major mechanical and electrical subsystems." HVAC systems are qualified as major mechanical subsystems, because they consume 38% of total energy in commercial buildings (DOE 2011). The understanding of the energy usage distribution allows energy professionals to identify energy deficiencies and improve system performance. This contributes to an objective in the Meter Data Management section of the Policy, which states that it will "enable energy professionals within each component to identify cost-effective energy investments…"
  - The elimination of manual data entry is one of the objectives described in the Meter Data Management section of the Policy. The BAS embedment of proposed virtual meters allows automatic data collection at any desired time interval.

2.0 TECHNOLOGY DESCRIPTION

2.1 TECHNOLOGY OVERVIEW

The demonstrated technology includes two major elements: virtual meter technology and performance degradation detection algorithms.

Virtual meter technology:

- Description: The virtual flow meter technology is a key component of the PDD in the proposed project. Three different types of virtual meters significantly enhance the measurement capacity of the BAS. In Type 1) meters, the whole building level chilled water flow rate and hot water flow rate are virtually obtained using pump operational characteristics, namely a **pump flow meter.** In Type 2) meters, the airflow rate in each air handling unit (AHU) is virtually obtained using fan operational characteristics, namely a **fan flow meter**. Finally, in Type 3) meters, the chilled water flow rate in each AHU is virtually obtained using control valve operational characteristics, namely a **control valve flow meter**. The water flow rate through the cooling coil, airflow rate, and chilled water and hot water flow rate through each main duct or pipe are regulated by the valve movement and the fan and pump speed adjustment. As a result, the virtual meters installed in this project used both the available or inexpensive/easy-to-obtain measurements of operational variables, such as valve position, differential pressure across the valve, fan/pump head and motor input power and frequency, and device characteristic curves that relate the behavior of these devices to the desired virtual values and commonly measurable variables. Device characteristic curves can be determined empirically using measurements or analytically from first principles. The desired virtual values can then be calculated using measured values of variables for which meters are commonly installed.

  – **Pump/fan flow meter**

  Both the virtual pump and fan flow meters work under the same principle. Motor input power (*W*) is determined by useful mechanical work imparted into fluid, the product of head (*H*) and flow rate (*Q*), fan/pump efficiency, and motor efficiency. Theoretically, the fan/pump efficiency ($\eta_{f/p}$) is a function of the ratio of head (*H*) to flow rate (*Q*) squared, while motor efficiency (η_{motor}) is theoretically a function of power (*W*), frequency (*f*), and voltage (*V*). Practically, head can be measured by a pressure differential sensor while voltage, power, and frequency can be obtained through the existing variable frequency drive (VFD). The motor equivalent circuit, defined by six circuit parameters (IEEE. 2004), can be applied to determine the motor efficiency under different frequencies and voltage. A break-through in this development was that Wang et al. (Wang, Song et al. 2013) successfully developed a method to estimate these six parameters based on the published motor efficiency and power factor under rated frequency. Meanwhile, the fan/pump efficiency curve can be calibrated through experiments on each system. Using calibrated motor and fan/pump efficiencies (η_{motor} and $\eta_{f/p}$), the flow rate (Q) can be obtained numerically based on the fan/pump head (H) and VFD output power (W) as well as the VFD output frequency (f) and voltage (V), shown in Equation (2-1) below. Wang *et al*. (Wang, Song et al. 2014) and Andiroglu *et al*. (Andiroglu, Wang et al. 2013) documented the accuracy comparison of the virtual meters.

The prior-to-demonstration studies also show that the coefficient of determination or R-square for the 2-week validation period was 0.81 for the airflow meter and 0.973 for the water flow meter. The schematic of the virtual pump/fan flow meter is shown in Figure 2-1, along with the photos of accessory sensors and equipment that are needed for virtual pump and fan flow calculations. These include the VFD and a differential pressure (DP) sensor.

$$Q = \frac{W \cdot \eta_{motor}(W,f,V) \cdot \eta_{f/p}(\frac{H}{Q^2})}{H} \quad (2\text{-}1)$$

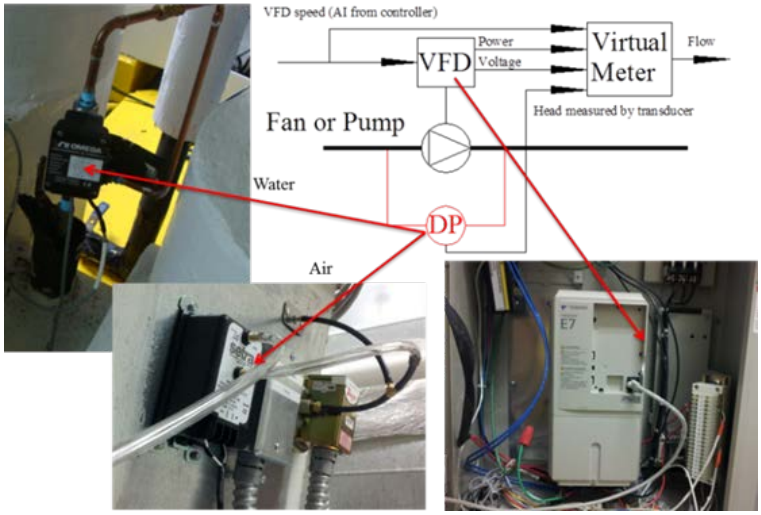

Figure 2.1. Virtual Pump/Fan Flow Meter.

– **Virtual valve flow meter**

A cooling or heating energy meter is typically not installed in an AHU because of high installation and maintenance costs and increased water loop pressure drop. It is often impossible to install one in existing AHUs due to space and system dimension limitations. The virtual valve flow meter uses existing coil control valve operational variables to indirectly obtain the water flow rates. Theoretically, the pressure drop through a valve is determined by valve position and flow rate for a given valve, which has a fixed valve characteristic curve. The pressure drop can be measured by a water pressure differential sensor and the valve position can be obtained by either valve command through a BAS or valve position feedback from the valve actuator. The valve characteristic curve needs to be obtained through a calibration process. Therefore, the flow rate (Q) can be obtained based on the pressure drop ($\Delta P_{L,x}$) and valve position (x) as well as calibrated valve curve ($F_{L.x}$) (Song, Swamy et al. 2011, Swamy, Song et al. 2012, Song, Joo et al. 2012a, Song, Wang et al. 2012b), as described in Equation (2-2). The schematic of the virtual valve flow meter is shown in Figure 2-2, along with the photo of accessory sensors that are parts of the virtual valve flow meter setting in the lab tests.

$$Q = F_{L.x}(x)\sqrt{\Delta P_{L,x}} \quad (2\text{-}2)$$

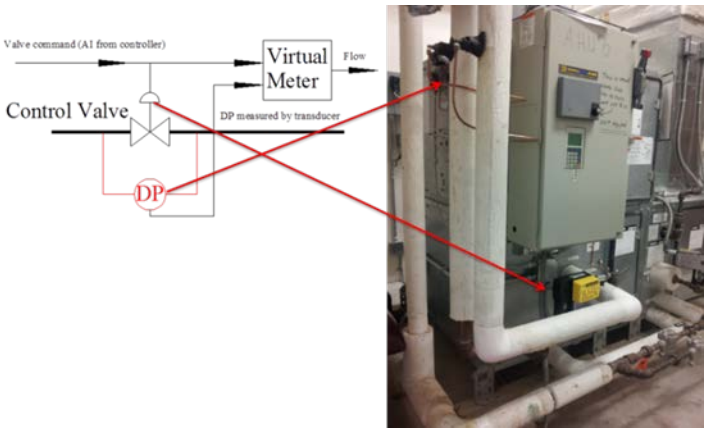

Figure 2.2. Virtual Valve Flow Meter.

- Visual Depiction: Figure 2-3 shows the different roles of proposed virtual meters in this project, which will greatly enhance the measurement capacity in a building. The virtual hot water flow meters were installed on the secondary hot water pumps to calculate the building heating energy and the virtual chilled water meter were installed on the secondary chilled water pump to calculate the building cooling energy. On the other hand, the virtual valve water flow meters were installed at the cooling coil of AHUs and the virtual fan airflow meters were installed at the supply fan of AHUs.

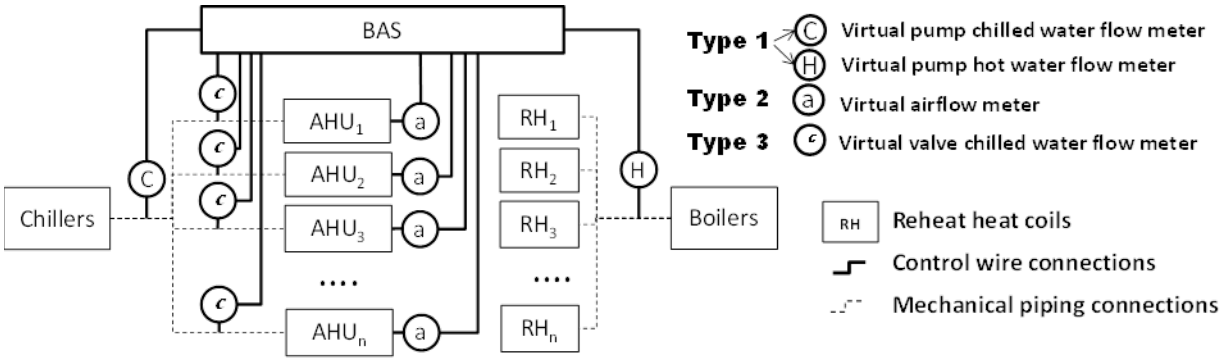

Figure 2.3. Measurement Results Comparison Between Virtual and Ultrasonic Water Flow Meters.

Performance degradation detection:

- Description: The PDD uses the available BAS data plus the measurements from the proposed virtual flow meters at pumps, fans, and valves to determine actual energy use of key building systems and subsystems. The energy use of energy efficient operations for those systems, i.e., reference values of energy consumption for practices conforming to standards and guidelines set by ASHRAE and other authorities, such as the static pressure reset requirements of ASHRAE 90.1(ASHRAE 2010b), can also be predicted through virtual flow measurements based on energy balance and/or mechanisms of subsystems.

As a result, the actual energy use and reference energy use for fans, reheats, cooling coils in AHUs and pumps, chillers and boilers in chilled and hot water systems can be automatically obtained in Phase I, Data Collection. Besides the energy comparisons, the duct and water loop pressure setpoints for fan and pump speed can be calculated based on the virtual flow measurements. The variation between the measured and simulated setpoints indicates a faulty setpoint or the incorrect damper or valve position. By comparing the actual energy use/setpoint with the reference energy use/setpoint, the energy degradation or system malfunction operations can be determined in Phase II, Online Diagnosis. The severity of the performance degradation or faults will trigger alarms and motivate facility operators for quick corrections, which is shown by the empty box to the right of the detector module.

- Visual Depiction: The mechanism of the detector is shown in Figure 2-4. The shaded box bordered by the dashed line represents an add-in PDD (a set of function modules) in a BAS. The two boxes on the left represent available sensor and command information in a BAS.

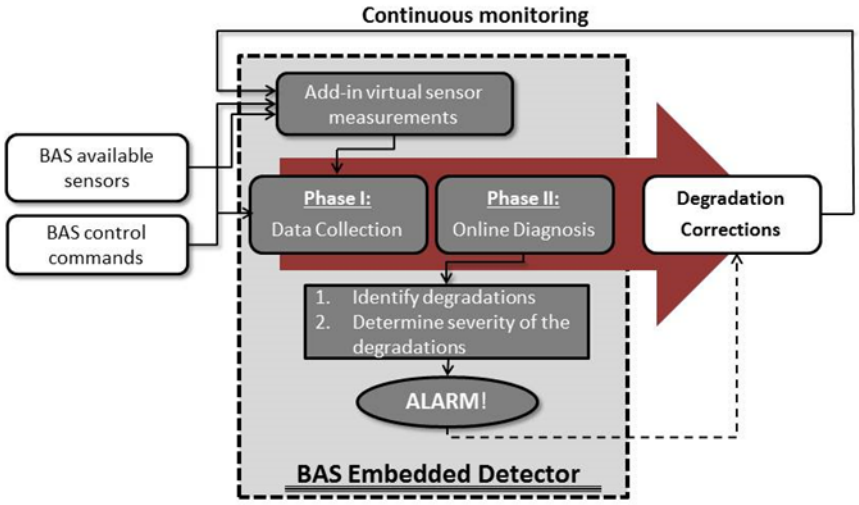

Figure 2.4. Flow Chart of the Embedded PDD.

Chronological Summary:

The concept of the technology was conceived during the inventors' combined 20-year commissioning experiences. The development effort was initiated in 2009 by OU's Building Energy Efficiency (BEE) laboratory, and continuing development was supported by DOE funds in 2011 and 2012 (Taasevigen, Huang et al. 2012). The concept of using virtual meters for performance diagnosis received recognition as one of five finalists for the 2011 ConocoPhillips Energy Prize. All three virtual meters have been experimentally tested in OU's BEE laboratory and the University of Miami (UM)'s HVAC laboratory. Test results have been compared with conventional meters and published in six journal papers (Wang, Liu et al. 2010, Swamy, Song et al. 2012, Song, Joo et al. 2012a, Wang, Song et al. 2013, Song, Wang et al. 2013a, Wang, Song et al. 2014) and five conference papers (Wang and Liu 2007, Song, Swamy et al. 2011, Song, Wang et al. 2012b, Andiroglu, Wang et al. 2013, Song and Wang 2013b). One patent has been filed through the OU research office. The technology is now ready for demonstration on a larger set of buildings to validate its performance and determine its true life-cycle cost.

Future Potential for DoD:

The technology is applicable to all existing and new buildings that possess a centralized HVAC system, which is estimated to be 0.95 billion ft^2 of DoD built infrastructure.

2.2 TECHNOLOGY DEVELOPMENT

An algorithm development was necessary prior to the field demonstration to successfully implement the technology in the specific demonstration building. Several other technology improvements have been made as a result of lessons learned during the demonstration to enhance the technology. They are summarized below:

- Explicit expression and algorithm of fan and pump flow meters had been developed to make the BAS-embedded virtual meters possible before the demonstration;
- A data-driven motor efficiency model in virtual fan and pump flow meters was developed to improve the meter accuracy during the demonstration. The new motor efficiency can cover the harmonic motor energy loss introduced by VFDs that was found in this demonstration project;
- Virtual valve flow meters were improved by developing a valve command correction algorithm and replacing the valve command by the valve position to reduce the valve hysteresis impacts;
- A mini-converter was developed to reduce the calculation load and measurement inputs introduced by the virtual flow meters. Having the technology embedded in a device makes the technology commercialization and mass production possible.
- A new fault detection method to detect reheat energy waste was developed using the virtual airflow rate measurement in each AHU rather than what we proposed using the whole building level hot water measurements by virtual hot water pump flow meters.
- A new fault detection method to detect loose belts in AHU fans was developed using the correlation between the VFD output power and frequency in addition to the fan control PDD.

2.2.1 Explicit Expression Conversion of Fan and Pump Flow Meters to facilitate the implementation for the demonstration.

Before the installation for the demonstration, it was found that two iterations in virtual flow calculations were barriers to implement the developed virtual fan and pump flow meters in BAS. This is because VFD voltage, frequency and motor slip are independent input variables to calculate motor power and efficiency using the motor equivalent circuit method. Therefore, motor efficiency must be implicitly determined by motor power, VFD frequency and voltage by a numerical iteration method. On the other hand, since fan and pump efficiencies were calibrated as a function of the ratio of fan or pump head to flow rate squared in our lab tests, an unknown flow rate results on both sides of the basic flow correlation equation, Equation (2-1). As a result, the flow rate must be calculated from available pump/fan shaft power and head through a numerical iteration process.

These two numerical processes made it impossible to achieve the virtual flow rate calculation in BAS for the demonstration building, which does not provide enough mathematical calculation capacity. Therefore, an explicit expression of fan/pump flow rate calculation was developed prior to the implementation of the virtual fan/pump flow meter for the demonstration.

Currently most VFDs on the market have three preset voltage controls – a linear V/f ratio, a squared V/f ratio and a flux optimizer -- that correlate the VFD output voltage to the VFD output frequency in different ways based on a selected voltage control. Therefore, the VFD output voltage is correlated to the VFD output frequency.

Moreover, the motor shaft power is ideally proportional to the VFD output frequency cubed if all valves or dampers remain in fixed positions for centrifugal pumps and fans. Even though valve or damper positions vary, the VFD output frequency is still approximately correlated to the motor shaft power as well as the motor input power.

As a result, the motor efficiency can be simplified as a function of the motor input power, which can be regressed using the simulation results.

$$\eta_{\mathrm{motor}} = \eta_{\mathrm{motor}}(\mathrm{W}) \tag{2-3}$$

The affinity laws state that the pump/fan flow rate is proportional to the pump/fan speed, the pump/fan head is proportional to the square of the pump/fan speed, and the shaft power is proportional to the cube of the pump/fan speed among all equivalent operating points.

Besides identical efficiency, all equivalent points have other unique identical ratios without the pump/fan speed, such as the ratio of head to flow rate squared (H/Q^2) and the ratio of shaft power squared to head to the power of 3 (W_{shaft}^2/H^3).

The pump/fan shaft power is the product of the measured motor input power and calculated motor efficiency. Consequently, the pump/fan efficiency can be regressed as a function of the ratio of pump/fan shaft power to pump/fan head to the power of 3/2 rather than the ratio of pump/fan head to water flow squared to avoid the unknown water/air flow rate in the pump efficiency calculation.

$$\eta_{\mathrm{f/p}} = \eta_{\mathrm{f/p}}\left(\frac{\mathrm{W}\cdot\eta_{\mathrm{motor}}(\mathrm{W,f,V})}{\mathrm{H}^{1.5}}\right) \tag{2-4}$$

Finally, with newly developed pump/fan efficiency function, the flow rate (Q) is correlated explicitly with the motor power (W_{motor}) and pump/fan head (H) (Wang, Kiamehr et al. 2016).

$$Q = \frac{W\cdot\eta_{motor}(W)\cdot\eta_{f/p}\left(\frac{W\cdot\eta_{motor}(W)}{H^{1.5}}\right)}{H} \tag{2-5}$$

To eliminate the direct impact of the motor input power, which is always dynamic, Equation (2-5) is rearranged as a correlation of the ratio of airflow to the squared root of head with the ratio of shaft power to head to the power of 3/2.

$$\frac{\mathrm{Q}}{\mathrm{H}^{0.5}} = \frac{W\cdot\eta_{motor}(W)\cdot\eta_{f/p}\left(\frac{W\cdot\eta_{motor}(W)}{H^{1.5}}\right)}{H^{1.5}} = \mathrm{f}\left(\frac{\mathrm{W}\cdot\eta_{\mathrm{motor}}(\mathrm{W})}{\mathrm{H}^{1.5}}\right) \tag{2-6}$$

As a result, the flow rate can be directly obtained from the calibrated correlation.

$$Q = H^{0.5} f\left(\frac{W \cdot \eta_{motor}(W)}{H^{1.5}}\right) \quad (2\text{-}7)$$

2.2.2 Data-driven Motor Efficiency Curve Calibration for Fan and Pump Flow Meters.

In our lab tests, prior to the demonstration, the motor efficiency was theoretically calculated using the motor equivalent circuit with consideration of the constant additional energy loss of 0.5 to 1.5% due to harmonic in the power supply from the VFD to the motor (Manz and Morgan 1996, WEG 2010). It is true that the harmonic impacts were approximately constant when the fans and pumps in the demonstration site always operated at a narrow high speed or VFD output frequency range before we implemented energy efficiency measures. However, what we found in our fan speed overrides, for obtaining full range of fan operation curves for efficiency calibration, was that the harmonic impacts significantly increased as the VFD output frequency decreased from an initial high value to a minimum value such as 15hz. This observation is very critical, and it means that the accuracy of the virtual fan/pump flow meters was not as good as we had predicted. In the first half of the demonstration project, until we submitted the mid-progress report that documented the accuracy of the virtual flow meters (attached in Appendix E), we could not identify an effective approach to correct the efficiency losses caused by the harmonics. Although the mid-progress report, which includes the fan airflow meters in three units with relatively large errors, was approved by the ESTCP office in March 2016, we have continued our efforts to improve the accuracy of the flow meters. As a result, to project the motor efficiency with significant frequency variation, a new data-driven calibration method for motor efficiency was developed in late 2016.

Since the VFD output frequency is easily controlled, the new motor efficiency function uses the VFD output frequency rather than the motor input power as the input. The motor efficiency is calibrated by manually overriding the VFD output frequency with fixed valve or damper positions from the rated frequency (f_d) to any frequency (f).

$$\eta_{motor} = \eta_{motor}(f) = \frac{(W)_f}{(W)_{fd}} \quad (2\text{-}8)$$

With a newly-developed motor efficiency function, the pump and air flow rate (Q) is correlated explicitly with the motor power input (W) and pump head (H) (Wang, Wang et al. 2018).

$$Q = \frac{W \cdot \eta_{motor}(f) \cdot \eta_{f/p}\left(\frac{W \cdot \eta_{motor}(f)}{H^{1.5}}\right)}{H} \quad (2\text{-}9)$$

Moreover, it is more accurate to regress the pump/fan efficiency curve than the correlation defined by Equation (2-6). The new calibration method was implemented for secondary chilled water pumps, the secondary chilled and hot water pumps, and AHU 2 and AHU 13 using the improved virtual flow meter models. As a result, we are confident that the accuracy of the virtual flow meter is less than 2% relative error compared with measured flow rates by a calibrated, physical flow meter at any motor frequency.

2.2.3 Valve Command Correction Algorithm for Valve Flow Meters

The valve flow meter experienced something similar. In our original proposal to the ESTCP, as well as in our lab tests, the virtual valve flow rate was calculated using the DP across the valve and the valve command, which represents the valve opening positions. With limited lab testing conditions, the results were very good, and we proposed to ESTCP with 2% error as the performance objective criteria for the valve flow meter as well.

However, in the demonstration, with real operational conditions, we found out that the valve commands cannot completely represent the valve opening positions, especially when a valve experiences slow movement.

As shown in Figure 2-5, measured water flow rate and virtual flow rate are compared with the reference of the valve commands. When the measured flow rate experiences a big change, the virtual flow follows the measured flow well. However, when the measured flow remains relatively constant, as shown by the lines in the red box, the virtual flow still experiences drastic decreases. The decrease in the virtual flow calculations is because the valve commands are experiencing the same slowly descending patterns. The measured flow reflects the actual valve position. This disagreement indicates that the slow valve command changes do not cause the valve actual movement. For this particular valve, the slow one-directional descending command can last for almost an hour; the hourly averaged virtual flow rate results in a large error compared with the measured flow rate. This phenomenon explains the outliers of the valve flow meters in our mid-progress report.

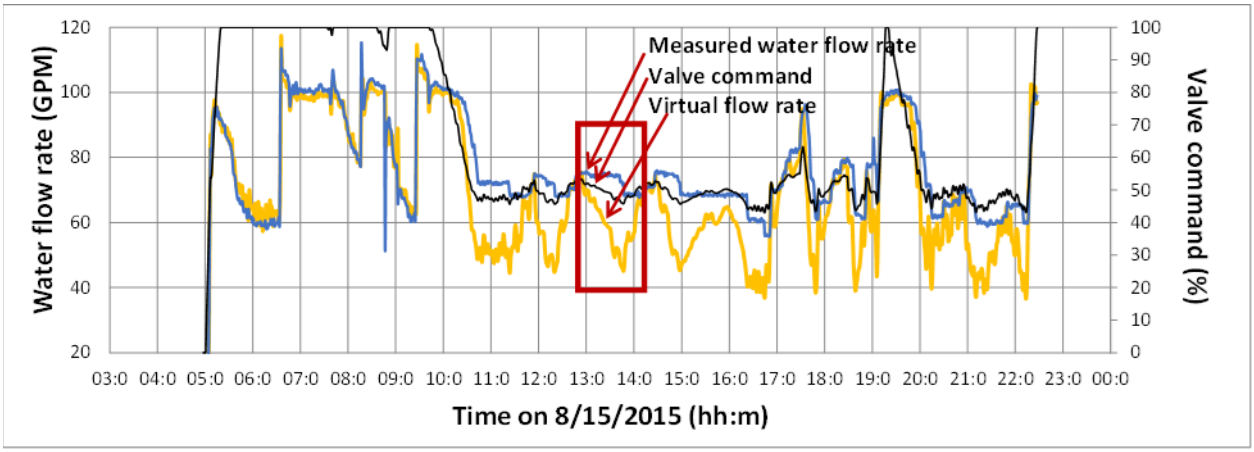

Figure 2.5. The Mismatch of Valve Command and Valve Positions.

Although the mid-progress report, along with the accuracy of the valve flow meters, was approved by the ESTCP office in March 2016, we have continued our efforts to improve the accuracy of the virtual valve flow meter. One method was implemented to predict the valve positions by correcting valve commands using empirically obtained stiction and deadband. The other method was to wire the valve position feedback signals directly to the BAS. The valve position feedback signal is usually available in the valve actuator. However, since it is not needed for basic valve control and operation, this signal is usually not connected to the BAS. Hence, there are additional costs to wire the signal into the BAS for virtual valve flow meter application. This additional wiring will increase the costs of the virtual valve flow meter implementation.

A BAS-programmable algorithm was developed to convert the valve commands to the true valve position by factoring in the impacts of resolution errors, stiction, and deadband. This is an alternative method that eliminates the need for additional wiring costs. Figure 2-6 shows the detailed flow chart that can be programmed into the BAS (Shahahmadi and Song 2018). The correction algorithm was implemented in AHU 2 and AHU 13 for test purposes.

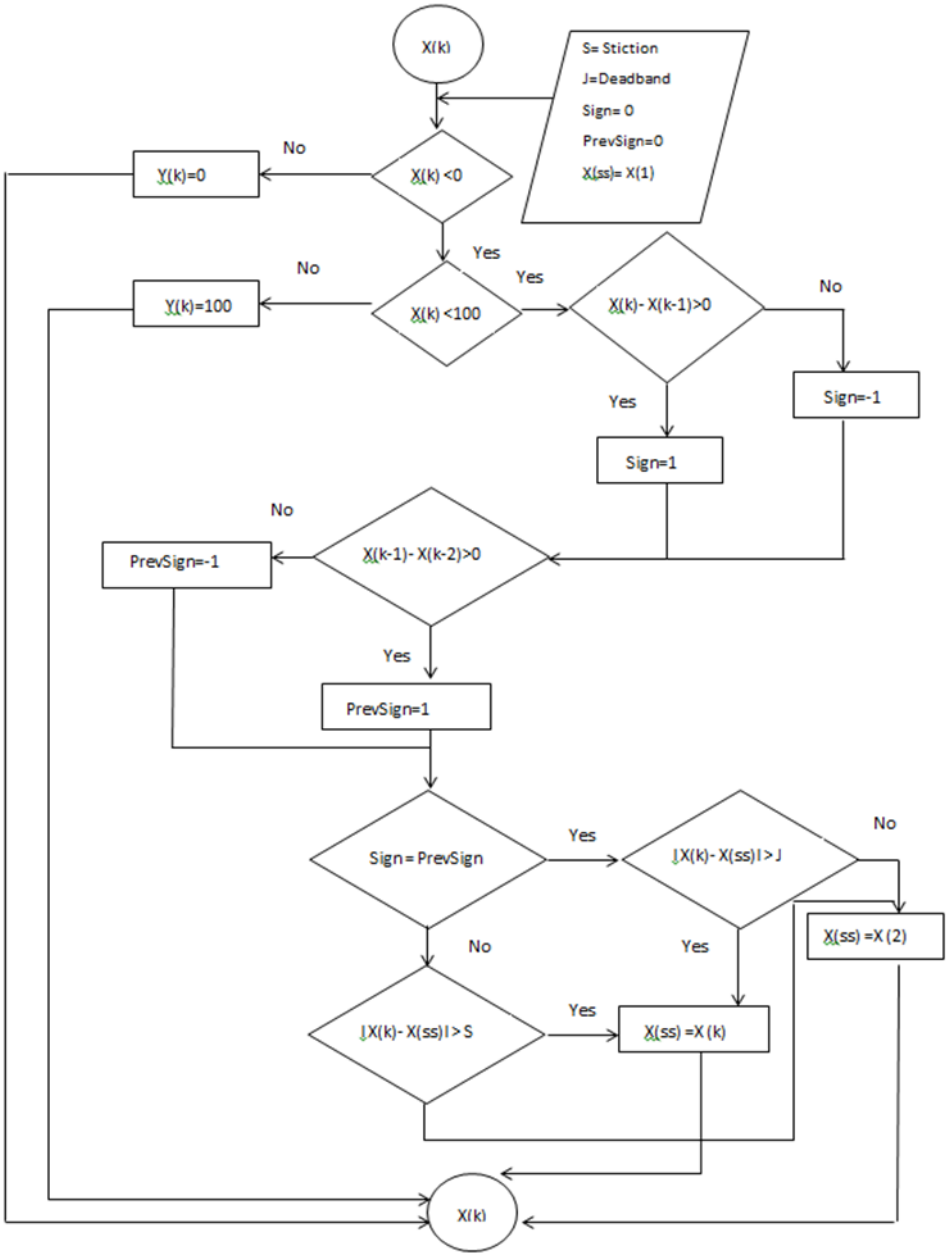

Figure 2.6. Flow Chart of Correcting Valve Commands into Valve Positions.

2.2.4 Development of a mini-converter

A mini-converter device was developed with leveraged funding support from the Oklahoma Center of Advanced Science and Technology (OCAST) to connect the valve position feedback signal that is provided in the valve actuator as the true valve position signal, instead of using the valve command signal for the virtual valve flow rate calculation.

The mini-converter was successfully developed and possesses a processor to calculate the virtual valve flow rate and integrate an I/O connection to receive input DP signal and valve feedback position signal and output the calculated flow rate. We have found that in addition to the virtual valve flow meter, the mini-converter can be applied to the fan and pump flow meter to reduce the calculation load and measurement inputs of existing controllers introduced by the virtual flow meters. Figure 2-7 shows the mini-converter prototype; the prototype was used in the tests of AHU 13 in the demonstration building. The mini-converter was tested in AHU 2 as well. Both prototypes were removed after the tests because they are not commercial-grade products and we did not want to leave them permanently in the demonstration building. We have also successfully conducted a test of using a mini-converter as a virtual pump flow meter at another site.

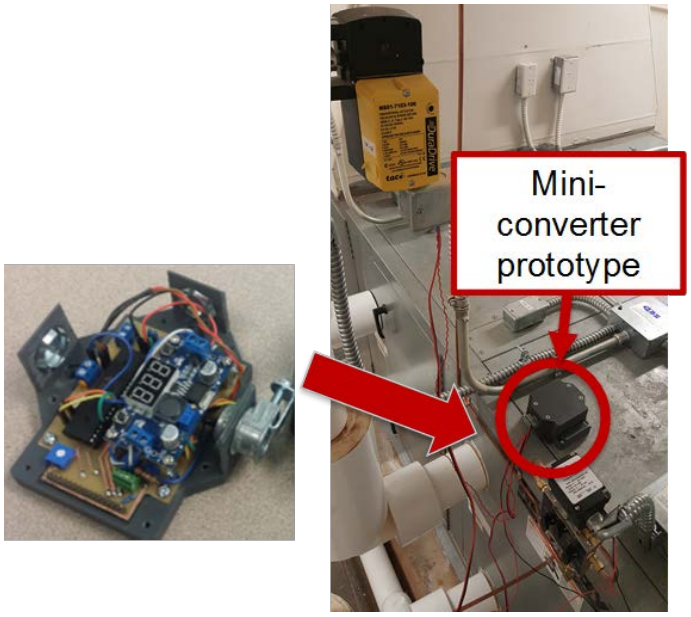

Figure 2.7. A Mini-converter Prototype in Testing.

2.2.5 Using the Virtual Airflow Rate Measurements in Each AHU to Detect Reheat Energy Waste

We proposed using a virtual hot water pump flow meter to calculate the whole building level reheat energy consumption, by multiplying it with the temperature difference between the hot water supply and return water shown in Equation (2-10), for simultaneous heating and cooling detection, i.e., the minimum supply air flow rate is too high so that unnecessary reheat energy is enabled. The temperature difference is calculated using the measurements from the temperature sensors installed on the hot water supply and return pipes, which were originally installed for monitoring building operations.

$$q_{rh} = 500Q_{hw}(T_{hws} - T_{hws}) = \sum(1.1Q_{TB}(T_{rm} - T_{rm}) - q_s) \qquad (2\text{-}10)$$

However, during the demonstration, we found that in summer season, detection for the simultaneous heating and cooling is the most needed. The temperature sensor errors on the hot water supply and return pipes are more pronounced when the temperature differences between the supply and return water are small in summer. As shown in Figure 2-8, the calculated reheat energy use in July experienced almost 50% oscillation over a two-day profile. The calculated reheat in September showed much a smoother pattern with distinctive day time and nighttime differences. Therefore, the calculated reheat in July was not reliable enough for fault detection purposes.

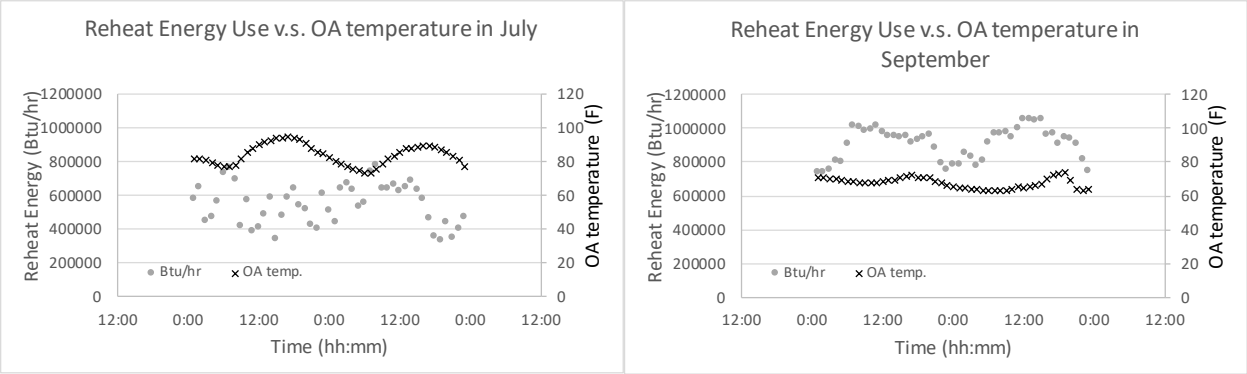

Figure 2.8. Calculated Reheat Energy Use Comparison Between July and September.

Because the calculated reheat was not precise enough, an alternative method was developed to accomplish fault detection more effectively. The air flow rate through the supply fan of an AHU reflects the minimum air flow setpoints of connected terminal boxes, which determine the heating energy use of reheat coils. Therefore, the calibrated fault-free minimum supply airflow ratio during occupied and unoccupied periods can be compared with the actual supply airflow rate to identify the high terminal box minimum airflow setpoints, in lieu of the fault detection method using hot water heating energy measurements.

2.2.6 Develop a fault detection method for loose belts on AHU fans.

A loose fan belt on a supply or/and return air fan of AHU does not impact the system energy performance but results in the reduced supply airflow and consequently impact the space thermal and health conditions. Multiple AHUs in the demonstration building experienced severe loose fan belt problems. One of the AHUs could only provide 0.36-inch static pressure when we started the project, while the duct pressure set point was required to be 1.3 inch, shown in Figure 2-9, which we snapshot in 2014. When this occurred, it was mostly treated as a faulty duct static pressure sensor. It is costly for building operators to identify the location of the duct static pressure and diagnose the problem; therefore we have developed an automated algorithm to detect loose fan belts. The algorithm is based on a calibrated correlation between the VFD output power and frequency when the belt is under normal operation. *Without necessary information provided by the virtual fan flow meter, the automated loose fan belt detection would not be possible.* The loose belt can be detected when the actual VFD output power is less than the power calculated based on the actual VFD output frequency along with the calibrated correlation (Kiamehr, Wang et al. 2016).

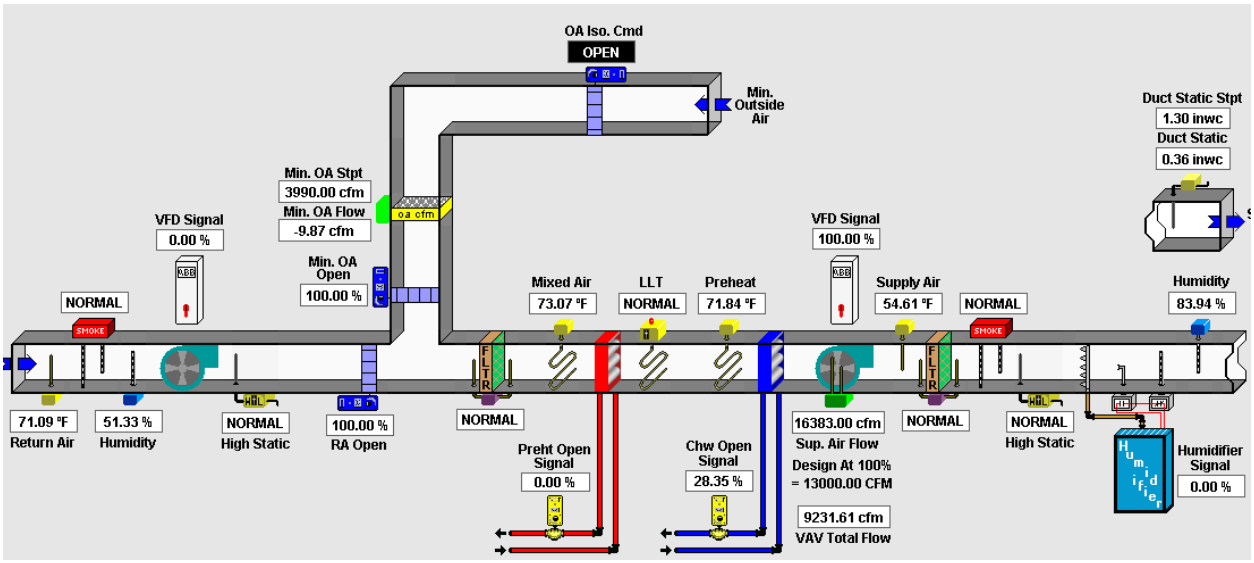

Figure 2.9. A Snapshot of an AHU with a Loose Fan Belt (taken in 2014).

2.3 ADVANTAGES AND LIMITATIONS OF THE TECHNOLOGY

Currently, the only alternative for the proposed technology is a physical flow meter that is costly and unreliable and sometimes impossible to install due to lack of the space in an HVAC mechanical room.

The advantage of the proposed technology is to make the flow rate measurements, the most critical information needed for energy performance assessment, available at extremely low cost and acceptable accuracy with no need for installation space, and consequently develop the PDD as an automatic commissioning agent using the virtual flow meters. The performance and cost advantages are summarized below:

- Performance Advantages: No matter whether the physical flow meters use velocity pressure or heat flux, the cleanliness of air and water significantly impacts the pressure and heat flux measurements. The accuracy will become worse without regular maintenance and calibration. Accuracy losses in physical flow meters were observed numerous times in this project. Because we needed to install our portable, recently-certified flow meter for virtual flow meter calibration, we had a chance to compare the measurement results of our portable meters with the readings from the flow meters that were installed in the building when the building was constructed. Significant discrepancies in the values were observed. Figure 2-10 shows the comparison of the readings from a physical hot water flow meter and our calibrated ultrasonic flow meter, which represent typical 10% to 20% errors. On the other hand, the developed virtual flow meters are less sensitive to air and water cleanliness and can provide less than 2% relative errors consistently over the long run. The reliable virtual meters then are applied to develop the PDD. In a meta-analysis using 643 non-residential buildings (99 million ft^2), Mills (Mills 2011) concluded that commissioning results in a 16% median whole-building energy savings in existing buildings with payback periods of 1.1 to 4.2 years.

The proposed PDD will contribute significantly to the DoD's stated goal of saving $1.5 Billion per year, as stated in Defense Budget Priorities and Choices – FY 2014 document (DoD 2013a). The improved building operation efficiency will result in less energy dependence on fossil fuels, thus reducing greenhouse gas emissions and enhancing energy security. The technology is applicable to all existing and new buildings that possess a centralized HVAC system, which is estimated to be 0.95 billion ft^2 of DoD's built infrastructure. The estimate assumes that 43.1% of DoD-cooled floor area is conditioned by centralized HVAC systems. The assumption is made based on a comprehensive energy assessment of 43 Army installations that collectively represent 39% of the Army's 1.1 billion square feet of floor space. Therefore, with 16% energy savings as summarized by Mills (Mills 2011), the proposed PDD will reduce DoD energy costs by approximately $0.3 Billion per year, assuming $4 billion energy expenses for DoD buildings and that the technology is applied to 43.1% of the DoD buildings.

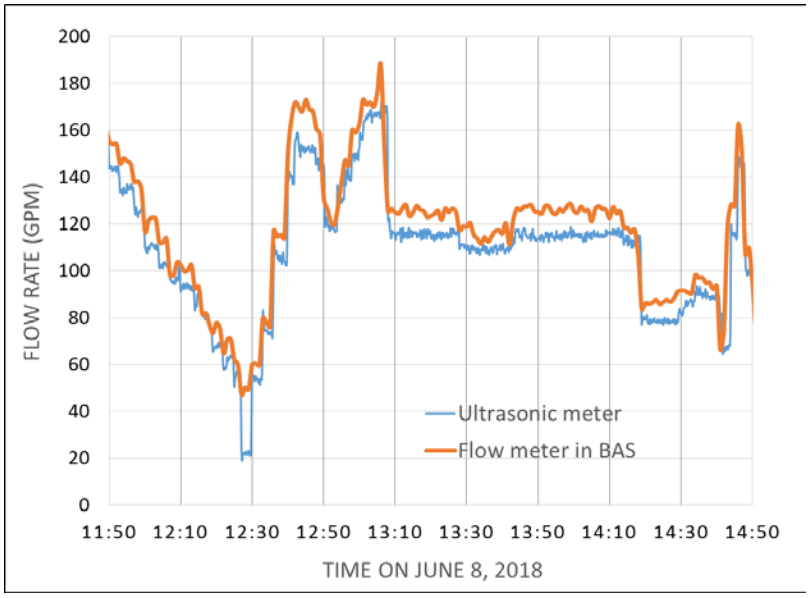

Figure 2.10. Comparison to Show the Accuracy Losses of a Physical Flow Meter Over Time.

- Cost Advantages: Physical flow meters cost $3,000 to $5,000 per unit, depending on system pipe sizes plus labor costs for installation and periodical calibration (usually 6 to 12 months), which can be substantially reduced by the demonstrated virtual meter technology. In addition, the demonstrated technology will eliminate the cost of data collection and analysis, which are the costliest activities in a typical commissioning process. In general, the commissioning cost, which is estimated at $0.30/$ft^2$ median normalized rate to deliver commissioning for existing buildings (Mills 2011), can be avoided by using the PDD.

The limitations of the proposed technology are summarized below:

- Performance Limitations: Equipment wear may result in less accurate virtual flow readings. However, according to valve, fan and pump manufacturers, the occurrence of noticeable plug and propeller wear in valves and fans/pumps should take 5 to 10 years.

This extends the calibration to a 5 to 10-year interval, significantly reducing the calibration cost compared with physical meters. Over the five-year duration of the ESTCP project, we did not notice any obvious accuracy losses caused by equipment deterioration. The virtual fan and pump flow meters need the fans and pumps to operate under functional operating conditions. For instance, the fan should have a positive fan head. However, faulty system design can make the meters operate under abnormal conditions, where the physical model cannot correlate the flow rate to the motor input power and fan head.

- Cost Limitations: All the virtual meters require a calibration process to obtain in-situ fan/pump efficiency curves and in-situ valve characteristic curves. Limitations on on-site skill levels and labor costs for generating the in-situ curves might provide a scale-up risk if adequately skilled engineers are not available. With the mini-converter being developed, we are in the process of developing an automated calibration algorithm to streamline the calibration.
- Potential Barriers to Acceptance: Faults might be identified by the demonstrated technology while systems seem to operate correctly, i.e., no comfort issues. This is because energy wastes are not always noticeable. Thus, alarms released through installation of the demonstrated technology might potentially increase and thus preventive maintenance efforts might increase. However, it is beneficial to have the demonstrated technology identify the problems before they occur and when they have not yet caused comfort issues, so the problems can be addressed.

3.0 PERFORMANCE OBJECTIVES

3.1 SUMMARY OF PERFORMANCE OBJECTIVES

We have planned two categories of performance objectives in Table 3-1, as shown below.

Table 3.1. Performance Objectives

Objective	Metric	Data Reqirements	Success Criteria	Results
Quantitative Performance Objectives for Virtual Meters				
Virtual water pump flow (3 condensing pumps; 3 primary; 3 scondary pumps; 2 hot wate secondarly pumps)	Difference between the virtual water flow rate determined from virtual measurements and the same flow rate measured with physical flow meters(GPM or L/s)	Water flow rate measurements by virtual and conventional meters	2% uncertainty at 95% confidence compared with a conventional meter	Met*
Virtual valve flow meter accuracy (cooling coils in AHU1-AHU13)	Difference between the virtual water flow rate determined from virtual measurements and the same flow rate measured with physical flow meters(GPM or L/s)	Water flow rate measurements by virtual and conventional meters	2% uncertainty at 95% confidence compared with a conventional meter	Met*
Airflow meter accuracy (supply air fans in AHU1-AHU13 and return air fans in AHU1-11)	Difference between the airflow rate determined from virtual measurements and the same flow rate measured with physical flow meters(GPM or L/s)	Water flow rate measurements by virtual and conventional meters	2% uncertainty at 95% confidence compared with a conventional meter	Met*

*: In our mid-progress report, we documented that we had 85% of virtual fan flow meters, 30% of valve flow meters and 75% of virtual pump flow meters passing the success criterion, which is less than 2% error at 95% confidence. Over 90% virtual meters passed 3% error at 95% confidence. With the improvements we made afterwards, now 93% of all the virtual flow meter had errors of less than 1.2% at 95% confidence. The remaining 7% meters had errors between 2% to 3% at 95% confidence.

Table 3-1. Performance Objectives (Continued)

Objective	Metric	Data Requirements	Success Criteria	Results
Quantitative Performance Objectives for PDD				
Outdoor air intake FDD (AHU1-13)	Difference between measured cooling energy use and estimated fault-free cooling energy use	Cooling energy use of a cooling coil in each AHU	Alarm when OA flow rate is beyond the OA flow required by	Met**
Hourly reheat usage (Hot water system)	Heating uses (MMBtu/hr. or kJ/hr.)	Virtual thermal meter readings	Alarm when heating occurs for non-minimum airflow rate defined	Not met, but an alternative was developed in Section 2.2.5
Fan control by SCC (AHU1-13)	Calculated SCC values	Virtual fan airflow rate and measured fan head	Alarm when SCC is beyond ±10% of the design value	Met and additional loose belt detection was added in Section 2.2.6
Secondary pump control by SCC	Calculated SCC values	Virtual pump flow rate and measured pump head	Alarm when SCC is beyond ±10% of the design value	Met
Variable primary chilled water pumps	Pump power savings (kWh)	Pump power measurements using the input to virtual pump flow meter	Alarm when actual pump power is higher than the power calculated by actual flow rate.	Not met. The chillers are having problems since the bldg. in operation. We were not allowed to make operation changes .
Variable condensing pumps	Pump power savings (kWh)	Pump power measurements using the input to virtual pump flow meter	Alarm when actual pump power is higher than the power calculated by actual flow rate.	Not met. The chillers are having problems since the bldg. in operation. We were not allowed to make operation changes .
Facility energy use reduction	The percentage difference between annual energy consumption before and after the corrections identified by PDD (%)	Whole-building electricity and gas meters	16% whole-building energy reduction	Met. Overall 13% annual electricity reduction and 25% annual gas reduction.
Environmental impact reduction	The difference between annual greenhouse gas emission reduction before and after the corrections identified by PDD (%)	Calculation based on electricity and gas sources.	16% reduction compared with the baseline	Met. GHG emission is reduced accordingly.
Qualitative Performance Objectives for PDD				
Cold/hot complaints	Degree of satisfaction	Call logs	0% increase in	Met***
Ease of use	Degree of satisfaction	Survey forms	80% or above satisfactory	Not met. Detailed discussions are in lessons learned.

**: Using the cooling energy use to detect outdoor air (OA) fault is not as effective as we expected because there is no OA humidity sensor available. Therefore, the estimated fault-free cooling energy use is only based on OA temperature. For hot and humid Oklahoma weather, latent OA load is not negligible. Therefore, this method is not effective when the fault that causes less than 15% or 20% cooling energy use deviations compared with measured cooling use.

3.2 PERFORMANCE OBJECTIVES DESCRIPTIONS

A detailed description for each performance objective listed in Table 1 is given below:

PO1:

- Name and Definition: Virtual water pump flow meter accuracy (Meters to be installed on 3 condenser water pumps; 3 primary CHW pumps; 3 secondary CHW pumps; 2 hot water secondary pumps).
- Purpose: To ensure that the virtual pump flow meter can accurately measure the water flow rate that can be used for performance degradation detection.
- Metric: Difference between the water flow rate determined from virtual measurements and the concurrent flow rate measurements with physical flow meters (GPM).
- Data: Water flow rate measurements by virtual and portable ultrasonic flow meters. The data were logged at each of the pumps where virtual meters were installed at 1-minute intervals for one week to cover a wide operation range for each pump.
- Analytical Methodology: Statistical analysis.
- Success Criteria: 2% uncertainty at 95% confidence compared with a conventional flow meter.
- Results: In our mid-progress report, we documented that we had 75% of virtual pump flow meters passing the success criterion, which is less than 2% error at 95% confidence. Over 90% of the virtual meters passed 3% error at 95% confidence. With the improvements we made, as described in Section 2.2, now 100% of pump virtual flow meter had errors of less than 1.2% at 95% confidence, exceeding the success criterion of 2%.

PO2:

- Name and Definition: Virtual valve flow meter accuracy (cooling coils in AHU1-AHU13).
- Purpose: To ensure that the virtual valve flow meter can accurately measure the water flow rate through a coil that can be used for performance degradation detection.
- Metric: Difference between the virtual water flow rate determined from virtual measurements and the same flow rate measured with physical flow meters (GPM).
- Data: Water flow rate measurements by virtual and portable ultrasonic meters. The data were logged at 1-minute intervals for one week to cover a wide operational range of the valves.
- Analytical Methodology: Statistical analysis.
- Success Criteria: 2% uncertainty at 95% confidence compared with a conventional meter.
- Results: In our mid-progress report, we documented that we had 30% of the fan flow meters passing the success criterion, which is less than 2% error at 95% confidence. Over 90% of the virtual meters passed 3% error at 95% confidence. With the improvements we made, 10 of 13 valve virtual flow meters had errors of less than 1.1% at 95% confidence, exceeding the success criterion of 2% and the remaining 3 had errors between 2% to 3% at 95% confidence.

PO3:

- Name and Definition: Airflow meter accuracy (supply air fans in AHU1-AHU13 and return air fans in AHU1-11).
- Purpose: To ensure that the virtual fan air flow meter can accurately measure air flow rates, which can be used for performance degradation detection.
- Metric: Difference between the airflow rate determined from virtual measurements and the same flow rate measured with physical flow meters (CFM).
- Data: Air flow rate measurements by virtual and conventional flow stations. The data were be logged at each of the fans where virtual meters were installed at 1-minute intervals for one week to cover a wide operational range of fans.
- Analytical Methodology: Statistical analysis.
- Success Criteria: 2% uncertainty at 95% confidence compared with a conventional meter.
- Results: In our mid-progress report, we documented that we had 85% of the valve flow meters passing the success criterion, which is less than 2% error at 95% confidence. Over 90% of the virtual meters passed 3% error at 95% confidence. With the improvements we made, as described in Section 2.2, 100% of the virtual fan airflow meters, including the ones in AHU2 and 13 that were tested for the new algorithm, passed the success criterion.

PO4:

- Name and Definition: Outdoor air intake FDD (AHU1-13).
- Purpose: To ensure that minimum outdoor air intake is properly controlled as required by ASHRAE Standard 62.1.
- Metric: The fault-free cooling coil energy is projected by fan energy use, supply air flow rate, actual outdoor air temperature and the required outdoor airflow rate (Song and Wang, 2015). The difference between measured cooling energy use using the virtual valve flow meter and the predicted fault-free cooling coil energy in percentage is used to determine if there are any outdoor air intake faults.
- Data: In addition to fan energy use, supply air flow rate and outdoor air temperature and humidity, virtual valve flow rate and chilled water supply and return water temperatures were used to calculate cooling energy use. The data were logged at 5-minute intervals for one year to cover a wide operational range of AHUs.
- Analytical Methodology: statistical analysis.
- Success Criteria: Alarm when the OA flow rate (related to cooling coil energy) is beyond the projected cooling energy using ASHRAE Standard 62.1.
- Results: The proposed method would be effective in detecting OA intake fault if the fault caused more than 15% errors when comparing the measured cooling use with the predicted fault-free one. However, it was not as sensitive because of the lack of the OA humidity sensor in the BAS. Therefore, the fault-free energy calculation was not as precise since only the OA temperature was used during the hot and humid Oklahoma summer weather.

PO5:

- Name and Definition: Hourly reheat usage (Hot water system) and supply airflow rate at AHUs.
- Purpose: To ensure that no simultaneous heating and cooling occurs during non-minimum airflow operations as defined by ASHRAE Standard 90.1.
- Metric: Heating hot water uses for reheat (MMBtu/hr or kJ/hr) versus cooling use (MMBtu/hr or kJ/hr), outdoor air conditions and total airflow rate for the entire building and supply airflow rate versus the outdoor air conditions for each AHU.
- Data: Virtual thermal meter readings and virtual supply fan meter readings. The data were logged at 5-minute intervals for one year.
- Analytical Methodology: Statistical analysis using scatter and time-series graphics.
- Success Criteria: Alarm when heating occurs for non-minimum airflow rate defined by ASHRAE 90.1 or when the actual supply airflow is higher than the supply airflow rate calculated based on the outdoor air temperature along with a calibrated code-compliant supply airflow rate versus outdoor air temperature correlation.
- Results: The direct measurement on the significantly reduced heating energy was not achieve the required accuracy in order to identify the reheat waste. However, the supply airflow rate was selected to indirectly identify the reheat use as an alternative.

PO6:

- Name and Definition: Fan control by SCC and loose belt (AHUs 1-13).
- Purpose: To ensure energy efficient fan operations.
- Metric: Calculated SCC values and VFD output power.
- Data: Virtual fan airflow rate and measured fan head and VFD output power and frequency. The data were logged at 5-minute intervals for one year to cover the full operational ranges for each fan.
- Analytical Methodology: Statistical analysis using scatter and time-series graphics.
- Success Criteria: Alarm when SCC is beyond ±10% of the design value or when the actual power is less than 10% of the predicted frequency-related power.
- Results: The SCC change was applied to identify the overridden duct pressure setpoint and consequently avoided the excessive fan speed as well as power input. Meanwhile, the VFD out power was applied to identify the loose fan to avoid space thermal and health issues.

PO7/8/9:

- Name and Definition: Variable primary chilled water/condensing pumps and secondary chilled water pump control by SCC.
- Purpose: To ensure energy-efficient pump operations.
- Metric: Calculated SCC values.
- Data: Virtual pump flow rate and measured pump head. The data were logged at 5-minute intervals for one year to cover full operational ranges for pumps.

- Analytical Methodology: Statistical analysis using scatter and time-series graphics.
- Success Criteria: Alarm when SCC is beyond ±10% of the design value.
- Results: The SCC change was applied to identify the overridden loop differential pressure setpoint and consequently avoid the excessive pump speed as well as power input of the secondary chilled water pump. PO9 was achieved. However, the variable flow operation for primary pumps and condensing pumps was not adopted by the facility management team. We did not have a chance to demonstrate the proposed PDD. PO7 and PO8 were not achieved.

PO10:

- Name and Definition: Facility energy use reduction.
- Purpose: To verify that the use of the PDD coupled with virtual metering will result in an overall reduction in building energy use.
- Metric: The percentage difference between annual energy consumption before and after the corrections identified by PDD (%) and total kWh and BTU.
- Data: Natural gas and electricity usage by the meters installed in the demonstration BAS. The data were logged at 15-minute intervals for two years including before and after corrections were made.
- Analytical Methodology: Statistical analysis using scatter and time-series graphics.
- Success Criteria: A 16% whole-building energy reduction that will be achieved and presented by kWh and BTU savings, respectively.
- Results: The major system operation changes and corrections were initiated in Spring 2016. Overall, by comparing the monthly utility bills from 2014 to 2017, with prior to May 2016 as before and post May 2016 as after, after correcting for weather conditions, the average annual whole building level electricity and natural gas savings was 13% and 25% respectively, which met our success criteria of a total of 16% energy reduction for the building.

PO11:

- Name and Definition: Environmental impact reduction.
- Purpose: To verify the amount of greenhouse gas emission reductions.
- Metric: The difference between annual greenhouse gas emissions before and after the corrections identified by PDD (%).
- Data: Natural gas and electricity usage by the meters installed in the demonstration BAS. The monthly utility data were collected for two years including before and after corrections were made.
- Analytical Methodology: Statistical analysis using scatter and time-series graphics.
- Success Criteria: 16% whole-building carbon dioxide (eCO2) emission reduction.
- Results: 13% electricity and 25% natural gas savings, resulting in a similar percentage of carbon dioxide emission reduction.

PO12:

- Name and Definition: Improved indoor comfort.
- Purpose: To verify that indoor thermal comfort and indoor air quality is not sacrificed by energy efficiency gains.
- Metric: Compare the cold/hot or complaint call logs before and after the project implementation.
- Data: Trouble call logs.
- Analytical Methodology: Statistical analysis.
- Success Criteria: Reduced or no increases in complaint calls to the facilities staff.
- Results: There was no evidence showing increased comfort complaints.

PO13:

- Name and Definition: System Ease of Use
- Purpose: To ensure the ease of use of the demonstrated technology.
- Metric: Degree of satisfaction of building operators.
- Data: Evaluation from building operations and building administrators using survey forms provided in Appendix B.
- Analytical Methodology: Statistical analysis.
- Success Criteria: 80% or above satisfactory.
- Results: We were not successful in achieving this PO. Throughout the entire five years of the project, all the data we collected through BAS and our virtual meters were utilized by the project team for the analysis and for fault detection and corrections. Once faults were identified, we corrected the faults if they could be done by changes in algorithms or set points. If parts such as a loose fan belt needed to be replaced, we notified the facility operators to replace them. However, we could not guarantee that they would replace them in a timely manner because those faults do not cause operational problems but only result in reduced energy efficiency. We also observed other issues that impacted the success of this PO. *First*, the facility operations team in the demonstration building was understaffed. Operators needed to prioritize handling the tasks that ensure the normal operations of the building, but not necessarily the energy efficient operations of the building. It was very difficult to get them involved in our project while we were working in the building. *Second*, the facility operators used BAS as a monitoring tool to check equipment status and space temperature to ensure comfort. The entire operation algorithms behind the scene were a black box to them. They cannot make algorithm corrections and they did not feel comfortable in making set point adjustments unless there was a comfort problem. However, this failure is a precious lesson learned in this project. It provides us an insight into how we should commercialize our technology. The DoD facility operators should not be the end users of the technology, but rather control service contractors, consulting service providers or technology licensees would be more appropriate to utilize the technology and achieve energy savings.

Page Intentionally Left Blank

4.0 FACILITY/SITE DESCRIPTION

The newly constructed clinic building at the Tinker Air Force Base (TAFB), in Oklahoma City, OK, was chosen and confirmed as the demonstration site. TAFB has shown strong commitment to collaborate on this project. TAFB occupies 5,500 acres, owns 472 facilities, consumes 3,461BBtu energy and has $3.41 billion economic impact annually. TAFB ranks as the top energy user among all Air Force Material Command facilities according to Fiscal Year 2010 energy consumption data. With such a high energy profile and economic impact, TAFB has been chosen by the Air Force to lead and pilot energy conservation efforts. Consequently, it is likely to have a broader impact across the Air Force and DoD once the technology is successfully demonstrated at TAFB.

TAFB is within 20 miles of the PI's research laboratory and the OU campus. According to TAFB Information Assurance requirements, no remote network access from the outside is allowed. To ensure the quality of the project, frequent on-site visits for collecting data and managing equipment retrofits were possible and cost-effective. This proximity enabled the project team to visit TAFB on a weekly basis since the project was awarded.

4.1 FACILITY/SITE LOCATION AND OPERATIONS

The demonstration building is a clinic building with a floor area of 162,000ft^2. It has standard building operating hours from 8:00am to 5:00pm. A total of thirteen AHUs condition the entire building. Among them, eleven AHUs have both supply air return air fans and two AHUs have supply air fans only. Figure 4-1 shows the serving area of each AHU. The black texts show the AHU location while the red texts show their service areas.

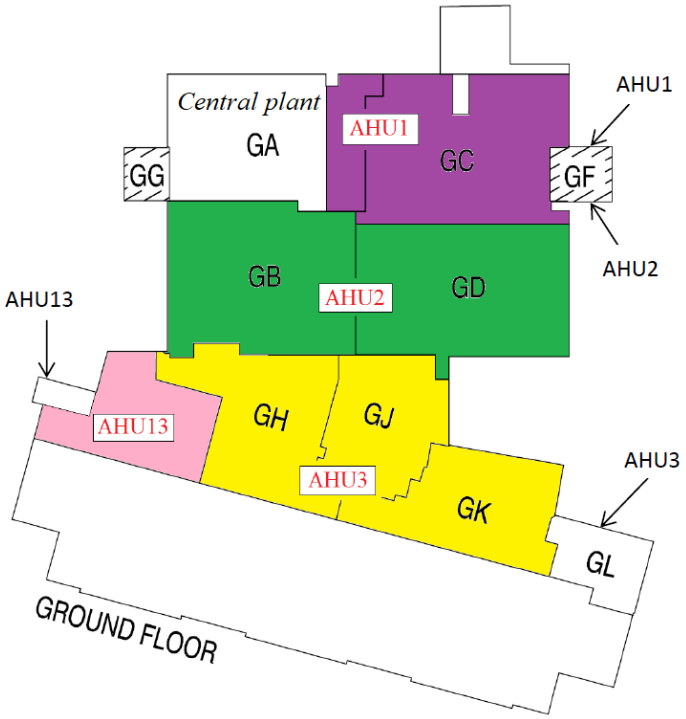

(a) Ground floor.

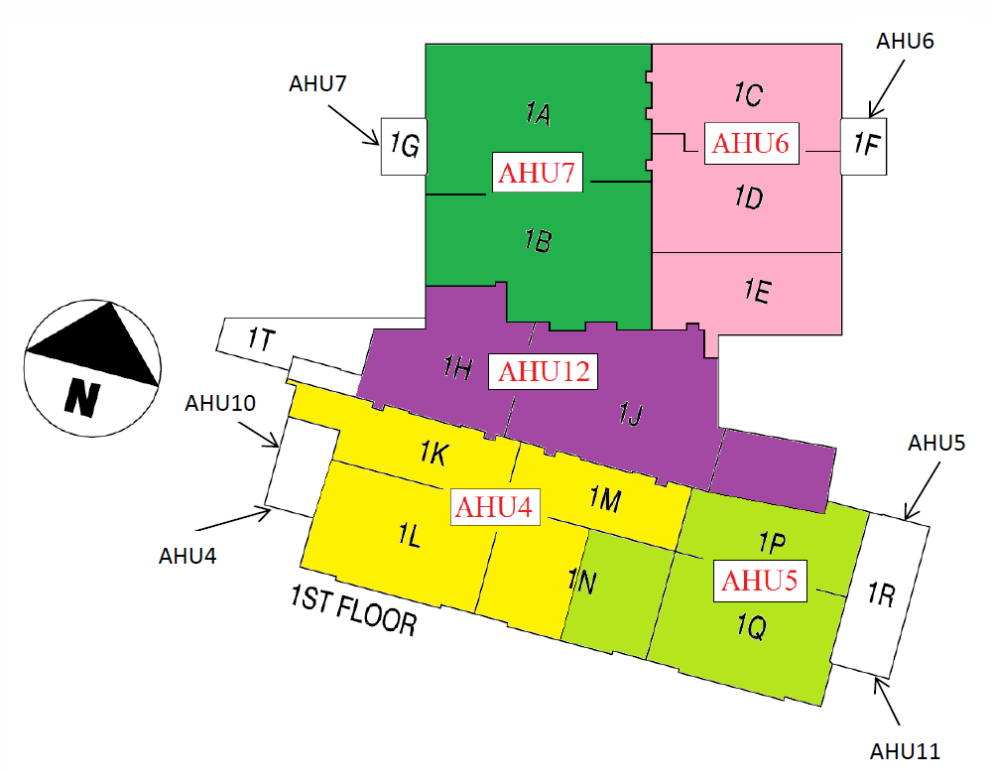

First floor.

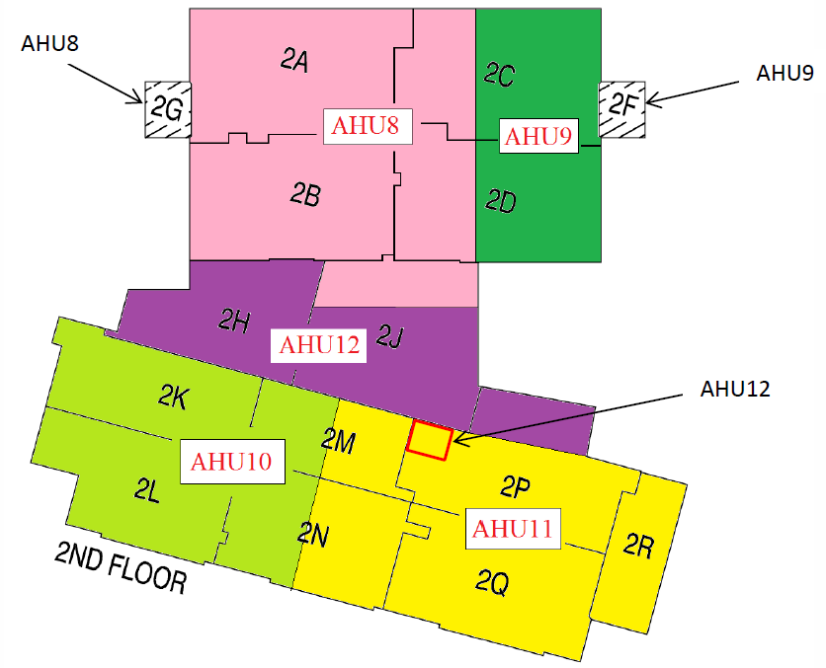

(b) Second floor.

Figure 4.1. The Floor Plan and Service Areas of Each AHU.

The building consists of two (300 tons each) chillers along with three primary chilled water pumps at 7.5 HP each, three secondary chilled water pumps at 20HP each, and three condensing water pumps at 20 HP each. The heating system is served by two (3,348MBH each) boilers with three primary hot water pumps at 3HP each and two secondary pumps at 25HP each. The central plant is located on the ground floor, as shown in Figure 4-1(a). Both chilled water and hot water loops are formed as primary and secondary water loop systems.

These are the major pieces of HVAC equipment on which we installed virtual flow meters for the technology demonstration. Table 4-1 shows a summary of information on the supply fan, return fan, cooling coil and valve of each AHU, while Table 4-2 shows the simplified information of the chilled water and hot water pumps in the central plant. We also have summarized the detailed HVAC information in Appendix C. The location and site map of the building is shown in Figure 4-2.

Table 4.1. AHU Design Information.

Component	SF			RF			Cooling coil		
Parameters	Motor	Airflow	Head	Motor	Airflow	Head	Valve	Coil DP	Valve DP
Unit	HP	CFM	inch.w	HP	CFM	inch.w	GPM	ft. water	ft. water
AHU1	10	6,200	1.5	2	4,905	0.9	43.2	12	11
AHU2	20	13,000	2.55	7.5	9,010	1.75	101	14.6	14.7
AHU3	25	13,380	3	7.5	10,735	1.5	95	13	13
AHU4	20	13,115	2.65	7.5	10,750	1.1	92.2	12.5	12.2
AHU5	15	9,885	2.75	5	7,965	1.25	65.8	7	6.2
AHU6	15	11,250	1.5	3	7,020	1.1	84.1	13	10
AHU7	15	12,490	1.5	7.5	9,845	7.5	85.1	9	**10**
AHU8	25	18,570	2	10	15,065	1.25	129.9	17	12.4
AHU9	15	9,735	1.75	5	7,785	1	66.3	7	6.3
AHU10	20	13,570	2	7.5	11,325	1.5	90.2	11.7	11.9
AHU11	20	14,875	2	7.5	11,725	1.5	102.3	13.5	16.5
AHU12	40	32,650	1.5	-	-	-	212.5	15.5	14.4
AHU13	5	2,480	1.5	-	-	-	23.9	10	13

Table 4.2. Design Information of Pumps.

Component	Quantity	Motor	Flow rate	Head	Virtual meter
Unit		HP	GPM	ft. water	
Primary chilled water pump	3	7.5	600	32	Yes
Secondary chilled water pump	3	20	600	80	Yes
Condensing water pump	3	20	900	68	Yes
Primary hot water pump	3	3	280	27	No
Secondary hot water pump	2	25	560	85	Yes

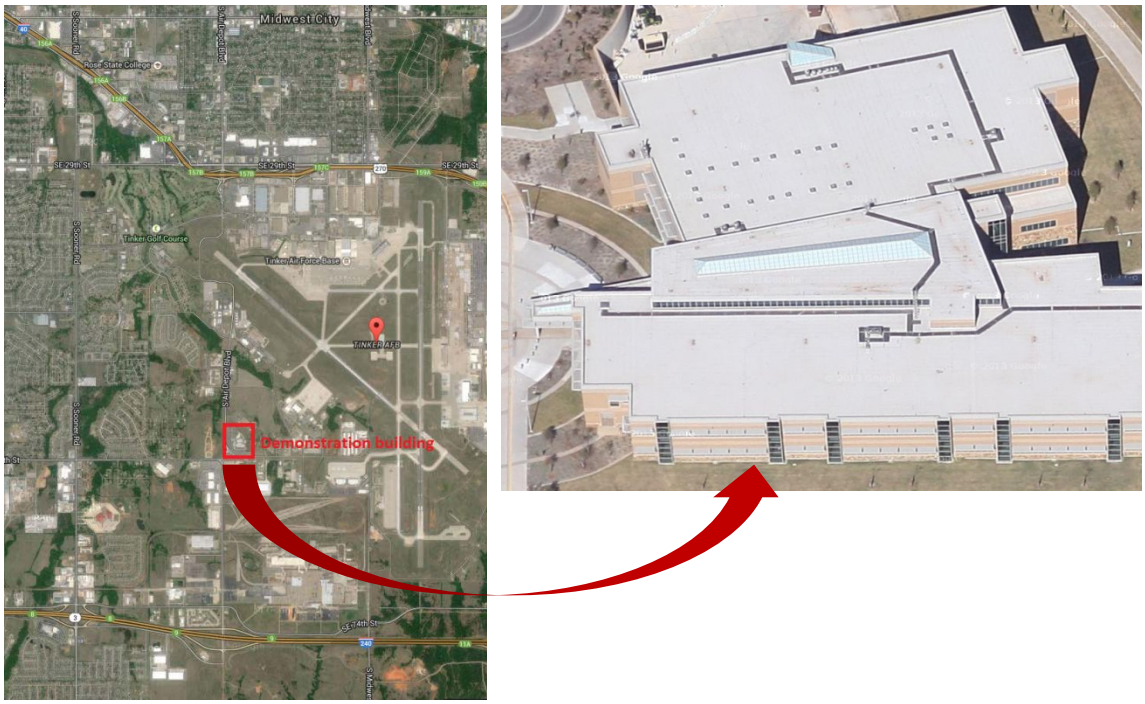

Figure 4.2. Demonstration Site and Building Layout.

4.2 FACILITY/SITE CONDITIONS

The demonstration building is a LEED certified building. It was constructed in 2008, with a full BAS system in place. The building is in Oklahoma City, OK, ASHRAE Climate Zone 3A.

5.0 TEST DESIGN

- Fundamental Problem: The demonstrated technology may provide the availability of low-cost air and water flow meters that can be utilized for continuous commissioning of energy-consuming HVAC systems
- Demonstration Question: This demonstration may answer the question "Can the use of "virtual" meters as part of a performance degradation continuous commissioning system produce energy savings?".

5.1 CONCEPTUAL TEST DESIGN

The following test design was used to evaluate the performance objectives, in Tables 5-1, 5-2 and 5-3.

Table 5.1. Test Design for PO1 to PO3

Items	Pump virtual meter	Valve virtual meter	Fan virtual meter
Hypothesis	Pump water flow can be virtually measured from VFD power, frequency, and pump head within accuracy of 99. 5% at 95% confidence compared with an ultrasonic meter.	Water flow through a coil can be virtually measured from the valve position and the pressure drop over both the coil and control valve within accuracy of 99.5% at 95% confidence compared with a conventional flow meter.	Fan airflow can be virtually measured from VFD power, frequency, and fan head within 98% accuracy at 95% confidence compared with a conventional air flow station.
Independent variable	The use of pump virtual meter	The use of valve virtual meter	The use of fan virtual meter
Dependent variable(s)	Actual pump water flow rate, VFD power, frequency, and pump head	Actual water flow rate through the coil, control valve position, pressure drop across the valve/coil.	Actual fan airflow rate, VFD power, frequency, and static pressure
Controlled variable(s)	Design of hydronic system, system setpoints	Design of hydronic system between the DP transducers, system setpoints	Design duct and fan system, system setpoints
Test Design	Compare measured and virtually calculated water flow rates	Compare measured and virtually calculated water flow rates	Compare measured and virtually calculated airflow rates

Table 5-1. Test Design for PO1 to PO3 (continued).

Items	Pump virtual meter	Valve virtual meter	Fan virtual meter
Pre-Test Phase	1. Install accessories, including: a) Portable ultrasonic flow meter is installed to calibrate and validate virtual meter; b) VFD power and frequency are obtained from VFD panel; c) Pressure differential transducer is installed to measure pump head at the inlet and outlet of the pumps; 4) VFDs are installed on condensing water and primary chilled water pumps (detailed retrofit list see Appendix D). 2. Program flow calculation algorithms.	1. Install accessories, including: a) Portable ultrasonic water flow meter is installed to calibrate and validate virtual meter; b) Pressure differential transducer is installed to measure pressure loss across the valve and coil (detailed retrofit list see Appendix D). 2. Program flow calculation algorithms.	1. Install accessories, including: a) Calibrate conventional airflow meters that have been installed in AHUs; b) VFD power and frequency are obtained from VFD panel; c) Pressure differential transducer is installed to measure fan static pressure(detailed retrofit list see Appendix D). 2. Program flow calculation algorithms.
Test Phases	1. Calibration - determine the relationship between the water flow and VFD power, frequency, and pump head. 2. Validation: compare the actual water flow and virtually calculated water flow.	1. Calibration - determine the relationship between the water flow and valve position and pressure drops across the valve. 2. Validation: compare the actual water flow and virtually calculated water flow.	1. Calibration - determine the relationship between the airflow and VFD power, frequency, and fan head. 2. Validation: compare the actual air flow and virtually calculated air flow.
Data Collection	All variables are recorded by the project team every one-minute, sometimes one-second, for the testing period using the existing building automation system in the demonstration site. The test period was up to a few week (including full and partial flow conditions.)	All variables are recorded by the project team every one-minute for the testing period using the existing building automation system in the demonstration site. The test period can be up to 5 days.	All variables are recorded by the project team every one-minute for the testing period using the existing building automation system in the demonstration site. The test period can be up to 5 days.

Table 5.2. Test Design for PO4-PO9.

Items	PO4 OA intake	PO5 Reheat usage	PO6 Fan controls	PO7/8/9 Pump controls
Hypothesis	The cooling coil consumption can reflect outdoor airflow intake under given supply airflow, supply and return air temperatures as well as fan power.	The supply airflow rate can reflect the minimum airflow setting for all the terminal boxes served by an AHU. Too high airflwo rate at low OA temp reflects reheat wastes.	The SCC, the ratio of fan head to the airflow squared, can be represented by the overall resistance of the air distribution system, which is determined by duct system resistance.	The SCC, the ratio of pump head to the water flow squared, can be represented by the overall resistance of the piping distribution system, which is determined by pipe system resistance.
Independent variable	The use of PDD algorithm.	The use of PDD algorithm.	The use of PDD algorithm.	The use of PDD algorithm.
Dependent variable	Cooling coil cooling energy.	Supply air flow rate in each AHU.	SCC of duct systems.	SCC of pipe systems.
Controlled variable	OA damper position or return fan speed.	Water supply temperature; water loop differential pressure; terminal box minimum airflow setpoint.	AHU damper positions; Balancing damper positions; Duct static pressure set point; Supply air fan speed.	Coil control valve positions; Balancing valve positions; Differential pressure set point; pump speed.
Test Design	Test whether alarms are enabled after generation of faulty outdoor air intake.	Test whether alarms are enabled after generation of high minimum airflow rate for all the terminal boxes served by the AHU.	Test whether alarms are enabled after generation of faulty damper positions.	Test whether alarms are enabled after generation of faulty valve positions.
Pre-test phase	Valve flow meter is installed.	Virtual fan airflow meter is installed.	Virtual fan airflow meter is installed.	Virtual pump water flow meter is installed.
Test Phase	The fault-free cooling coil cooling consumption function is built up and compared with measured value.	The fault-free airflow rate v.s. time schedule correlation is built up and compare with measured value.	The fault-free SCC function is built up and compare with measured data.	The fault-free SCC function is built up and compare with measured data.
Data Collection	All variables are recorded by the project team every one-minute for three days.	All variables is recorded by the project team every one-minute for three days.	All variables is recorded by the project team every one-minute for three days.	All variables is recorded by the project team every one-minute for three days.

Table 5.3. Test Design for PO10-PO13.

Items	Energy reduction	Comfort	Easy-to-use interface
Hypothesis	Energy will be reduced by 16% after the installation of detectors based on virtual flow meters are implemented.	The number of comfort trouble calls will not increase after the PDD and control optimizations are in place.	The PDD is accepted and adopted for continued use by facility operators.
Independent variable	The use of PDD algorithms	The use of PDD algorithms	The use of PDD algorithms
Dependent variable(s)	Electrical and gas consumption	Trouble Call logs	-
Controlled variable(s)	Controlled variables will include the intended use and occupancy of the space, occupancy schedules, major HVAC equipment, etc. These are all items that are not intended to be changed between the baseline and demonstration phases.	Controlled variables will include the intended use and occupancy of the space, occupancy schedule, major HVAC equipment, etc. These are all items that are not intended to be changed between the baseline and demonstration phases.	-
Test Design	Compare the electrical and gas consumption before and after implementation of the PDD	Compare the volume of call logs before and after the use of the PDD	Develop a user survey form to quantify the user satisfaction rate.
Pre-Test Phase	None, since both electrical and gas meters are installed and connected with the building automation system.	None, since the trouble call log system is in place.	Design the survey form.
Test Phases	1. Measure baseline energy consumption (already started after the kick-off call on 11/6). 2. PDD implementation. 3. Measure energy consumption after any necessary improvements have been made.	1. Collect the space air temperature for before and after comparison. 2. PDD implementation.	1. Invite the participants to fill out the survey form. 2. Improve the interface design until the satisfaction rate reaches 80% if needed.

5.2 BASELINE CHARACTERIZATION

- Reference Conditions include:
  - Building operating and occupancy schedules
  - Weather conditions, such as monthly average outdoor air temperature, heating degree days and cooling degree days
  - Indoor air temperature and humidity, and indoor air quality
  - Selected system operating conditions
    - The outdoor air flow rate and damper position
    - The AHU supply air temperature and cooling coil valve position
    - The supply air duct static pressure and supply air fan speed
    - The terminal box minimum and maximum airflow settings
    - The water pipe differential pressure and pump speed in secondary hot water and chilled water loops
    - The condensing water temperature and cooling tower fan speed
  - Building electricity and natural gas consumption
- Baseline Collection Period:
  - We have collected energy baseline data (including electricity and natural gas) since November 6, 2014. The original system operation was not altered until the beginning of 2016. We had a total of 14 months for baseline data collection, which would provide us enough redundancy to ensure data quality.
- Existing Baseline Data:
  - Building operation hours were obtained from the BAS and the occupancy schedules were collected from the building manager.
  - Outdoor condition data were downloaded from a nearby weather station.
  - Indoor air temperature and humidity and outdoor airflow data were collected based on the current control using BAS.
  - Energy consumption was measured by the existing electricity and natural gas meters.
- Baseline Estimation:
  - The building operation and outdoor air conditions during the baseline collection period were used to establish baseline costs.
  - The desired baseline indoor conditions are defined as
    - The indoor air temperature ranges from 70°F to 75°F in general.
    - The indoor air relative humidity ranges from 30% to 60% (ASHRAE 2015).
    - The outdoor air intake is determined by ASHRAE Standard 62.1 (ASHRAE 2010a) to maintain the indoor CO_2 level at 700PPM above the outdoor air CO_2 level.
  - The baseline energy consumption data would use the actual energy data if the indoor conditions satisfied the defined baseline conditions. If the indoor conditions were less than satisfactory, the energy consumption would be adjusted to accommodate the

impacts of the indoor condition corrections. The adjustment did not occur since the indoor conditions always satisfied the baseline conditions during collection periods.

  - After the improvements, the energy consumption would be adjusted before the savings calculations if the actual building operations and outdoor air conditions were different from the reference conditions during the baseline data collection. The regressions of energy consumption versus outdoor air temperature were generated to take into account the weather impacts.

- Data Collection Equipment:
  - Building energy consumption, including electricity and natural gas, was collected using the existing meters for utility charge purposes.
  - The indoor air conditions, including space air temperature and humidity ratio and outdoor airflow, as controlled variables, were collected based on the previous control strategies and were validated by the existing sensors, hobo loggers, and TSI meters for a short period.
  - The outdoor air conditions were obtained from weather station data.

5.3 DESIGN AND LAYOUT OF TECHNOLOGY COMPONENTS

- System Design: The demonstration project covers all 13 AHUs, one chilled water system, and one hot water system (see Appendix C for HVAC system summary). Overall, we have installed 24 virtual fan air flow meters on 13 supply air fans and 11 return air fans, 13 virtual valve flow meters on 13 AHU cooling coil valves, and 11 virtual pump flow stations on three primary chilled water pumps, three secondary chilled water pumps, three condensing water pumps and two secondary hot water pumps. To facilitate the virtual pump flow meter installations, we also installed six VFDs on the three condensing water pumps and three primary chilled water pumps (see Appendix D for HVAC system implementation plan). However, the VFDs were set at 60Hz since the facility was not ready to move from a primary/secondary loop to a variable primary- only loop due to consistent problems the chillers were having.
  - The chilled water system includes two electrical chillers and provides the chilled water to the cooling coils of the 13 AHUs. The chilled water system is a decoupled loop system, with three constant speed pumps in the primary loop and three variable speed pumps in the secondary loop. The condensing water loop has three constant speed pumps and two cooling towers, each with variable speed fans. Virtual pump flow meters were installed on three primary pumps, three secondary pumps, and three condensing water pumps, along with the PDD installation to identify the pump speed control faults. However, since the chilled water loop and condensing water loop were not converted to variable flow primary and condensing water loops, the use of the virtual flow meter on the primary chilled water pumps and condensing water pumps was limited.
  - The hot water system includes two natural gas boilers and provides the hot water to the preheating coil of the thirteen AHUs and the reheat coils of all terminal boxes. The hot

water system is a decoupled loop system with three constant speed pumps in the primary loop and two variable speed pumps in the secondary loop. Virtual pump flow meters were installed on two secondary pumps. The PDD was installed on the hot water system to identify the pump speed faults.

– The building is served by 13 AHUs, each with a cooling coil, a preheating coil, a supply air fan, a return air fan (excluding AHU12 and AHU13), and an outdoor intake path with a control damper and an outdoor air fan (excluding AHUs 2-5 and AHU13). Virtual fan airflow meters were installed on all supply fans and return fans. Virtual valve water flow meters were installed on all cooling coil valves. The PDDs were installed to identify the fan speed and damper-related faults using the airflow data and the outdoor air-related fault using the virtual valve energy data.

- Components of the System:
  – Virtual fan/pump flow meters: The virtual fan airflow or pump water flow rate was obtained from the measured fan or pump head and the VFD output power and frequency along with an installed fan/pump efficiency curve and an installed motor efficiency curve. As shown in Figure 2-1, the VFD power or frequency data is directly obtained through the VFD without any sensors and the fan or pump head is measured by a pressure transducer. Since the VFD output voltage is exactly correlated to the VFD output frequency, the VFD output voltage was calculated using the correlation rather than what was measured. A calibration process to obtain the installed fan/pump and motor efficiency curves was carried out onsite by the project team, as shown in Figure 5-1. We set up data logging in BAS for fan/pump speed (VFD output frequency), fan/pump heads, and motor power signals, and in portable flow measurement devices at one-minute intervals for up to 24 hours. Temporary airflow/water flow rates through the supply and return fans and the pumps were measured by multiple-point measurements using air velocity sensors and the water flow rate was measured by a portable ultrasonic flow meter during the calibration.

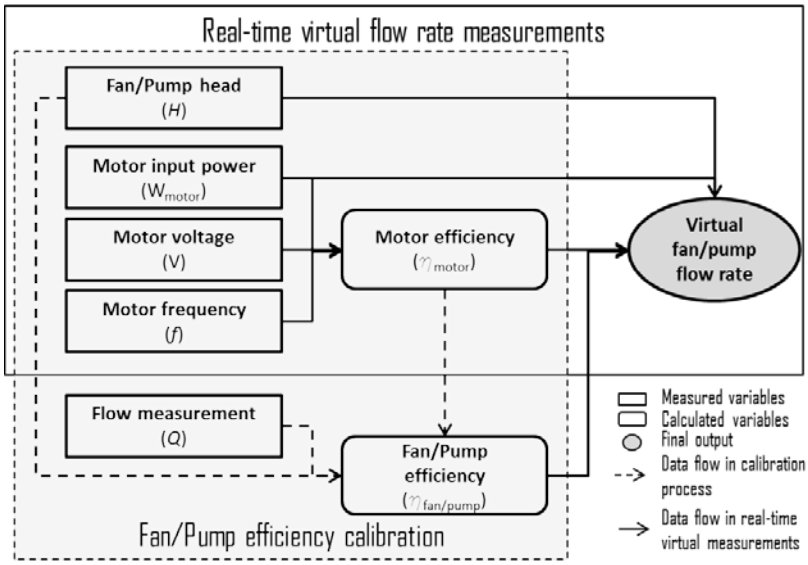

Figure 5.1. Fan/pump Efficiency Calibration Process.

– Virtual valve flow meter: The water flow through the valve was obtained based on the valve position, the pressure drops over the valve and coil, and an installed valve characteristic curve that needed to be calibrated for the valves. As shown in Figure 2-2, the valve position was obtained from the valve command and the pressure drop was measured by a pressure transducer. The calibration process for the installed valve characteristic curve was carried out onsite by the project team during the valve installation. We set up data logging in BAS for valve command (x), which is used to represent the valve stem position (z) and the DP across the loop ($\Delta P_{L,z}$) and in a portable ultrasonic meter for the water flow rate through the valve (Q_z) at one-minute intervals for up to 24 hours. Then the installed valve characteristic curve ($F_{L.x}$) at different valve stem positions (z) was calculated using Equation (5-1).

$$F_{L.x}(z) = \frac{Q_z}{\sqrt{\Delta P_{L,z}}} \qquad (5\text{-}1)$$

- System Depiction:
  – Virtual pump flow meters on the chilled water system: As shown by the red circles in Figure 5-2, nine virtual pump flow meters were installed on the three condensing water pumps, three primary chilled water pumps, and three secondary chilled water pumps.

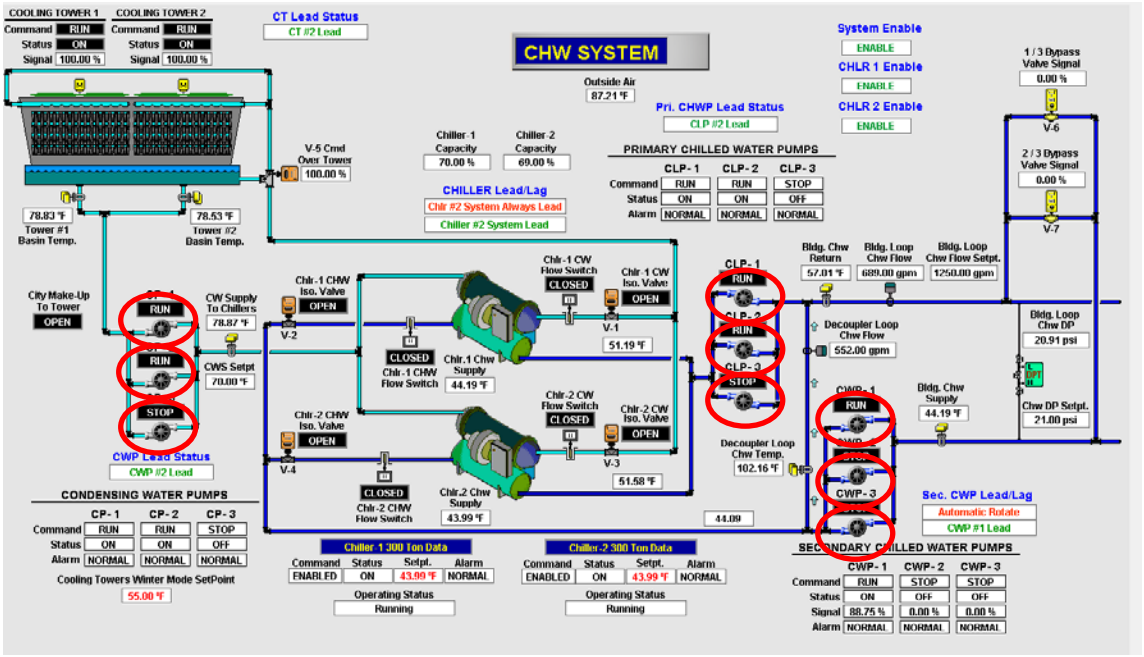

Figure 5.2. Virtual Pump Flow Meter Installation on the Chilled Water System.

– Virtual pump flow meters on the hot water system: As shown by the red circles in Figure 5-3, two virtual pump flow meters were installed on two secondary hot water pumps.

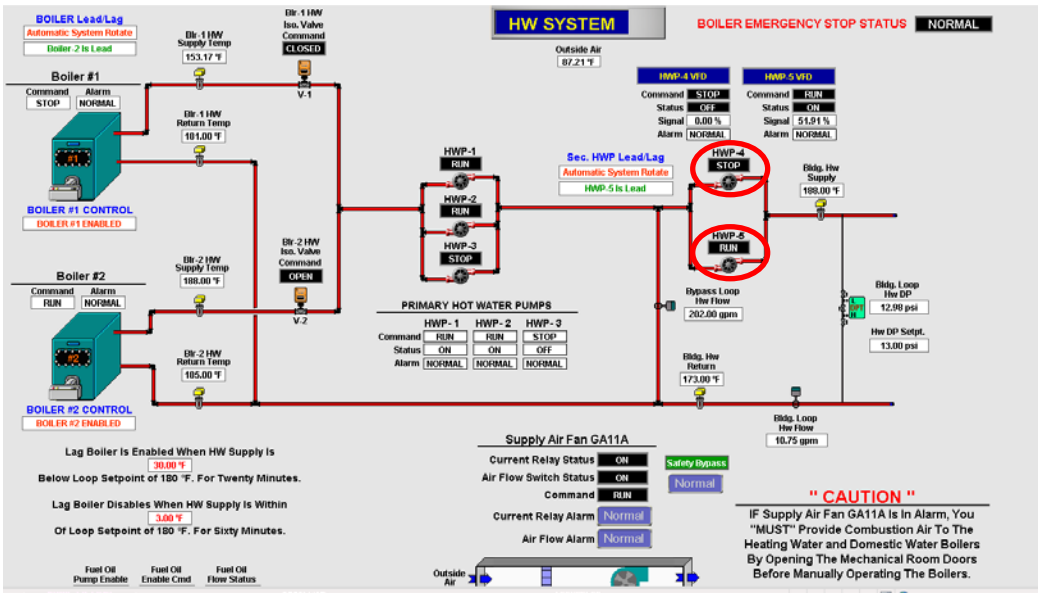

Figure 5.3. Virtual Pump Flow Meter Installation on the Hot Water System.

– Virtual fan flow meter and virtual valve meters on the AHUs: two virtual fan flow meters on both supply and return air fans and one virtual valve flow meter on the cooling coil control valve were installed in each of 13 AHUs except AHUs 12 and 13 which do not have a return air fan. The changes on AHU-1 are shown in Figure 5-4 as an example. All other AHUs had a similar configuration.

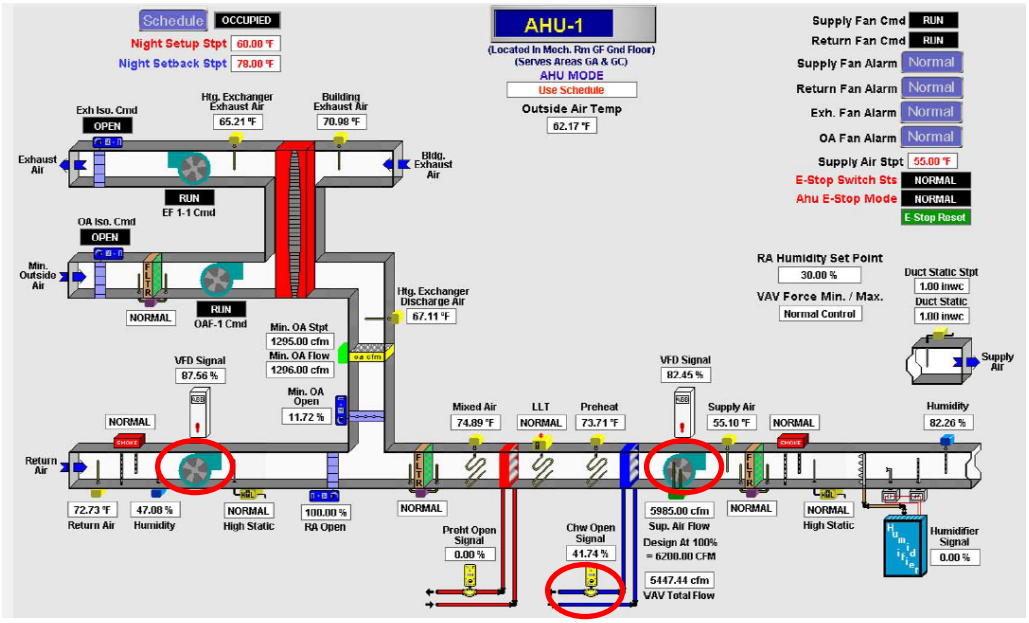

Figure 5.4. Virtual Fan Flow Meter and Valve Flow Meter Installation on AHU1.

- System Integration: See Appendix D of the HVAC system implementation plan.
  - Virtual fan airflow meters

- Differential pressure transducers were installed across both supply air fans on all 13 AHUs and return air fans for 11 AHUs, as shown in Figure 5-5(a), for fan head measurement.
- Fan motor power and frequency signals were wired from VFD drives to the BAS for the virtual airflow calculations.
- New BAS panels were installed to accommodate additional control inputs, as shown in Figure 5-5(b).

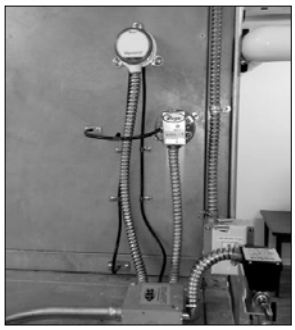

(a) Installed air differential pressure transducer

(b) Installed new BAS panel to accommodate additional signal communication

Figure 5.5. Permanent Equipment Installation for Virtual Fan Flow Meters.

- For virtual air flow meter calibration and validation, a physical flow measurement device needed to be in place. To have a full range of calibration, one-time flow measurement, as was done in the TAB process, was not adequate. Thus, a custom bracket was designed and built for this project as shown in Figure 5-6. Multiple TSI Alnor Air Velocity probe and transducers (8455) were selected. The device has an accuracy of ±0.5% of full scale of the selected range.

(a) Available holes for traverse measurements

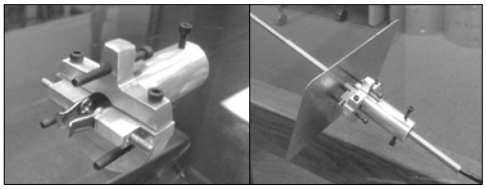

(b) Custom design and built bracket for portable yet extended period airflow measurements

(c) Installed brackets with holding velocity probes

(d) Velocity probe transducer in custom built case

Figure 5.6. Temporary Velocity Probe Installation for Virtual Fan Flow Meters.

- Virtual fan flow rate calculation blocks were also programmed in the BAS, shown in Figure 5-7. Figure 5-7 also shows related fault detections using the calculated virtual flow rate.

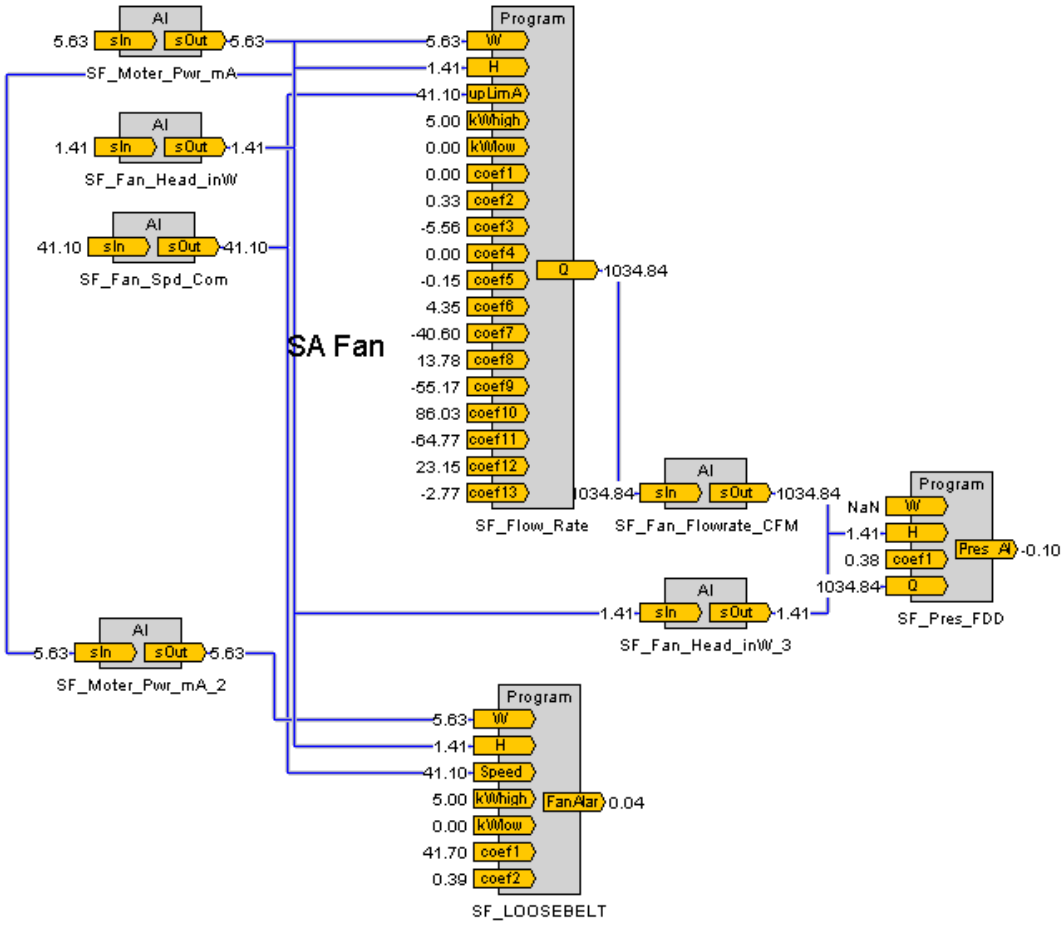

Figure 5.7. Virtual Fan Flow Rate Calculation and Associated PDD blocks in the BAS Monitoring System.

– Virtual valve flow meters

- Differential pressure transducers were installed across the cooling coil valves in 13 AHUs, shown in Figure 5-8.
- Valve command from the BAS was used for virtual flow calculations.
- For virtual valve flow meter calibration and validation, an ultrasonic meter was installed temporarily to obtain the data for valve characteristic curve calculations and virtual flow validations, shown in Figure 5-9.
- The supply water temperature and return water temperature sensors were installed across the cooling coils of 13 AHUs for cooling coil energy calculations. The virtual valve flow rate calculation blocks and associated cooling energy calculation block and the PDD blocks that use the virtual valve flow rates were also added in the BAS, shown in Figure 5-10.

Figure 5.8. Permanent Water DP Installation for Virtual Valve Flow Meters.

Figure 5.9. Temporary Installed Ultrasonic Meter and Its Accessories.

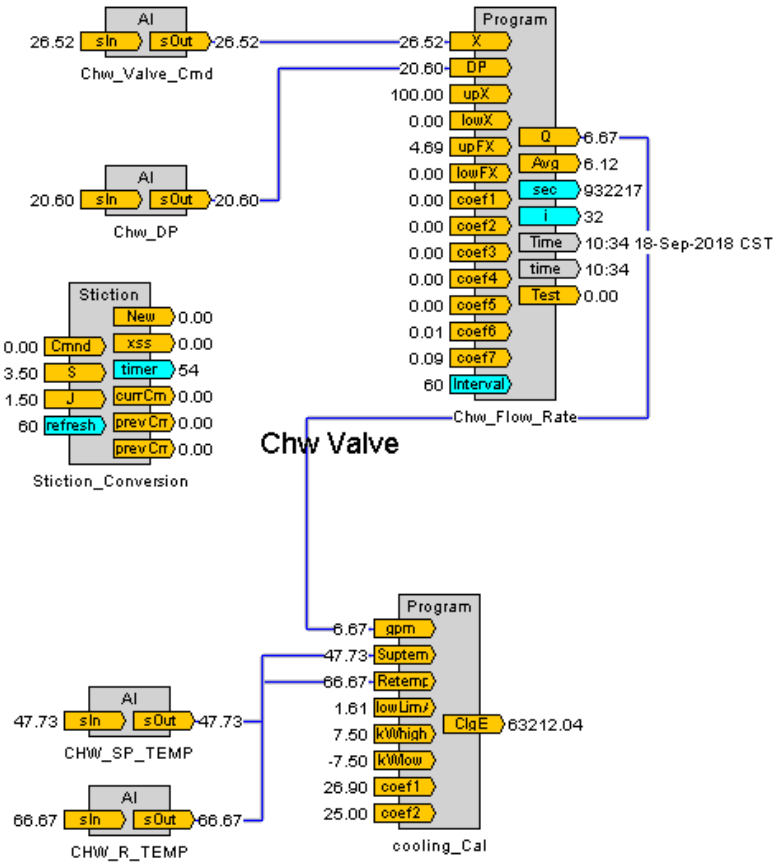

Figure 5.10. Virtual Valve Flow Rate Calculation and Associated PDD Blocks in the BAS Monitoring System.

– Virtual pump flow meters

- VFDs were installed on three condensing water pumps and three primary chilled water pumps, as shown in Figure 5-11.
- Differential pressure transducers were installed across pumps on three chilled water primary pumps, three chilled water secondary pumps, three chilled water condensing pumps and two hot water secondary pumps, as shown in Figure 5-12.
- Pump motor power and frequency signals were also wired from VFD drives to the BAS for the virtual pump flow calculations.
- For virtual pump flow meter calibration and validation, a physical flow measurement device--an ultrasonic meter—needed to be in place, as shown in Figure 5-13.
- The pump flow rate calculation blocks were added in the BAS as shown in Figure 5-14, with three inputs, including pump head, pump power and pump frequency, and a few coefficients to calculate the flow rate as an output. The PDD blocks that use the virtual pump flow rate were also programmed and shown in Figure 5-14.

Figure 5.11. Permanent VFD Installation on Condensing Pumps.

Figure 5.12. Permanent Differential Pressure Transducer Installation for Virtual Pump Flow Meters.

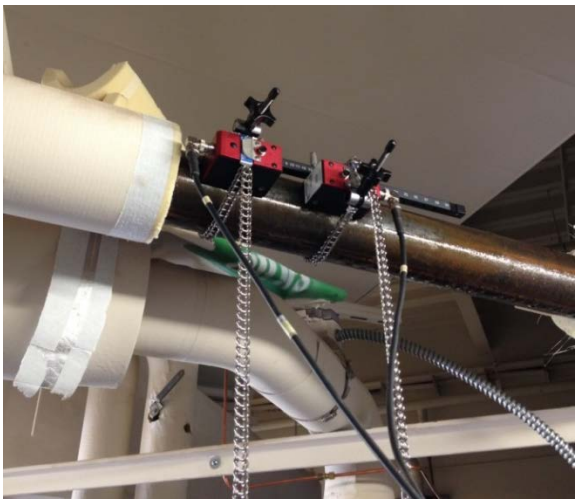

Figure 5.13. Temporary Ultrasonic Meter Installation on the Secondary Chilled Water Loop.

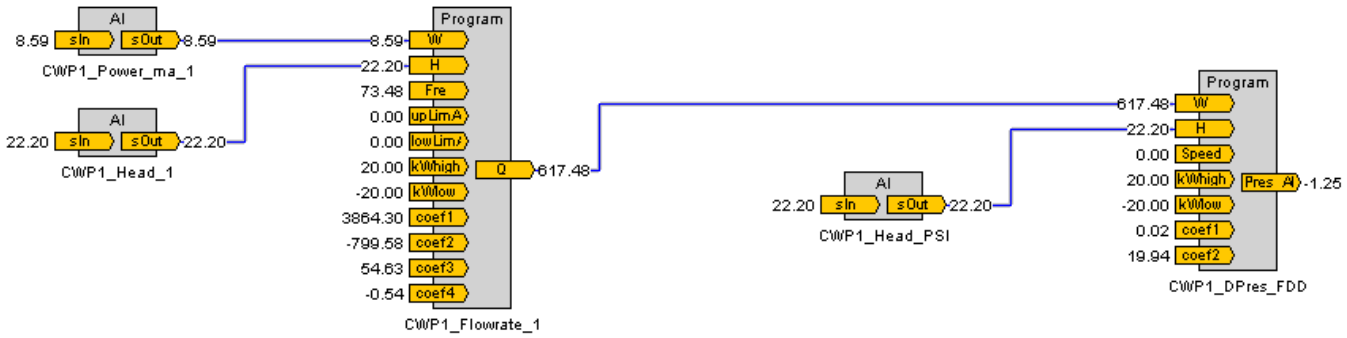

Figure 5.14. Chilled Water Flow Rate Calculation Blocks in the BAS.

- System Controls:
  - Unless inefficient operations were detected by the PDD and then corrected by the project team with consensus from the building operators, the control sequences remained unchanged with corrected control setpoints.

5.4 5.4 OPERATIONAL TESTING

- Operational Testing of Cost and Performance: This phase included a six-month virtual meter test, four-month PDD test, and one-year energy savings test. The virtual meter and PDD tests were conducted during normal building operations with created faults. The one-year energy consumption data after the PDD test were used for comparison with the energy baseline data for the energy savings test.
  - The virtual meter tests included the virtual fan airflow meter tests on 13 AHU supply fans and 11 AHU return fans, the virtual valve water flow meter tests on 13 AHU cooling coils, the virtual pump water flow meter tests on three primary chilled water pumps, three secondary chilled water pumps, three condensing water pumps and two secondary hot water pumps.
    - For the virtual fan/pump flow meter, the airflow/water flow, fan/pump head, and VFD power and frequency were measured to develop the coefficients in a virtual flow calculation formula during the calibration process, and then the flow calculated using the identified formula was compared with the measured flow to validate the installed virtual meter.
    - For the valve flow meter, the water flow, pressure drop, and valve position were measured to develop the coefficients in the virtual flow calculation formula during the calibration process, and then the flow calculated using the identified formula was compared with the measured flow to validate the developed virtual meter.
  - The PDD test included the pump and valve-related fault detection for three chilled water primary pumps, three chilled water secondary pumps, three condensing pumps, and two hot water secondary pumps, fan and damper-related fault detection for 13 AHU supply fans and 11 AHU return fans, outdoor intake related fault detection for 13 AHUs, and reheat-related fault detection for 13 AHUs. We commissioned all the systems in the building first to create fault-free operations as a reference to be built in the PDD.

Then, faults were created to test the effectiveness of the PDD. At the completion of the PDD test, the system was continuously monitored for 12 more months to verify whether the PDD could detect possible performance deteriorations.

- For the pump and valve-related fault detection, the pump head and water flow relationship were developed under fault-free conditions. One fault, such as a partially closed valve, was created to verify the pump head offset from the reference pump head calculated by this relationship to test the effectiveness of the PDD. The pump performance was evaluated by comparing the power usage before the PDD installation with the data after the completion of the PDD test.
- For the fan and damper-related fault detection, the fan head and air flow relationship were developed under fault-free conditions. One fault, such as a partially-closed damper or a high static pressure setpoint, was created to verify the fan head offset from the reference fan head calculated by this relationship. The fan performance was evaluated by comparing the power usage before the PDD installation with the usage after the completion of the PDD test.
- For the outdoor air intake fault detection, in general, the ideal outdoor air intake is determined by the number of occupants based on ASHRAE Standard 62.1. Since the outdoor air intake in the demonstration building is controlled based on a fixed set point in each unit, the reference cooling coil energy model was developed based on the supply airflow rate, outdoor air flow rate and outdoor air temperature based on the measured data. Then one fault, such as a high outdoor air setpoint or stuck outdoor air damper, was created to verify the projected cooling coil energy reference model.
- For reheat fault detection, the terminal box minimum airflow setpoint was commissioned first. The fault-free minimum supply airflow ratio was developed as a function of time of day based on the measured supply airflow rate in each AHU through the virtual fan airflow meter. One fault, such as increasing the terminal box minimum airflow setpoint, was created and the actual airflow ratio was compared with the fault-free airflow rate ratio.

– Building energy test to validate the robustness of the PDD. The system faults were automatically detected by the PDD and were corrected by the operator after detection to maximize energy savings. Energy consumption was measured using four-year utility bills to validate the energy savings with the PDD.

- Modeling and Simulation: the models used in virtual flow calculations and the PDD are introduced separately in this section.

  – Virtual flow calculation models:

  Both the virtual pump and fan flow meters work under the same principle. Power consumption is determined by useful mechanical work imparted into fluid (product of head and flow rate), fan/pump efficiency and motor efficiency. Theoretically, the fan/pump efficiency is a function of the ratio of power to head to the power of 1.5, while motor efficiency is a function of power, frequency, and voltage. Practically, head is measured by a pressure differential sensor while power and frequency are obtained through the existing variable frequency drive (VFD) and voltage is obtained based on its correlation with frequency.

The motor equivalent circuit, defined by six circuit parameters (IEEE. 2004, Wang, Song et al. 2013), can be applied to determine the motor efficiency under different power, frequencies and voltage. For the improved approach, using calibrated motor and fan/pump efficiencies, the flow rate can be obtained, shown in Equation (2-5) or (2-7) in Section 2.2 (Wang, Kiamehr et al. 2016).

The **virtual valve meter** uses existing cooling coil control valve operational variables to indirectly obtain the water flow rates. Theoretically, the pressure drop through a valve is determined by valve position and flow rate for a given valve, which is defined by a valve characteristic curve. The pressure drop is measured by a water pressure differential sensor and the valve position is obtained by valve command through a BAS and for the improved approach corrected to reflect the true valve positions. The valve characteristic curve was obtained through a calibration process. Therefore, the flow rate is obtained by pressure drop and valve position as well as calibrated valve curve (Song, Swamy et al. 2011, Swamy, Song et al. 2012, Song, Joo et al. 2012a, Song, Wang et al. 2012b), as described in Equation (2-2) in Section 2.1.

– Models adopted in the PDD:

Pump and valve related fault detection: The SCC of a water loop is correlated to the pump head (H), the pump water flow rate (Q) and the loop pressure setpoint (H_{sp}), as described in Equation (5-2). The fault-free SCC is used as a reference to compare with operational SCC and the difference between the two is used as an indicator to detect faults.

$$H = SCC \cdot Q^2 + H_{sp} \tag{5-2}$$

Fan and damper related fault detection: The SCC of a ductwork is correlated to the fan head (H), the fan airflow rate (Q), and the duct static pressure setpoint (H_{sp}), as described in Equation (5-3). The fault-free SCC is used as a reference to compare with operational SCC and the difference between the two is used as an indicator to detect faults.

$$H = SCC \cdot Q^2 + H_{sp} \tag{5-3}$$

Fan loose belt fault detection: The VFD output power is correlated to the VFD output frequency, as described in Equation (5-4). The fault-free VFD output power is used as a reference to compare with actual VFD output power and the difference between the two is used as an indicator to detect the loose belt faults.

$$W = a \cdot f^b \tag{5-4}$$

OA flow-related fault detection: Cooling coil load (q_{cc}) is the summation of the fan load (q_{fan}), space sensible cooling load (q_s), and latent cooling load (q_l) and terminal box reheat load (q_{rh}) and outdoor air cooling load, which is the product of air density (ρ), outdoor airflow rate (Q_{oa}) and the difference between outdoor air enthalpy (i_{oa}) and space air enthalpy (i_{rm}) , as shown in Equation (5-5). Therefore, the cooling coil load can be expressed as a function of supply airflow and outdoor airflow as well as outdoor air temperature and humidity. The reference fault-free cooling coil load is calculated using Equation (5-5) and desired control setpoints. The difference between calculated and measured cooling coil load indicates the fault (Song and Wang 2015).

$$q_{cc} = q_{fan} + \sum(q_s + q_l) + \sum q_{rh} + \rho Q_{oa}(i_{oa} - i_{rm}) \tag{5-5}$$

Hot water reheats related fault detection: Due to the lack of the precision in the temperature measurements for hot water supply and return, especially in summer when the reheat energy use is low and the fault detection is the most critical, we have adopted an alternative method to detect the reheat energy waste. The alternative method is to commission the terminal box minimum airflow setpoint first. The fault-free minimum supply airflow ratio is calibrated as a function of the time of the day. The function is used to calculate required minimum airflow ratio based on the time of the day. A higher measured minimum airflow ratio than the calculated one indicates the fault of too high of minimum supply airflow rate and therefore results in reheat energy waste.

5.5 SAMPLING PROTOCOL

- Data Collector(s): Graduate students in the OU BEE lab.
- Data Recording: Most (90%) of data were logged and achieved through the BAS. Some additional data were logged through portable data loggers if they were not available in the BAS.
- Data Description: Table 5-3 summarizes the data samples for each application and is followed by the detailed description of data samples.

Table 5.4. Data sample summary.

PO	Data sample	Meters or sensors
PO1/PO3	VFD output power and frequency Pump and fan head Fan or pump flow rate for calibration	VFD Pressure transducer Ultrasonic flow meter
PO2	Valve command Valve/coil pressure drop Valve flow rate for calibration	BAS Pressure transducer Ultrasonic flow meter
PO4	Valve virtual flow Chilled water supply and return temp	Virtual meter (PO2) Temperature sensors
PO5	Supply airflow in AHU	Virtual meter (PO3)
PO6	Fan head Fan airflow	Same in PO3 Virtual meter (PO3)
PO9	Pump head Pump flow	Same in PO1 Virtual meter (PO1)
PO10/11	Electricity consumption Natural gas consumption	Electrical meter Gas meter
PO12	Space temperature and occupants' feedback	Space thermostats Call logs

– The virtual fan airflow rate or pump water flow rate was calculated from the measured fan or pump head and the VFD output power or frequency along with the calibrated motor and fan/pump efficiency curves. As shown in Figure 2-1, the required sampling data to install the virtual flow meters and validate the accuracy of the flow meter are listed below. The sampling time of one minute was usually applied.

        - The VFD output power and frequency was directly obtained through the VFD control panel without any sensors.
        - The fan or pump head was measured by a pressure transducer, as shown in Figure 5-5 for the fan head and in Figure 5-12 for the pump head.
        - In order to calibrate the motor and fan/pump efficiency, a ultrasonic water flow meter was installed to measure the pump water flow rate, as shown in Figure 5-13, while six TSI Alnor Air Velocity probes and transducers (8455) were installed inside a duct section along with a custom bracket to measure the air velocity at multiple points, as shown in Figure 5-6, which was then converted to the airflow rate.
    - The water flow through the valve was obtained based on the valve position, the pressure drops over the valve and coil along with a calibrated valve characteristic curve. As shown in Figure 2-2, the operating data were recorded with a sampling time of one minute. The required sampling data were:
        - The valve position was obtained from the valve command.
        - The pressure drop was measured by a pressure transducer, as shown in Figure 5-8.
        - In order to calibrate the valve characteristic curve, a portable ultrasonic meter was installed to measure the water flow rate, as shown in Figure 5-9.
    - The system operating data for the PDD test were recorded at one-minute intervals for a minimum of three days including before and after the fault was introduced. The required sampling data are listed below:
        - For the OA flow-related fault detection, the cooling coil valve flow rate was calculated by the developed virtual valve flow meter along with the chilled water supply and return temperature.
        - For the reheat coil-related fault detection, the AHU supply airflow rate was measured by the developed virtual fan flow meter.
        - For the damper- and setpoint-related fan fault detection, the supply airflow rate was measured by the developed virtual fan flow meter along with the duct static pressure setpoint. For the loose fan belt, the VFD output power and frequency were obtained from the VFD control panel.
        - For the valve- and setpoint-related secondary pump fault detection, the pump water flow rate was measured by the developed virtual pump flow meter along with the loop pressure differential setpoint.
    - The building level electricity and natural gas usage were monitored using monthly utility bills as long as the demonstration was ongoing, including one year for the baseline and one year after improvement in the energy savings calculations.

- Data Storage and Backup: Logged data were downloaded from the BAS or the portable meters to two different hard drives for backup every two weeks.
- Survey Questionnaires: A PDD user interface survey was developed for the facility operators. However, the survey could not be successfully executed because we learned through the project that the facility operators should not be the end users of the technology.

Rather, experienced BAS contractors or potential PDD technology licensees/installers should be the end users of the technology. Therefore, we did not conduct this survey. No data were collected in this regard.

5.6 SAMPLING RESULTS

The demonstration building has multiple equipment for the same type, such as 13 single-duct AHUs, each with a VFD on the supply air fan and a control valve on the chilled water-cooling coil, and three secondary chilled water pumps and two secondary hot water pumps each with a VFD. Although we have implemented the technology in all the applicable equipment in order to obtain 16% of the whole building-level energy savings, in this section, we only show the data using one of the same type equipment as a representative.

5.6.1 Sampling results for the demonstration of virtual pump water flow meters:

1. VFD output power

Figure 5-15 shows the measured VFD output power for secondary chilled water pump 1 at one-minute interval for one week.

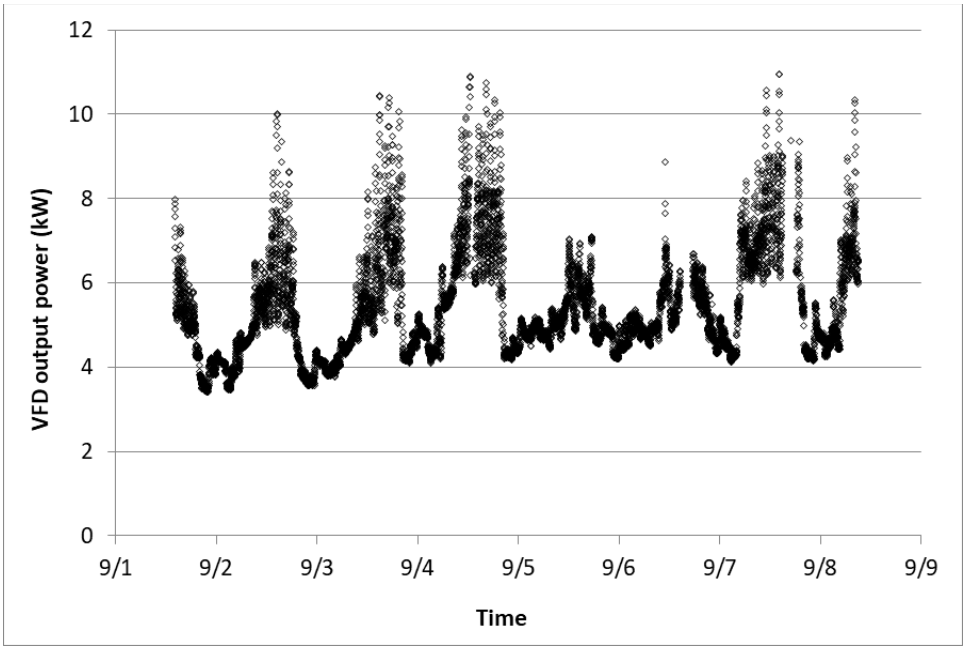

Figure 5.15. Measured VFD Output Power for Secondary Chilled Pump 1.

2. VFD output frequency

Figure 5-16 shows the measured VFD output frequency for secondary chilled pump 1.

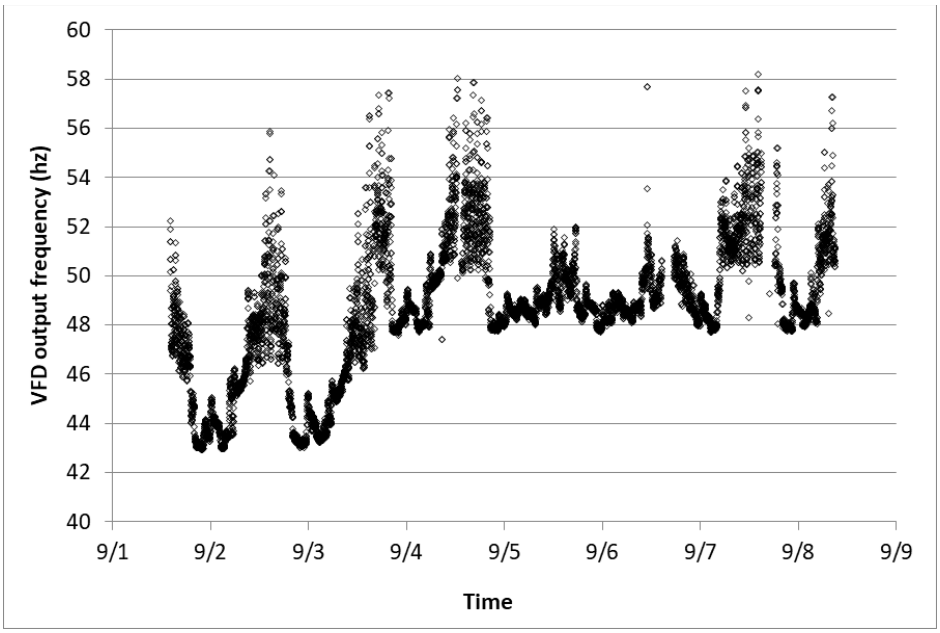

Figure 5.16. Measured VFD Output Frequency for Secondary Chilled Pump 1.

3. Pump head

Figure 5-17 shows the measured pump head for secondary chilled pump 1.

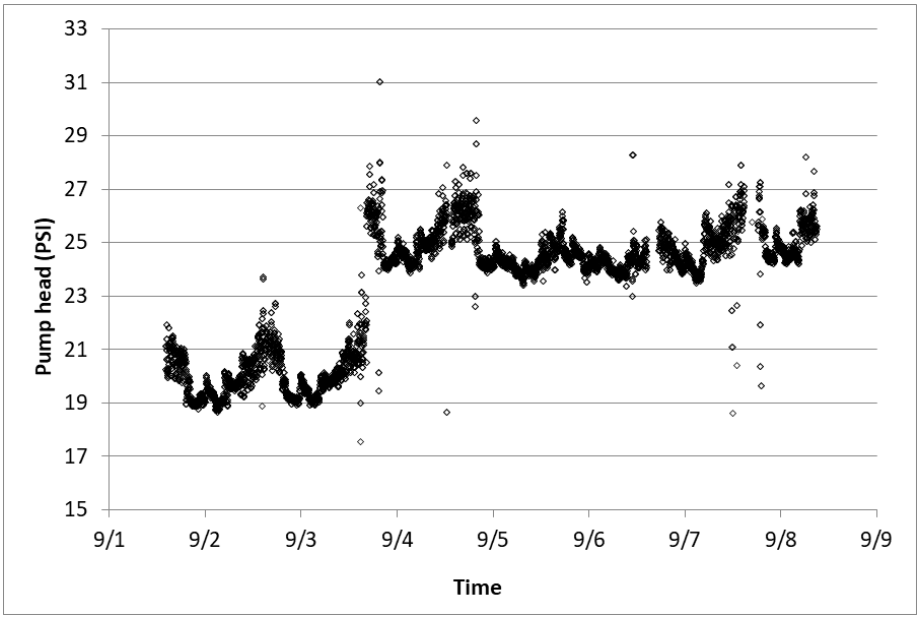

Figure 5.17. Measured Pump Head for Secondary Chilled Pump 1.

4. Pump water flow rate

Figure 5-18 shows the measured pump water flow rate for secondary chilled pump 1 by a portable ultrasonic water flow meter as shown in Figure 5-13.

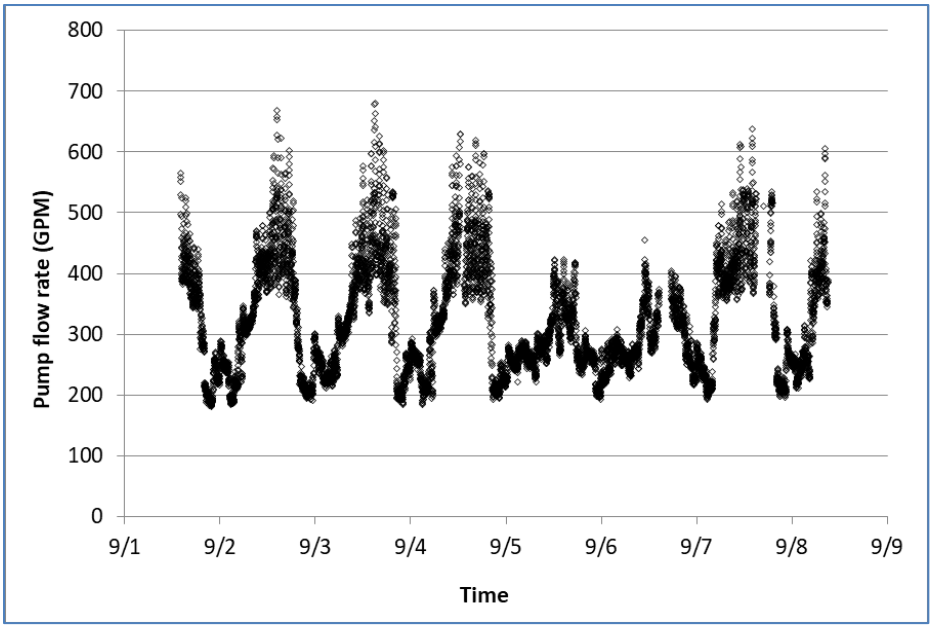

Figure 5.18. Measured Pump Water Flow Rate for Secondary Chilled Pump 1.

5.6.2 The virtual valve water flow meter

1. Pressure drop through the valve and coil

Figure 5-19 shows the pressure drop (differential pressure) through the cooling coil control valve and coil in AHU10 at one-minute intervals.

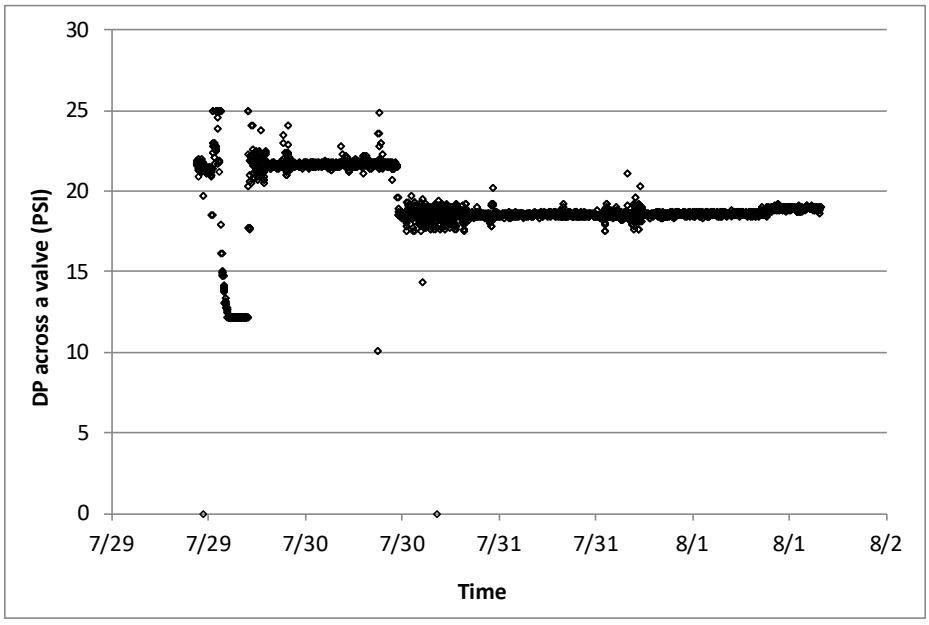

Figure 5.19. Measured Pressure Drop Across the Cooling Coil Control Valve in AHU10.

2. Valve command

Figure 5-20 shows the pressure drop (differential pressure) through the cooling coil control valve and coil in AHU10 at one-minute intervals. The cooling coil valve was overridden at 80% to purposely generate the variations of the water flow rate.

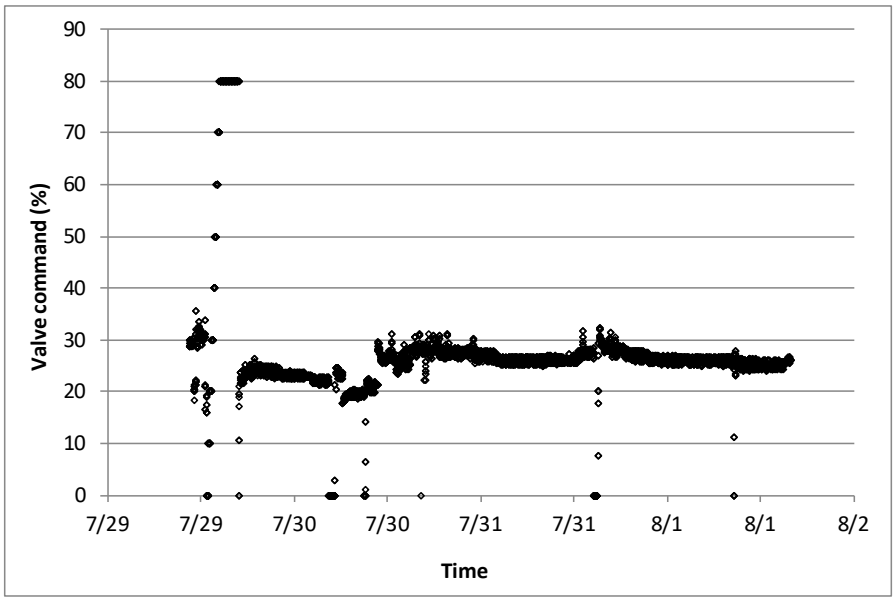

Figure 5.20. Valve Command Signal of the Cooling Coil Control Valve in AHU10.

3. Valve water flow rate

Figure 5-21 shows the measured chilled water flow rate through the cooling coil in AHU10 at one-minute intervals. This measurement was used for virtual valve flow meter validation. The water flow variations were generated by the control valve overrides shown in Figure 5-20.

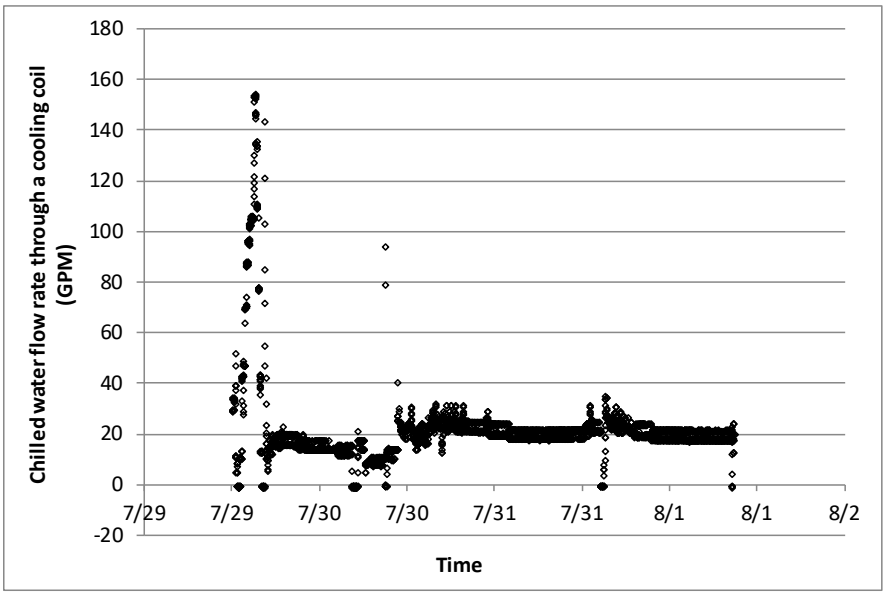

Figure 5.21. Measured Chilled Water Flow Rate through the Cooling Coil in AHU10.

5.6.3 Sampling results for the demonstration of virtual fan airflow meters

1. VFD output power

Figure 5-22 shows the measured VFD output power for the supply fan of AHU2 at one-minute intervals for one week.

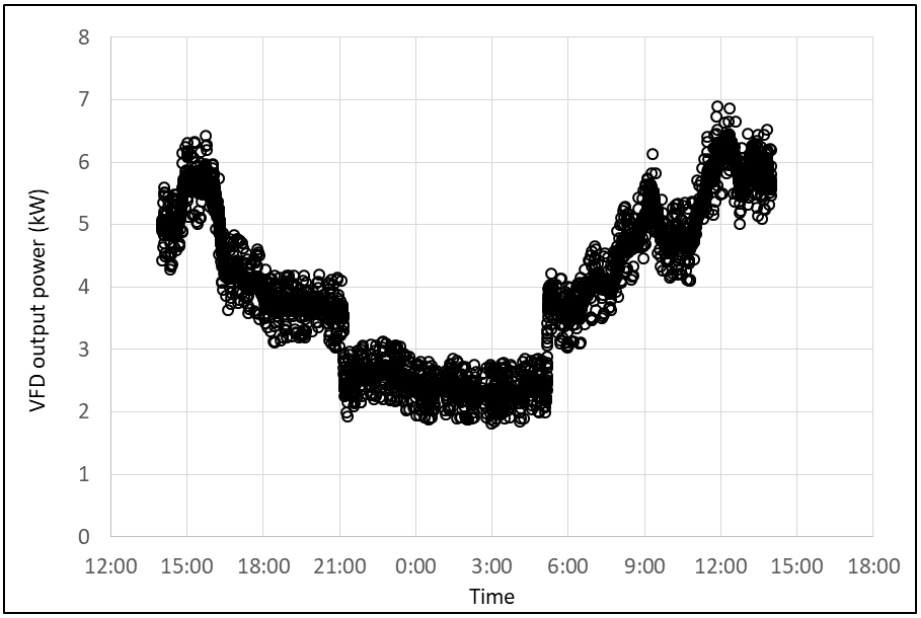

Figure 5.22. Measured VFD Output Power for the Supply Fan of AHU 2.

2. VFD output frequency

Figure 5-23 shows the measured VFD output frequency for the supply fan of AHU 2.

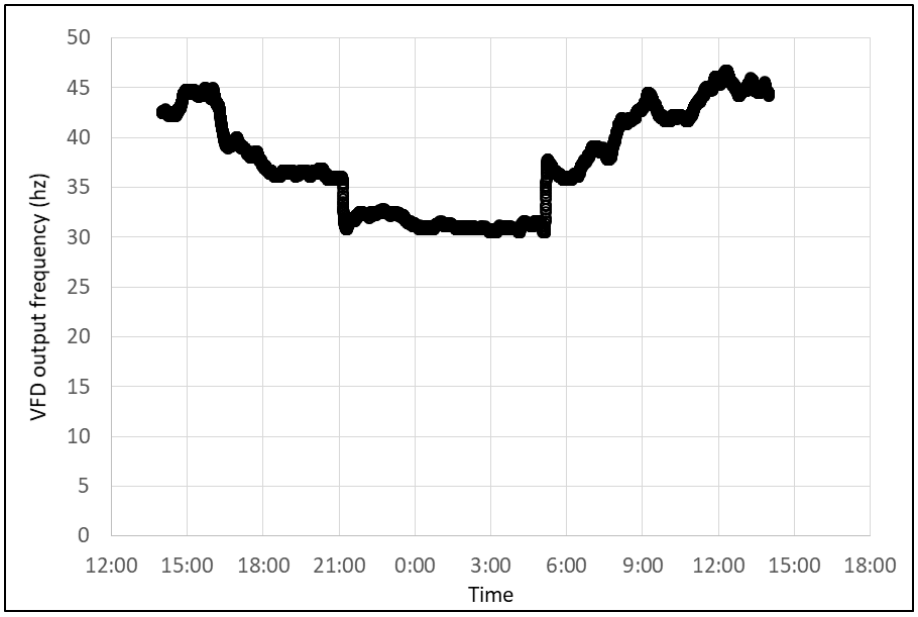

Figure 5.23. Measured VFD Output Frequency for the Supply Fan of AHU 2.

3. Fan head

Figure 5-24 shows the measured fan head for the supply fan of AHU2.

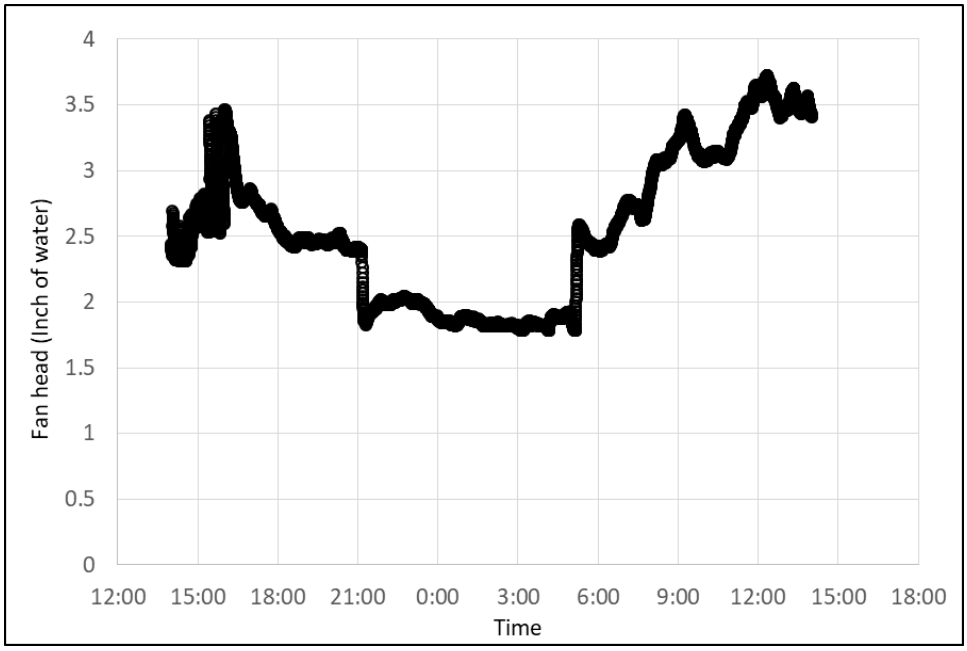

Figure 5.24. Measured Fan Head for the Supply Fan of AHU2.

4. Fan air flow rate

Figure 5-25 shows the measured fan airflow rate for the supply fan of AHU2 by multiple air velocity probes, as shown in Figure 5-6.

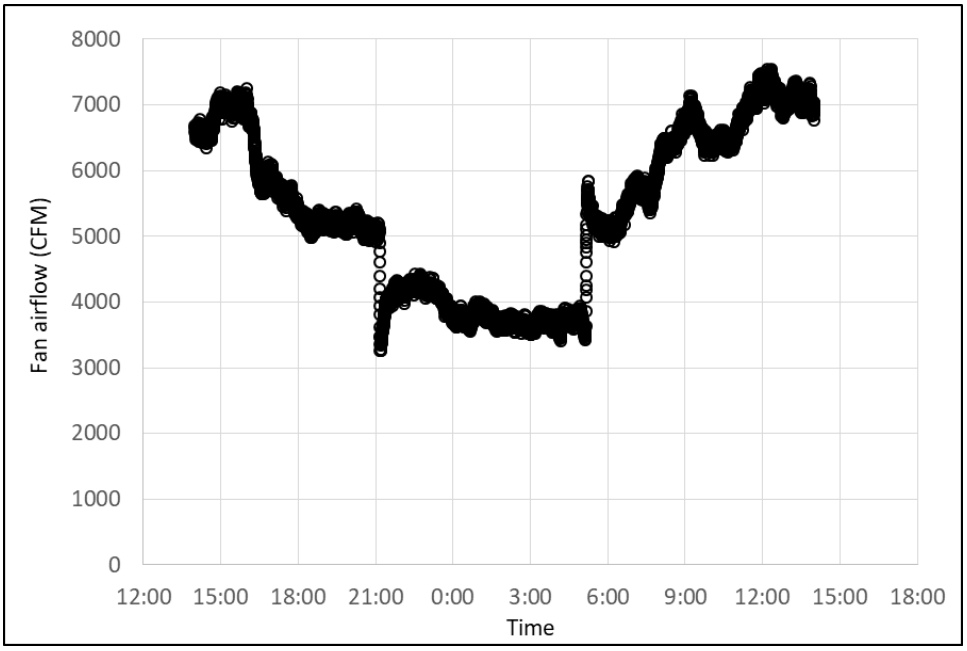

Figure 5.25. Measured Fan Airflow Rate for the Supply Fan of AHU2.

5.6.4 The PDD

1. OA fault

Figure 5-26 shows the measured chilled water supply and return temperature across the cooling coil in AHU13. The measurements were used for OA intake fault detection.

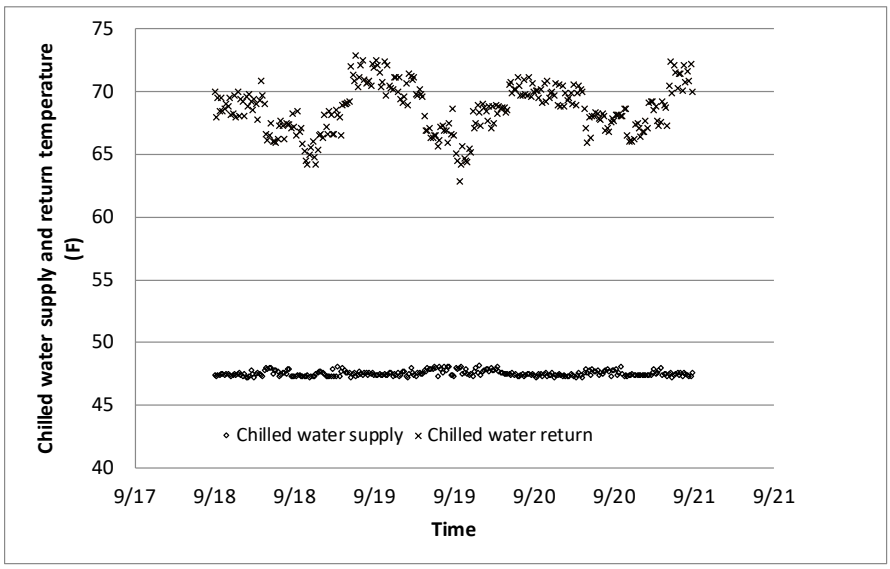

Figure 5.26. Measured Chilled Water Supply and Return Temperature in AHU13.

2. Reheat fault

The supply airflow rate was obtained by virtual meters. Figure 5-27 shows the virtual supply airflow rate for AHU 13. For comparison purposes, outdoor air temperature is also shown in Figure 5-27. It can be seen that the supply airflow rate was mainly impacted by the occupancy schedule rather than the outdoor air temperature.

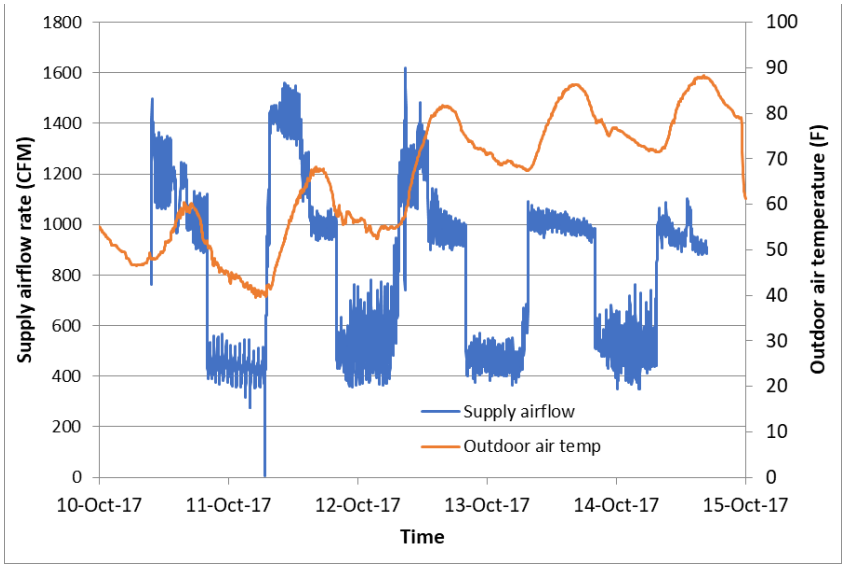

Figure 5.27. Supply Airflow Rate and Outdoor Air Temperature for AHU13.

3. Fan-related fault

The fan air flow rate was measured by a virtual flow meter and fan head was measured by a pressure differential sensor, the same sensor in the virtual flow meter. The fan airflow rate and head as well as the duct static pressure setpoint were applied to calibrate the fault-free SCC based on Equation (5-3).

To detect the fan loose belt fault, both the VFD output power and frequency were obtained from the VFD, similar to the virtual flow meter. Even though there is no additional data sample required for this PDD, to demonstrate the fan loose belt FDD, Figure 5-28 shows the measured VFD output power and Figure 5-29 shows the measured VFD output frequency in AHU3.

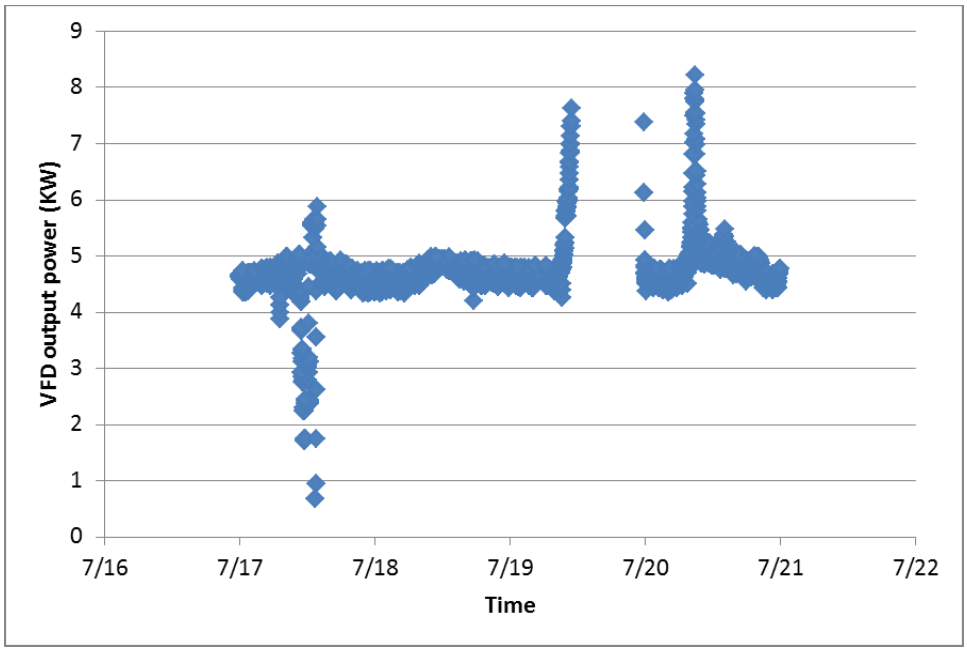

Figure 5.28. VFD Output Power in AHU3.

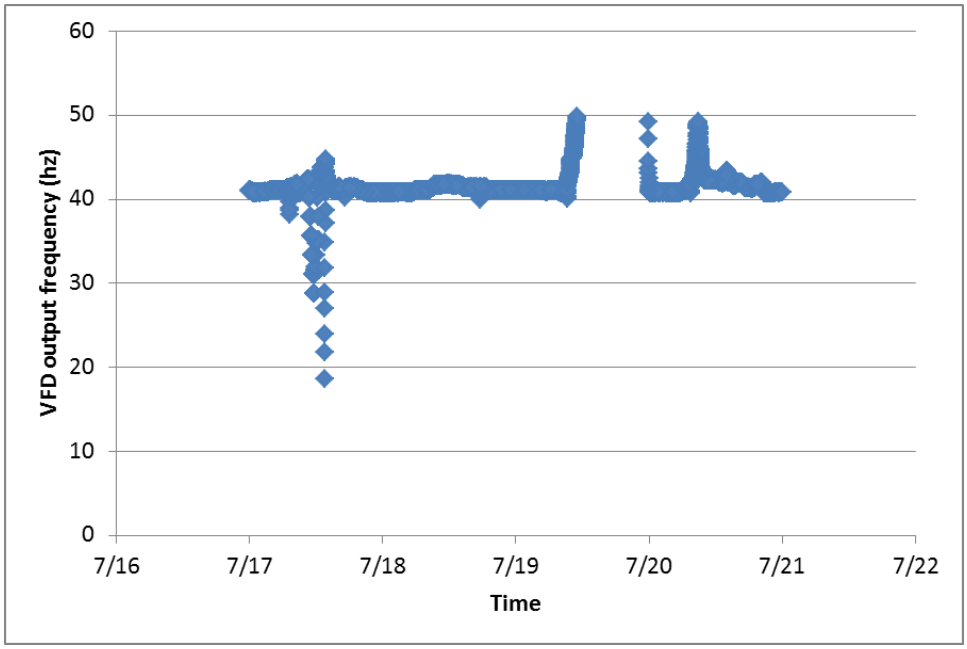

Figure 5.29. VFD Output Frequency in AHU3.

4. Pump-related fault

The pump water flow rate was measured by the developed virtual pump flow meter and pump head was measured by a differential pressure transducer, the same device in the virtual flow meter. The pump water flow rate and head, as well as the loop differential pressure setpoint, were applied to calibrate the fault-free SCC based on Equation (5-2). There is no additional data sample required for this PDD.

6.0 PERFORMANCE ASSESSMENT

6.1 PO EVALUATION OF THE THREE VIRTUAL FLOW METERS

- Performance Objective Analysis Overview: Compared water flow and airflow rate measurements of the virtual flow meters with those of physical flow meters.
- Statistical Methodologies: The data comparison was carried out using standard deviation, two-sigma confidence interval analysis in absolute and relative scales for the two types of measurements.
- Graphical Methodologies: Time series charts and scatter plots were used for data analysis and comparison.
- Industry Standards: No industry standards are available for virtual meter assessments because the technology is still new. Typical industry standards for physical flow meters are the error over full measurement scale at 95% confidence (two sigma), which we used in our analysis for the virtual flow meter report (the mid-term project report).
- External Validity: Other military installations might not have direct digital control systems in place. Implementations of this technology require retrofits of the existing control system first.

6.1.1 PO evaluation for the virtual pump flow meter

Two phases of the results are shown in this subsection. One is the results using our original proposed algorithm to calculate the flow rate and the other describes the results using the improved algorithm.

Using the original proposed algorithm, to calculate the virtual pump flow rate, a simulated motor efficiency curve and a calibrated pump curve in the form of $H/Q^{0.5}$ versus $Ws/H^{1.5}$ were needed. Figure 6-1 shows the simulated motor efficiency versus VFD output power. Figure 6-2 shows the calibrated $H/Q^{0.5}$ versus $Ws/H^{1.5}$ curve. Figure 6-3 compares the calculated water flow rate using our original proposed method and measured water flow rate on September 21, 2015. Statistical analysis results were RSME=18 GPM or 1.5% error over the design flow rate.

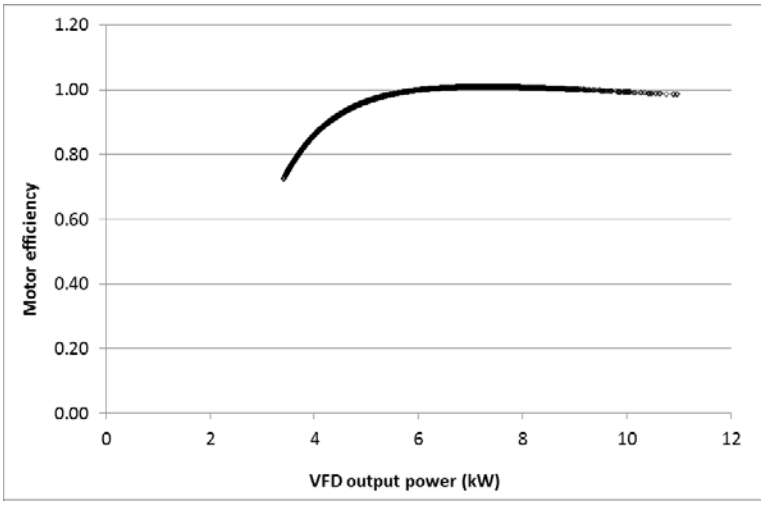

Figure 6.1. Simulated Motor Efficiency.

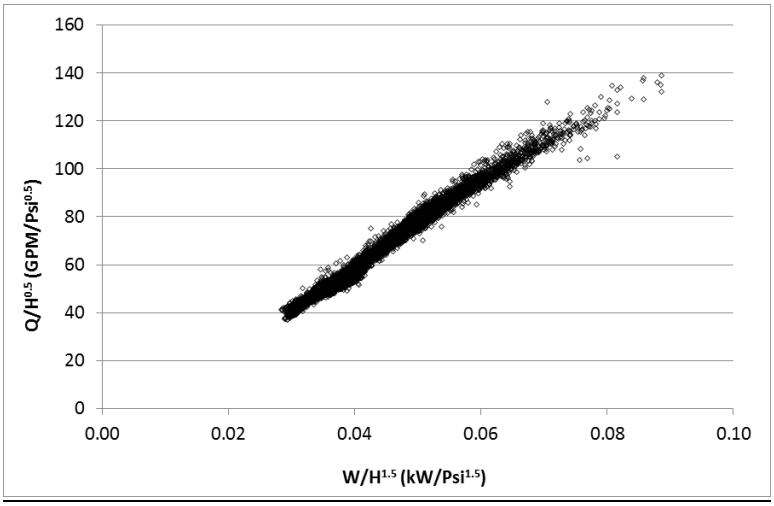

Figure 6.2. Calibrated Pump $H/Q^{0.5}$ versus $Ws/H^{1.5}$ Curve.

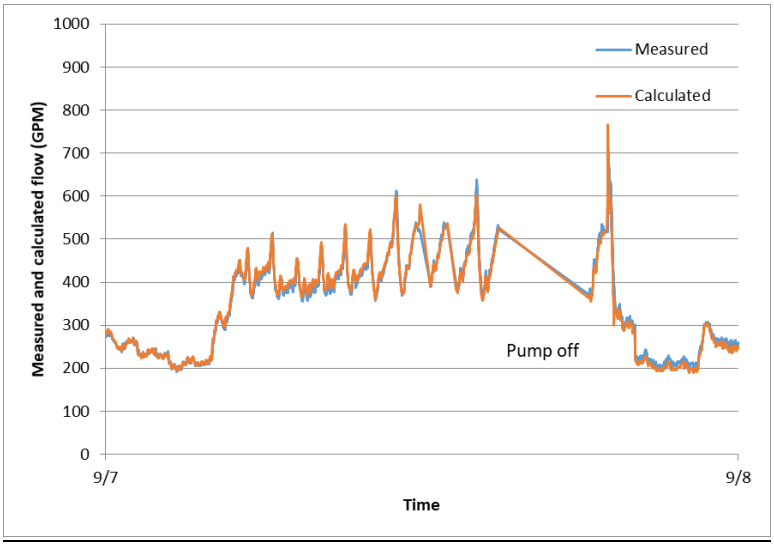

Figure 6.3. Comparison of Calculated and Measured Water Flow Rate.

Although the results are acceptable, the comparison on September 23, 2015 as shown in Figure 6-4, reveals noticeable errors (around 5% of full range measurements) at the lower VFD output frequency and power for this pump, as shown by the areas marked using the red circle. It reveals that the simulated motor efficiency in Figure 6-1 cannot accurately represent the actual motor efficiency at lower frequencies.

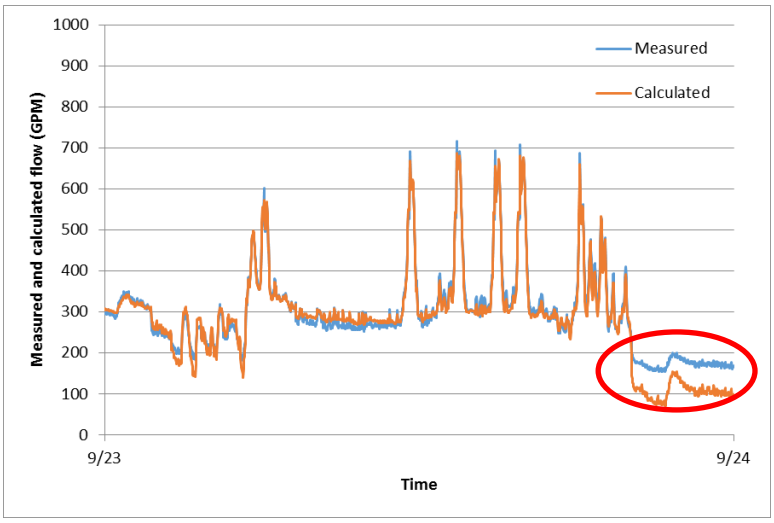

Figure 6.4. Measurement Errors at Lower VFD Output Frequency and Power.

Per the improved method, both motor efficiency curve and pump efficiency curve that are actually relative efficiency curves were needed, and they were obtained through calibration. Figure 6-5 shows the calibrated motor efficiency versus VFD output frequency rather than VFD output power. Figure 6-6 shows the calibrated pump efficiency versus $W/H^{1.5}$ curve. Figure 6-7 compares the calculated and measured water flow rate on September 7 using the improved method. The statistical analysis of the improved results was RSME=15 GPM or 1.2% error over the design flow rate. Meanwhile, Figure 6-8 shows the measurement improvement at the lower VFD output frequency and power by comparing the data on September 23, 2015.

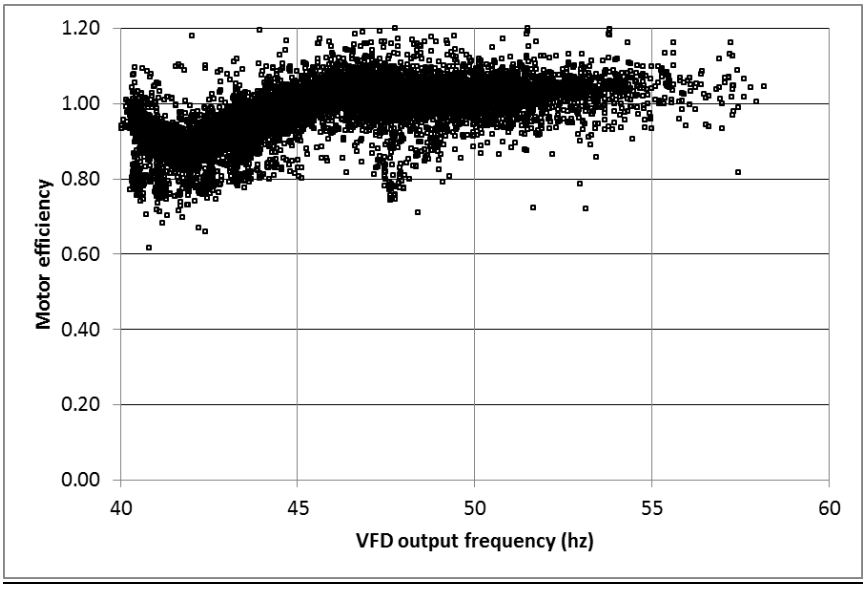

Figure 6.5. Calibrated Motor Efficiency.

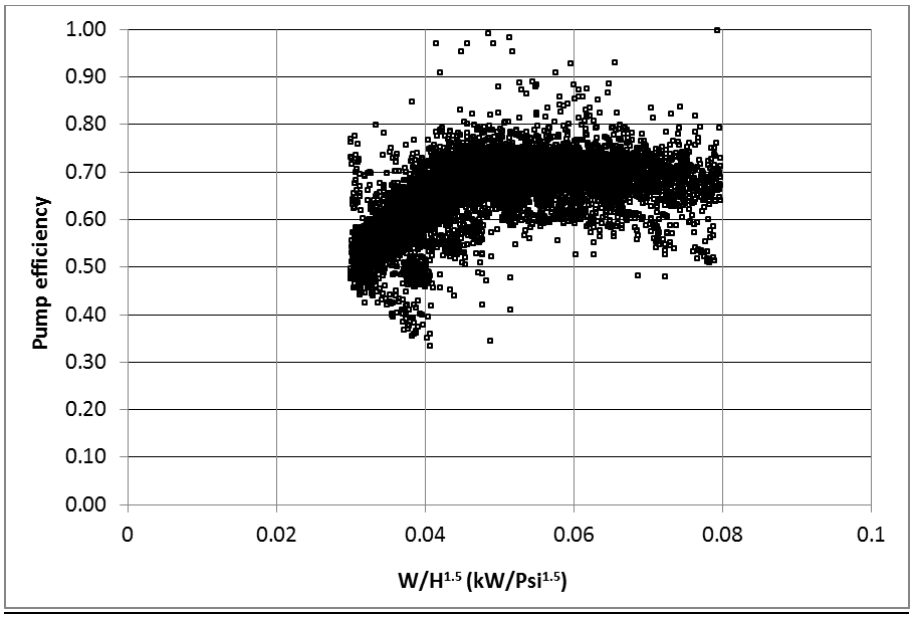

Figure 6.6. Calibrated Pump Efficiency.

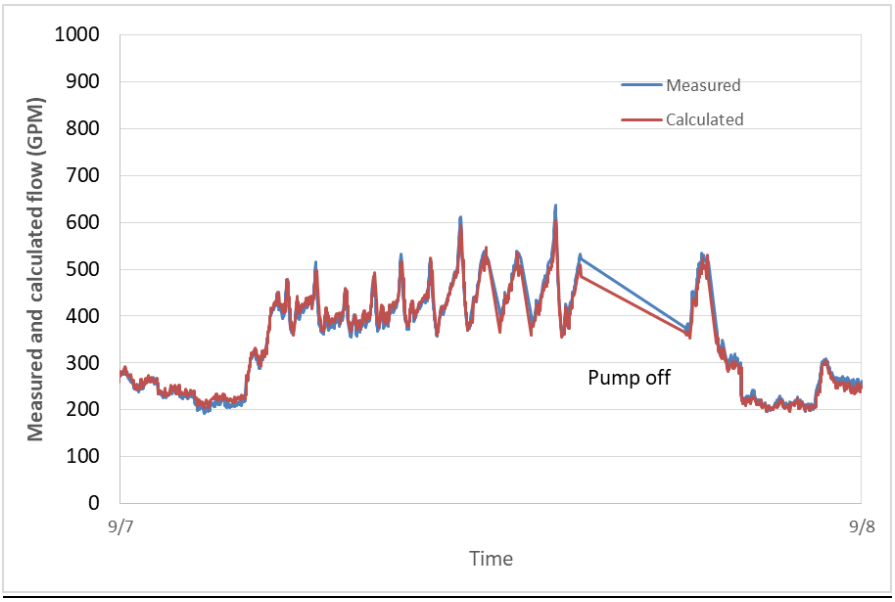

Figure 6.7. Comparison of the Calculated and Measured Pump Flow Rate with Improvement.

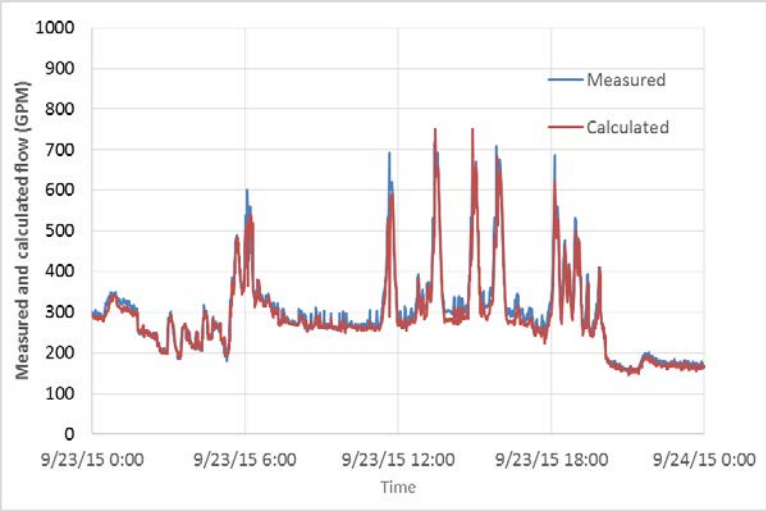

Figure 6.8. Comparison of the Improved Flow Rate and Measured Pump Flow Rate.

6.1.2 PO evaluation of the virtual valve flow meter

Two phases of the results are shown in this subsection. One is the results using our original proposed algorithm to calculate the flow rate and the other phase is the results using the improved algorithm.

Using the originally proposed method, where the valve commands were used to represent the valve opening position, the valve characteristic curve was obtained, shown in Figure 6-9, using the valve command as the valve opening indicator. Figure 6-10 shows the calculated flow rate comparison with the measured flow rate using an ultrasonic meter. Statistical analysis results were RSME=0.347GPM or 1.5% error over the design flow rate. However, as shown by the areas marked using the red circles, the comparison has a consistent bias when the valve experiences oscillations.

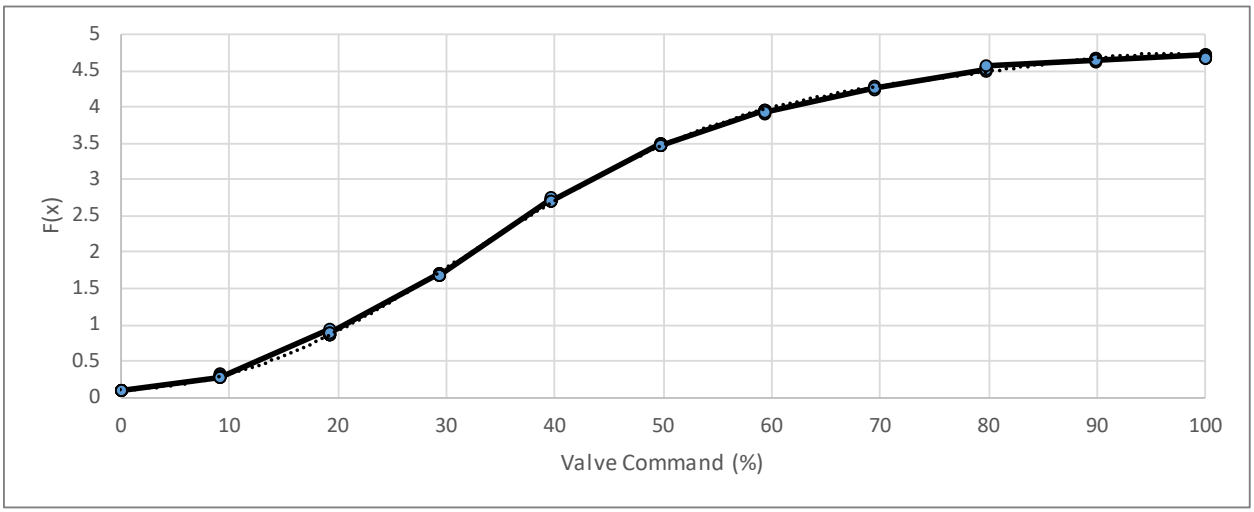

Figure 6.9. Valve Characteristic Curve Using the Valve Command as an Input.

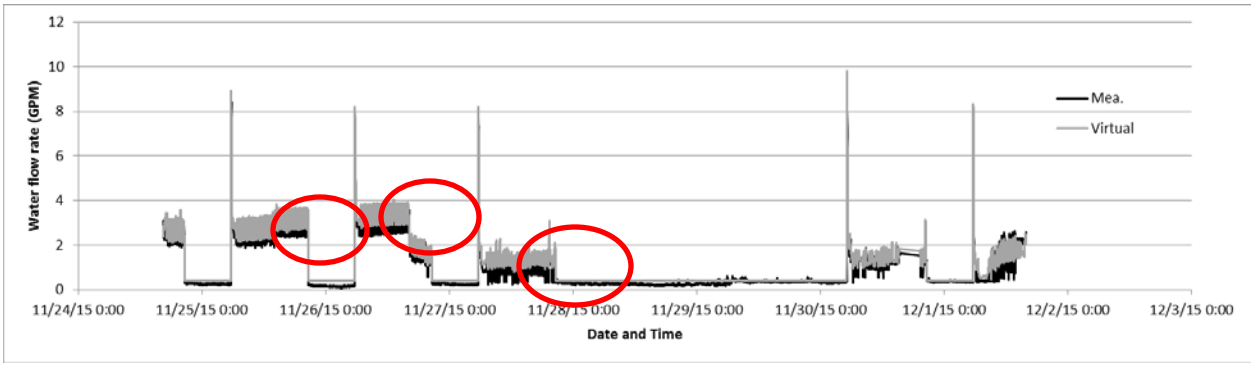

Figure 6.10. Comparison of the Calculated and Measured Valve Flow Rates.

Using the improved method, the valve command was corrected by using valve stiction, hysteresis and valve actuator resolution error. The constants used to correct the valve command were obtained by learning valve dynamic behavior, which is shown in Figure 6-11. Figure 6-12 shows the comparison with the improved method. The statistical analysis of the improved results was RSME=0.231GPM or 0.97% over the design flow rate

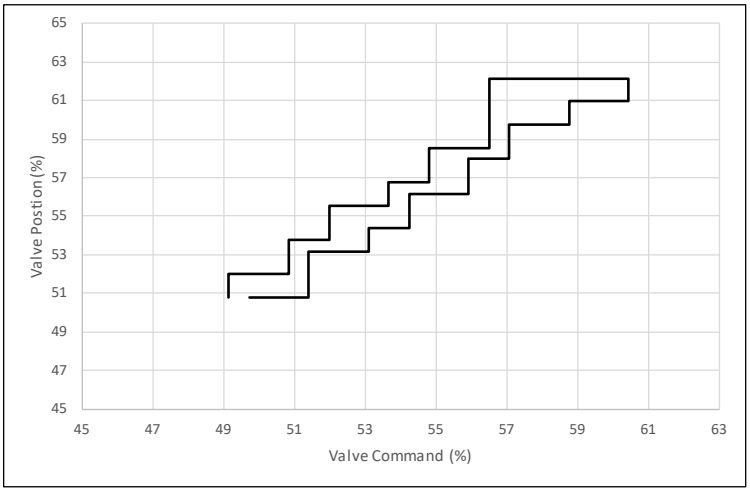

Figure 6.11. Valve Dynamic Behavior Study for Determination of Valve Hysteresis and Stiction.

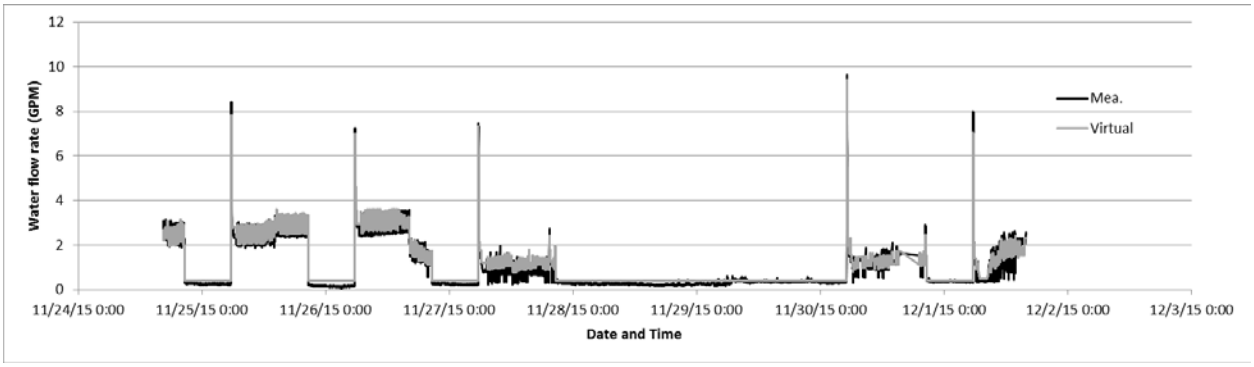

Figure 6.12. Comparison of the Improved Valve Flow Rate Calculation and Measured Valve Flow Rate.

6.1.3 PO evaluation of the virtual fan airflow meter

Only the improved results are shown in this subsection.

Per the improved method, both motor efficiency curve and fan efficiency curve that are actually relative efficiency curves were needed. Moreover, they were obtained through calibration. Figure 6-13 shows the calibrated motor efficiency versus VFD output frequency rather than VFD output power. Figure 6-14 shows the calibrated fan efficiency versus $Ws/H^{1.5}$ curve. Figure 6-15 compares the calculated and measured water flow rates using the improved method. The statistical analysis of the improved results was RSME=154CFM GPM or 1.1% error over the design flow rate. The RSME was 166 CFM or 1.3% error in the initial report.

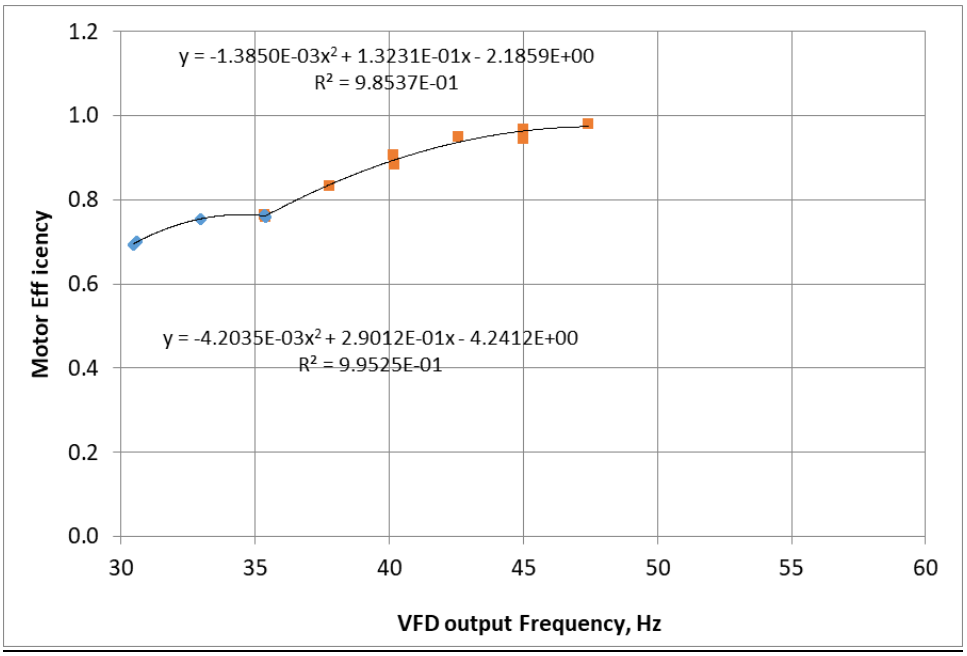

Figure 6.13. Calibrated Motor Efficiency.

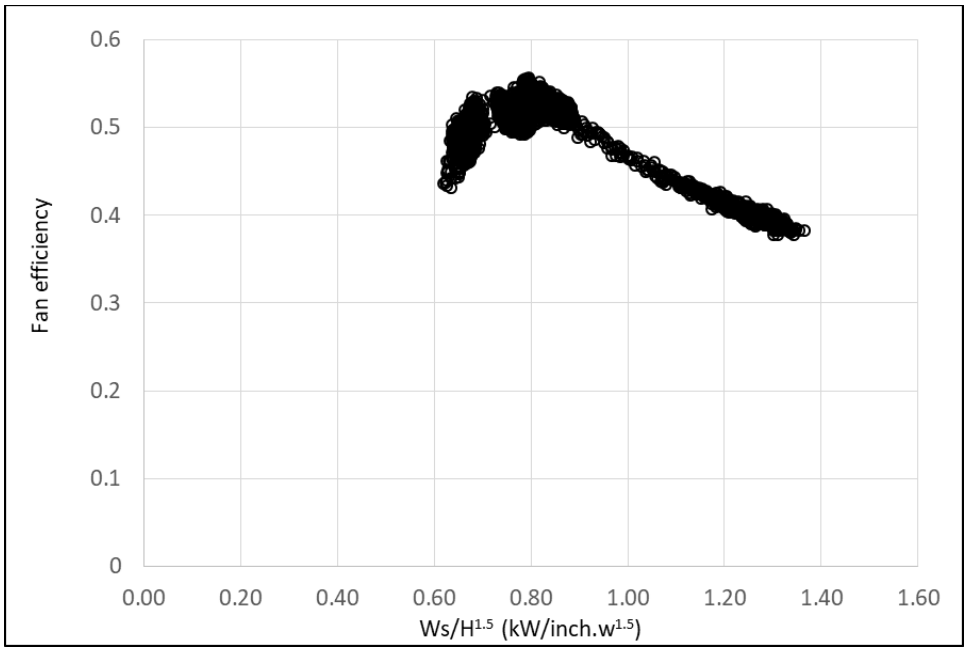

Figure 6.14. Calibrated Fan Efficiency.

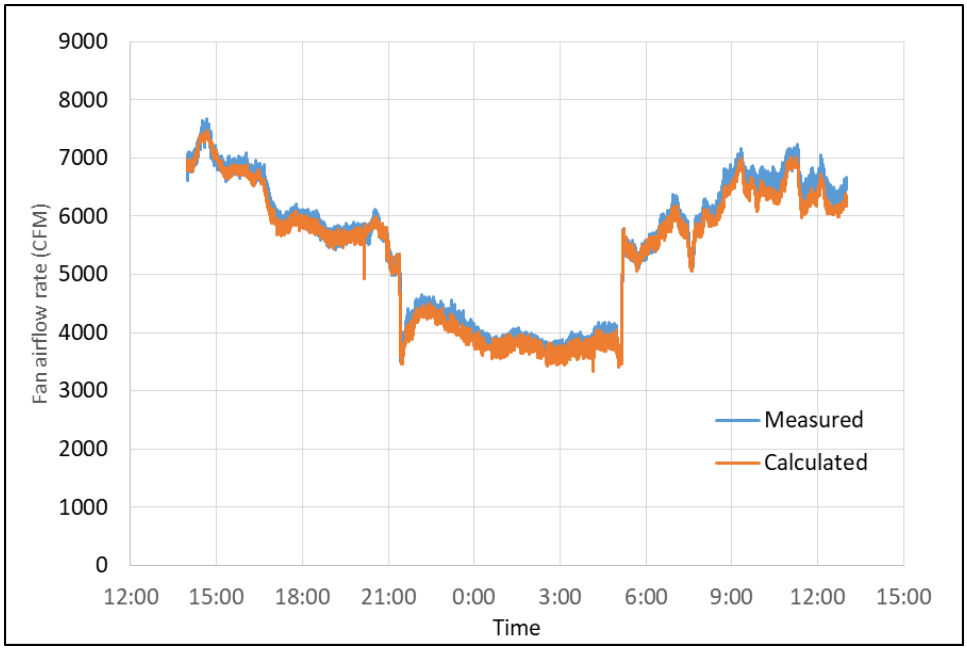

Figure 6.15. Comparison of the Calculated and Measured Pump Flow Rates with Improvement.

6.2 PO EVALUATION OF THE PDD

- Performance Objective Analysis Overview: Compared actual system operations with fault-free reference system operations.
- Statistical Methodologies: The data comparison was carried out using standard deviation, three-sigma confidence interval analysis in both absolute and relative scales.
- Graphical Methodologies: Time series charts and/or scatter plots were used for data analysis and comparison.
- Industry Standards: No industry standard available.
- External Validity: Other military installations might not have direct digital control systems in place. Implementations of this technology require retrofits of the existing control system first.

6.2.1 PO evaluation of the outdoor air intake faults

Excessive outdoor air intake can significantly increase the cooling energy use in each AHU. Therefore, by comparing the actual cooling energy use measured by the virtual valve flow meter (multiplied by the supply and return chilled water temperature difference) and the calculated fault-free cooling energy usage using Equation (5-5), the significant difference can indicate the faults related to the outdoor air intake. However, the demonstration building does not have an outdoor air humidity sensor; therefore, we have used the outdoor air temperature only to represent the outdoor air conditions. This assumption results in uncertainty of the fault-free cooling baseline model. Figure 6-16(a) compares the calculated fault-free energy baseline with measured cooling energy use without fault per hour. The difference between the two is represented by the red squares in the same figure. It is noticeable that the difference has some clear patterns which indicate the cooling fault-free baseline model can be improved. The lack of the humidity sensors, resulting in ignorance of the latent outdoor air load, might be one of the large contributors to this error. Figure 6-16(b) compares the fault-free cooling baseline with the measured cooling when the outdoor air damper was stuck, i.e., there was significantly reduced outdoor air intake. Although the uncertainty embedded in the cooling fault-free baseline model still existed, the orange line is consistently higher than the blue line when outdoor air was hotter, which indicate insufficient outdoor air intake to the building.

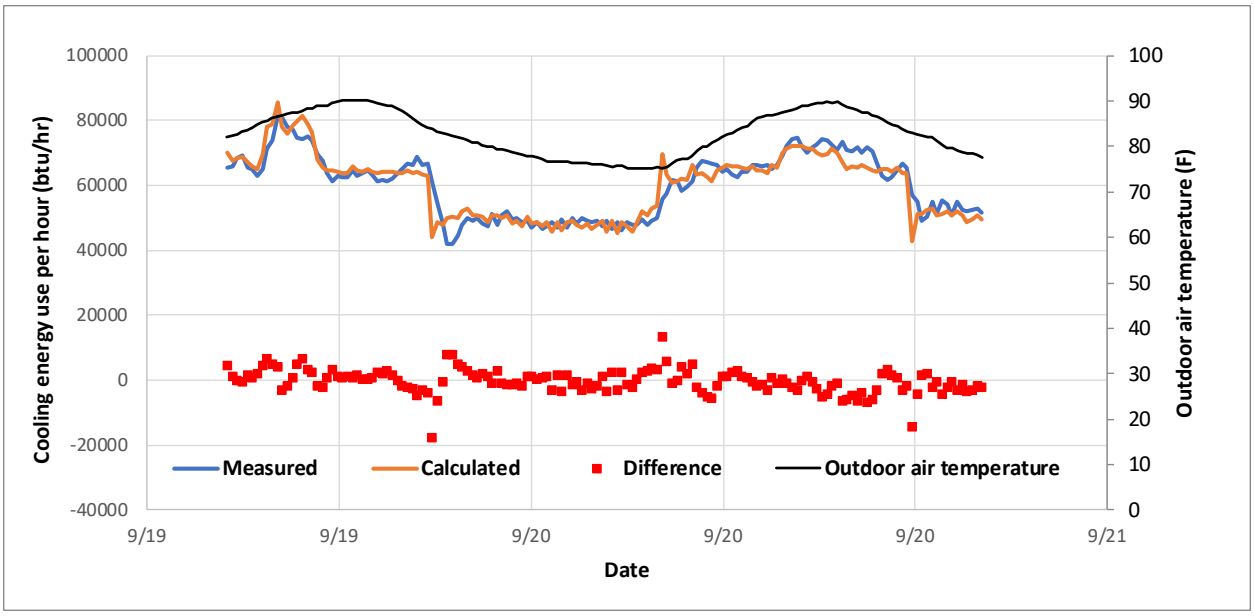

Figure 6.16(a). Comparison Between the Calculated Fault-free Cooling and Measured Cooling Rates When There is No Outdoor Air Fault.

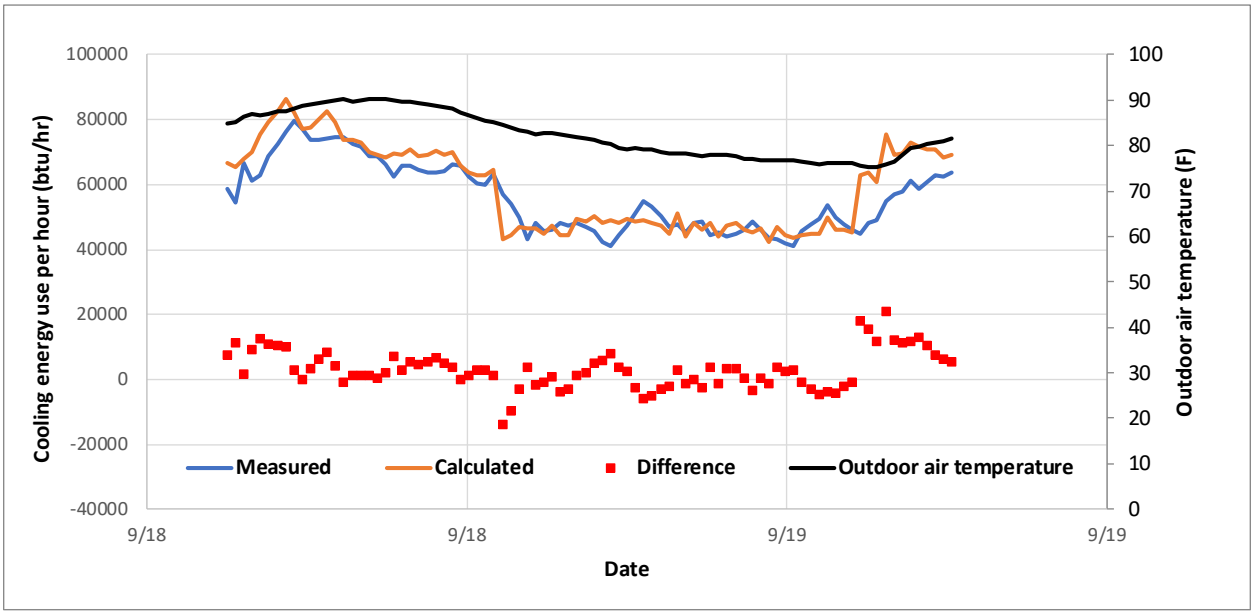

Figure 6.16(b). Comparison of the Calculated and Measured Cooling Rates When an Outdoor Air Fault is Introduced.

The two differences with fault and with no fault are also compared in Figure 6-17, using a scatter chart versus outdoor air temperature. The green line is the average of the green triangles, which are the differences between the measured and calculated cooling rates when there was no fault and. The red line is the average of the red diamonds, which are the differences when outdoor air intake faults were present. Through the average line comparison, it is more obvious that less outdoor air intake, resulting in sacrificed indoor air quality, can be detected by the cooling energy use, although the sensitivity of the detection would still be enhanced if an outdoor air humidity sensor was available.

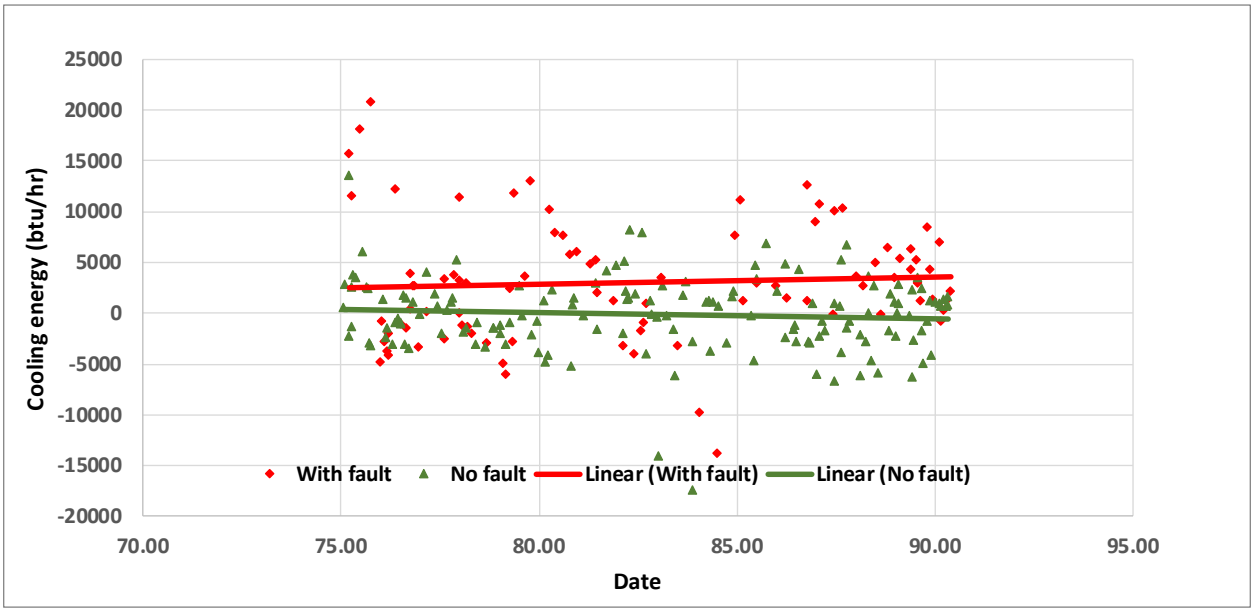

Figure 6.17. Comparison of Cooling Differences with and Without an Outdoor Air Fault.

6.2.2 PO evaluation of the reheat energy waste

The minimum supply airflow ratio was calibrated based on the fault-free supply airflow during occupied and unoccupied periods. Figure 6-18 shows the calculated supply airflow ratio of AHU 13. It reveals that the minimum supply airflow ratio was 40% during the occupied period from 7AM to 8PM and 20% during the unoccupied period from 20PM to 7AM. The PDD was validated using the operating data before the energy efficiency measures were implemented. Figure 6-19 compares the actual supply airflow ratio (blue line) with required minimum airflow ratio (red line). The figure reveals that the actual flow ratio almost remained constant at 62%, which is more than the required ratio of 40% for daytime and 20% for nighttime. The significant supply airflow reduction resulted in significant reheat energy savings in addition to cooling energy and fan electrical savings.

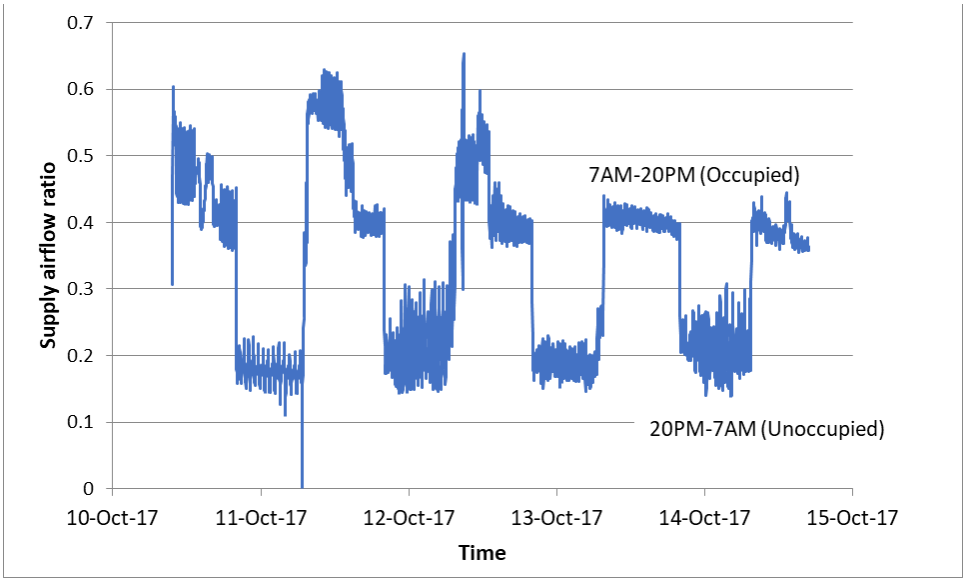

Figure 6.18 Calibrated Minimum Supply Airflow Ratios.

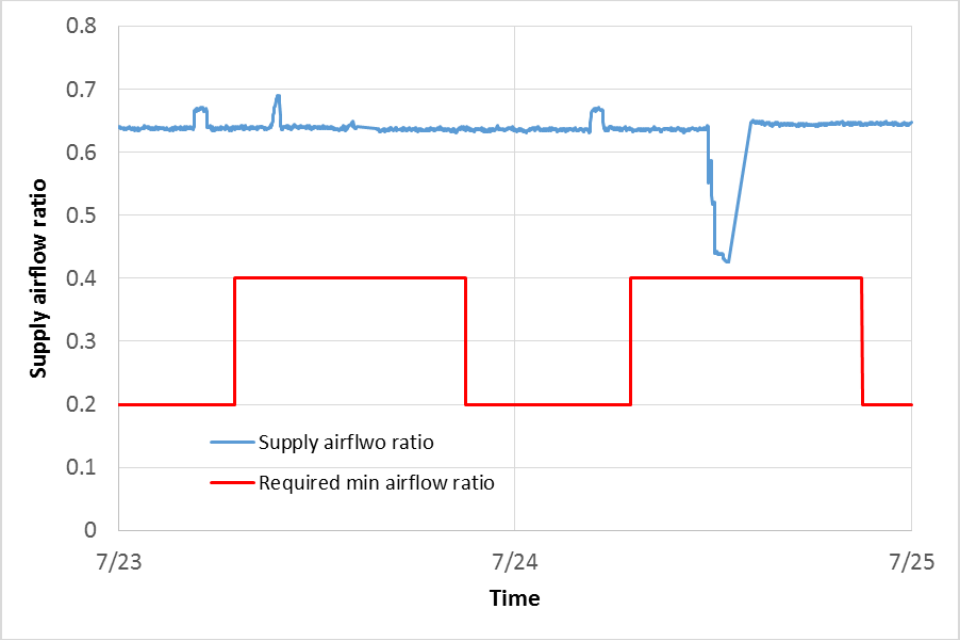

Figure 6.19 Actual Supply Airflow Ratios.

6.2.3 PO evaluation of the fan operation-related faults

1. Fan damper and pressure setpoint-related faults

Figure 6-20 shows the calibrated fault-free SCC for the supply fan of AHU 13 based on the data in Figure 5-22, 23 and 24.

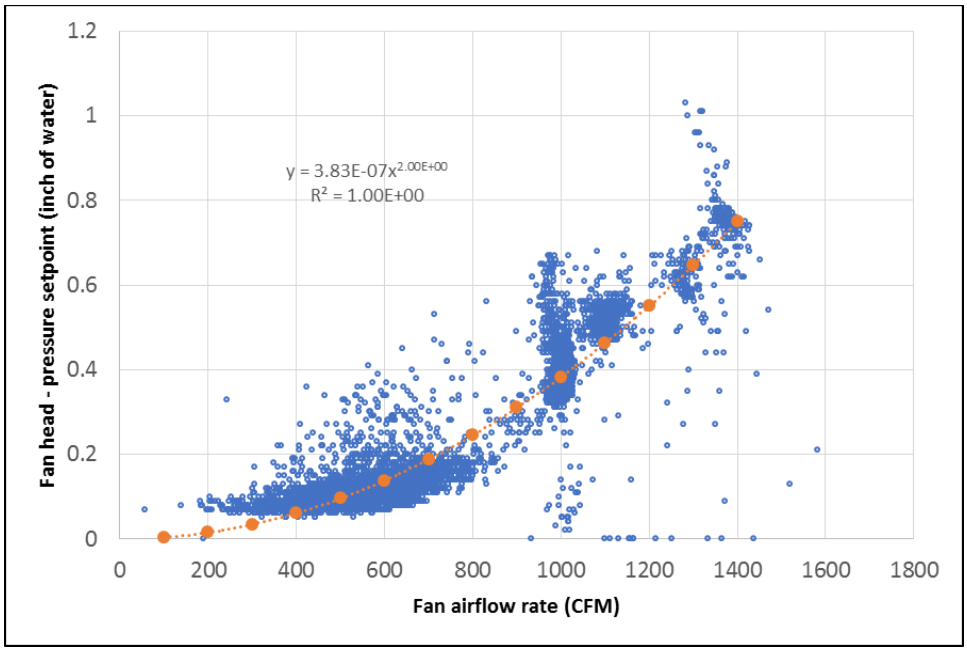

Figure 6.20 Calibrated SCC of AHU13.

2. Fan loose belt faults

Figure 6-21 shows the calibrated fault correlation between the VFD output frequency and power for AHU3 based on the data in Figures 5-28 and 5-29.

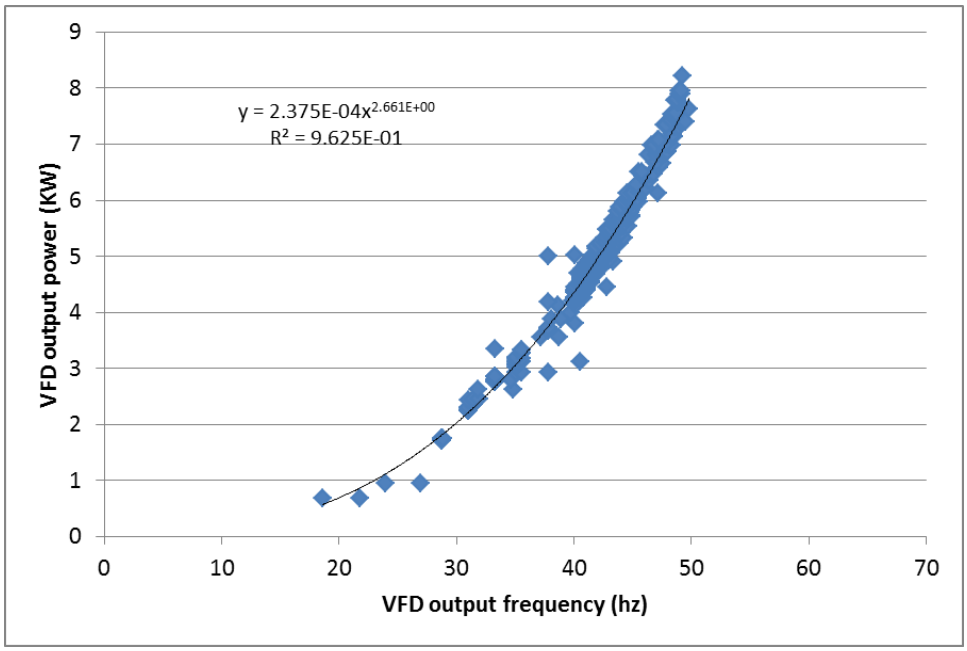

Figure 6.21 Calibrated Correlation Between VFD Output Power and Frequency for AHU3.

With the calibrated fault-free correlations, the free-fault VFD output power can be calculated based on the VFD output frequency and then compared with the actual VFD output power. The fault alarm will be triggered if the actual VFD output power is much less than the fault-free power. Figure 6-22 shows the actual frequency (green line) and its associated fault-free power (black line) as well as the actual power (red line). It is clear the fan belt was loose when the frequency was higher than 50hz.

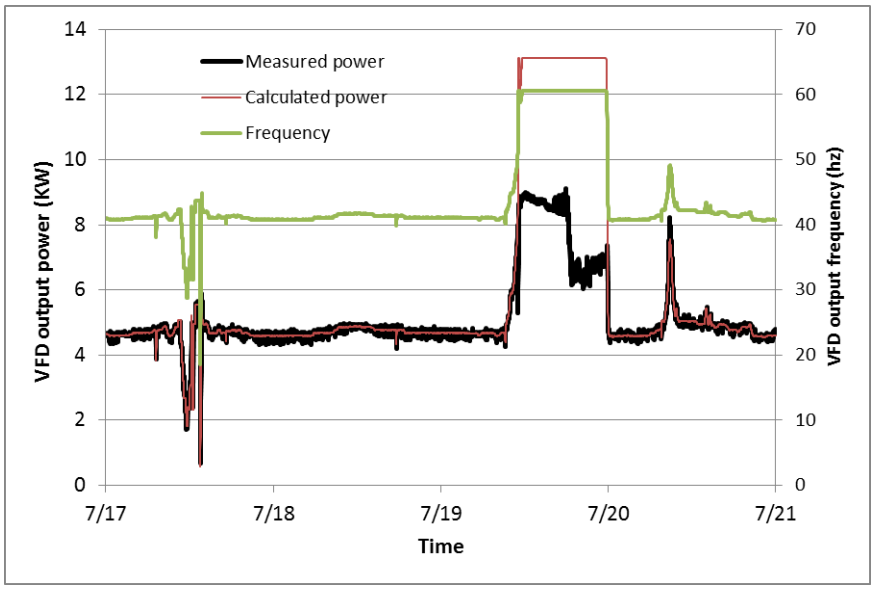

Figure 6.22 Calculated Fault-free and Actual Power as Well as Actual Frequency for AHU3.

6.2.4 PO evaluation of the pump operation-related faults

Figure 6-23 shows the calibrated fault-free SCC for the secondary chilled pump 1 based on the data in Figures 5-15, 5-16 and 5-17.

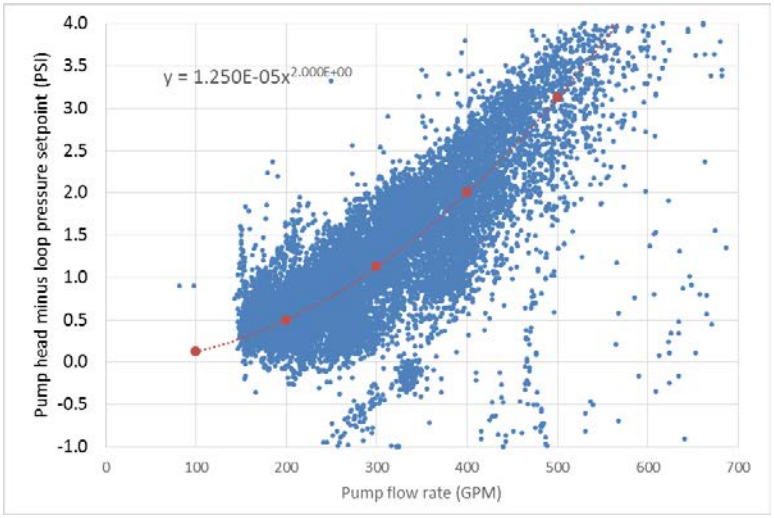

Figure 6.23 Calibrated SCC for Secondary Chilled Water Pump 1.

A fault alarm is triggered if the fault-free loop pressure setpoint calculated based on the pump water flow rate and head using the calibrated SCC is different than the actual measured loop pressure. Figure 6-24 shows the calculated fault-free loop pressure setpoint (red line) and actual measured loop pressure (blue line). It can be seen that the calculated loop pressure setpoint tracked the actual measured loop pressure very well.

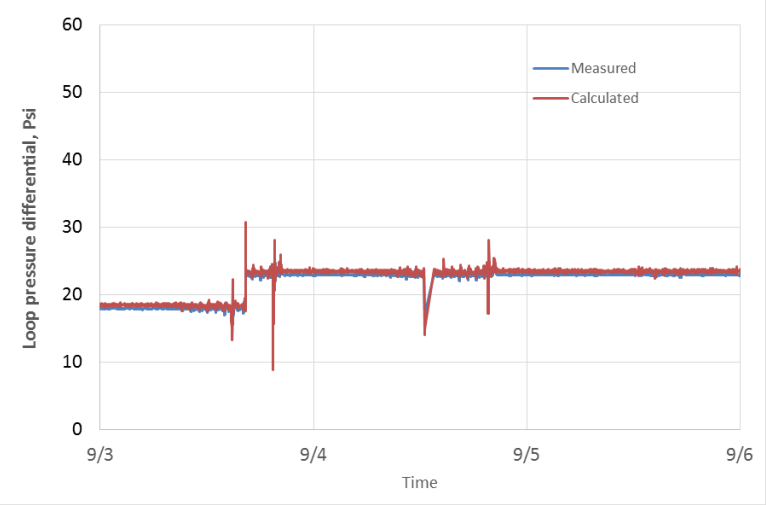

Figure 6.24 Comparison of the Calculated and Measured Loop Pressure Differences.

6.3 PO EVALUATION OF THE END-USE ENERGY

- Performance Objective Analysis Overview: The ultimate goal of the PDD was to capture 16% energy savings in the demonstration building through the PDD. Our approach was to correct the problems identified by the PDD and measure the energy usage before and after the corrections to validate the amount of the energy savings. In this project, we collected monthly utility bills from January 2014 to December 2017, a total of four years' data, to validate the proposed savings. The original utility data is shown in Figure 6-25: Figure 6-25(a) shows the monthly electricity use and Figure 6-25(b) shows the natural gas monthly use. The improvements by the project team were primarily made from January 2016 to May 2016. The facility experienced a mold problem in summer 2016. One of the solutions was suggested by a consulting firm was to override all the AHUs to 24-hour operations with 5°F lower supply air temperature starting in mid-July 2016. The overrides significantly altered the energy performance of the building. Therefore, we have selected the energy usage in Year 2015 as a baseline and the energy usage in Year 2017 for the after changes. Although the supply air temperature overrides were released in late 2016, the schedule overrides were still not completely released, i.e., there were still several AHUs running 24x7 at the present time. The savings were compromised by this operations change.

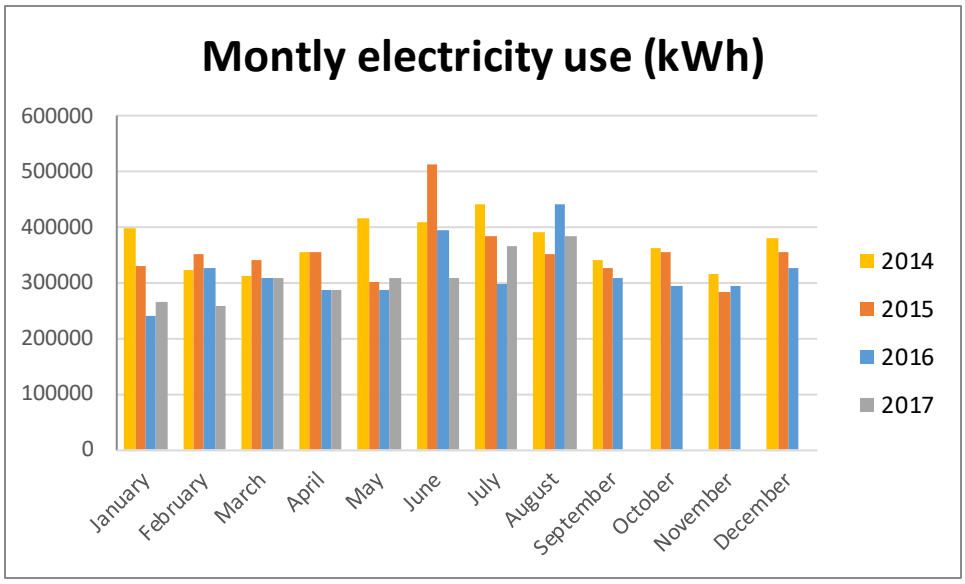

Figure 6.25(a). Raw Values for Collected Monthly Electricity Data.

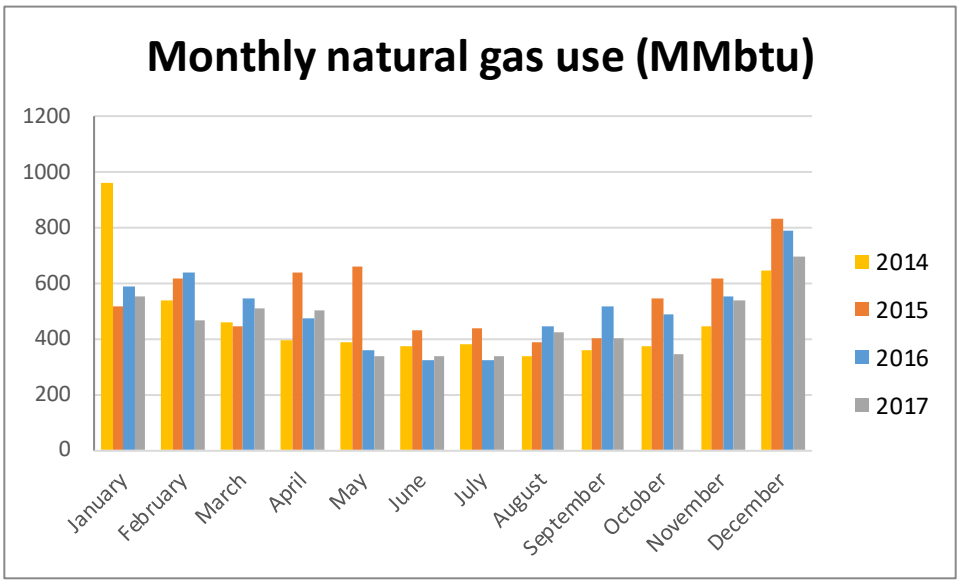

Figure 6.25(b). Raw Values for Collected Monthly Natural Gas Data.

- Statistical Methodologies: The energy savings was the difference between the baseline energy (2015) and the energy usage after the PDD implementation (2017). However, the weather impacts needed to be considered. We have utilized a scatter chart to regress the energy use versus average outdoor air temperature before and after the corrections to eliminate the weather impacts. Figure 6-26 (a) shows the monthly electricity use versus average outdoor air temperature in the month, while Figure 6-26 (b) shows the monthly natural gas use before and after the correction versus average outdoor air temperature in the month.

Red triangles are for the months before the correction and green dots represent the months after the correction. By using the linear regression of the red triangles and green dots respectively, shown by the solid lines in both figures, the average electricity and natural gas usage versus outdoor air temperature are obtained. The difference between the two solid lines in Figure 6-26 (a) was the electricity savings, equivalent to 14.7% of the electricity use baseline, while the difference between the two solid lines in Figure 6-26 (b) was the natural gas savings, equivalent to 16.9% of the natural gas use baseline. For Year 2017 weather conditions, the average annual total cost savings was $74,629 for the whole building level energy use based on the lumped utility rate of $0.0522/kWh for electricity and $4.02/MMbtu (the utility rates were calculated using the average rates from 2014 to 2017 due to the rate changes over time), equivalent to 15% annual energy cost savings overall.

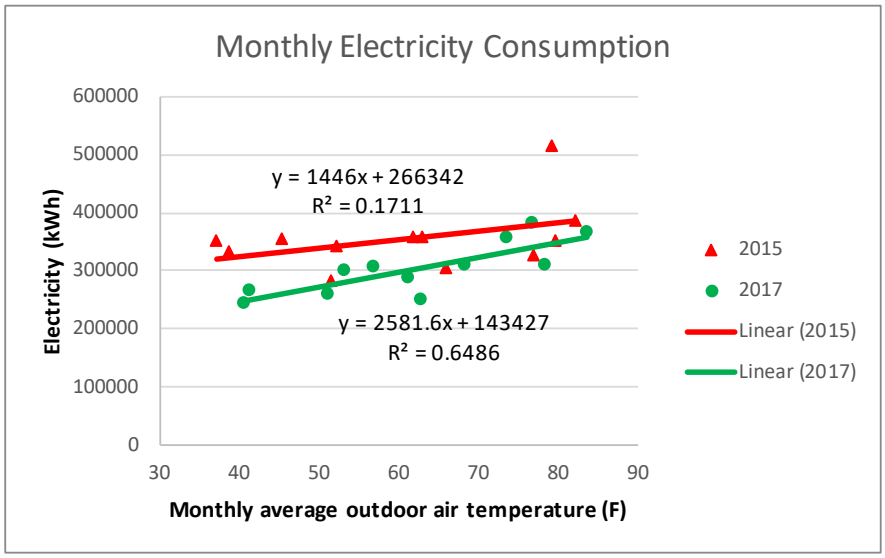

Figure 6.26(a). Monthly Electricity Use versus Monthly Average Outdoor Air Temperature.

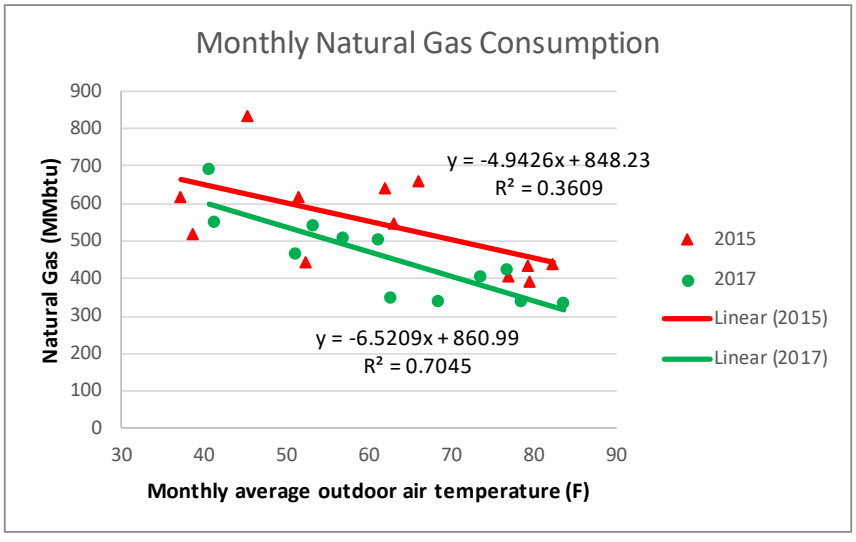

Figure 6.26(b). Monthly Natural Gas Use versus Monthly Average Outdoor Air Temperature.

- Graphical Methodologies: Both time series charts and scatter plots were used to present the energy usage differences between before and after corrections.
- Modeling and Simulation: Although there were still a few AHUs running 24 by 7 operations, the energy penalty was not significant compared with the supply air temperature overrides which were done in late 2016. Therefore, by choosing Years 2015 and 2017 for energy performance calculations, there was no need for modeling and simulation to validate the savings. The weather impacts can be quantified by the scatter chart.
- Anecdotal Perspectives: Facility operators would provide timely notice of the system operations, changes and any unexpected alarms from PDD for us to improve the technology.
- Industry Standards: Using the scatter chart to regress the energy use versus the outdoor air temperature for before and after corrections complies with International Performance Measurement and Verification Protocols (IPMVP) and ASHRAE guide 14-Measurement of Energy and Demand savings.
- External Validity: Other military installations might not have direct digital control systems in place. Implementation of the technology requires a retrofit of the existing control system first.

7.0 COST ASSESSMENT

7.1 COST MODEL

The actual cost of the demonstration is summarized in Table 7-1.

Table 7.1. Cost Model for the Demonstration Technology.

Cost Element	Data Tracked During the Demonstration	Estimated Costs
Hardware capital costs	Subcontractor's invoice	$62,705 (the costs of six VFDs was deducted because they did not contribute to the savings we obtained)
Installation costs	Subcontractor's invoice	$19,465 (the costs of six VFDs was deducted because they did not contribute to the savings we obtained)
Programming and PDD implementation costs	Estimates based on the engineering programming effort by the project team	$15,000 (estimated by assuming 200 engineering hours are needed at a rate of $75 per hour)
Facility operational costs	Reduction in energy required vs. baseline data	$74,629 (The savings were obtained by correcting the faults/deficiencies identified through PDD.)
Maintenance	• Frequency of required maintenance • Labor and material per maintenance action	$0 (not beyond routine maintenance costs. Particularly for this project, no equipment replacement was needed for the 15% savings we obtained. However, our team made soft corrections on fan and pump operation set points, outdoor air intake and VAV box minimum airflow setting, estimated at $13,125 one-time engineering cost for the correction at $75 per hour for a total of 175 hours.)
Hardware lifetime	Estimate based on components degradation during demonstration	30 years
Annual service costs	Based on 50 engineering hours annually	$3,750 ($4^{+}$ hours per month)

- Hardware capital costs: As explained in the technology description section, the virtual fan/pump flow meters need to have input signals such as fan/pump head, VFD power, and frequency for the flow rate calculations. The virtual valve flow meter needs the differential pressure across the valve. The input information requires the installation of differential pressure sensors and necessary control wires.
- Installation costs: The BAS service provider for the demonstration building was hired to install the hardware required as described in the last bullet.
- Programming and PDD implementation costs: Although the flow rate calculation algorithms and the PDD algorithms are straightforward to implement, a few coefficients needed to be calibrated to make the algorithms work properly. This work was done by the project team, so there was no contractor's invoice for that expense. However, based on the effort we have put in and the size of the demonstration building, we estimated that 200 engineering hours would be needed at the cost of $75 per hour.

- Maintenance: We did not include any maintenance costs in the estimation because the demonstration building did not need any equipment replacement. There were no additional maintenance costs associated with the savings. However, our team made soft corrections on fan and pump operation set points, outdoor air intake and VAV box minimum airflow setting, estimated at $13,125 one-time engineering cost for the correction at $75 per hour for a total of 175 hours.
- Hardware lifetime: We estimated the lifetime of the installed differential pressure sensor and VFD is about the same as any other HVAC equipment, with a lifetime of 30 years at Tinker.
- Annual service costs: As we experienced in the demonstration building, we do not think it is realistic to let facility operators keep up with fault corrections, especially when the faults are related to operation sequences. It will add more workload to the facility operator and potentially generate the need for more hires. Also, the facility operators will need to call the BAS service provider to fix the problem. In this case, an annual service fee paid to a BAS service provider or a PDD licensee is a more economical way to implement the technology and receive the savings.

7.2 COST DRIVERS

Potential cost drivers include the Executive Orders and The Meter Policy as discussed in Section 1.3. Specifically, Tinker Air Force Base has several ongoing ESPC and UESCs that are over $500 million to enhance base resilience and energy efficiency. The virtual flow meters are low cost and provide energy savings to help ESCO and utilities enable the ESCP and UESC project by offering reduced project payback.

7.3 COST ANALYSIS AND COMPARISON

The current approach of providing similar monitoring and fault detection services is through a retro-commissioning service, where engineers physically audit building systems using portable meters to manually collect data. At Tinker, a four-year payback is the threshold to make a retro-commissioning project happen. This four-year threshold covers the service costs only and does not include the costs for the equipment retrofit. Therefore, the retro-commissioning cost is equivalent to what the virtual meter and PDD technology can offer. If we use a four-year payback, to save the same amount of energy as we saved for the demonstration building, the cost of the retro-commissioning would be $298,516 for the one-time service. Additional costs are usually incurred if continuous monitoring or health checks are needed. Figure 7-1 shows the BLCC analysis for the virtual meter and PDD technology. Figure 7-2 shows the BLCC analysis for a typical retro-commissioning project.

Figure 7.1 BLCC Analysis for the Demonstrated Technology.

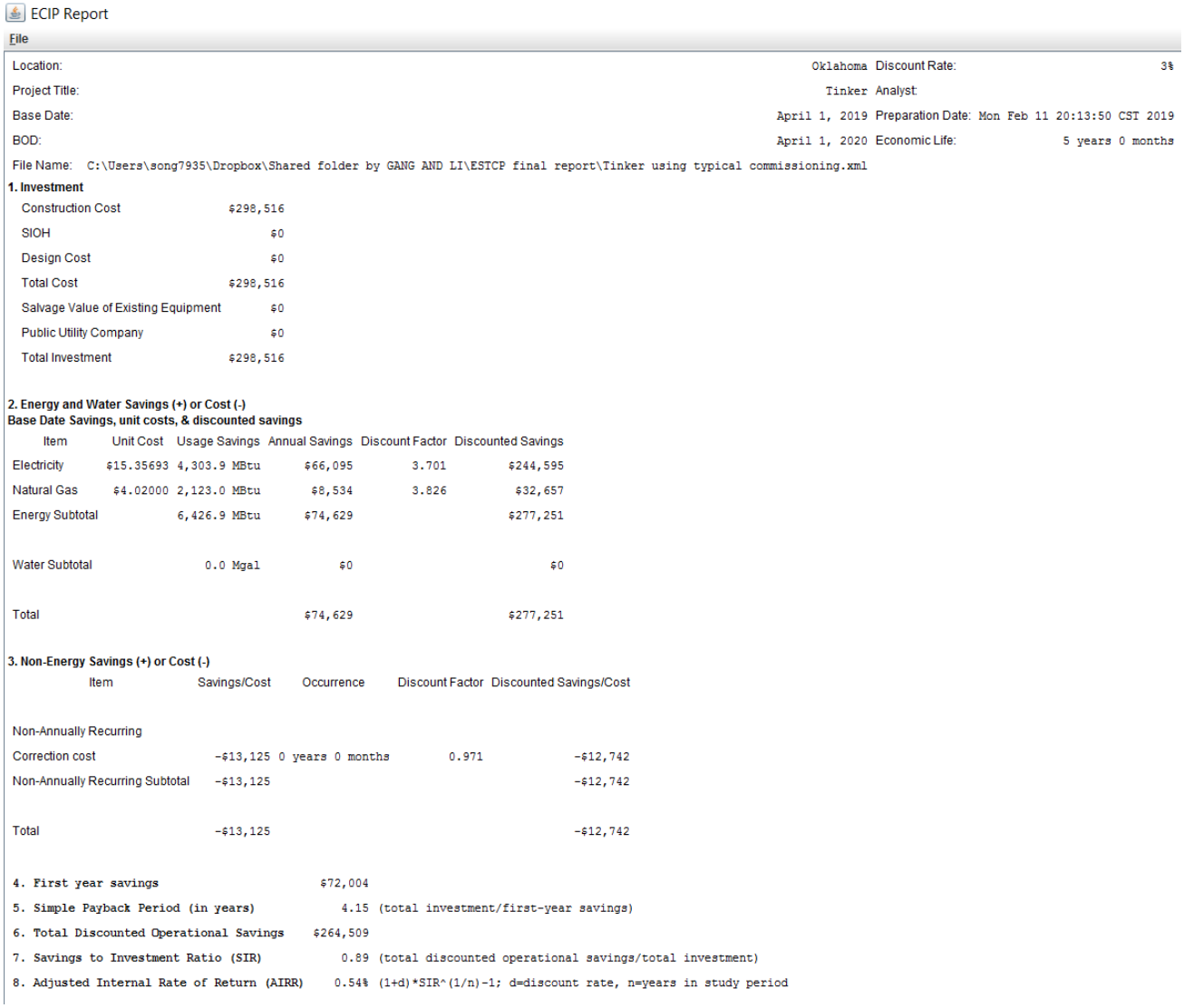

ECIP Report

File

Location:	Oklahoma	Discount Rate:	3%
Project Title:	Tinker	Analyst:	
Base Date:	April 1, 2019	Preparation Date:	Mon Feb 11 20:13:50 CST 2019
BOD:	April 1, 2020	Economic Life:	5 years 0 months

File Name: C:\Users\song7935\Dropbox\Shared folder by GANG AND LI\ESTCP final report\Tinker using typical commissioning.xml

1. Investment

Construction Cost	$298,516
SIOH	$0
Design Cost	$0
Total Cost	$298,516
Salvage Value of Existing Equipment	$0
Public Utility Company	$0
Total Investment	$298,516

2. Energy and Water Savings (+) or Cost (-)
Base Date Savings, unit costs, & discounted savings

Item	Unit Cost	Usage Savings	Annual Savings	Discount Factor	Discounted Savings
Electricity	$15.35693	4,303.9 MBtu	$66,095	3.701	$244,595
Natural Gas	$4.02000	2,123.0 MBtu	$8,534	3.826	$32,657
Energy Subtotal		6,426.9 MBtu	$74,629		$277,251
Water Subtotal		0.0 Mgal	$0		$0
Total			$74,629		$277,251

3. Non-Energy Savings (+) or Cost (-)

Item	Savings/Cost	Occurrence	Discount Factor	Discounted Savings/Cost
Non-Annually Recurring				
Correction cost	-$13,125	0 years 0 months	0.971	-$12,742
Non-Annually Recurring Subtotal	-$13,125			-$12,742
Total	-$13,125			-$12,742

4. First year savings	$72,004	
5. Simple Payback Period (in years)	4.15	(total investment/first-year savings)
6. Total Discounted Operational Savings	$264,509	
7. Savings to Investment Ratio (SIR)	0.89	(total discounted operational savings/total investment)
8. Adjusted Internal Rate of Return (AIRR)	0.54%	(1+d)*SIR^(1/n)-1; d=discount rate, n=years in study period

Figure 7.2 BLCC Analysis for a Typical Retro-commissioning Process.

8.0 IMPLEMENTATION ISSUES

We have learned a lot through the demonstration project. The technology-related lessons and related solution/improvements have been discussed in Section 2.2. Here, a few implementation-related issues are summarized.

- Potential regulation issues: The major regulation issue is cybersecurity clearance. Although we did not have this trouble during this project, the BAS we needed to access is a standalone system and is not on the Tinker network system, the time and effort to obtain necessary cybersecurity clearances can potentially increase the project cost.
- End-user concerns: As we have explained in PO13 in Section 3, it is not realistic to train facility operators to use the PDD technology, including reading the alarms and making necessary corrections for energy savings. This approach would potentially increase their job responsibilities and potentially increase the need for additional staffing. The capacities of the facility operators in the demonstration site allow them to maintain normal BAS operation by performing time schedule changes and some overrides with the override windows preset by BAS contractor. They call in the BAS contractor for additional needful such as making the operation sequence changes etc. Therefore, it would be extremely difficult to train the building operators for the use of PDD technology that is built upon BAS. The training would be required for both understanding BAS system and then the PDD technology. Typically, BAS training provided by BAS manufacturers costs thousands of dollars and it would be only effective for the trainees who have certain prerequisite knowledge. Instead, we learned through the demonstration that a more economical and practical approach would be to hire contractors who can be either BAS service providers or our technology licensees (installers) by paying a monthly fee or long-term service contract package to receive the alarms, make necessary soft changes in programs if needed, and/or suggest hardware replacements to the facility operators.
- Procurement issues: There are two approaches to implement the technology. One is the same as we did in the demonstration project, i.e., implement the calculation algorithms into the existing BAS. Although the technology was demonstrated in a LEED building, it is applicable to any building regardless LEED certified or not. Non-LEED buildings will only provide more savings because they are expected to operate less efficient than a LEED certified building. However, this approach will not be feasible for a building that does not possess BAS. The other approach is to install our mini-converter, which includes flow rate calculations in the mini-converter and output the signal directly to the LCD display on the converter or BAS if available. The mini-converter is a stand-alone device that can possess a processor to calculate the flow rate, an LCD display to show the flow rate onsite and an I/O module to receive the needed inputs and send out the calculated flow rate in standard analog signal format that is compatible with all the BAS systems. The development of the mini-converter is to reduce the hardware cost of BAS panel expansion and wire connection and its associated labor cost, and to save the costs for programming and calibration for wide deployment. The first approach has no procurement issues, as all the accessories to be installed are off-the-shelf. The second approach may need special procurement procedures because our mini-converter is a custom-built prototype at the moment.

Page Intentionally Left Blank

9.0 REFERENCES

Andiroglu, E., G. Wang and L. Song (2013). Development of a Virtual Water flow Meter using Pump Head and Motor Power. Zero Energy Mass Customization Housing (ZEMCH2013) International Conference, Miami, FL.

ASHRAE (2010a). ANSI/ASHRAE Standard 62.1-2010, Ventilation for acceptable indoor air quality. Atlanta, GA, American Society of Heating, Refrigerating and Air-conditioning Engineers, Inc.

ASHRAE (2010b). ASHRAE Standard 90.1-2010. Energy Standard for Buildings except Low-Rise Residential Buildings. Atlanta, GA, American Society of Heating, Refrigerating and Air-conditioning Engineers, Inc.

ASHRAE (2015). ASHRAE handbook, HVAC Application. Atlanta, GA, American Society of Heating, Refrigerating and Air-conditioning Engineers, Inc.

DoD (2013a). Defense Budget Priorities and Choices, Fiscal Year 2014. Washington DC, Department of Defense.

DoD (2013b). Utilities Meter Policy. Washington DC, Department of Defense.

DOE (2011). 2010 Buildings Energy Data Book, Section 3.1.4.

DOE (2014). Executive Order 13514: Federal Leadership in Environmental, Energy, and Economic Performance. Washington, DC Federal Energy Management Program (FEMP).

IEEE. (2004). IEEE Standard 112-2004, IEEE standard test procedure for polyphase induction motors and generators. New York, IEEE Power Engineering Society.

Kiamehr, K., G. Wang, A. R. Prieto, W. M. Thomas and L. Song (2016). Evaluation of Fault Detection and Diagnosis Methods for Air and Water Distribution Systems. 2016 ASHRAE Annual Conference, St. Louis, MO.

Manz, L. B. and R. B. Morgan (1996). "Mating new variable frequency drives to existing motors." Electrical Construction & Maintenance **95**(3): 36-38.

Mills, E. (2011). "Building Commissioning: a golden opportunity for reducing energy costs and greenhouse gas emissions in the United States." Energy Efficiency **2011**(4): 145-173.

Shahahmadi, S. and L. Song (2018). "Valve Flowmeter Enhancement Through Computing Valve Dynamic Behaviors." ASHRAE Transactions **124**.

Song, L., I.-s. Joo and G. Wang (2012a). "Uncertainty analysis of a virtual water flow measurement in building energy consumption monitoring." HVAC&R Research **18**(5): 997-1010.

Song, L., A. Swamy, G. Shim and G. Wang (2011). Feasibility Study of Developing a Virtual Chilled Water Flow Meter at Air Handling Unit Level. International Conference of Enhanced Building Operation, New York City.

Song, L. and G. Wang (2013b). Uncertainty propagation in device characteristic based virtual sensors. Winter ASHRAE conference, Dallas TX.

Song, L. and G. Wang (2015). "Using a hybrid method to construct a computational efficient cooling coil model for an automated single-duct variable air volume system fault detection and diagnosis." Energy and Buildings **92**: 363-373.

Song, L., G. Wang and M. R. Brambley (2013a). "Uncertainty analysis for a virtual flow meter using an air-handling unit chilled water valve." HVAC&R Research **19**(3): 335-345.

Song, L., G. Wang, A. Swamy and G. Shim (2012b). In-Situ resistance coefficient curve and experimental analysis of a virtual chilled water flow meter at air handling unit level. ASME 2012 International Mechanical Engineering Congress and Exposition, Houston TX.

Swamy, A., L. Song and G. Wang (2012). "A virtual chilled water flow meter development at air handling unit level." ASHRAE Transactions **118**(1): 1013-1020.

Taasevigen, D. J., Y. Huang, R. Lutes, M. R. Bambley and L. Song (2012). Automated fault detection algorithms for use with a virtual chilled-water flow meter for air-handling units.

Wang, G., K. Kiamehr and L. Song (2016). "Development of a virtual pump water flow meter with a flow rate function of motor power and pump head." Energy and Buildings **117**: 63-70.

Wang, G. and M. Liu (2007). Development of motor power based fan airflow station. Energy Sustainability 2007, Long Beach, California.

Wang, G., M. Liu and D. E. Claridge (2010). "Development of an energy meter using a pump flow station

" ASHRAE Transactions **116**(2).

Wang, G., L. Song, E. Andiroglu and G. Shim (2014). "Investigations on a virtual airflow meter using projected motor and fan efficiencies." HVAC&R Research **20**(2): 178-187.

Wang, G., L. Song and S.-W. Park (2013). "Estimation of induction motor circuit parameters and efficiency under variable frequencies." ASHRAE Transactions **119**: 118.

Wang, G., Z. Wang and L. Song (2018). "Uncertainty Analysis for Different Virtual Pump Water Flow Meters. Science and Technology for the Built Environment." Science and Technology for the Built Environment **In press**.

WEG (2010). Technical Guide - Induction Motors Fed by PWM Frequency Inverters. S.A. Brazil, WEG ELECTRIC CORP.

APPENDIX A POINTS OF CONTACT

Point of Contact	Organization	Phone & E-mail	Role in Project
Li Song	OU	405.325.1714 lsong@ou.edu	Principal investigator
Gang Wang	UM	305.284.5555 g.wang2@miami.edu	Principal investigator
Michael Brambley	PNNL	509.375.6875 Michael.Brambley@pnnl.gov	Principal investigator
Benny Sisson	ABS	405.948.1794 Benny.sission@abscompanies.com	Contractor for equipment installation
Russell Jennings	Tinker AFB	405.734.7222 Russell.jennings@us.af.mil	Tinker Air Force Base energy manager
Deborah Burge	Tinker AFB	405.582.6100 Deborah.burge@us.af.mil	Facility manager of the demonstration building

Page Intentionally Left Blank

APPENDIX B PDD USER SURVEY FORM

Your experience with the product is an important aspect to consider in understanding how it is used and how well it works for its intended purpose. Please respond to the following survey items while thinking of the training provided, the performance of the product, and your overall experience.

Building Operator Survey

Q1 Please determine your level of agreement with each statement about the performance of the product.

	Strongly Disagree	Disagree	Neither Agree nor Disagree	Agree	Strongly Agree
1. The virtual meters monitor buildings effectively.	❍	❍	❍	❍	❍
2. The alarms are accurate.	❍	❍	❍	❍	❍
The product identifies faults correctly.	❍	❍	❍	❍	❍
3. The information provided by the product provides appropriate locations of faults.	❍	❍	❍	❍	❍
4. The information provided by the product is received timely.	❍	❍	❍	❍	❍
5. The product provides proper instructional information when the fault is indicated.	❍	❍	❍	❍	❍
6. When a problem is experienced with the product, it is easy to fix.	❍	❍	❍	❍	❍

Q2 Please determine your level of agreement with each statement about the impact this product has had on your daily work.

	Strongly Disagree	Disagree	Neither Agree nor Disagree	Agree	Strongly Agree
1. My work is completed more efficiently because of the product's use.	❍	❍	❍	❍	❍
2. I am more knowledgeable about my system operations.	❍	❍	❍	❍	❍
3. I am more knowledgeable about energy efficiency opportunities in my building.	❍	❍	❍	❍	❍

Q3 Please determine your level of agreement with each statement about the training provided.

	Strongly Disagree	Disagree	Neither Agree nor Disagree	Agree	Strongly Agree
1. The instructional manuals are easy to understand.	❍	❍	❍	❍	❍
2. The instructional training is offered often enough.	❍	❍	❍	❍	❍
3. The instructional training allows me to use the product the way it was intended to.	❍	❍	❍	❍	❍
4. Instructional training increases knowledge about the product.	❍	❍	❍	❍	❍

Q4 Please assess your overall evaluation of the product

	Strongly Disagree	Disagree	Neither Agree nor Disagree	Agree	Strongly Agree
1. I would recommend the product in some of buildings I operate.	❍	❍	❍	❍	❍
2. I would recommend the product in all the buildings I operate.	❍	❍	❍	❍	❍

Building Administrator Survey

Q1 Please determine your level of agreement with each statement

	Strongly Disagree	Disagree	Neither Agree nor Disagree	Agree	Strongly Agree
1. This product reduces the utility bills.	❍	❍	❍	❍	❍
2. Use of the product increases the building operators' work efficiencies.	❍	❍	❍	❍	❍
3. This product increases building operators' knowledge level about the systems they maintain.	❍	❍	❍	❍	❍
4. The cost of implementing this product (including training, installations and workforce) offsets long-term cost of loss of energy.	❍	❍	❍	❍	❍
5. The implementation of this product increases awareness of energy conservation.	❍	❍	❍	❍	❍
6. Increased energy conservation awareness leads to more self-regulated energy use from the employees.	❍	❍	❍	❍	❍

Page Intentionally Left Blank

APPENDIX C HVAC SYSTEM INFORMATION

C.1. AHU-1

1. Schematics

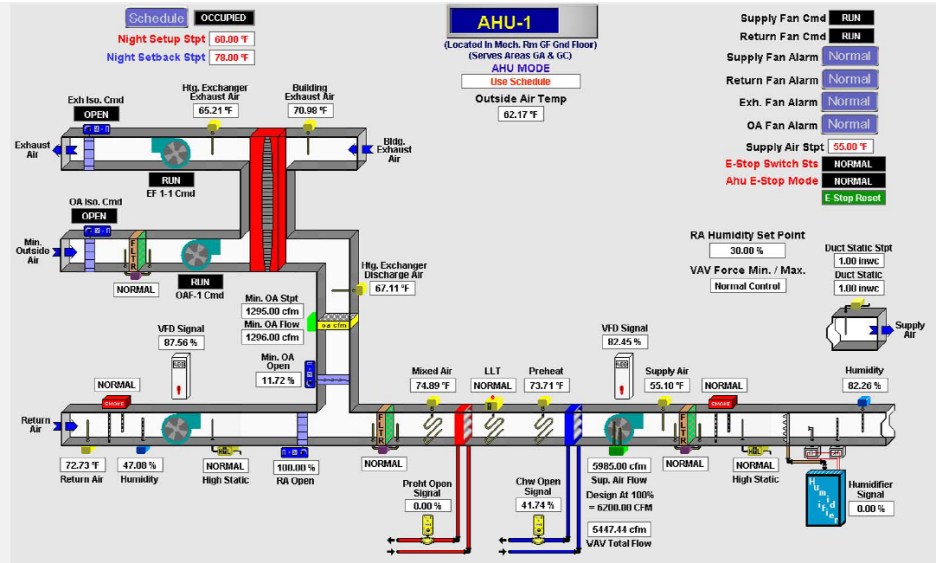

2. Design information

Supply air fan	Airflow (CFM)	6,200
	Motor power (HP)	10
	Voltage (V)/Phase	460/3
	Head (inch of water)	1.50
	VFD	Yes
	Duct size	D22
Return air fan	Return airflow (CFM)	4,905
	RF (HP)	2.0
	RF voltage (V)/PH	460/3
	RF Head (inch of water)	0.9
	VFD	Yes
	Duct size	36x18
Outdoor air fan	Outdoor airflow (CFM)	1,295
	OAF power (HP)	1.0
	OAF voltage (V)/PH	460/3
	OAF Head (inch of water)	1.6
	Duct size	20x10
	VFD	No
Relief air fan	EXF airflow (CFM)	1,020
	EXF power (HP)	1.0
	EXF voltage (V)/PH	460/3
	EXF Head (inch of water)	2.15
	Duct size	16x6
	VFD	No
Cooling coil	Capacity (MBH)	260
	Water flow (GPM)	43.2
	Pipe size (inch)	2 ½
	Coil DP (ft of water)	12
	Valve size	1-1/4

	Valve Cv	20
	Valve DP (ft of water)	11
Spare points	MNL-1	IN8
	MNL-2	None
	MNL-3	IN5 and IN6

3. AUH floor plan

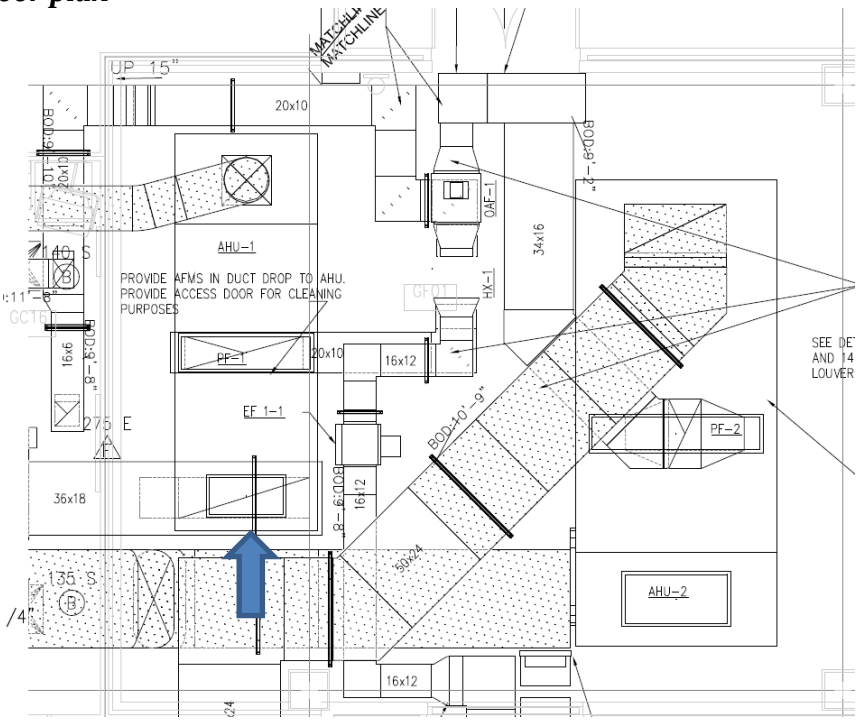

C.2. AHU-2

1. Schematics

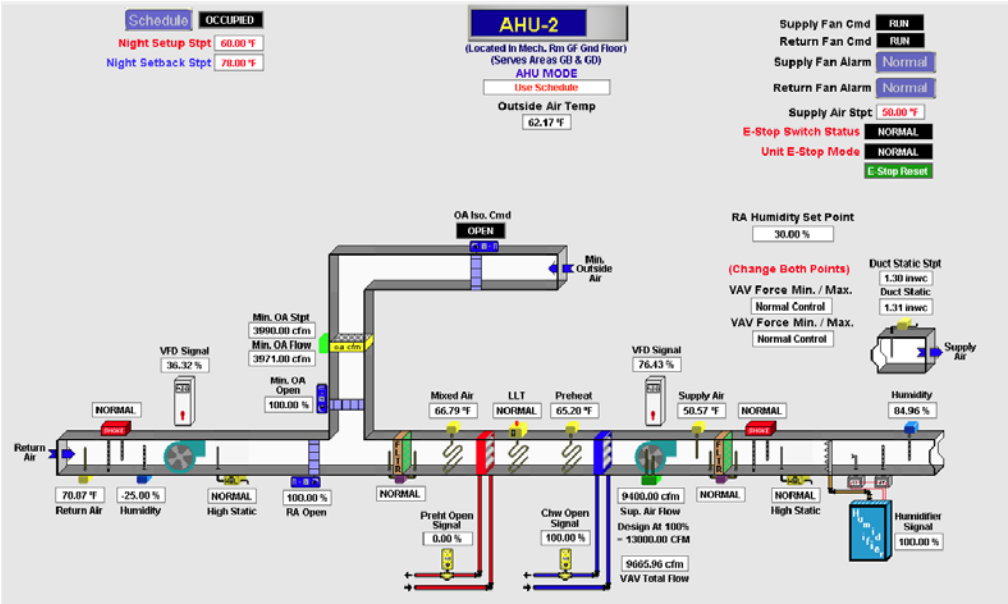

2. Design information

Supply air fan	Airflow (CFM)	13,000
	Motor power (HP)	20
	Voltage (V)/Phase	460/3
	Head(inch of water)	2.55
	VFD	Yes
	Duct size	48*20
Return air fan	Return airflow (CFM)	9,010
	RF (HP)	7.5
	RF voltage (V)/PH	460/3
	RF Head (inch of water)	1.75
	VFD	Yes
	Duct size	50*24
Outdoor air fan	Outdoor airflow (CFM)	3,990
	OAF power (HP)	N/A
	OAF voltage (V)/PH	N/A
	OAF Head (inch of water)	N/A
	Duct size	20*10
	VFD	N/A
Relief air fan	EXF airflow (CFM)	N/A
	EXF power (HP)	N/A
	EXF voltage (V)/PH	N/A
	EXF Head (inch of water)	N/A
	Duct size	N/A
	VFD	N/A
Cooling coil	Capacity (MBH)	608
	Water flow (GPM)	101
	Pipe size (inch)	3
	Coil DP (ft of water)	14.6
	Valve size	2.00
	Valve Cv	40
	Valve DP(ft of water)	14.674
Spare points	MNL-4	None
	MNL-5	None

3. AUH floor plan

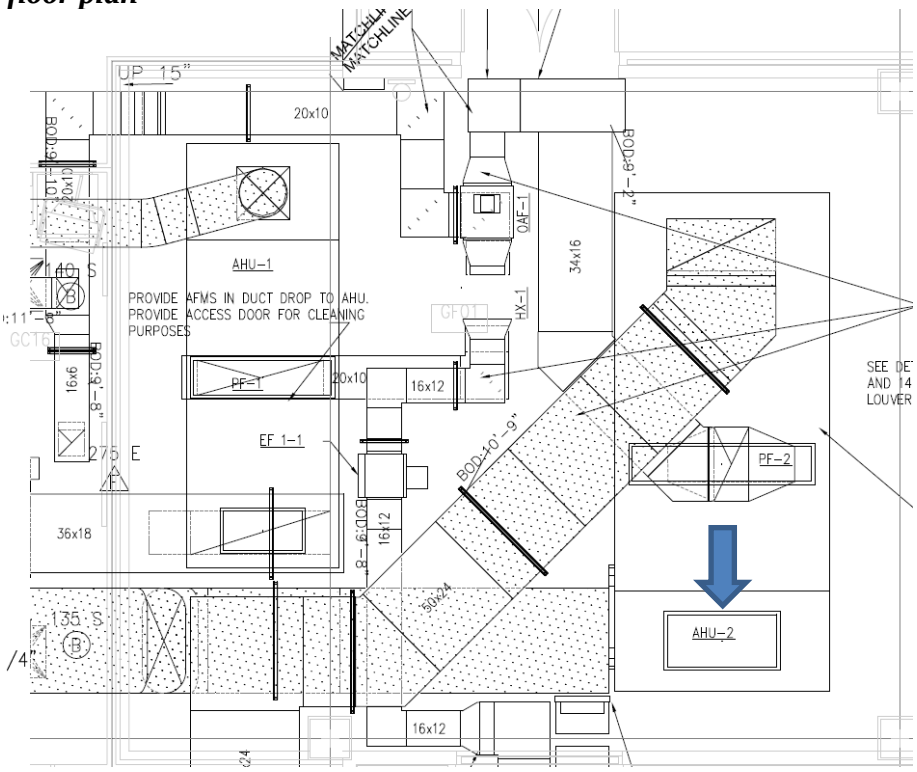

C.3. AHU-3

1. Schematics

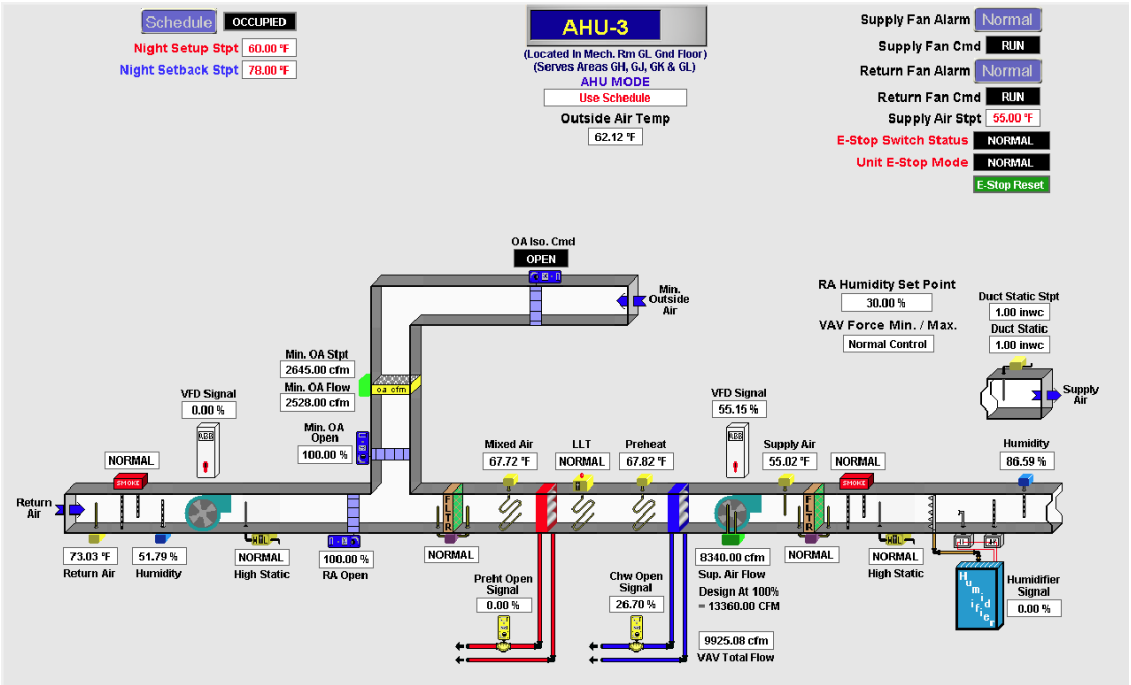

2. Design information

Supply air fan	Airflow (CFM)	13,380
	Motor power (HP)	25
	Voltage (V)/Phase	460/3
	Head(inch of water)	3
	VFD	Yes
	Duct size	48*20
Return air fan	Return airflow (CFM)	10,735
	RF (HP)	7.5
	RF voltage (V)/PH	460/3
	RF Head (inch of water)	1.5
	VFD	Yes
	Duct size	60*24
Outdoor air fan	Outdoor airflow (CFM)	2,645
	OAF power (HP)	N/A
	OAF voltage (V)/PH	N/A
	OAF Head (inch of water)	N/A
	Duct size	28*14
	VFD	N/A
Relief air fan	EXF airflow (CFM)	N/A
	EXF power (HP)	N/A
	EXF voltage (V)/PH	N/A
	EXF Head (inch of water)	N/A
	Duct size	N/A
	VFD	N/A
Cooling coil	Capacity (MBH)	572
	Water flow (GPM)	95
	Pipe size (inch)	3
	Coil DP (ft of water)	13
	Valve size	2.00
	Valve Cv	40
	Valve DP(ft of water)	12.972
Spare points	MNL-4	None
	MNL-5	IN4

3. AUH floor plan

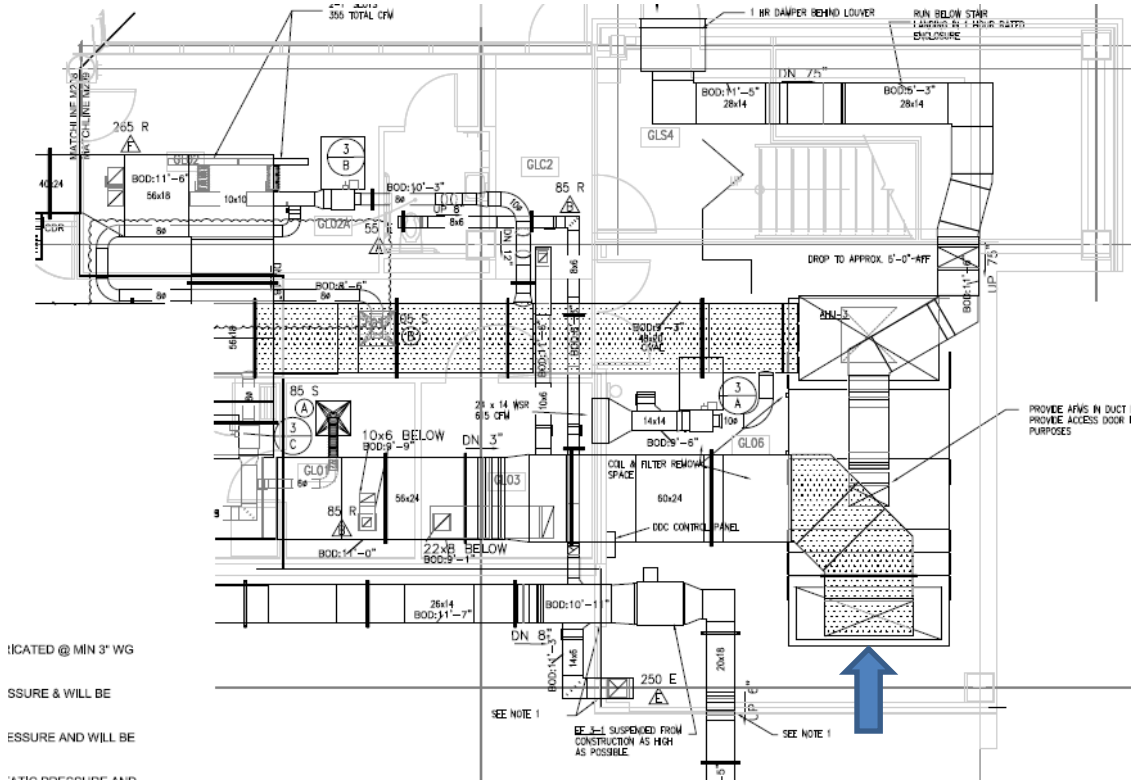

C.4. AHU-4

1. Schematics

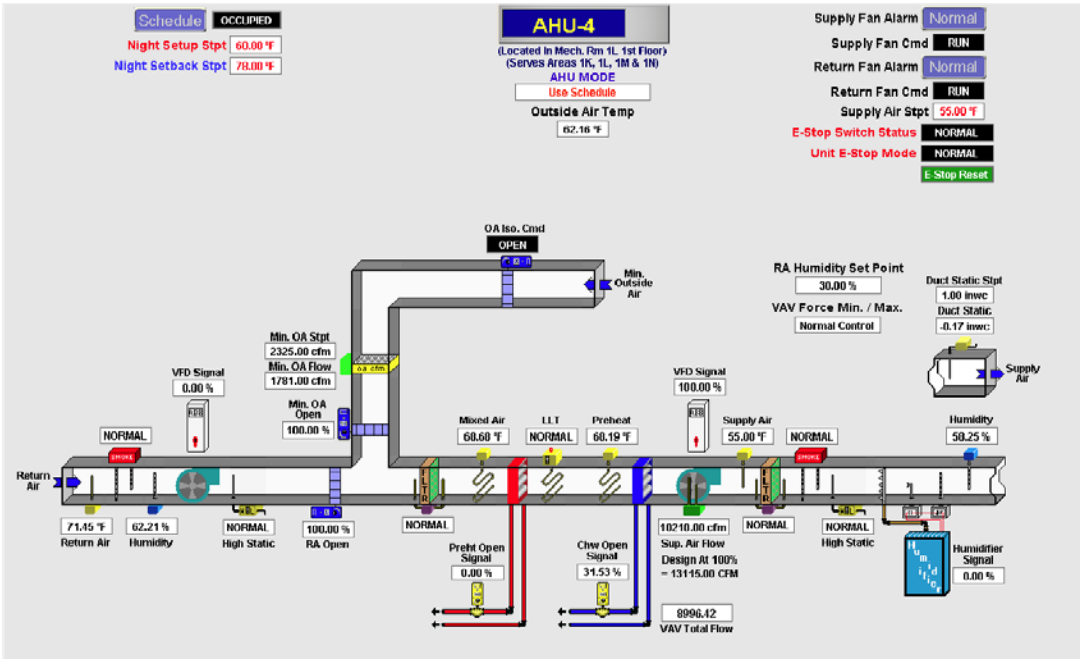

2. Design information

Supply air fan	Airflow (CFM)	13,115
	Motor power (HP)	20
	Voltage (V)/Phase	460/3
	Head (inch of water)	2.65
	VFD	Yes
	Duct size	D32
Return air fan	Return airflow (CFM)	10,750
	RF (HP)	7.5
	RF voltage (V)/PH	460/3
	RF Head (inch of water)	1.1
	VFD	Yes
	Duct size	30*30(to 3 branches: 24*16 / 30*14 & 30*22)
Outdoor air fan	Outdoor airflow (CFM)	2,365
	OAF power (HP)	N/A
	OAF voltage (V)/PH	N/A
	OAF Head (inch of water)	N/A
	Duct size	26*14
	VFD	N/A
Relief air fan	EXF airflow (CFM)	N/A
	EXF power (HP)	N/A
	EXF voltage (V)/PH	N/A
	EXF Head (inch of water)	N/A
	Duct size	N/A
	VFD	N/A
Cooling coil	Capacity (MBH)	555
	Water flow (GPM)	92.2
	Pipe size (inch)	3
	Coil DP (ft of water)	12.5
	Valve size	2.00
	Valve Cv	40
	Valve DP (ft of water)	12.213
Spare points	MNL-1	None
	MNL-2	None

3. AUH floor plan

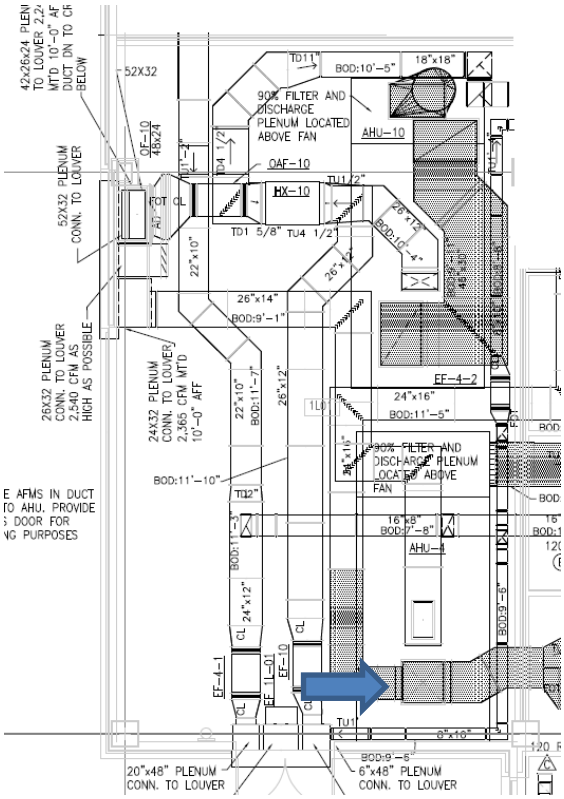

C.5. AHU-5

1. Schematics

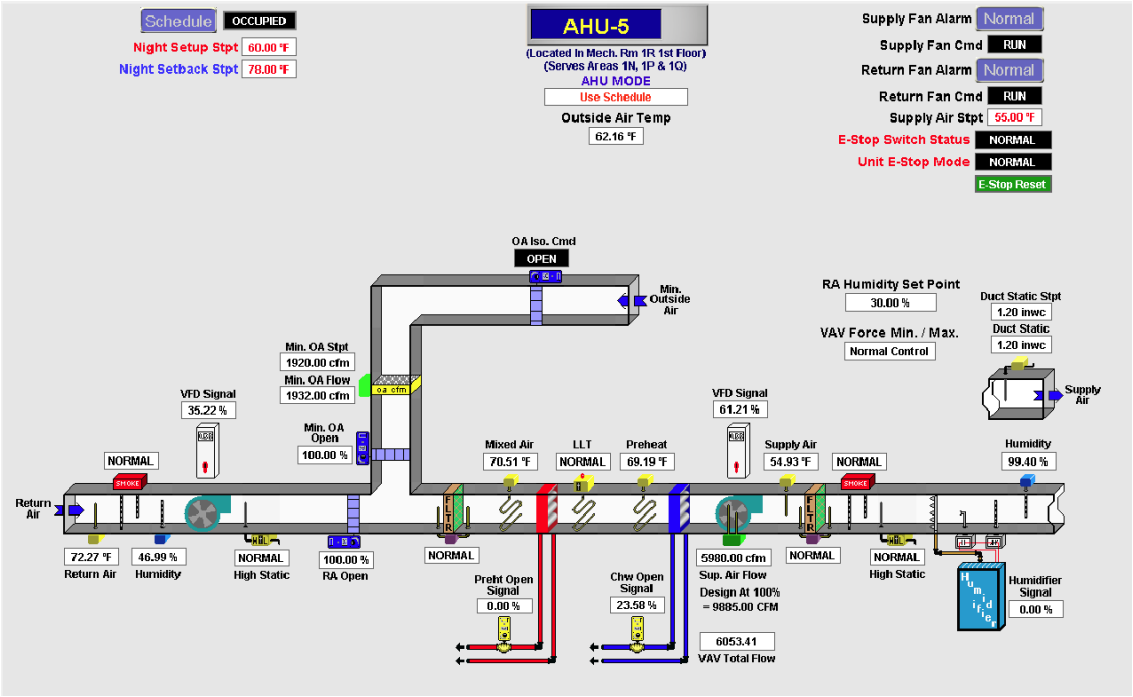

2. Design information

Supply air fan	Airflow (CFM)	9,885
	Motor power (HP)	15
	Voltage (V)/Phase	460/3
	Head (inch of water)	2.75
	VFD	Yes
	Duct size	36*20 oval
Return air fan	Return airflow (CFM)	7,965
	RF (HP)	5
	RF voltage (V)/PH	460/3
	RF Head (inch of water)	1.25
	VFD	Yes
	Duct size	30*28
Outdoor air fan	Outdoor airflow (CFM)	1,920
	OAF power (HP)	N/A
	OAF voltage (V)/PH	N/A
	OAF Head (inch of water)	N/A
	Duct size	20*14
	VFD	N/A
Relief air fan	EXF airflow (CFM)	N/A
	EXF power (HP)	N/A
	EXF voltage (V)/PH	N/A
	EXF Head (inch of water)	N/A
	Duct size	N/A
	VFD	N/A
Cooling coil	Capacity (MBH)	396
	Water flow (GPM)	65.8
	Pipe size (inch)	2 1/2
	Coil DP (ft of water)	7
	Valve size	2.00
	Valve Cv	40
	Valve DP (ft of water)	6.233
Spare points	MNL-1	None
	MNL-2	None

3. AUH floor plan

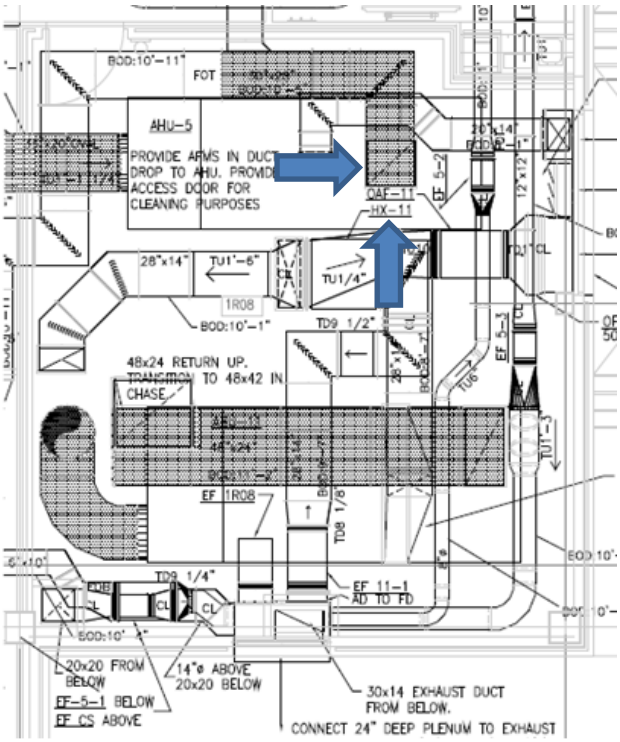

C.6. AHU-6

1. Schematics

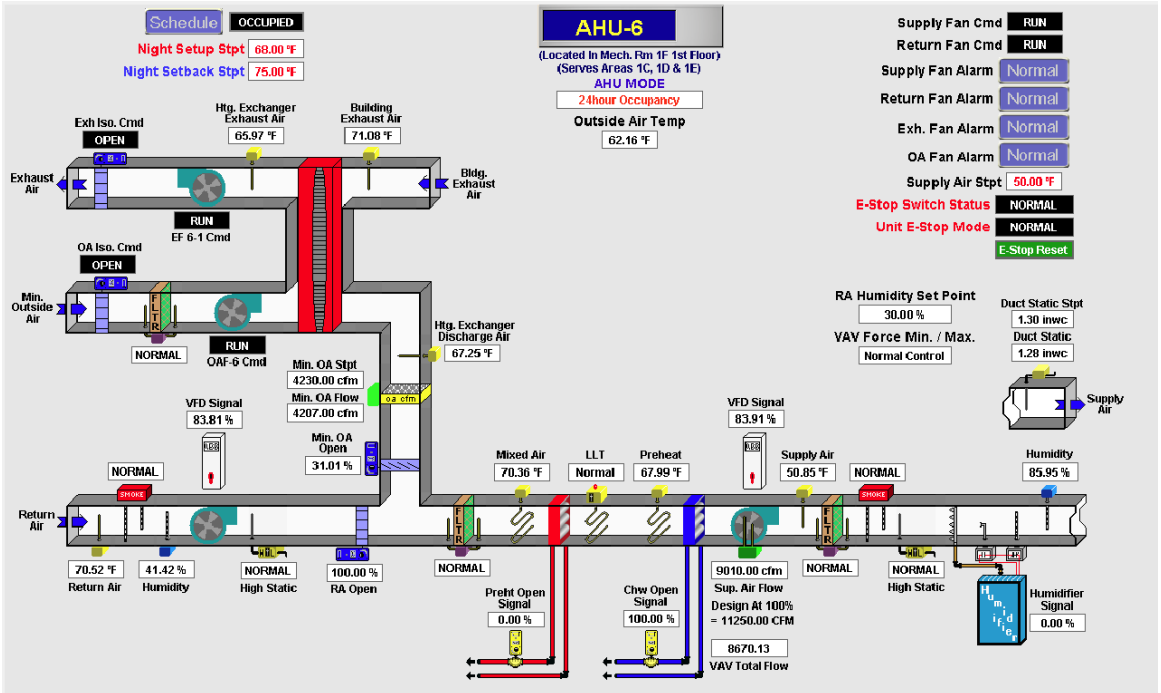

2. Design information

Supply air fan	Airflow (CFM)	11,250
	Motor power (HP)	15
	Voltage (V)/Phase	460/3
	Head (inch of water)	1.5
	VFD	Yes
	Duct size	46*18 oval
Return air fan	Return airflow (CFM)	7,020
	RF (HP)	3
	RF voltage (V)/PH	460/3
	RF Head (inch of water)	1.1
	VFD	Yes
	Duct size	24*14/24*22
Outdoor air fan	Outdoor airflow (CFM)	4,230
	OAF power (HP)	5
	OAF voltage (V)/PH	460/3
	OAF Head (inch of water)	2.05
	Duct size	20*48
	VFD	No
Relief air fan	EXF airflow (CFM)	3,225
	EXF power (HP)	3
	EXF voltage (V)/PH	460/3
	EXF Head (inch of water)	2.5
	Duct size	16*26
	VFD	No
Cooling coil	Capacity (MBH)	512
	Water flow (GPM)	84.1
	Pipe size (inch)	3
	Coil DP (ft of water)	13
	Valve size	2.00
	Valve Cv	40
	Valve DP (ft of water)	10.166
Spare points	MNL-1	None
	MNL-2	None
	MNL-3	IN5 and IN6

3. AUH floor plan

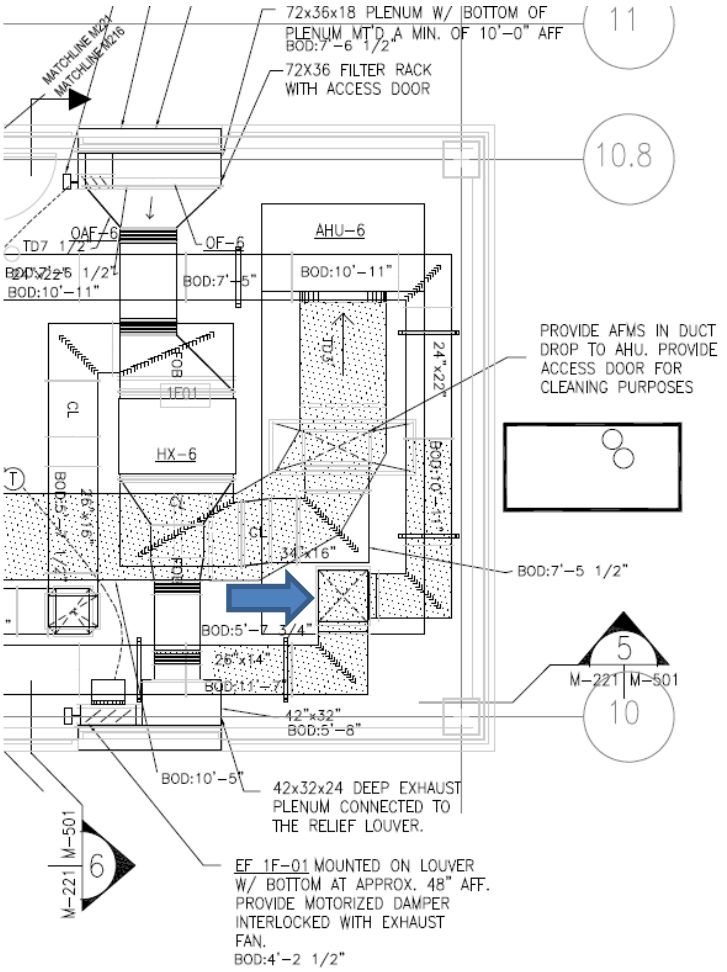

C.7. AHU-7

1. Schematics

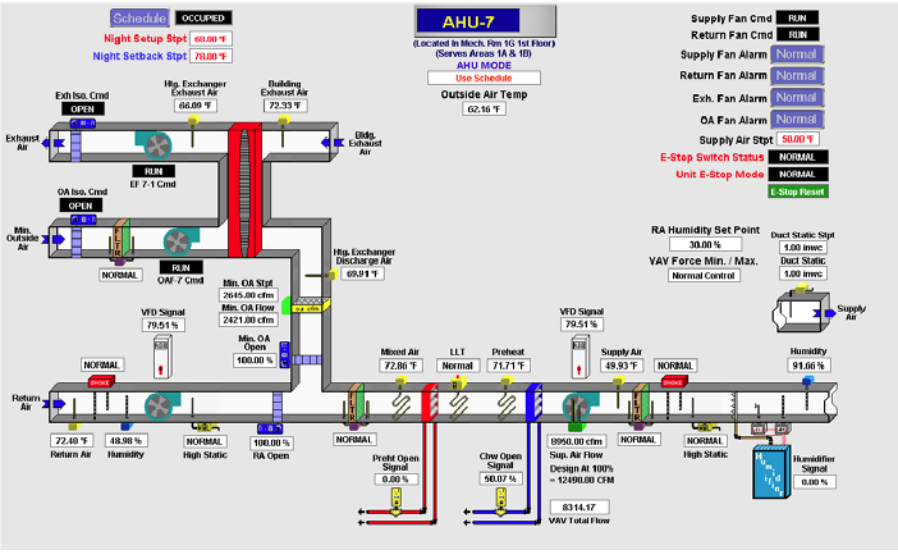

2. Design information

Supply air fan	Airflow (CFM)	12,490
	Motor power (HP)	15
	Voltage (V)/Phase	460/3
	Head (inch of water)	1.5
	VFD	Yes
	Duct size	48*20 oval
Return air fan	Return airflow (CFM)	9,845
	RF (HP)	7.5
	RF voltage (V)/PH	460/3
	RF Head (inch of water)	1.5
	VFD	Yes
	Duct size	42*24/20*18(the second one converts to 30*12)
Outdoor air fan	Outdoor airflow (CFM)	2,645
	OAF power (HP)	2
	OAF voltage (V)/PH	460/3
	OAF Head (inch of water)	1.9
	Duct size	14*30
	VFD	No
Relief air fan	EXF airflow (CFM)	2,430
	EXF power (HP)	1.5
	EXF voltage (V)/PH	460/3
	EXF Head (inch of water)	2.09
	Duct size	D24
	VFD	No
Cooling coil	Capacity (MBH)	512
	Water flow (GPM)	85.1
	Pipe size (inch)	3
	Coil DP (ft of water)	9
	Valve size	2.00
	Valve Cv	40
	Valve DP (ft of water)	10.419
Spare points	MNL-1	IN8
	MNL-2	None
	MNL-3	IN5 and IN6

3. AUH floor plan

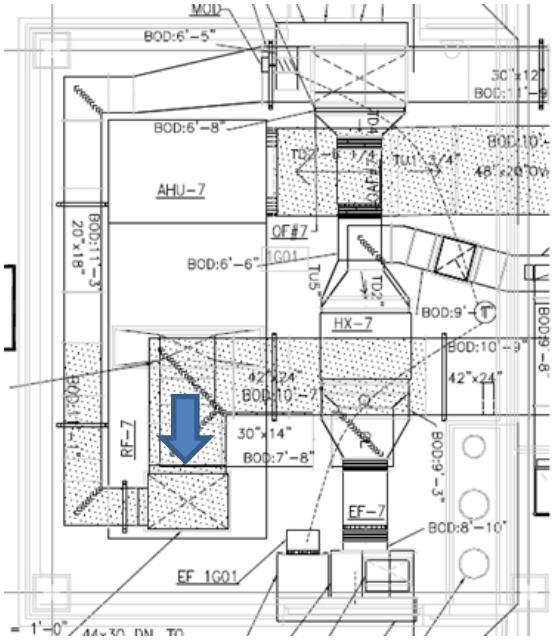

C.8. AHU-8

1. Schematics

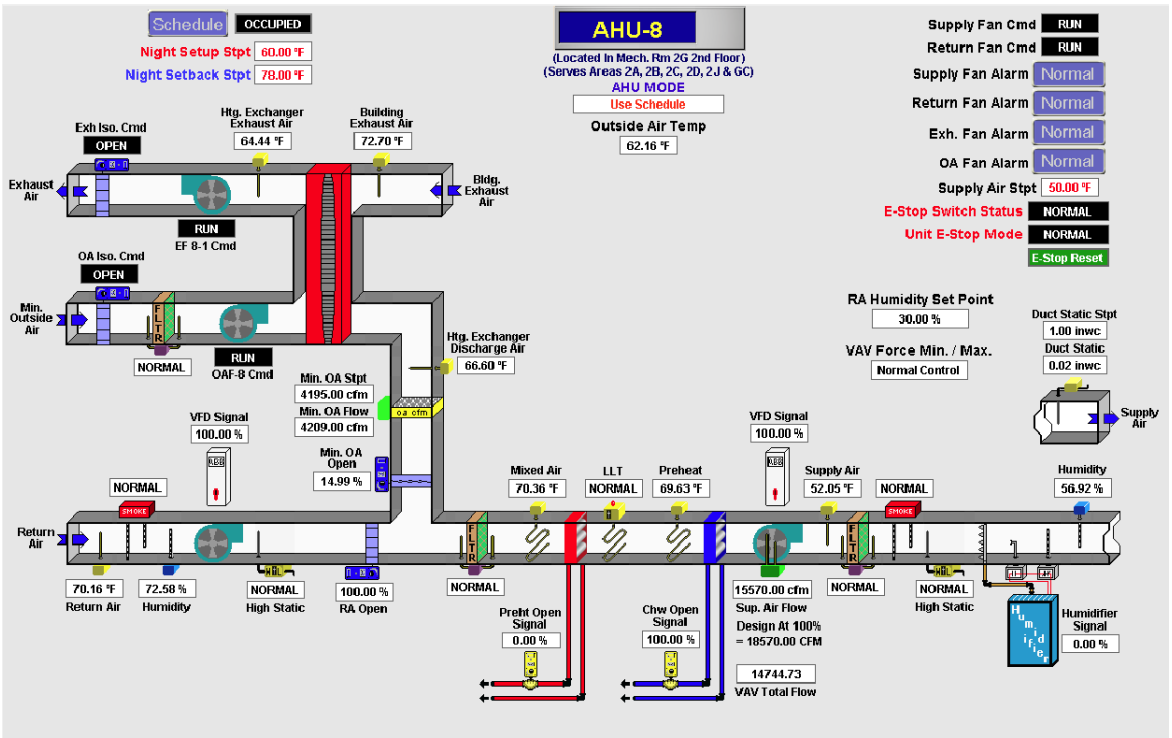

2. Design information

Supply air fan	Airflow (CFM)	18,570
	Motor power (HP)	25
	Voltage (V)/Phase	460/3
	Head (inch of water)	2
	VFD	Yes
	Duct size	D56x24 to D38
Return air fan	Return airflow (CFM)	15,065
	RF (HP)	10
	RF voltage (V)/PH	460/3
	RF Head (inch of water)	1.25
	VFD	Yes
	Duct size	48*28/16*30 to 24x20
Outdoor air fan	Outdoor airflow (CFM)	4,195
	OAF power (HP)	3
	OAF voltage (V)/PH	460/3
	OAF Head (inch of water)	1.3
	Duct size	42*14
	VFD	No
Relief air fan	EXF airflow (CFM)	4,025
	EXF power (HP)	3
	EXF voltage (V)/PH	460/3
	EXF Head (inch of water)	2.15
	Duct size	20*26
	VFD	No
Cooling coil	Capacity (MBH)	752
	Water flow (GPM)	129.9
	Pipe size (inch)	4
	Coil DP (ft of water)	17
	Valve size	2 1/2
	Valve Cv	56
	Valve DP (ft of water)	12.374
Spare points	MNL-1	None
	MNL-2	None
	MNL-3	IN6

3. AUH floor plan

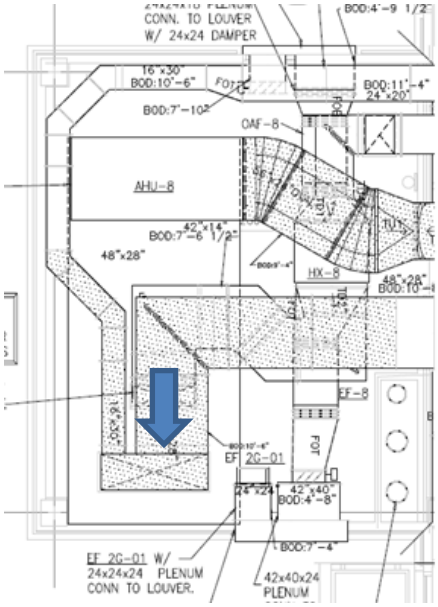

C.9. AHU-9

1. Schematics

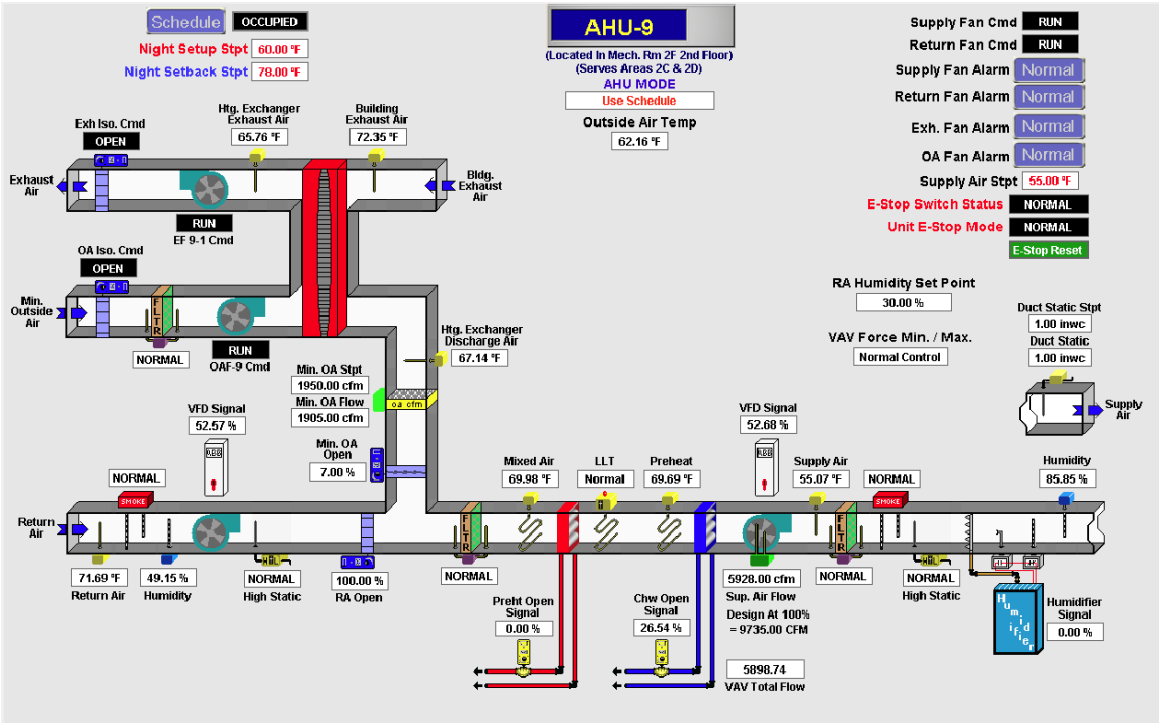

2. Design information

Supply air fan	Airflow (CFM)	9,735
	Motor power (HP)	15
	Voltage (V)/Phase	460/3
	Head (inch of water)	1.75
	VFD	Yes
	Duct size	44*16
Return air fan	Return airflow (CFM)	7,785
	RF (HP)	5
	RF voltage (V)/PH	460/3
	RF Head (inch of water)	1
	VFD	Yes
	Duct size	26*38
Outdoor air fan	Outdoor airflow (CFM)	1,950
	OAF power (HP)	1.5
	OAF voltage (V)/PH	460/3
	OAF Head (inch of water)	1.75
	Duct size	26*12
	VFD	No
Relief air fan	EXF airflow (CFM)	1,640
	EXF power (HP)	1.5
	EXF voltage (V)/PH	460/3
	EXF Head (inch of water)	2.2
	Duct size	12*26
	VFD	No
Cooling coil	Capacity (MBH)	399
	Water flow (GPM)	66.3
	Pipe size (inch)	3
	Coil DP (ft of water)	7
	Valve size	2
	Valve Cv	40
	Valve DP (ft of water)	6.325
Spare points	MNL-1	IN8
	MNL-2	None
	MNL-3	IN6

3. AUH floor plan

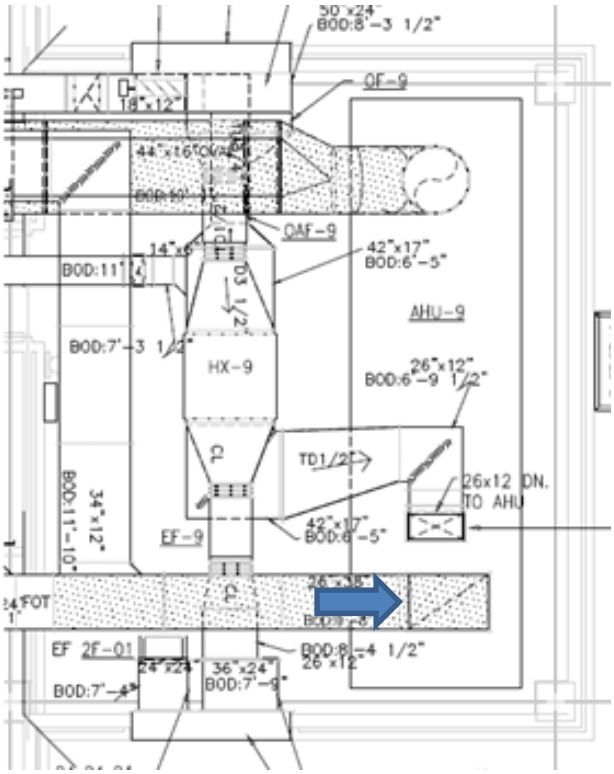

C.10. AHU-10

1. Schematics

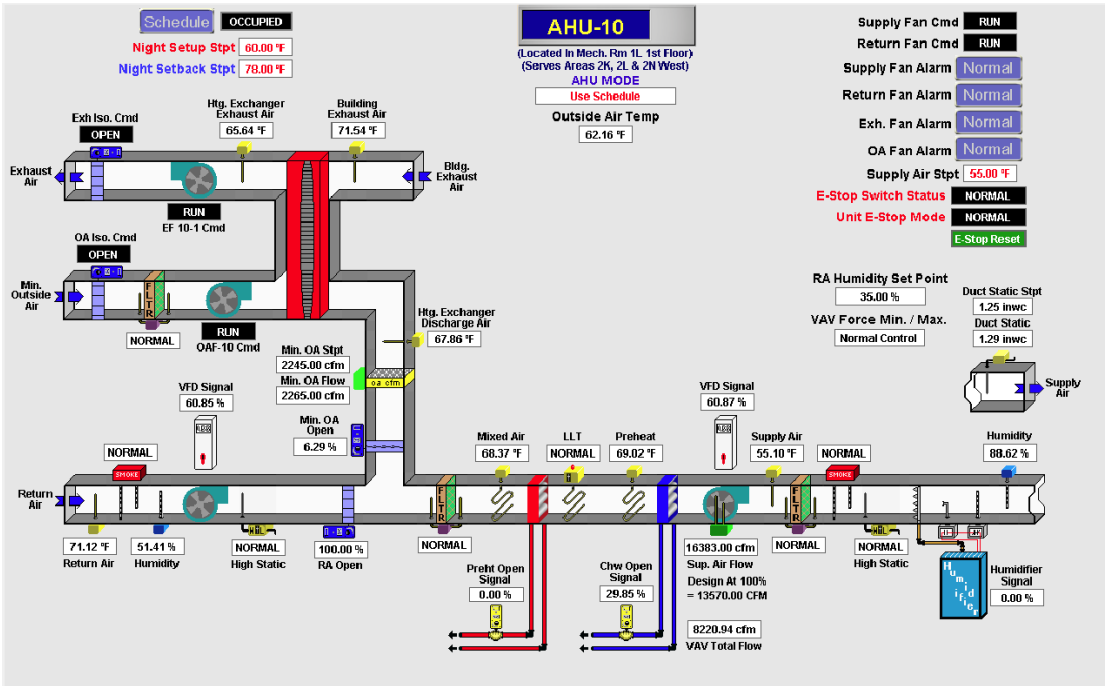

2. Design information

Supply air fan	Airflow (CFM)	13,570
	Motor power (HP)	20
	Voltage (V)/Phase	460/3
	Head (inch of water)	2
	VFD	Yes
	Duct size	D32
Return air fan	Return airflow (CFM)	11,325
	RF (HP)	7.5
	RF voltage (V)/PH	460/3
	RF Head (inch of water)	1.5
	VFD	Yes
	Duct size	46*30
Outdoor air fan	Outdoor airflow (CFM)	2,245
	OAF power (HP)	1.5
	OAF voltage (V)/PH	460/3
	OAF Head (inch of water)	1.85
	Duct size	26*12
	VFD	No
Relief air fan	EXF airflow (CFM)	2,105
	EXF power (HP)	2
	EXF voltage (V)/PH	460/3
	EXF Head (inch of water)	2.85
	Duct size	26*12
	VFD	No
Cooling coil	Capacity (MBH)	543
	Water flow (GPM)	90.2
	Pipe size (inch)	3
	Coil DP (ft of water)	11.9
	Valve size	2
	Valve Cv	40
	Valve DP (ft of water)	11.707
Spare points	MNL-3	IN8
	MNL-4	None
	MNL-5	IN6

3. AUH floor plan

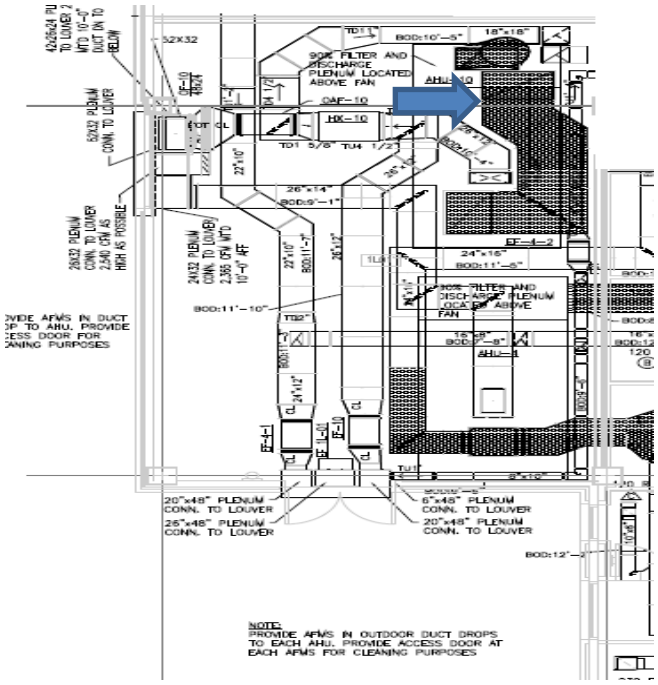

C.11. AHU-11

1. Schematics

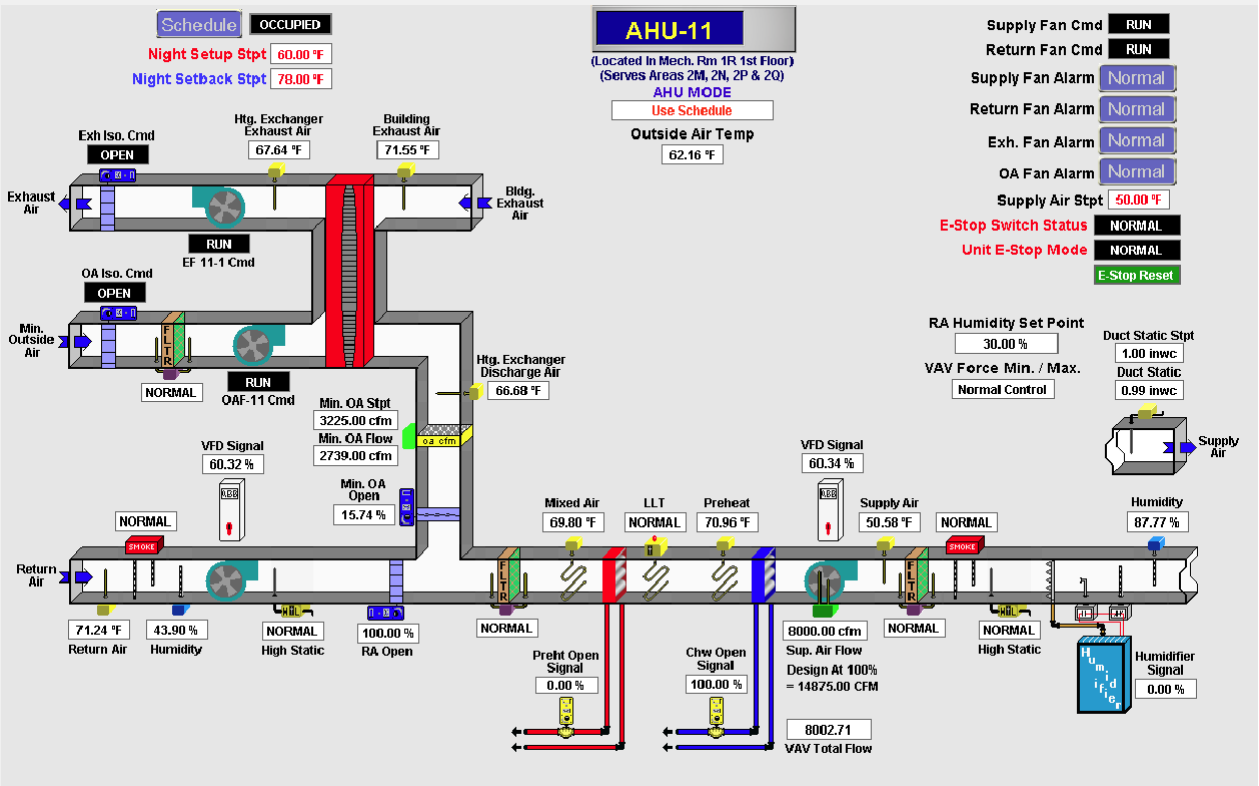

2. Design information

Supply air fan	Airflow (CFM)	14,875
	Motor power (HP)	20
	Voltage (V)/Phase	460/3
	Head (inch of water)	2
	VFD	Yes
	Duct size	D34
Return air fan	Return airflow (CFM)	11,725
	RF (HP)	7.5
	RF voltage (V)/PH	460/3
	RF Head (inch of water)	1.5
	VFD	Yes
	Duct size	48*24
Outdoor air fan	Outdoor airflow (CFM)	3,150
	OAF power (HP)	3
	OAF voltage (V)/PH	460/3
	OAF Head (inch of water)	2.15
	Duct size	14*28
	VFD	No
Relief air fan	EXF airflow (CFM)	2,685
	EXF power (HP)	3
	EXF voltage (V)/PH	460/3
	EXF Head (inch of water)	2.4
	Duct size	14*28
	VFD	No
Cooling coil	Capacity (MBH)	616
	Water flow (GPM)	102.3
	Pipe size (inch)	3
	Coil DP (ft of water)	13.5
	Valve size	2
	Valve Cv	40
	Valve DP(ft of water)	16.5462
Spare points	MNL-3	IN8
	MNL-4	None
	MNL-5	IN6
	MNL-6	None

3. AUH floor plan

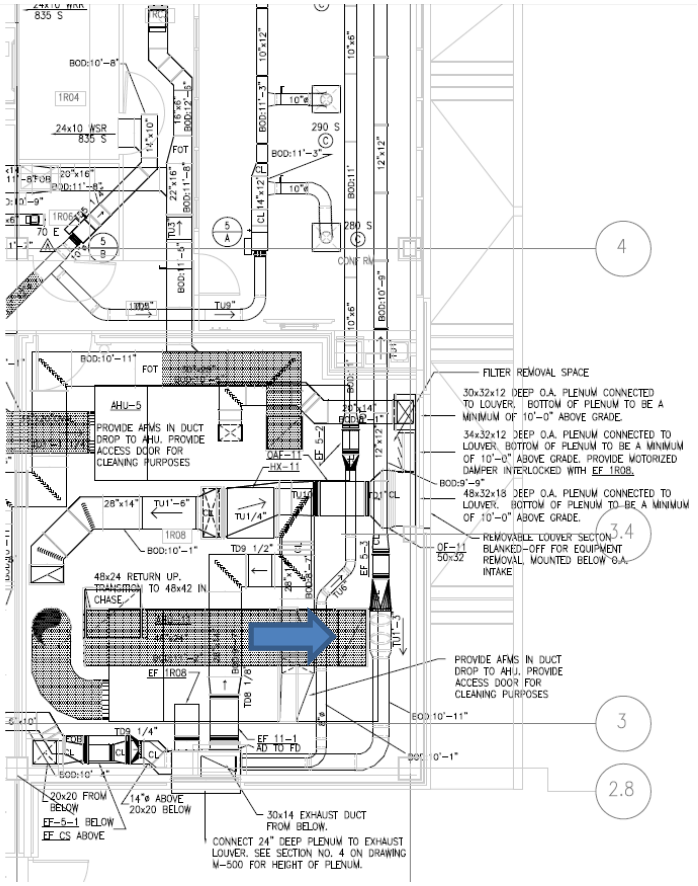

C.12. AHU-12

1. Schematics

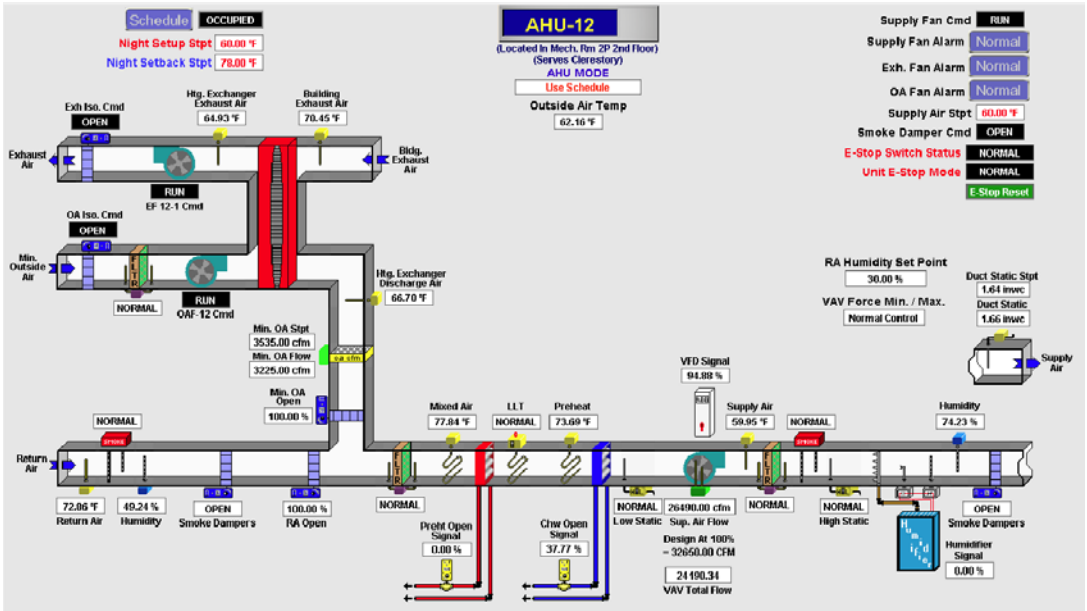

2. Design information

Supply air fan	Airflow (CFM)	32,650
	Motor power (HP)	40
	Voltage (V)/Phase	460/3
	Head (inch of water)	1.5
	VFD	Yes
	Duct size	D16/D16/D16/D20/D45
Return air fan	Return airflow (CFM)	N/A
	RF (HP)	N/A
	RF voltage (V)/PH	N/A
	RF Head (inch of water)	N/A
	VFD	N/A
	Duct size	N/A
Outdoor air fan	Outdoor airflow (CFM)	3,535
	OAF power (HP)	3
	OAF voltage (V)/PH	460/3
	OAF Head (inch of water)	2.75
	Duct size	?
	VFD	No
Relief air fan	EXF airflow (CFM)	2,340
	EXF power (HP)	2
	EXF voltage (V)/PH	460/3
	EXF Head (inch of water)	1.9
	Duct size	?
	VFD	No
Cooling coil	Capacity (MBH)	1279
	Water flow (GPM)	212.5
	Pipe size (inch)	4
	Coil DP (ft of water)	15.5
	Valve size	3
	Valve Cv	85
	Valve DP(ft of water)	14.375
Spare points	MNL-1	None
	MNL-2	None
	MNL-3	None

3. AUH floor plan

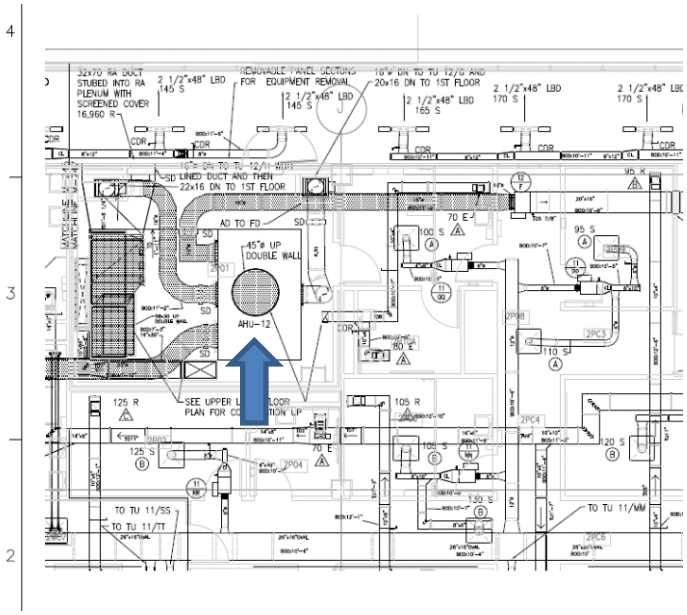

C.13. AHU-13

1. Schematics

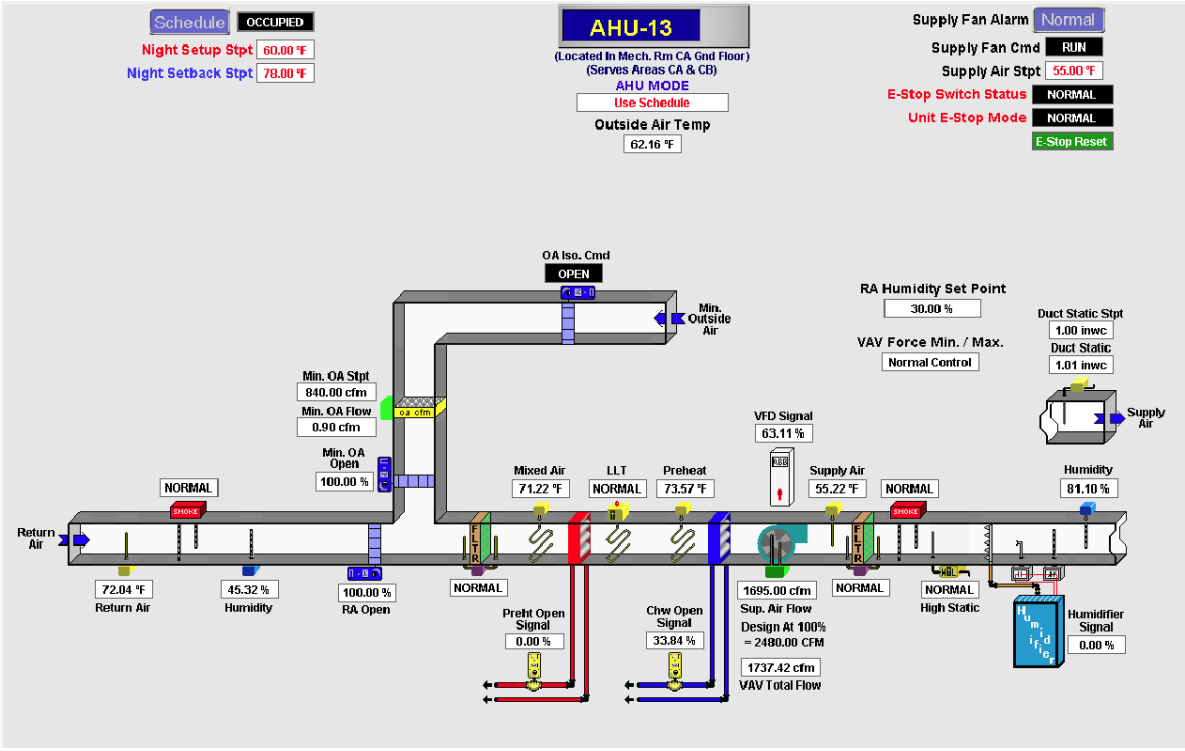

2. Design information

Supply air fan	Airflow (CFM)	2,480
	Motor power (HP)	5
	Voltage (V)/Phase	460/3
	Head (inch of water)	1.5
	VFD	Yes
	Duct size	D16
Return air fan	Return airflow (CFM)	N/A
	RF (HP)	N/A
	RF voltage (V)/PH	N/A
	RF Head (inch of water)	N/A
	VFD	N/A
	Duct size	28*10
Outdoor air fan	Outdoor airflow (CFM)	N/A
	OAF power (HP)	N/A
	OAF voltage (V)/PH	N/A
	OAF Head (inch of water)	N/A
	Duct size	14*12
	VFD	N/A
Relief air fan	EXF airflow (CFM)	N/A
	EXF power (HP)	N/A
	EXF voltage (V)/PH	N/A
	EXF Head (inch of water)	N/A
	Duct size	N/A
	VFD	N/A
Cooling coil	Capacity (MBH)	119.333
	Water flow (GPM)	23.9
	Pipe size (inch)	2
	Coil DP (ft of water)	10
	Valve size	3/4
	Valve Cv	10
	Valve DP (ft of water)	13.133
Spare points	MNL-4	IN8
	MNL-5	IN4

3. AUH floor plan

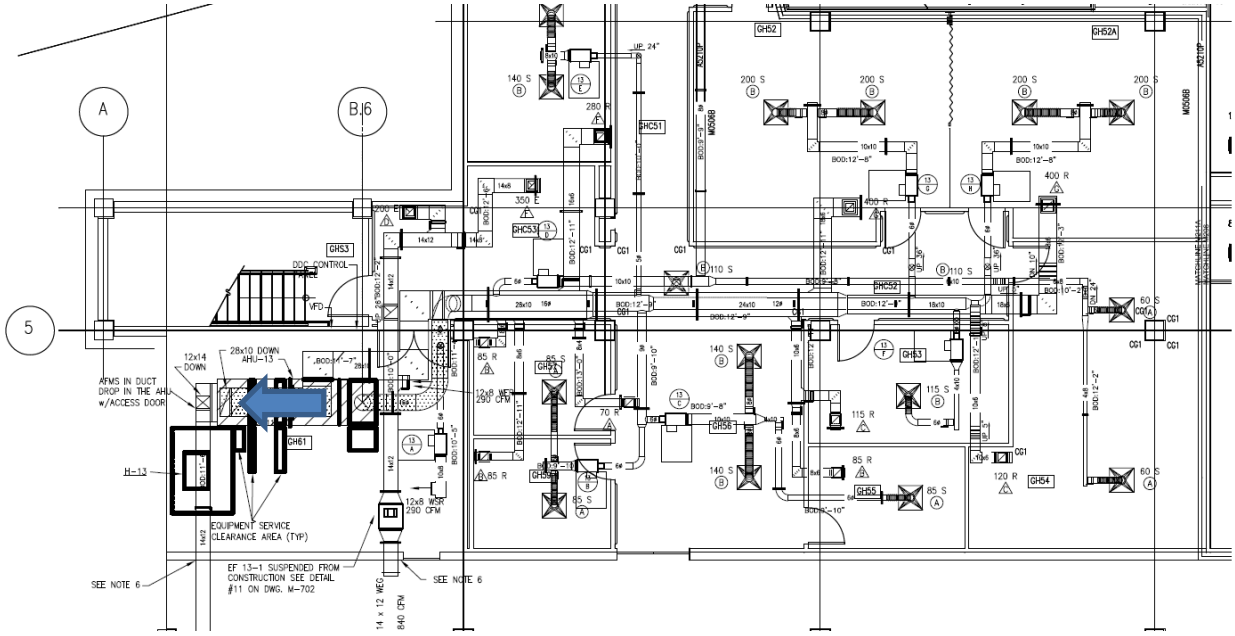

C.14. Chiller system

1. Schematics

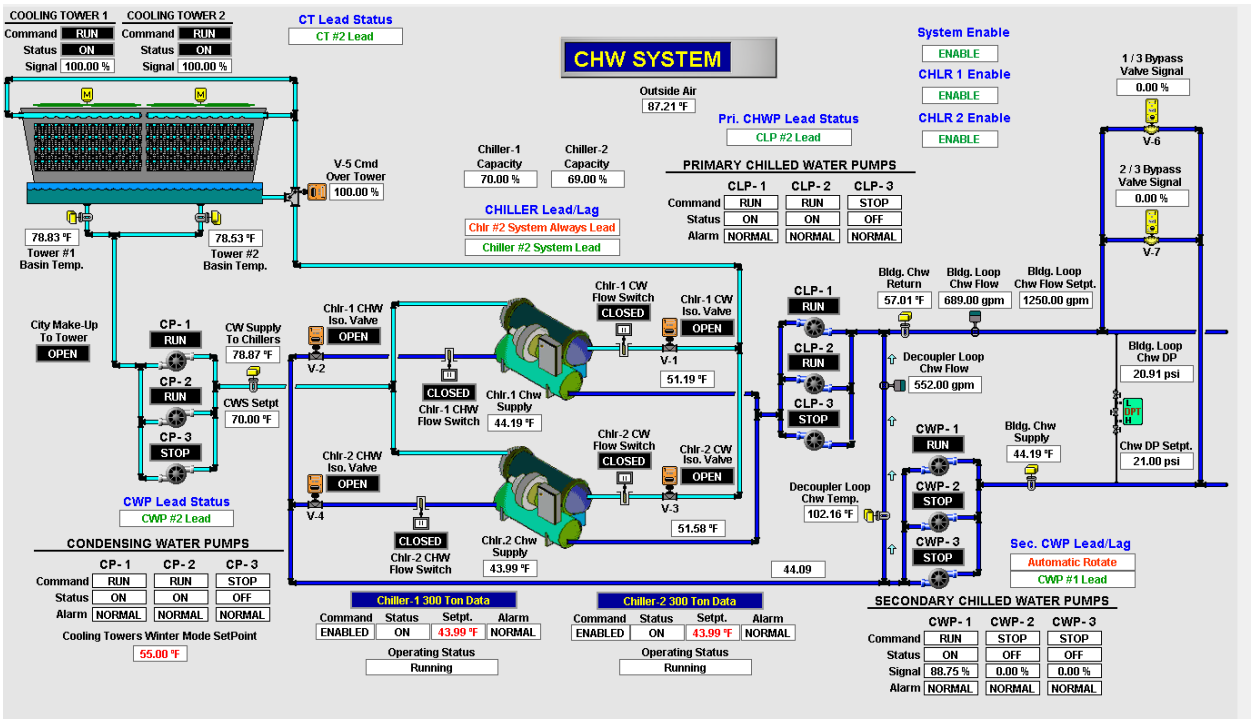

2. Design information

Primary pump (3)	Flow (GPM)	600
	Motor power (HP)	7.5
	Voltage (V)/Phase	460/3
	Head (ft of water)	32
	VFD	No
	Pipe size (inlet/outlet)	4” x4”
Secondary pump (3)	Flow (GPM)	600
	Motor (HP)	20
	Voltage (V)/PH	460/3
	Head (ft of water)	80
	VFD	Yes
	Pipe size(inlet/outlet)	6” x6”
Condensing pump (3)	Flow (GPM)	900
	Motor (HP)	20
	Voltage (V)/PH	460/3
	Head (ft of water)	68
	VFD	No
	Pipe size(inlet/outlet)	6” x5”

3. Chiller plant floor plan

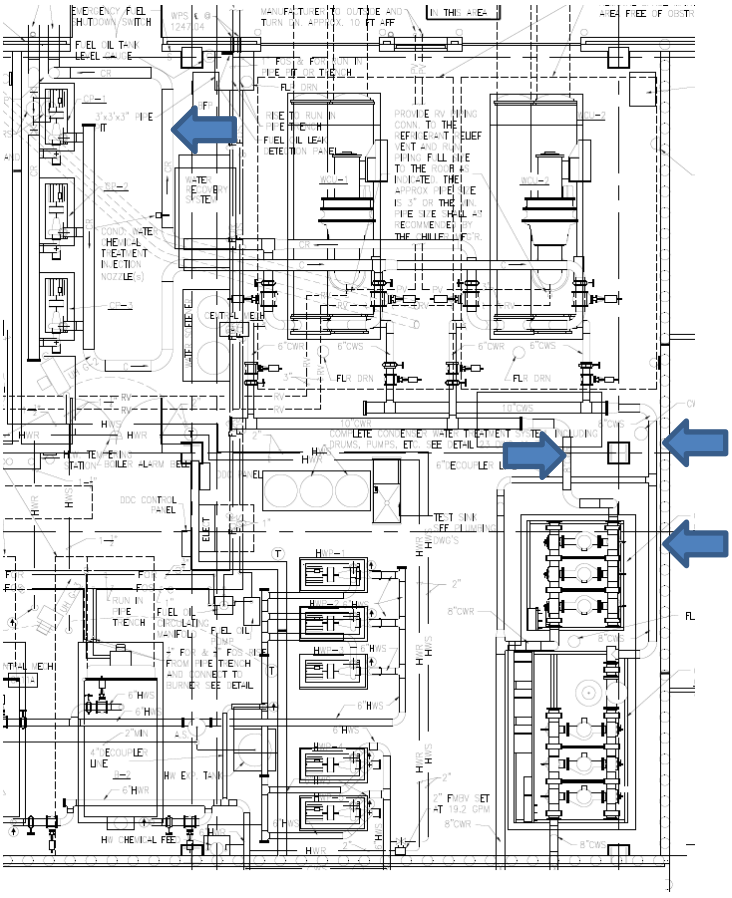

C.15. Hot water system

1. Schematics

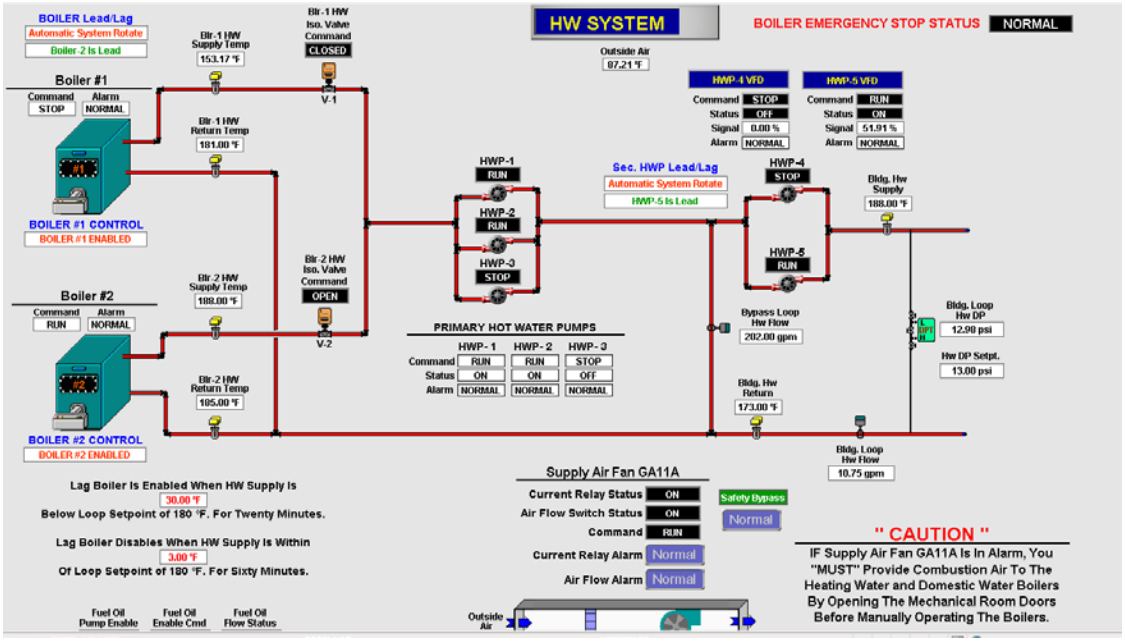

2. Design information

Primary pump (3)	Flow (GPM)	280
	Motor power (HP)	3
	Voltage (V)/Phase	460/3
	Head (ft of water)	27
	VFD	No
	Pipe size (inlet/outlet)	4” x3”
Secondary pump (2)	Flow (GPM)	560
	Motor (HP)	25
	Voltage (V)/PH	460/3
	Head (ft of water)	85
	VFD	Yes
	Pipe size(inlet/outlet)	5” x4”

3. Hot water plant floor plan

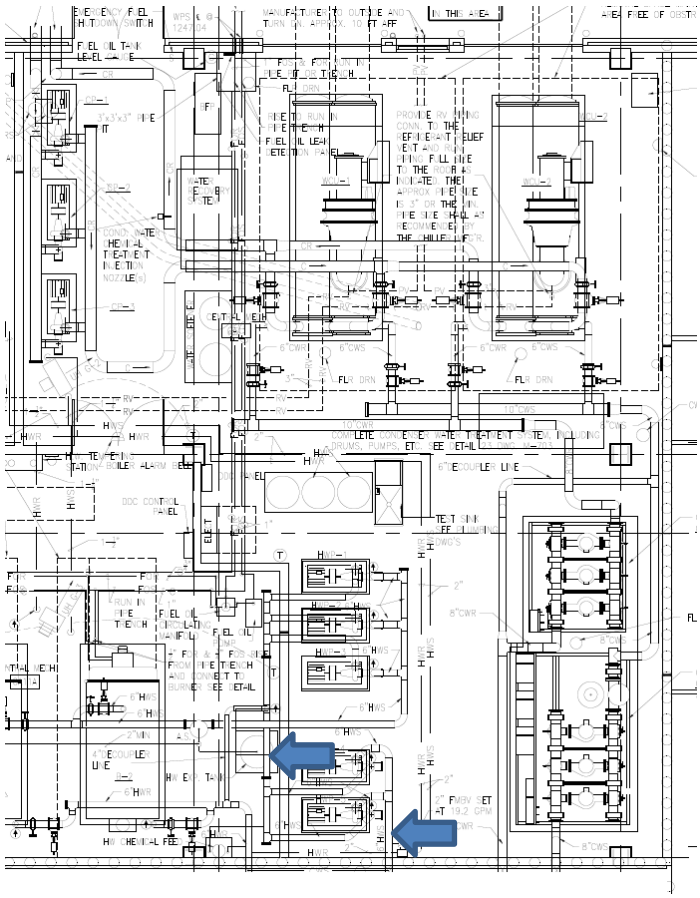

Page Intentionally Left Blank

APPENDIX D HVAC SYSTEM IMPLEMENTATION PLAN

D.1. AHU-1

Sensor	Air pressure	5 inch of water (1.5)	Supply fan head
	Air pressure	5 inch of water (0.9)	Return fan head
	Water pressure	20 Psig (10)	Coil/valve
	Water temperature		CHW supply
	Water temperature		CHW return
Controller	Air pressure	AI	Supply fan head
	VFD power	AI	Supply fan power
	Air pressure	AI	Return fan head
	VFD power	AI	Return fan power
	Water pressure	AI	Coil/valve
	Water temperature	AI	CHW supply
	Water temperature	AI	CHW return

D.2. AHU-2

Sensor	Air pressure	5 inch of water (2.5)	Supply fan head
	Air pressure	5 inch of water (1.75)	Return fan head
	Water pressure	20 Psig (13)	*Coil/valve*
	Water temperature		CHW supply
	Water temperature		CHW return
Controller	Air pressure	AI	Supply fan head
	VFD power	AI	Supply fan power
	Air pressure	AI	Return fan head
	VFD power	AI	Return fan power
	Water pressure	AI	Coil/valve
	Water temperature	AI	CHW supply
	Water temperature	AI	CHW return

D.3. AHU-3

Sensor	Air pressure	5 inch of water (3)	Supply fan head
	Air pressure	5 inch of water (1.5)	Return fan head
	Water pressure	20 Psig (11.29)	Coil/valve
	Water temperature		CHW supply
	Water temperature		CHW return
Controller	Air pressure	AI	Supply fan head
	VFD power	AI	Supply fan power
	Air pressure	AI	Return fan head
	VFD power	AI	Return fan power
	Water pressure	AI	Coil/valve
	Water temperature	AI	CHW supply
	Water temperature	AI	CHW return

D.4. AHU-4

Sensor	Air pressure	5 inch of water (2.65)	Supply fan head
	Air pressure	5 inch of water (1.1)	Return fan head
	Water pressure	20 Psig (10.74)	Coil/valve
	Water temperature		CHW supply
	Water temperature		CHW return
Controller	Air pressure	AI	Supply fan head
	VFD power	AI	Supply fan power
	Air pressure	AI	Return fan head
	VFD power	AI	Return fan power
	Water pressure	AI	Coil/valve
	Water temperature	AI	CHW supply
	Water temperature	AI	CHW return

D.5. AHU-5

Sensor	Air pressure	5 inch of water (2.75)	Supply fan head
	Air pressure	5 inch of water (1.25)	Return fan head
	Water pressure	20 Psig (5.75)	Coil/valve
	Water temperature		CHW supply
	Water temperature		CHW return
Controller	Air pressure	AI	Supply fan head
	VFD power	AI	Supply fan power
	Air pressure	AI	Return fan head
	VFD power	AI	Return fan power
	Water pressure	AI	Coil/valve
	Water temperature	AI	CHW supply
	Water temperature	AI	CHW return

D.6. AHU-6

Sensor	Air pressure	5 inch of water (1.5)	Supply fan head
	Air pressure	5 inch of water (1.1)	Return fan head
	Water pressure	20 Psig (10.07)	Coil/valve
	Water temperature		CHW supply
	Water temperature		CHW return
Controller	Air pressure	AI	Supply fan head
	VFD power	AI	Supply fan power
	Air pressure	AI	Return fan head
	VFD power	AI	Return fan power
	Water pressure	AI	Coil/valve
	Water temperature	AI	CHW supply
	Water temperature	AI	CHW return

D.7. AHU-7

Sensor	Air pressure	5 inch of water (1.5)	Supply fan head
	Air pressure	5 inch of water (1.5)	Return fan head
	Water pressure	20 Psig (8.44)	Coil/valve
	Water temperature		CHW supply
	Water temperature		CHW return
Controller	Air pressure	AI	Supply fan head
	VFD power	AI	Supply fan power
	Air pressure	AI	Return fan head
	VFD power	AI	Return fan power
	Water pressure	AI	Coil/valve
	Water temperature	AI	CHW supply
	Water temperature	AI	CHW return

D.8. AHU-8

Sensor	Air pressure	5 inch of water (2)	Supply fan head
	Air pressure	5 inch of water (1.25)	Return fan head
	Water pressure	20 Psig (12.77)	Coil/valve
	Water temperature		CHW supply
	Water temperature		CHW return
Controller	Air pressure	AI	Supply fan head
	VFD power	AI	Supply fan power
	Air pressure	AI	Return fan head
	VFD power	AI	Return fan power
	Water pressure	AI	Coil/valve
	Water temperature	AI	CHW supply
	Water temperature	AI	CHW return

D.9. AHU-9

Sensor	Air pressure	5 inch of water (1.75)	Supply fan head
	Air pressure	5 inch of water (1)	Return fan head
	Water pressure	20 Psig (5.79)	Coil/valve
	Water temperature		CHW supply
	Water temperature		CHW return
Controller	Air pressure	AI	Supply fan head
	VFD power	AI	Supply fan power
	Air pressure	AI	Return fan head
	VFD power	AI	Return fan power
	Water pressure	AI	Coil/valve
	Water temperature	AI	CHW supply
	Water temperature	AI	CHW return

D.10. AHU-10

Sensor	Air pressure	5 inch of water (2)	Supply fan head
	Air pressure	5 inch of water (1.5)	Return fan head
	Water pressure	20 Psig (10.26)	Coil/valve
	Water temperature		CHW supply
	Water temperature		CHW return
Controller	Air pressure	AI	Supply fan head
	VFD power	AI	Supply fan power
	Air pressure	AI	Return fan head
	VFD power	AI	Return fan power
	Water pressure	AI	Coil/valve
	Water temperature	AI	CHW supply
	Water temperature	AI	CHW return

D.11. AHU-11

Sensor	Air pressure	5 inch of water (2)	Supply fan head
	Air pressure	5 inch of water (1.5)	Return fan head
	Water pressure	20 Psig (13.06)	Coil/valve
	Water temperature		CHW supply
	Water temperature		CHW return
Controller	Air pressure	AI	Supply fan head
	VFD power	AI	Supply fan power
	Air pressure	AI	Return fan head
	VFD power	AI	Return fan power
	Water pressure	AI	Coil/valve
	Water temperature	AI	CHW supply
	Water temperature	AI	CHW return

D.12. AHU-12

Sensor	Air pressure	5 inch of water (1.5)	Supply fan head
	Water pressure	20 Psig (12.99)	Coil/valve
	Water temperature		CHW supply
	Water temperature		CHW return
Controller	Air pressure	AI	Supply fan head
	VFD power	AI	Supply fan power
	Water pressure	AI	Coil/valve
	Water temperature	AI	CHW supply
	Water temperature	AI	CHW return

D.13. AHU-13

Sensor	Air pressure	5 inch of water (1.5)	Supply fan head
	Water pressure	20 Psig (10.06)	Coil/valve
	Water temperature		CHW supply
	Water temperature		CHW return
Controller	Air pressure	AI	Supply fan head
	VFD power	AI	Supply fan power
	Water pressure	AI	Coil/valve
	Water temperature	AI	CHW supply
	Water temperature	AI	CHW return

D.14. Chiller system

Sensors	Water pressure (3)	20 Psig (13.4)	Primary pump head
	Water pressure (3)	40 Psig (35)	Secondary pump head
	Water pressure (3)	40Psig (30)	Condensing pump head
Hardware	VFD (3)	7.5HP 460/3	Primary pumps
	VFD (3)	20HP 460/3	Condensing pumps
Controller	Water pressure (3)	AI	Primary pump head
	VFD power (3)	AI	Primary pump power
	VFD speed (3)	AO	Primary pump speed
	Water pressure (3)	AI	Secondary pump head
	VFD power (3)	AI	Secondary pump power
	Water pressure (3)	AI	Condensing pump head
	VFD power (3)	AI	Condensing pump power
	VFD speed (3)	AO	Condensing pump speed

D.15. Hot water system

Sensors	Water pressure (3)	40 Psig (37)	Secondary pump head
Controller	Water pressure (3)	AI	Secondary pump head
	VFD power (3)	AI	Secondary pump power

Page Intentionally Left Blank

APPENDIX E THE MID-PROGRESS REPORT OF VIRTUAL FAN AIRFLOW METERS

E.1. AHU1

1. Supply fan

   a. Flow validation comparison (measured v.s. calculated) chart

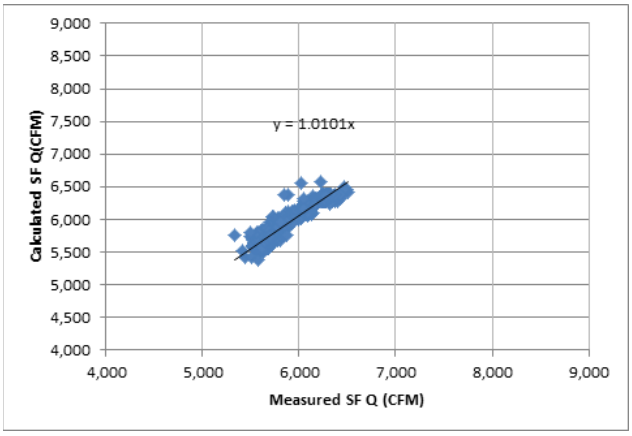

   b. Validation in the time series chart

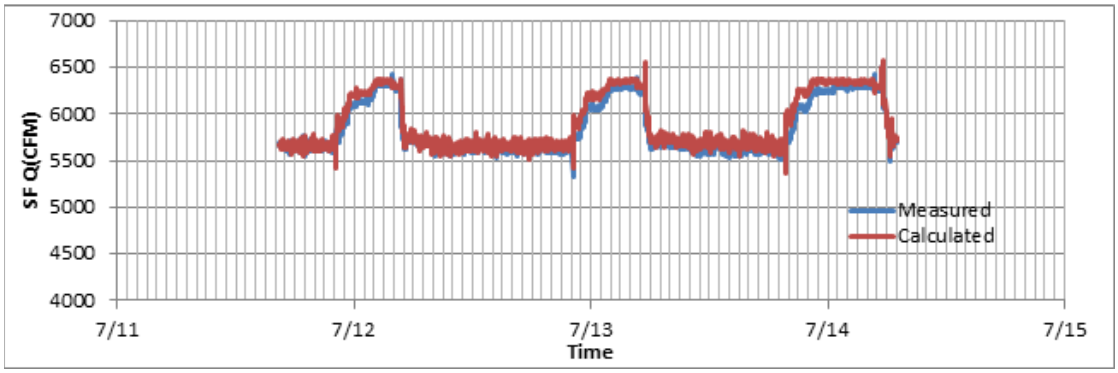

2. Return fan

   a. Flow validation comparison (measured v.s. calculated) chart

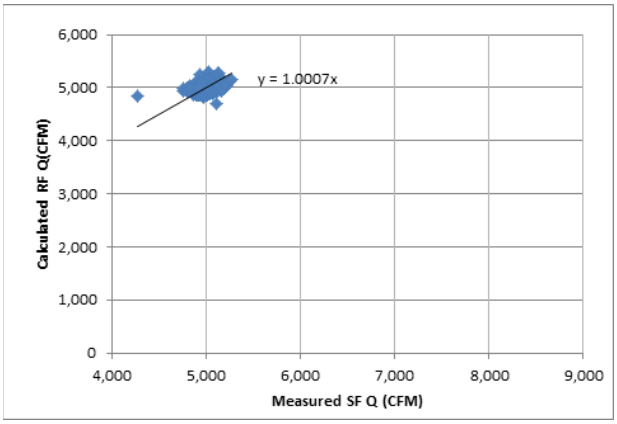

b. Validation chart

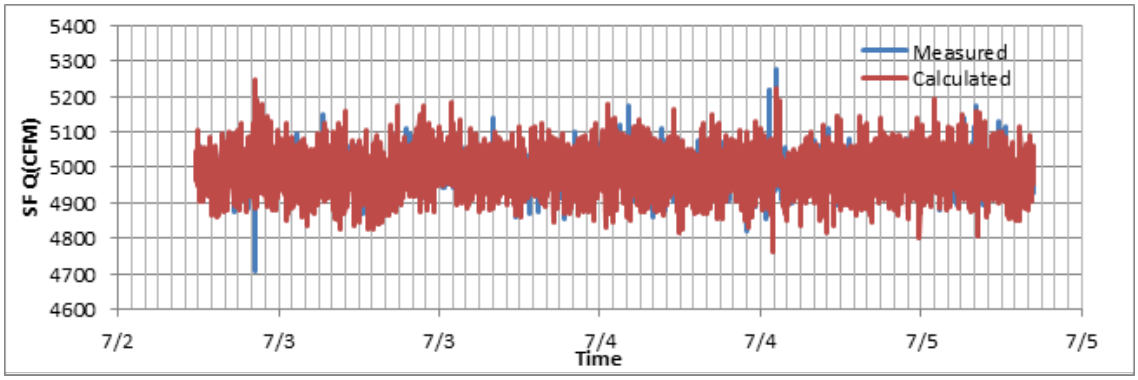

E.2. AHU2

1. Supply fan

a. Flow comparison (measured vs. calculated) chart

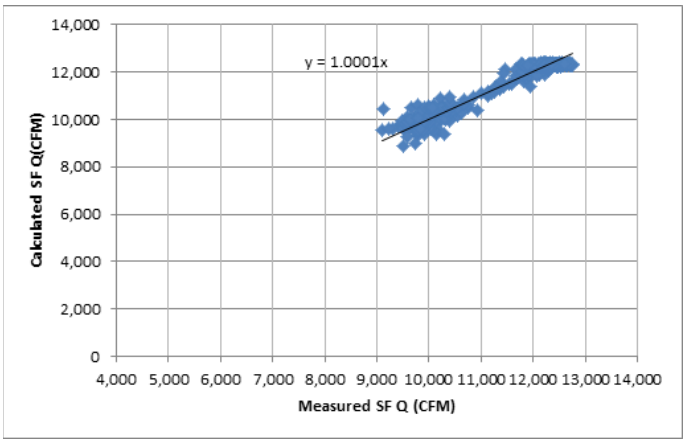

b. Validation chart

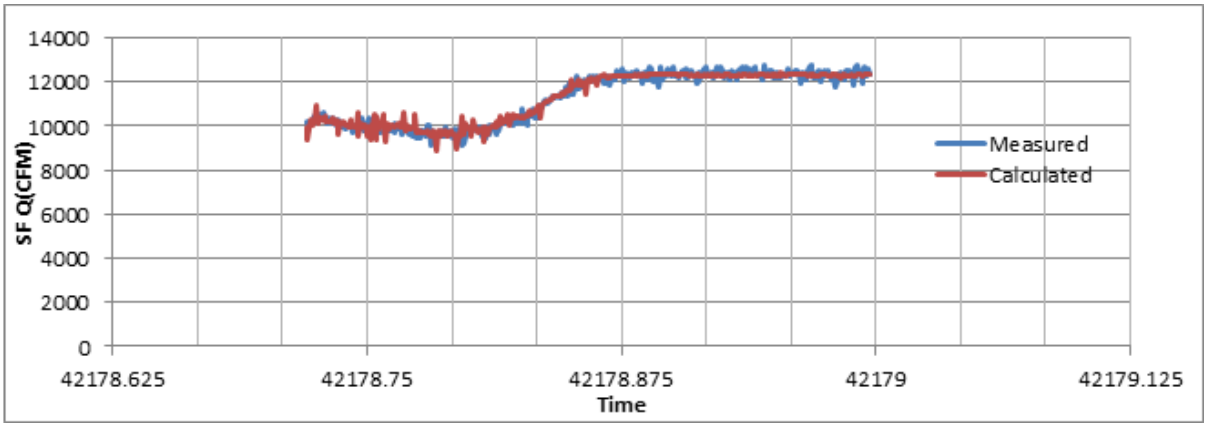

2. Return fan

a. Flow comparison (measured v.s. calculated) chart

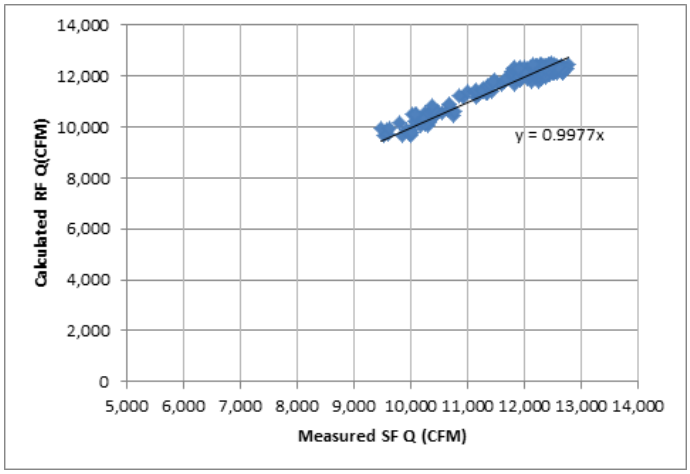

b. Validation chart

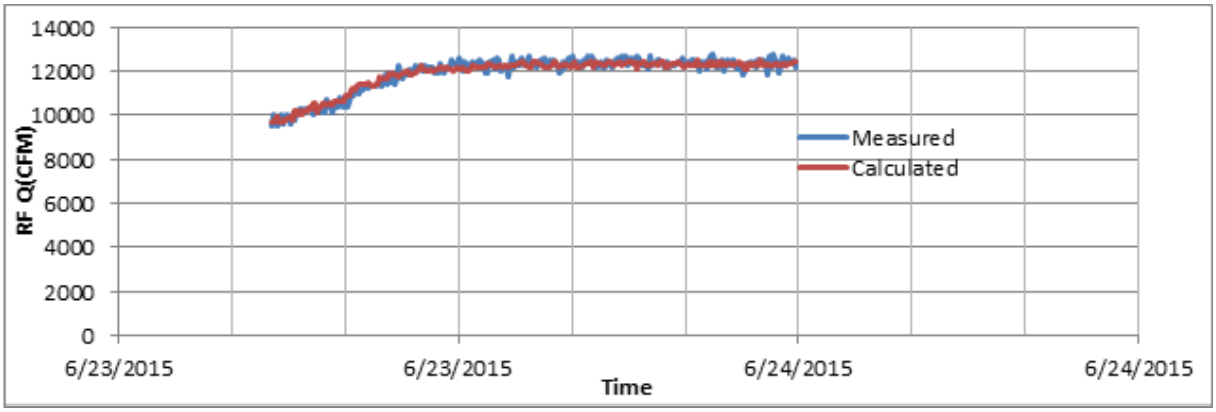

E.3. AHU3

a. Flow comparison (measured vs.. calculated) chart

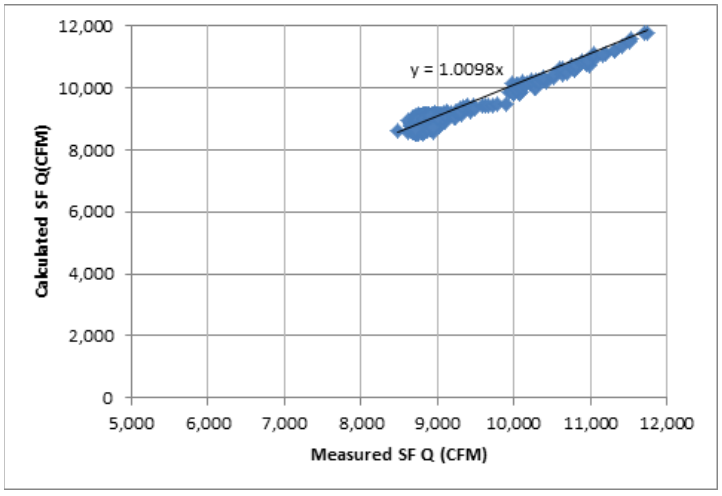

b. Validation chart

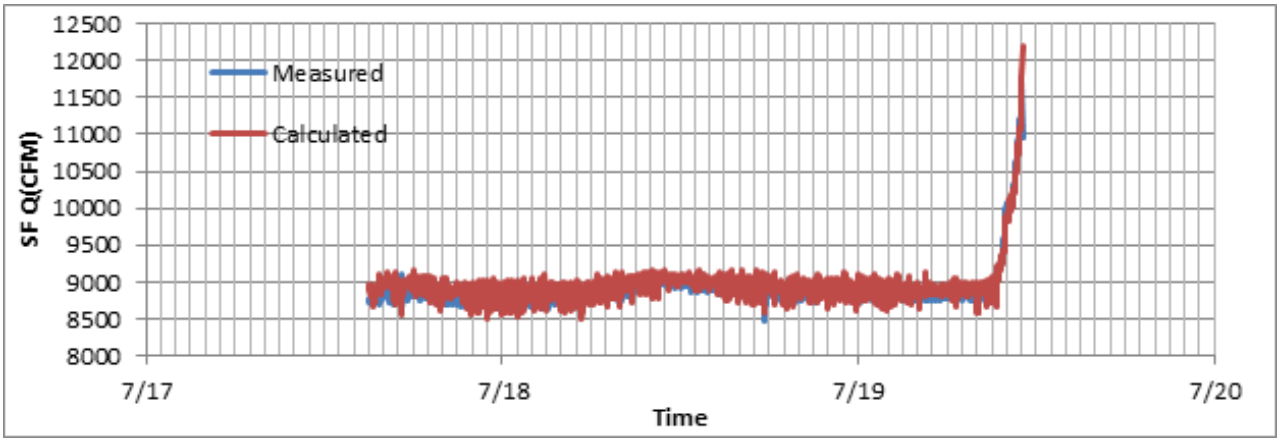

E.4. AHU4

1. Supply fan

a. Flow comparison (measured v.s. calculated) chart

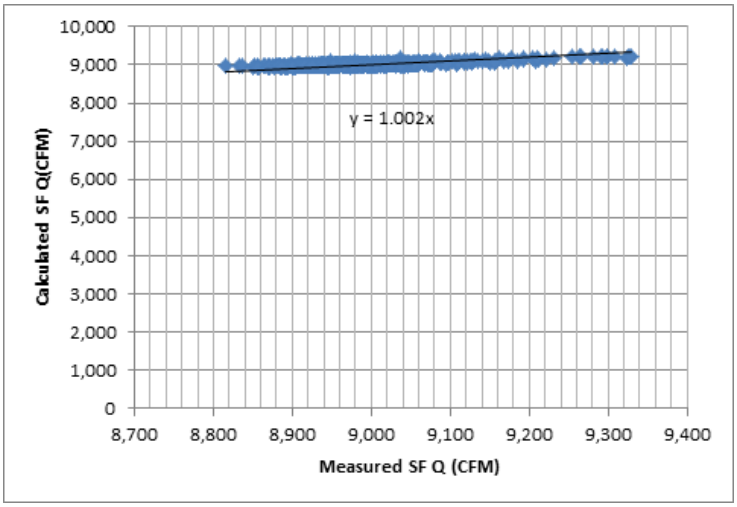

b. Validation chart

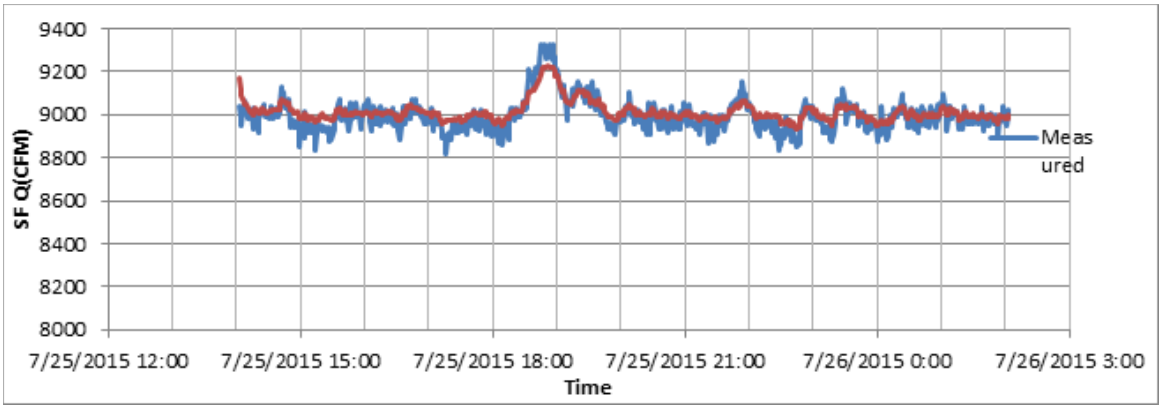

E.5. AHU5

1. Supply fan

a. Flow comparison (measured v.s. calculated) chart

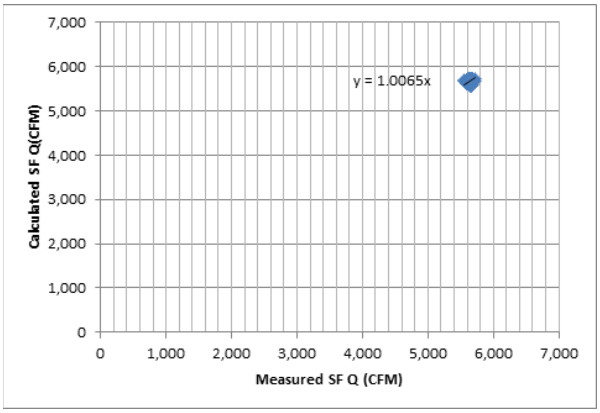

b. Validation chart

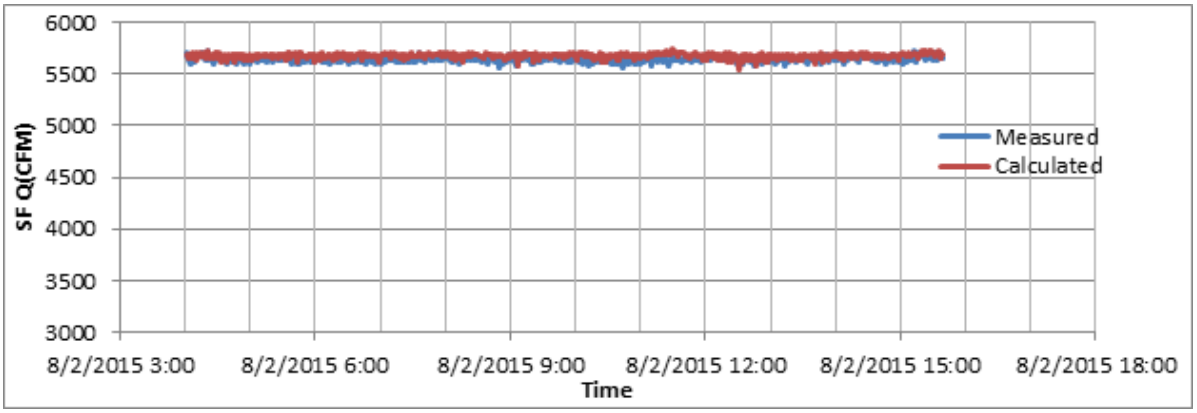

2. Return fan

a. Flow comparison (measured v.s. calculated) chart

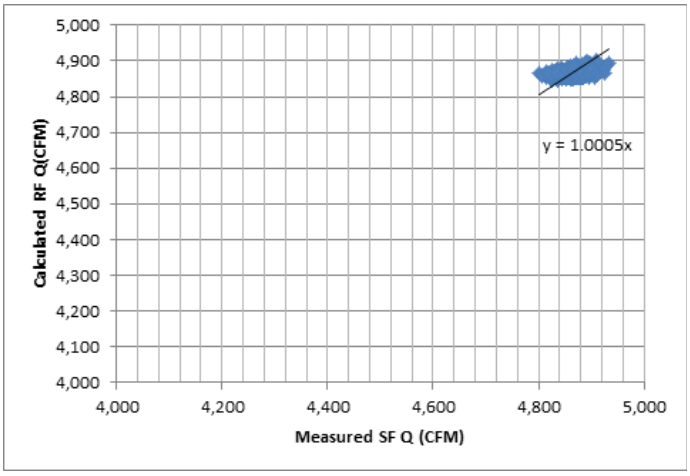

b. Validation chart

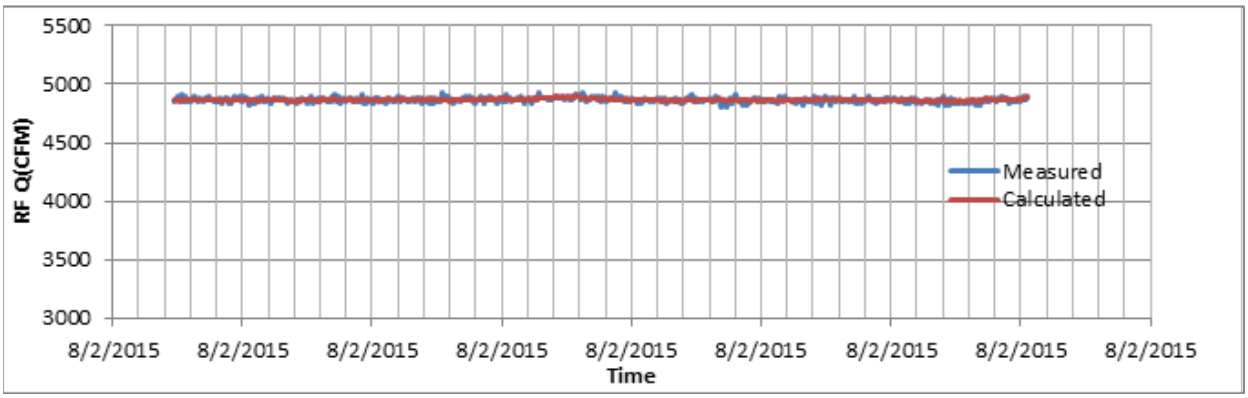

E.6. AHU6

1. Supply fan

a. Flow comparison (measured vs. calculated) chart

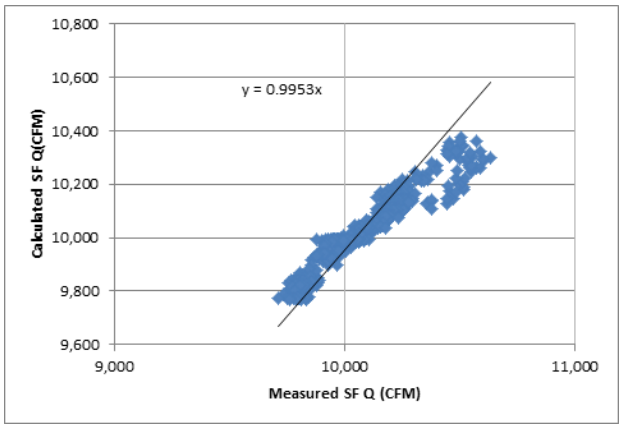

b. Validation chart

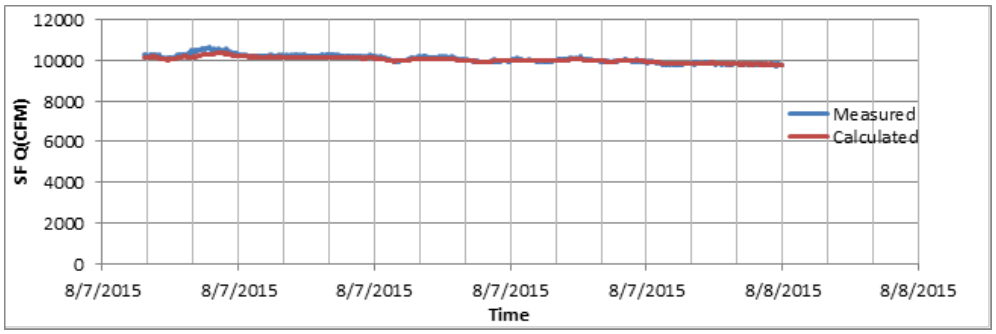

E.7. AHU7

1. Supply fan

a. Flow comparison (measured v.s. calculated) chart

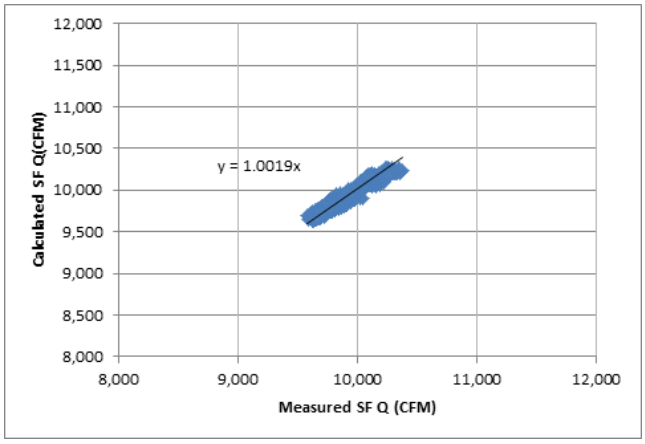

b. Validation chart

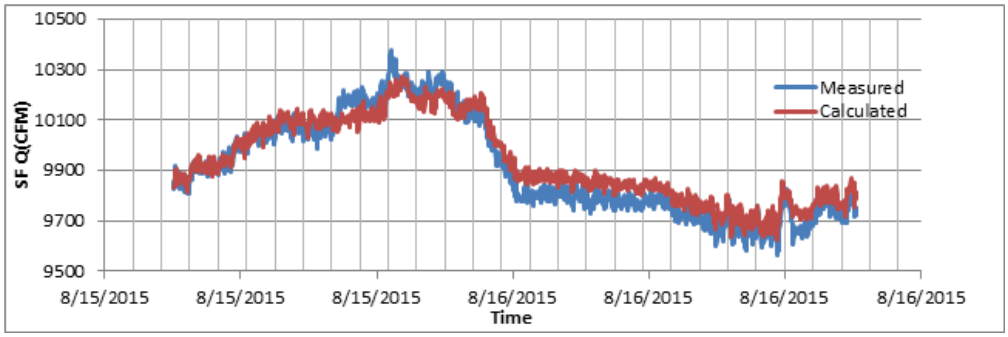

2. Return fan

a. Flow comparison (measured v.s. calculated) chart

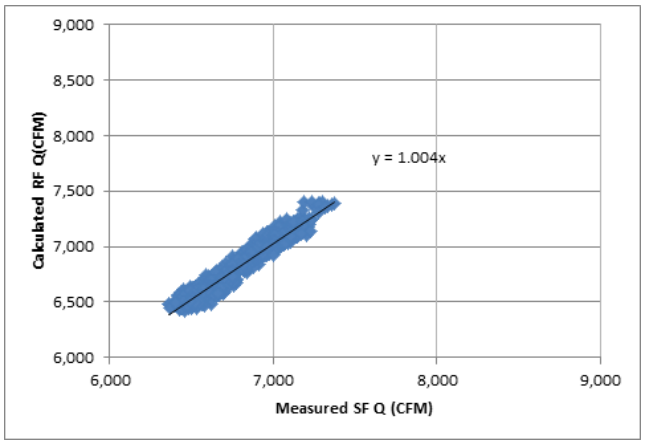

b. Validation chart

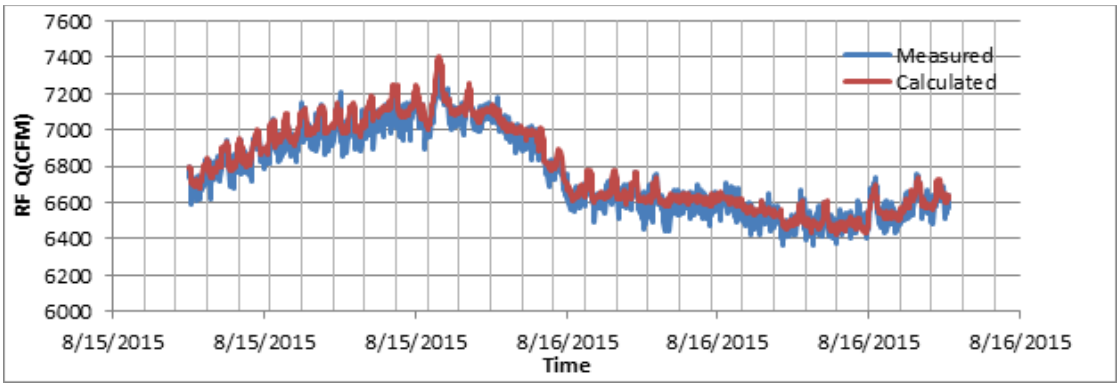

E.8. AHU8

1. Supply fan

a. Flow comparison (measured v.s. calculated) chart

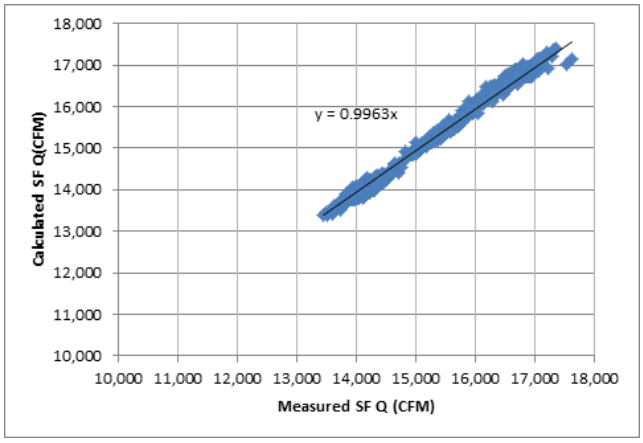

b. Validation chart

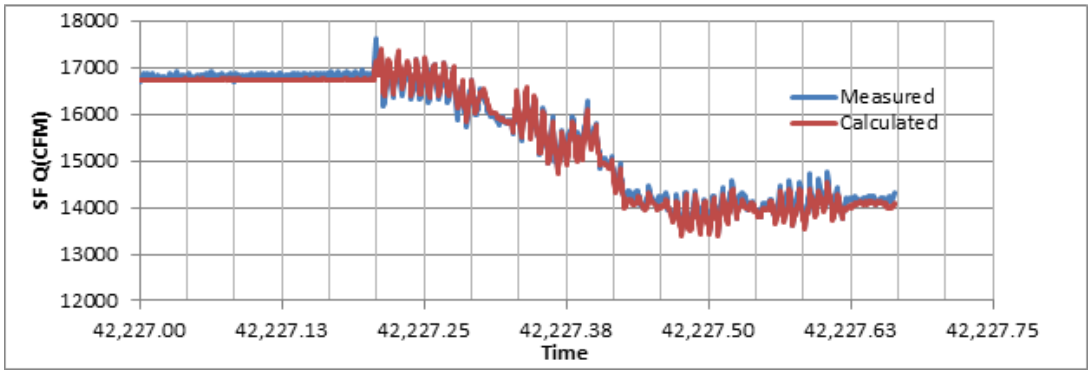

2. Return fan

a. Flow comparison (measured v.s. calculated) chart

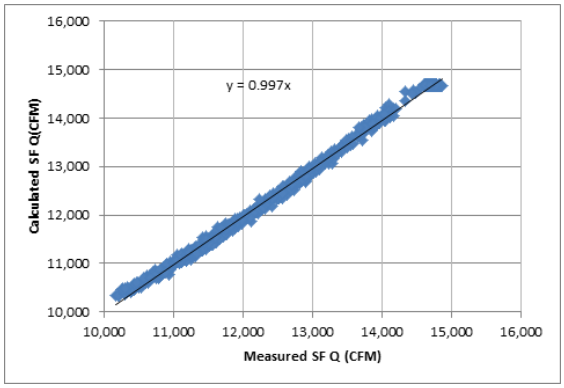

b. Validation chart

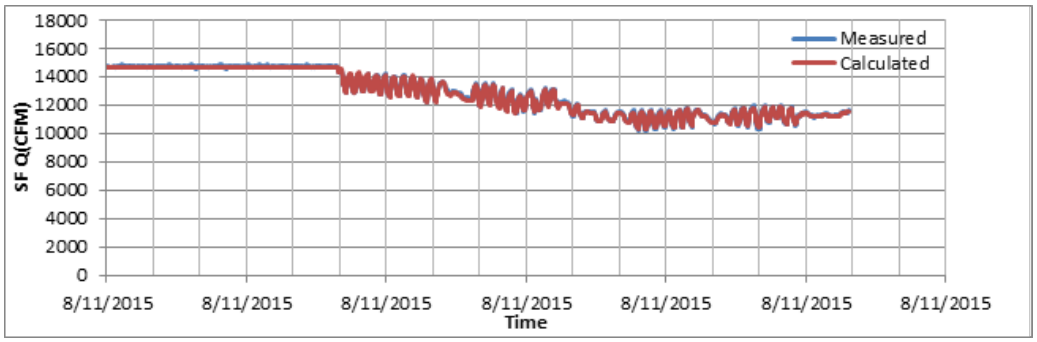

E.9. AHU9

1. Supply fan

a. Flow comparison (measured v.s. calculated) chart

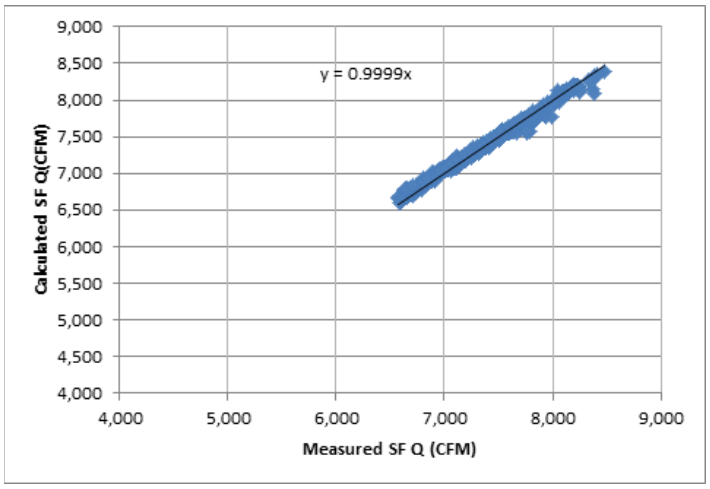

b. Validation chart

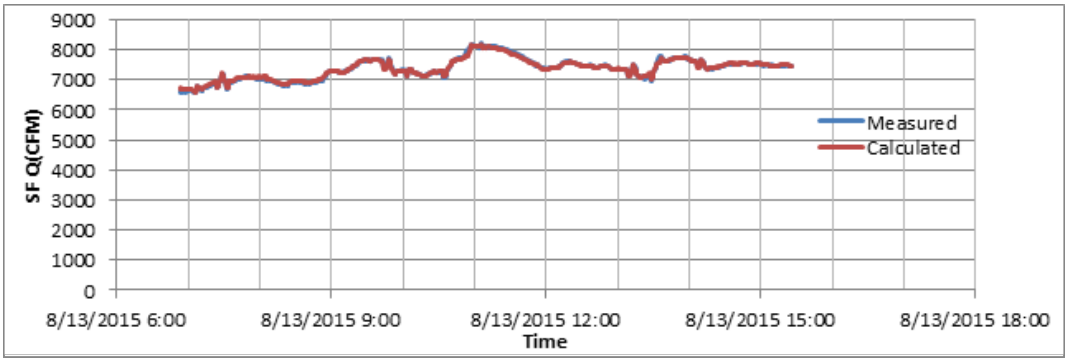

2. Return fan

a. Flow comparison (measured vs. calculated) chart

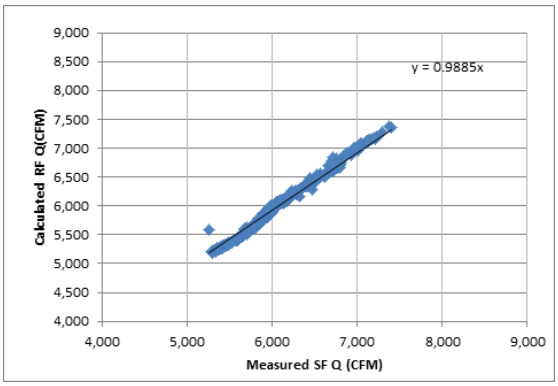

b. Validation chart

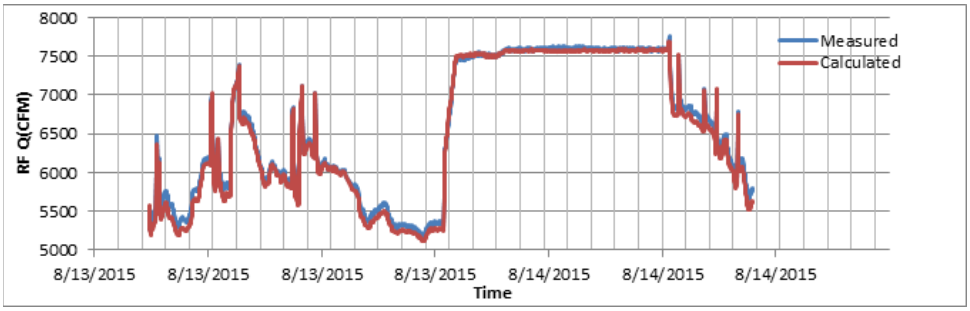

E.10. AHU10

1. Supply fan

a. Flow comparison (measured – calculated) chart

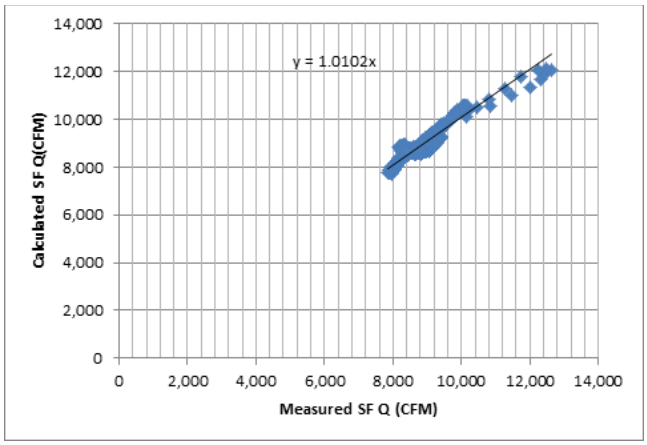

b. Validation chart

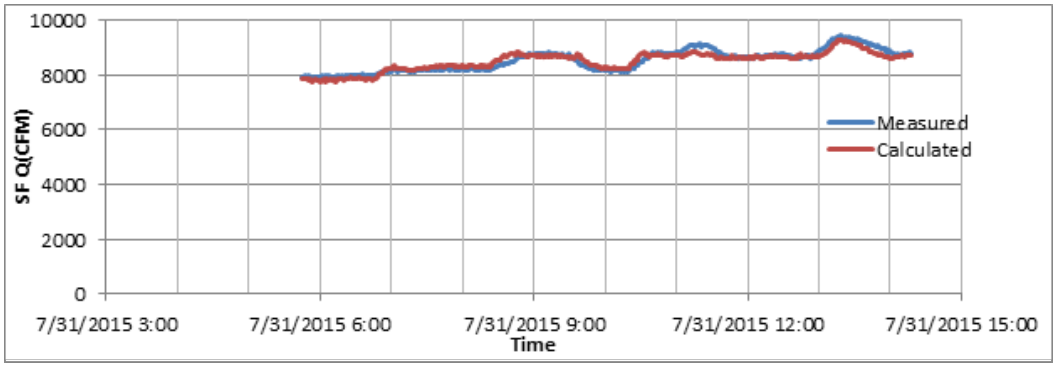

2. Return fan

a. Flow comparison (measured v.s. calculated) chart

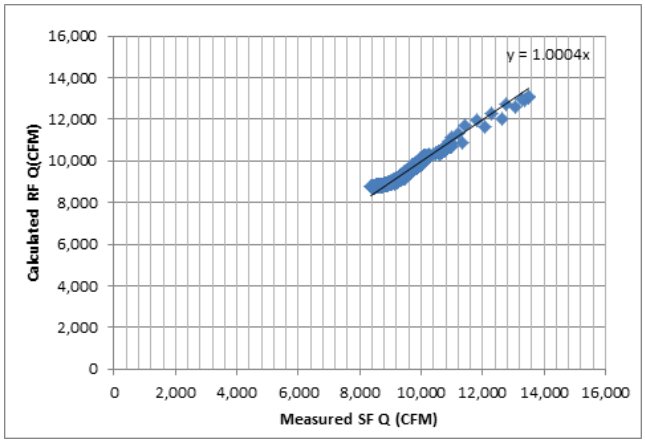

b. Validation chart

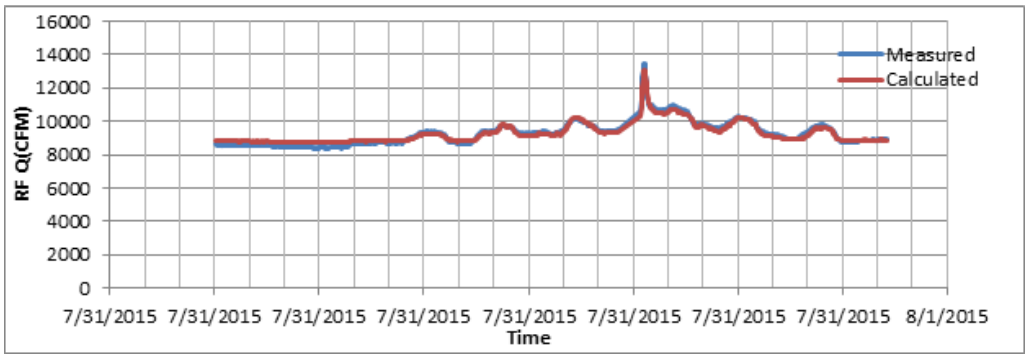

E.11. AHU11

1. Supply fan

a. Flow comparison (measured vs. calculated) chart

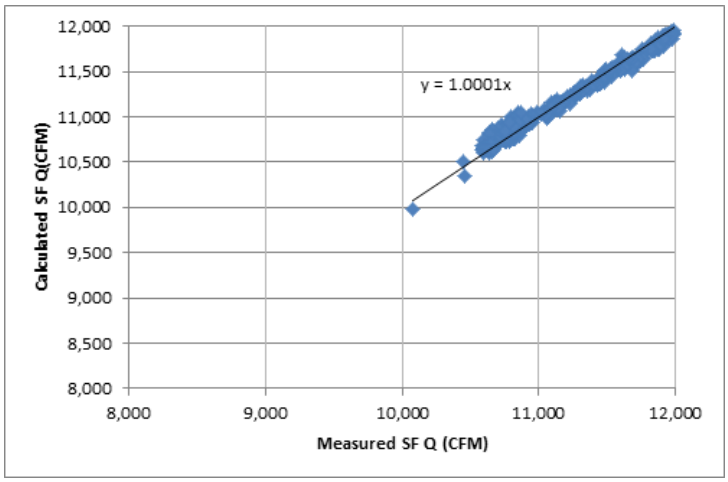

b. Validation chart

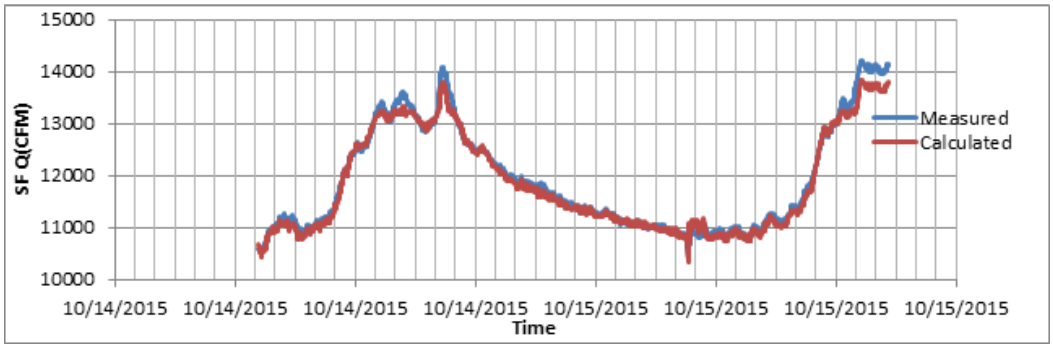

2. Return fan

a. Flow comparison (measured v.s. calculated) chart

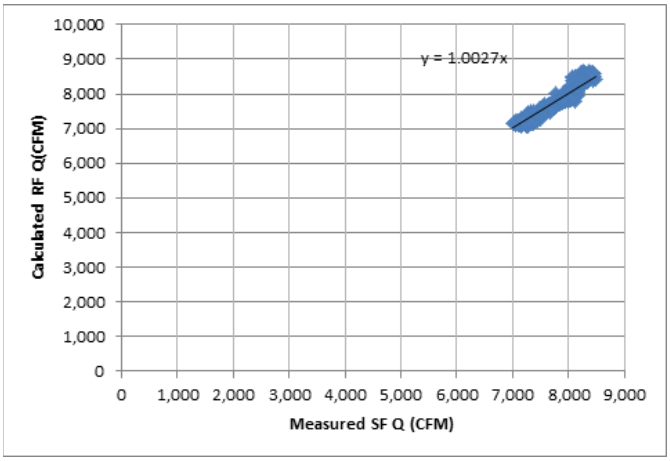

b. Validation chart

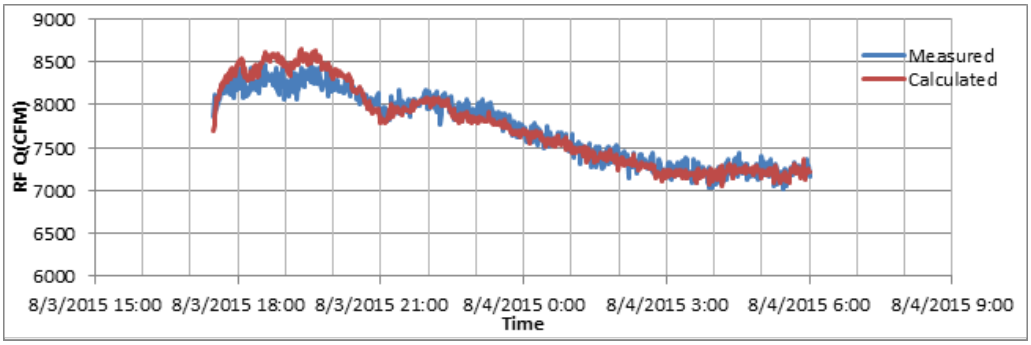

E.12. AHU12

1. Supply fan

a. Flow comparison (measured vs. calculated) chart

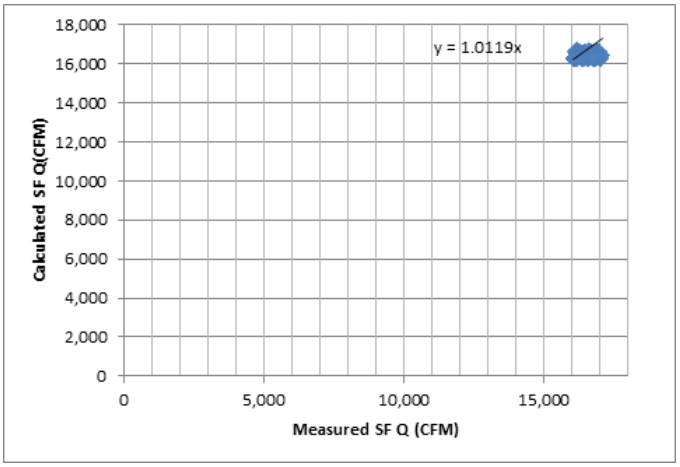

b. Validation chart

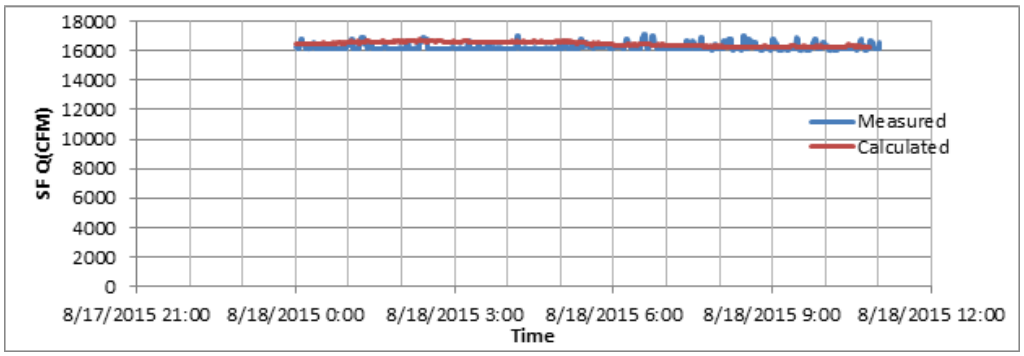

E.13. AHU13

1. Supply fan

a. Flow comparison (measured v.s. calculated) chart

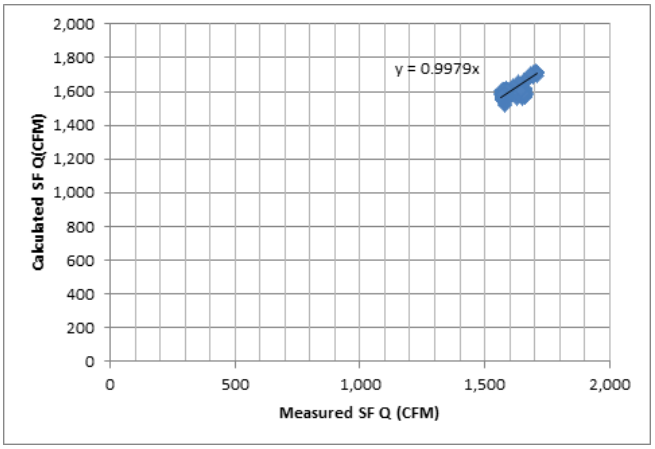

b. Validation chart

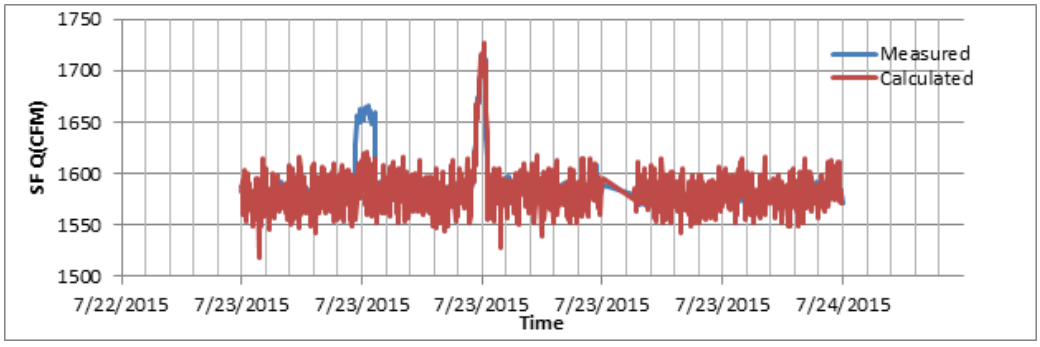

APPENDIX F MID-PROGRESS REPORT OF VIRTUAL VALVE FLOW METERS AT AHUS

F.1. AHU1

1. *Flow validation comparison (measured v.s. calculated) chart*

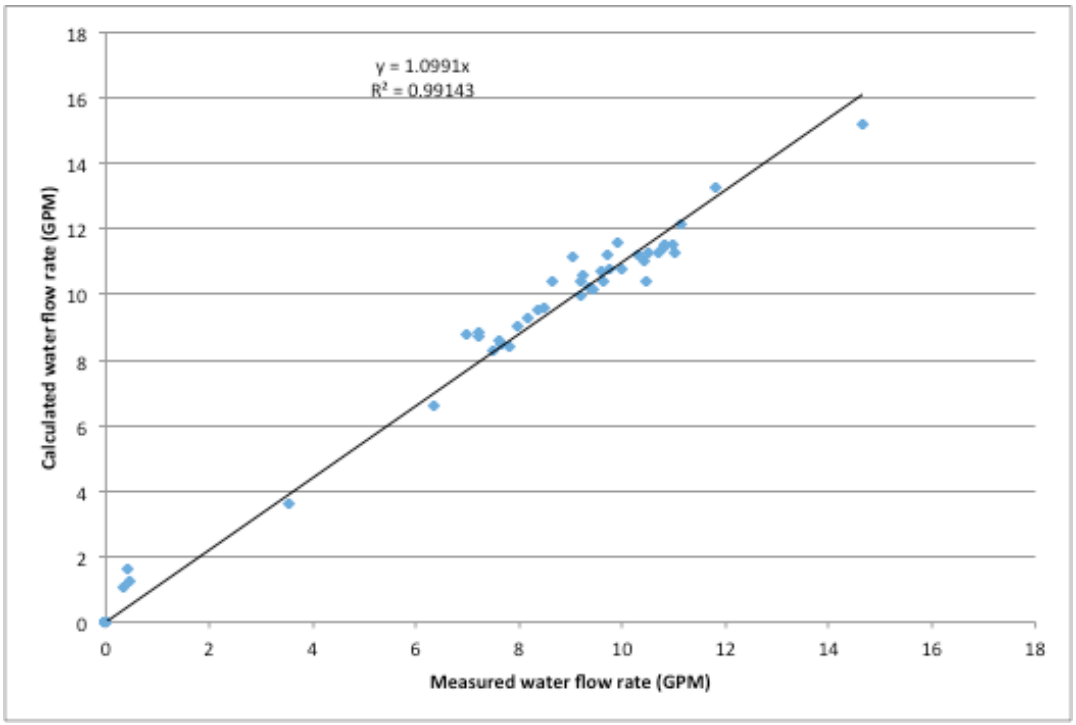

2. *Validation chart*

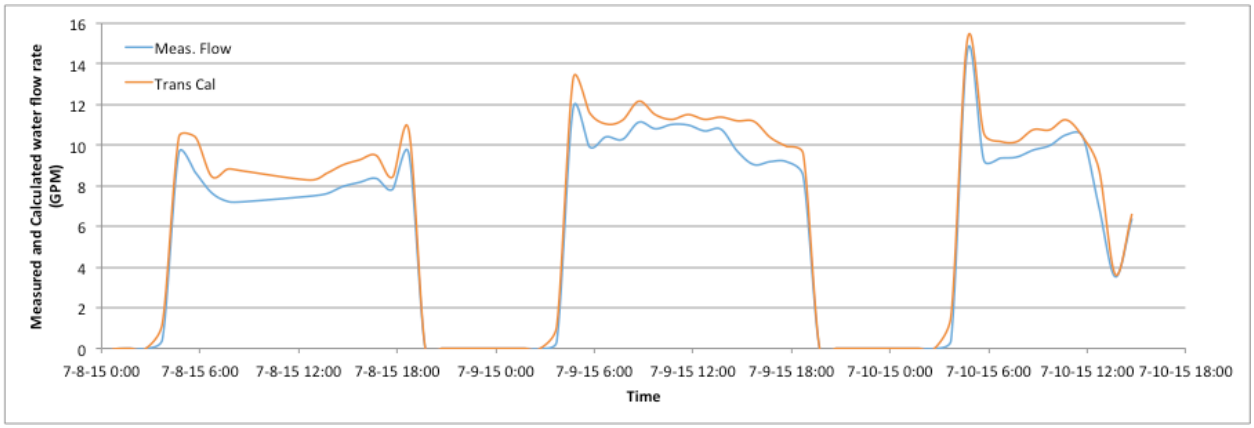

F.2. AHU2

1. Flow validation comparison (measured vs. calculated) chart

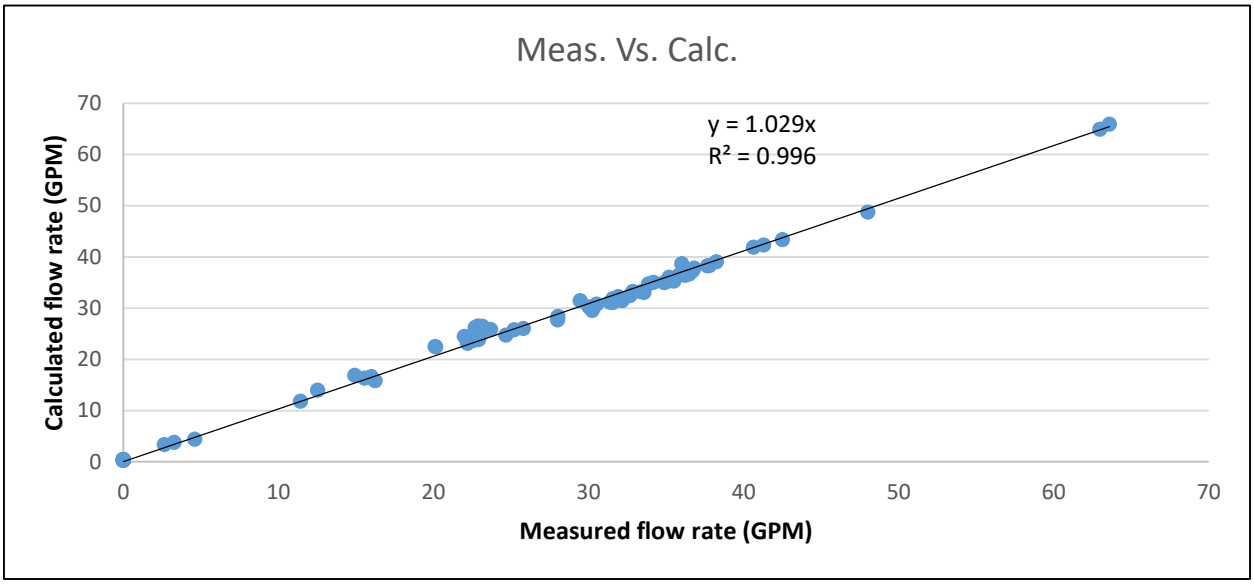

2. Validation chart

F.3. AHU3

1. ***Flow validation comparison (measured vs. calculated) chart***

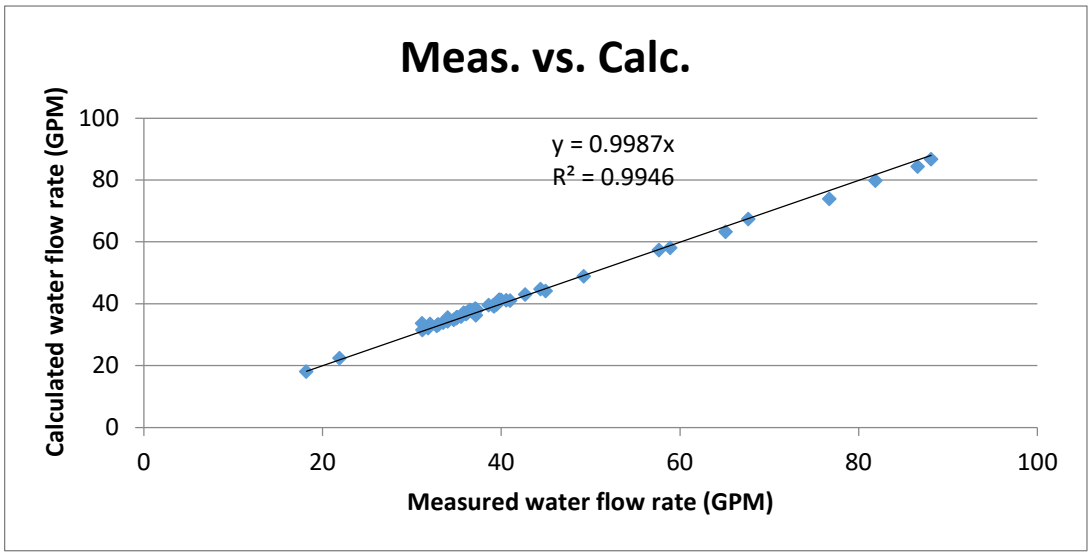

2. ***Validation chart: the empty periods are when the DP transducers were maxed out.***

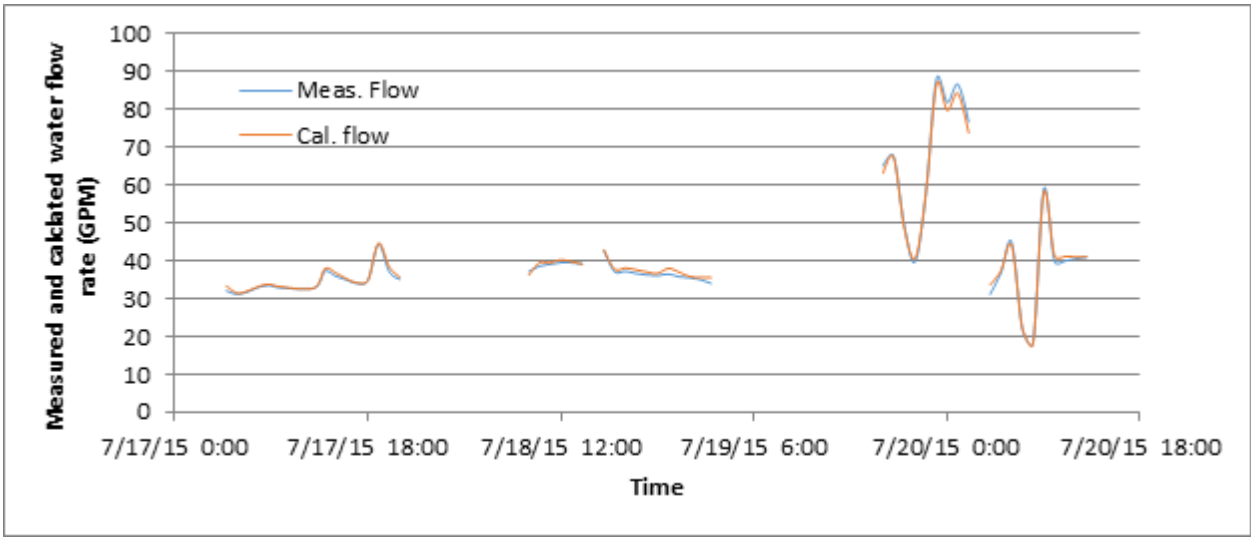

F.4. AHU4

1. *Flow validation comparison (measured v.s. calculated) chart*

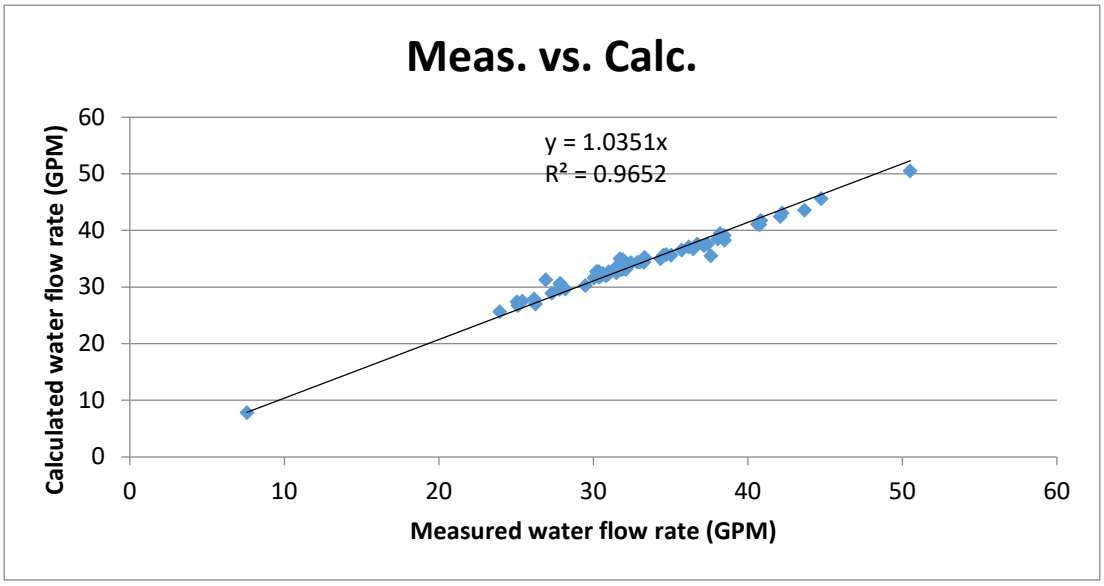

2. *Validation chart*

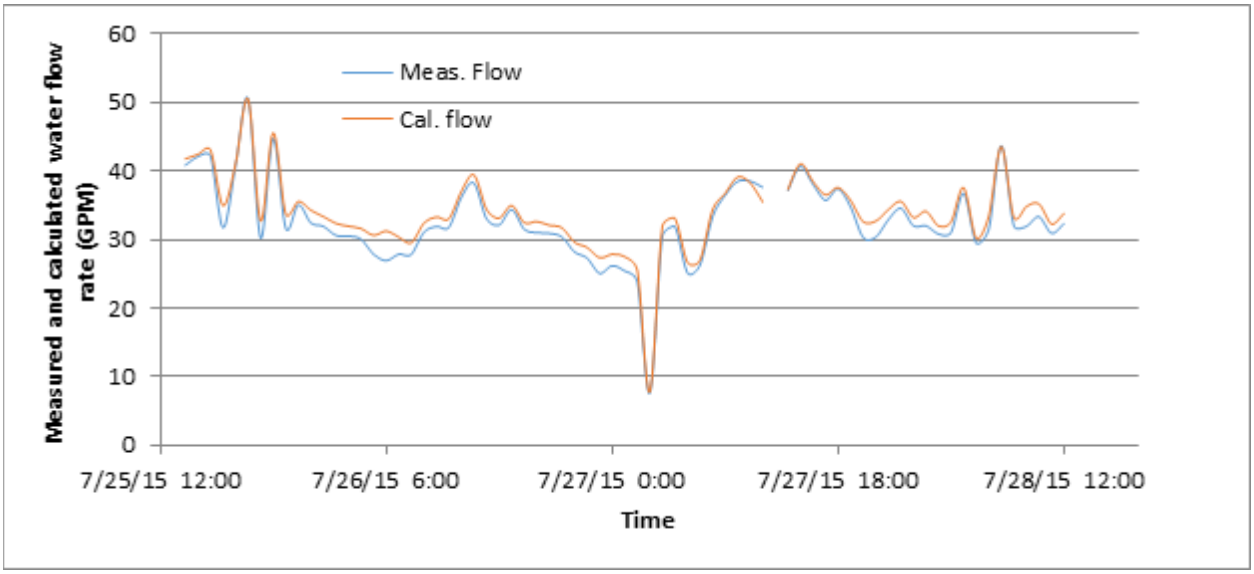

F.5. AHU5

1. *Flow validation comparison (measured vs. calculated) chart*

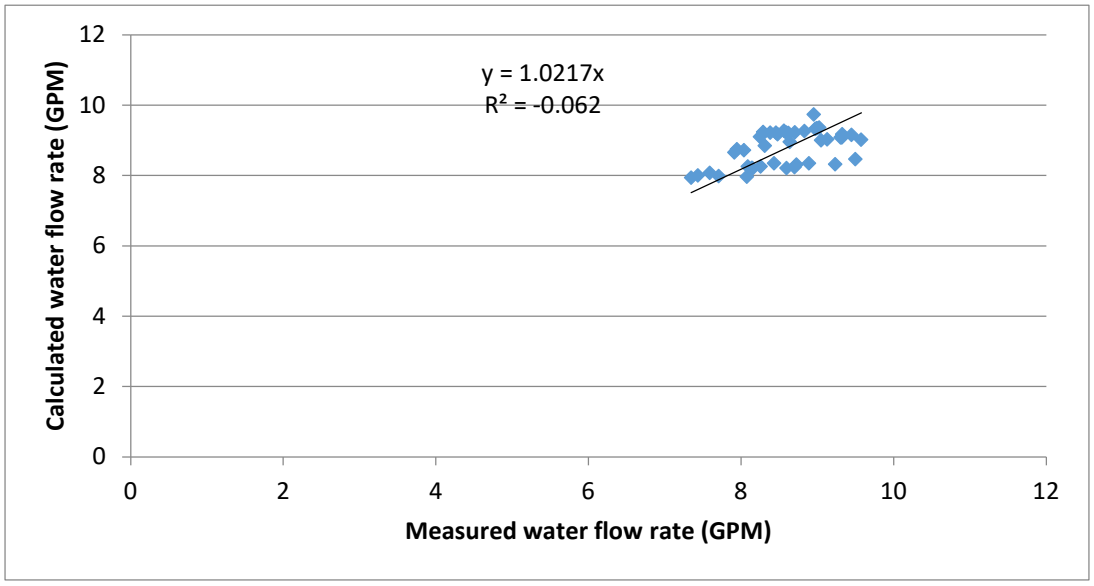

2. *Validation chart*

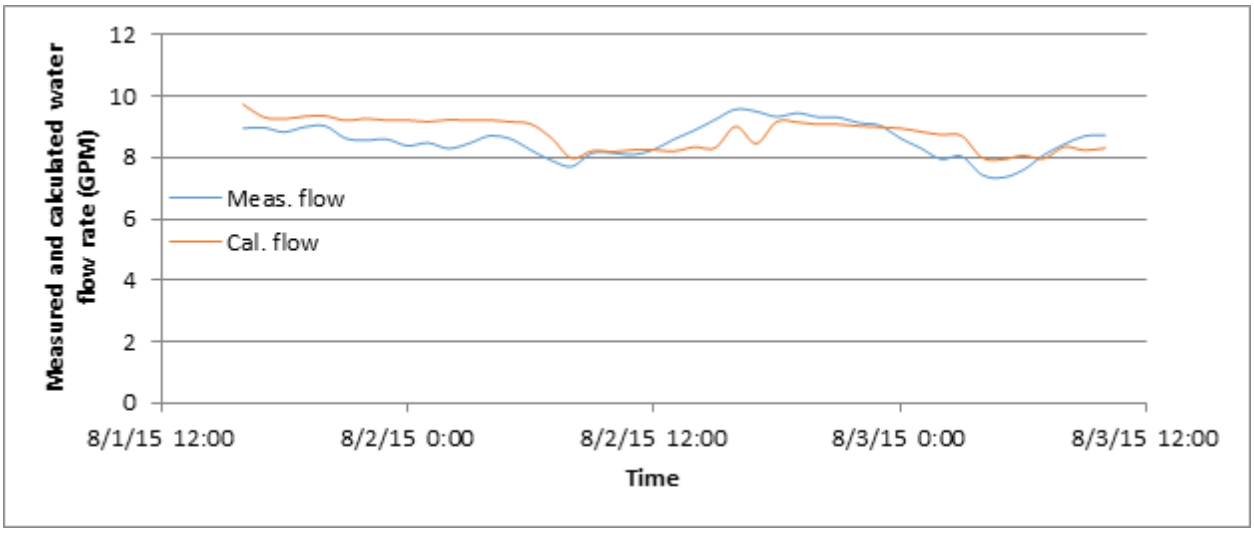

F.6. AHU6

1. *Flow validation comparison (measured v.s. calculated) chart*

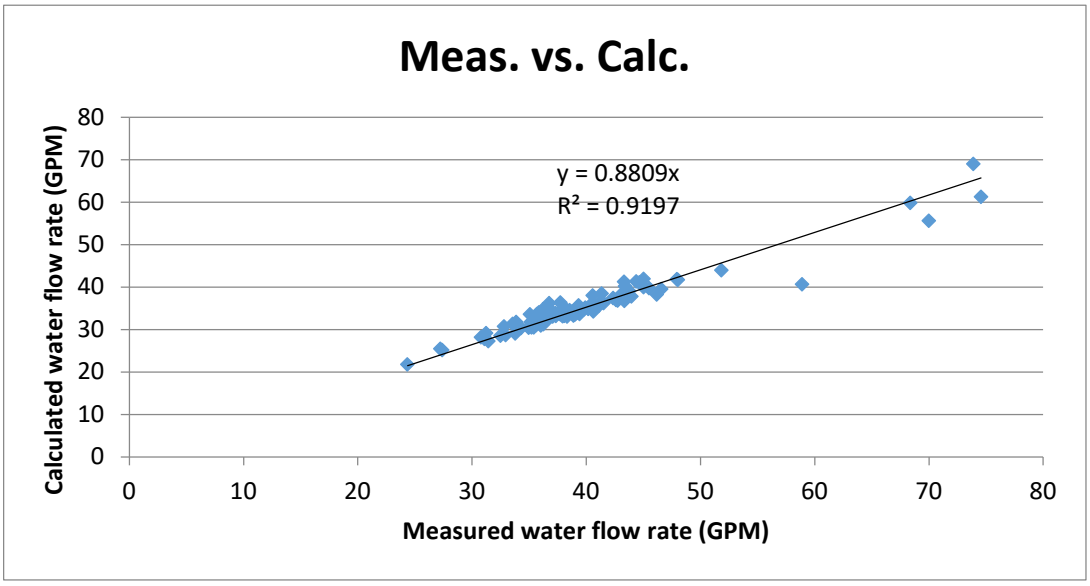

2. *Validation chart*

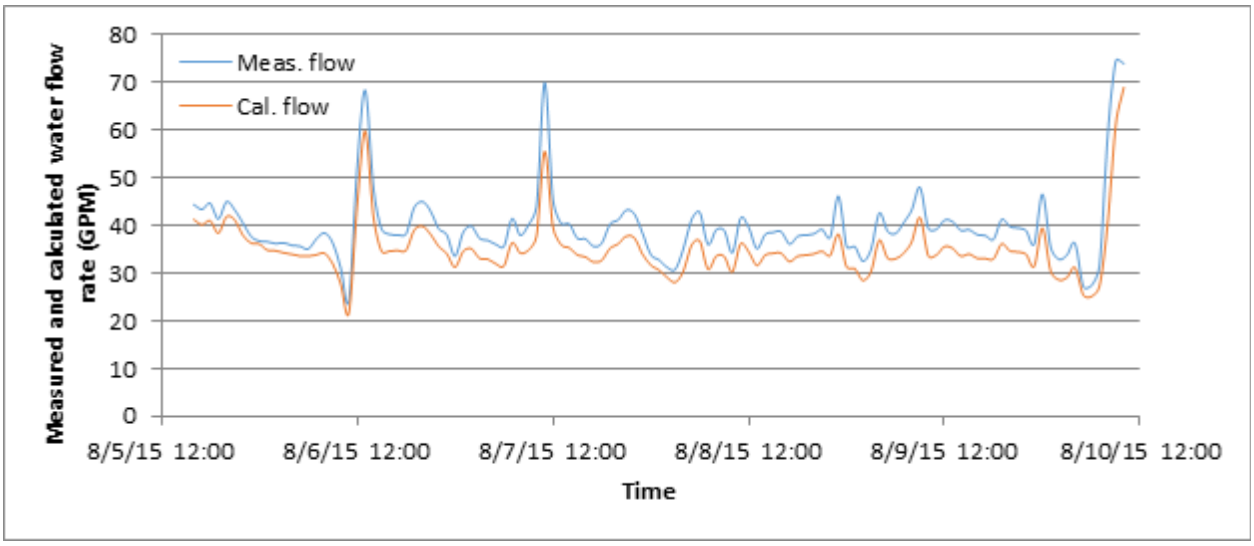

F.7. AHU7

1. *Flow validation comparison (measured v.s. calculated) chart*

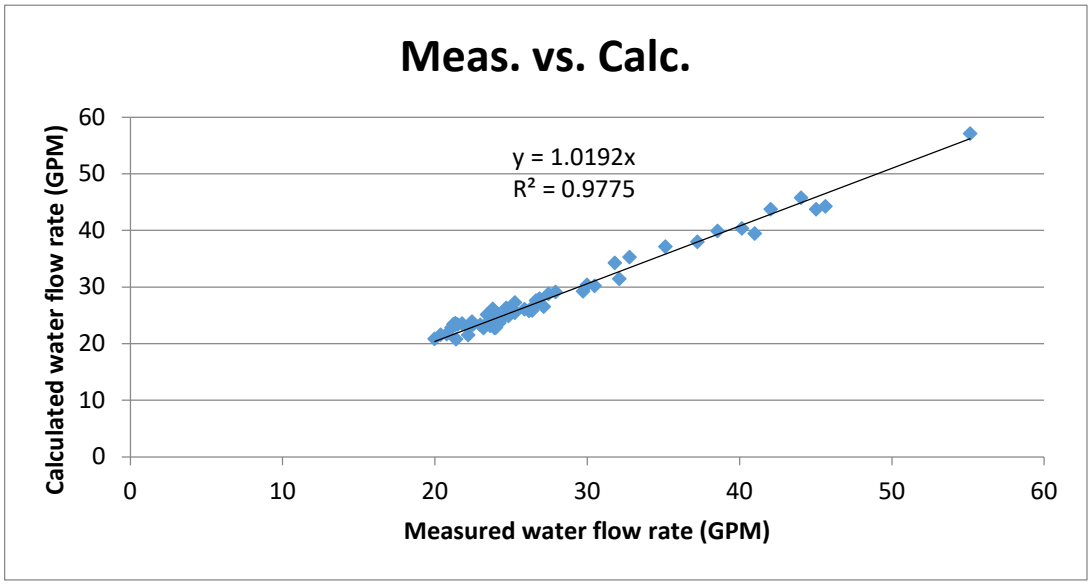

2. *Validation chart*

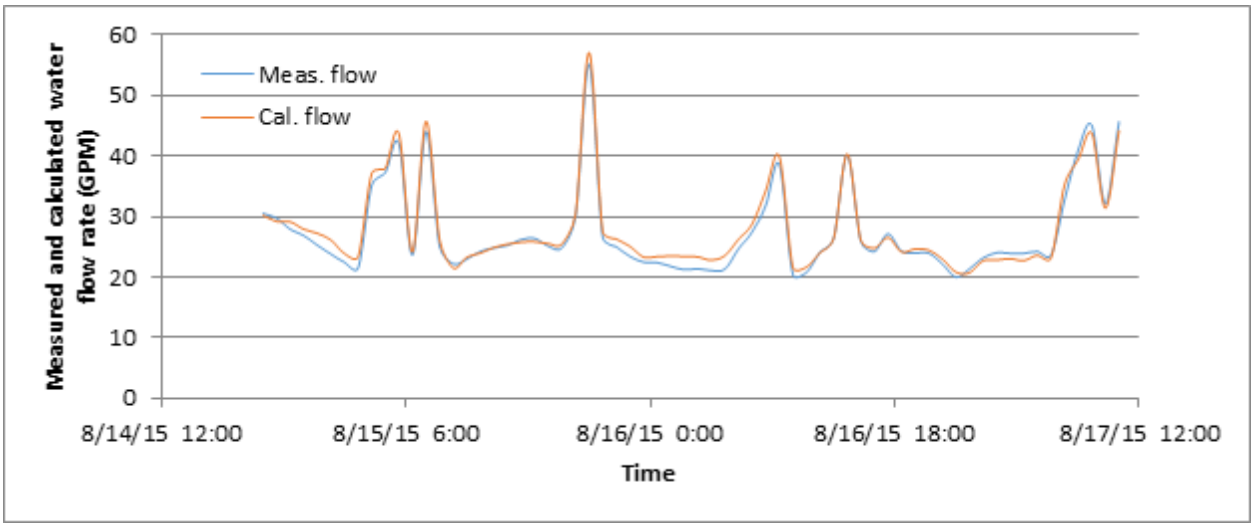

F.8. AHU8

1. *Flow validation comparison (measured v.s. calculated) chart*

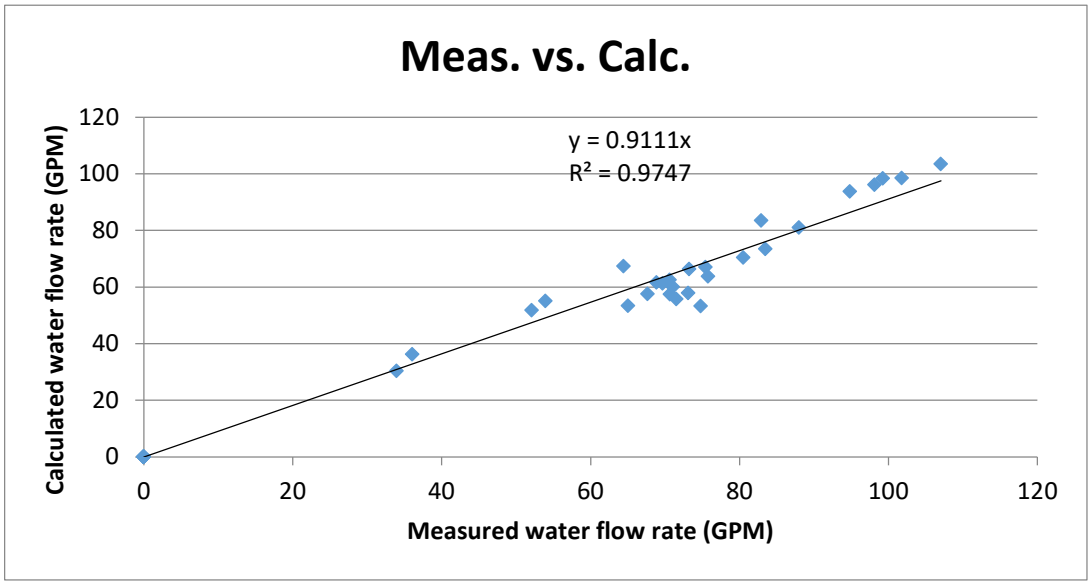

2. *Validation chart*

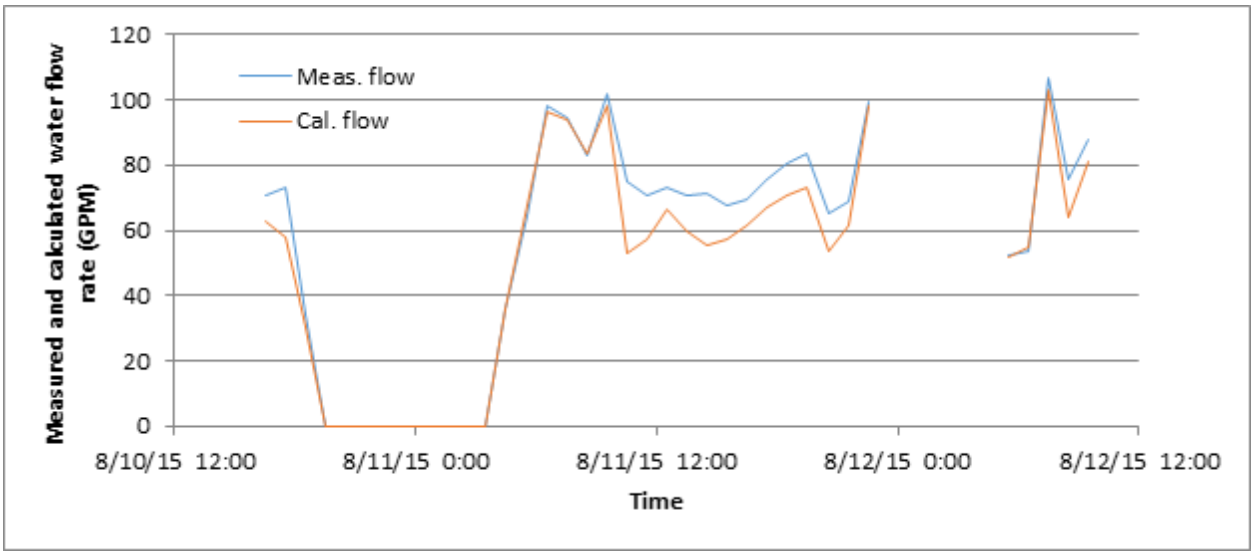

F.9. AHU9

1. *Flow validation comparison (measured vs. calculated) chart*

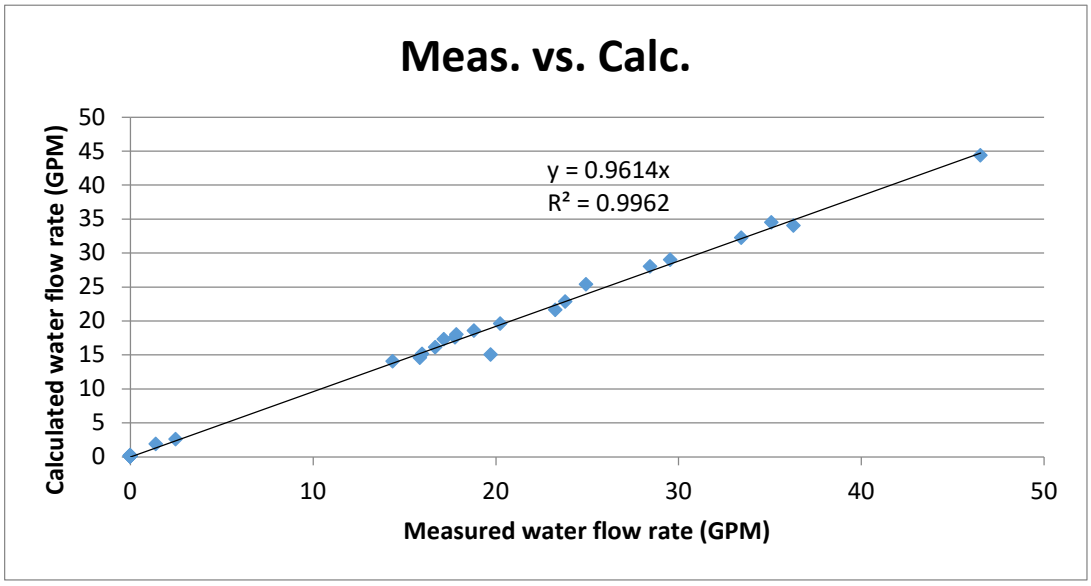

2. *Validation chart*

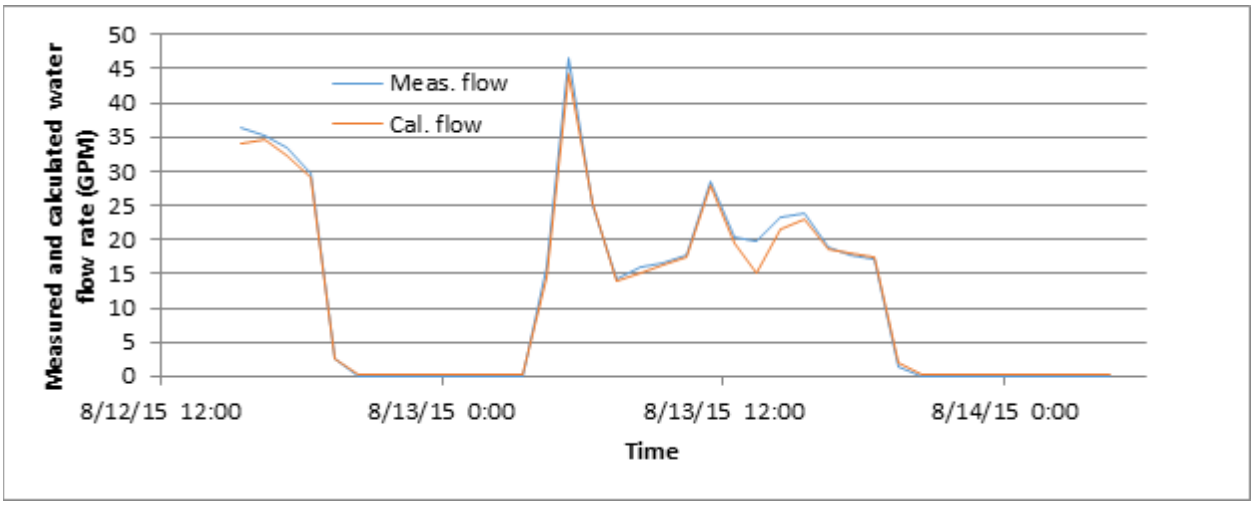

F.10. AHU10

1. *Flow validation comparison (measured vs. calculated) chart*

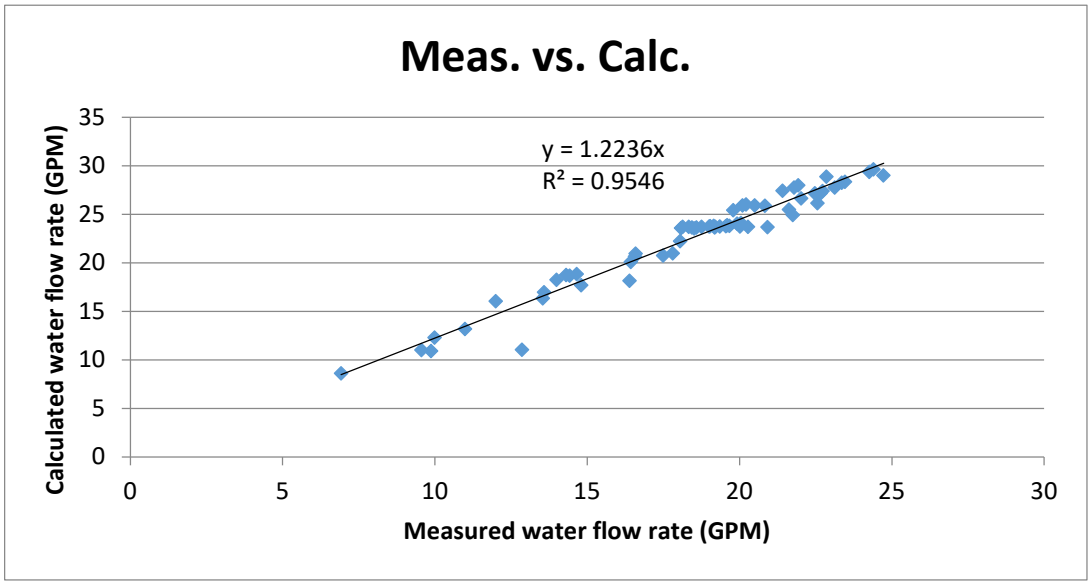

2. *Validation chart*

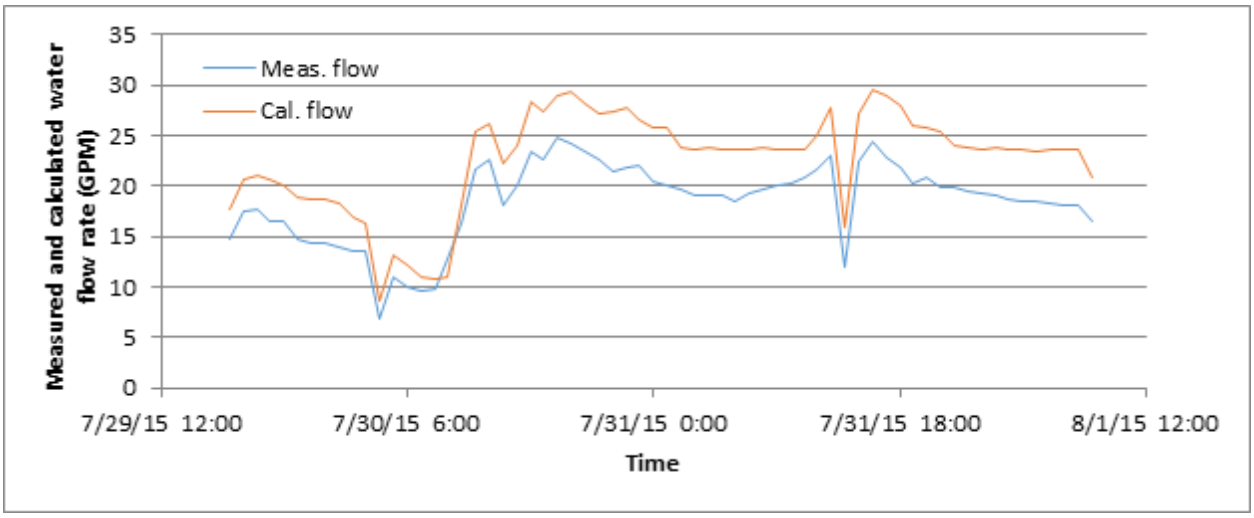

F.11. AHU11

1. *Flow validation comparison (measured v.s. calculated) chart*

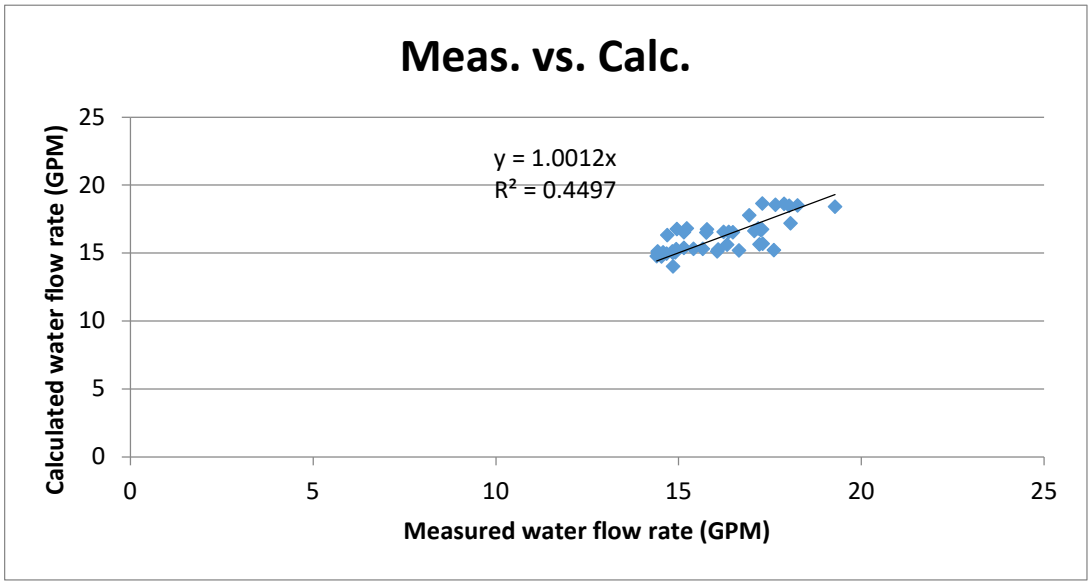

2. *Validation chart*

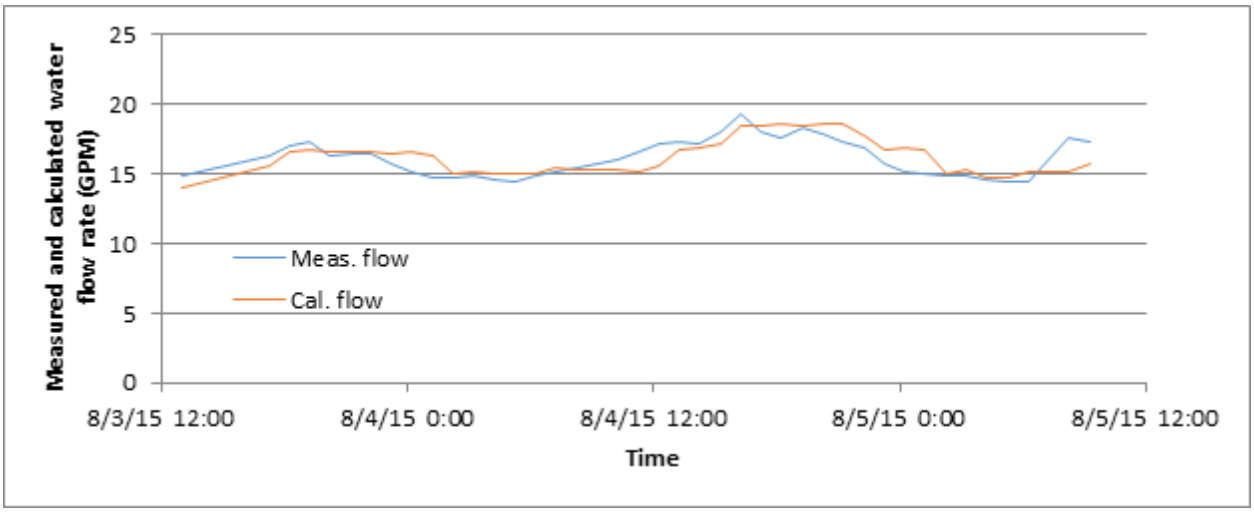

F.12. AHU12

1. *Flow validation comparison (measured vs. calculated) chart*

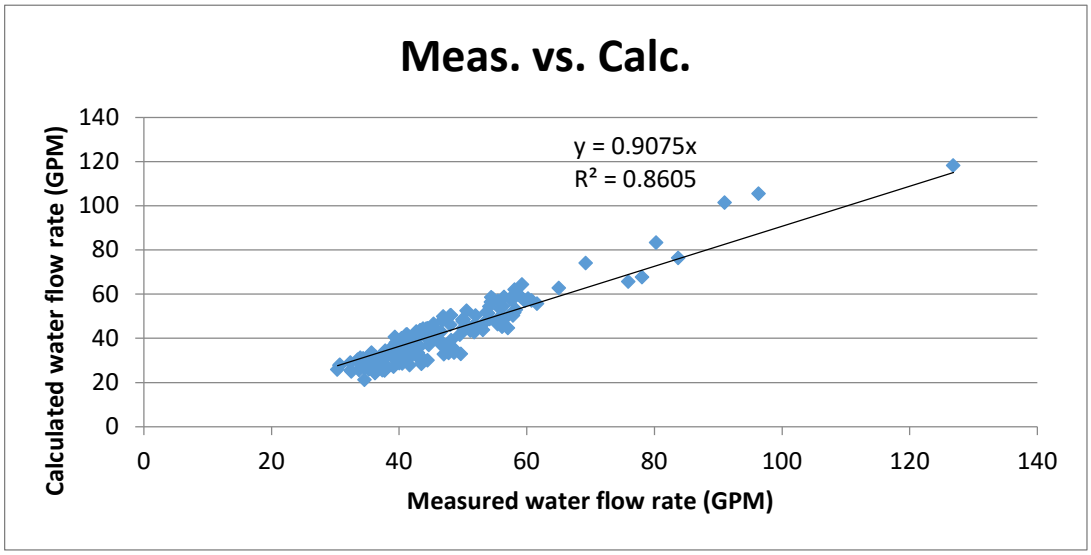

2. *Validation chart*

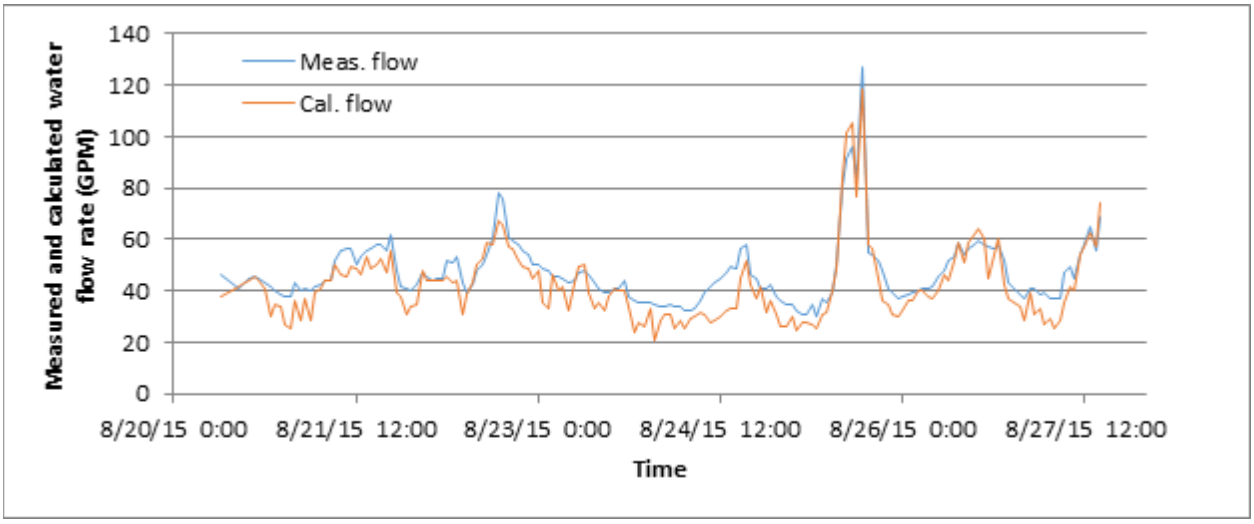

F.13. AHU13

1. Flow validation comparison (measured v.s. calculated) chart

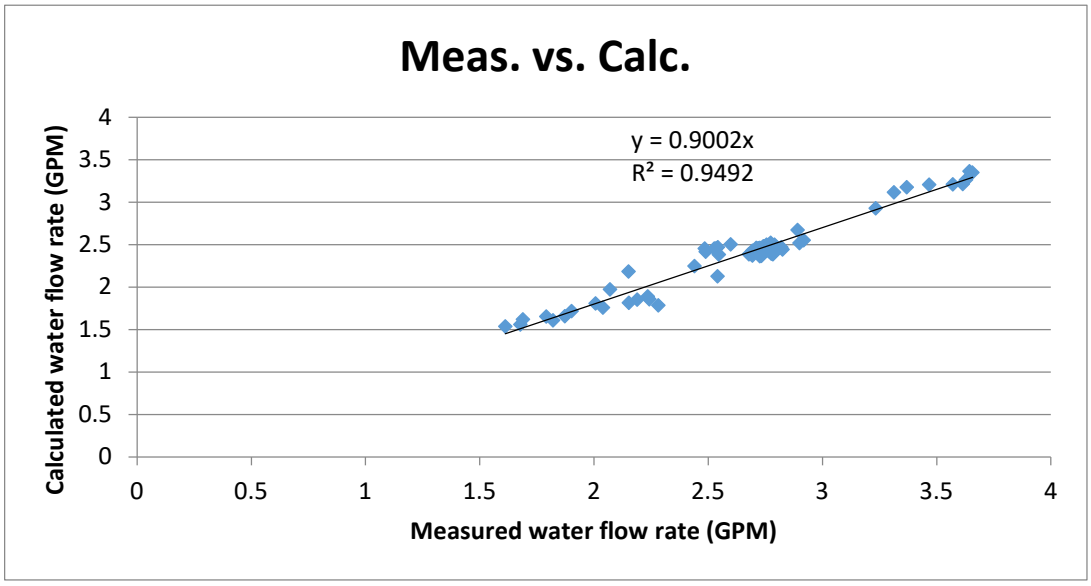

2. Validation chart

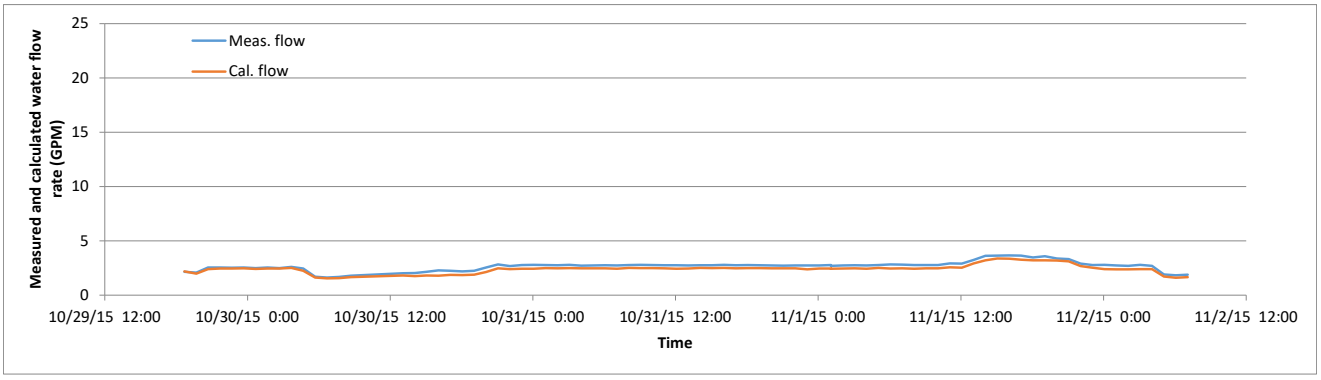

Page Intentionally Left Blank

APPENDIX G THE MID-PROGRESS REPORT OF VIRTUAL PUMP FLOW METERS

G.1. Hot water pumps

1. Flow validation comparison (measured vs. calculated) chart

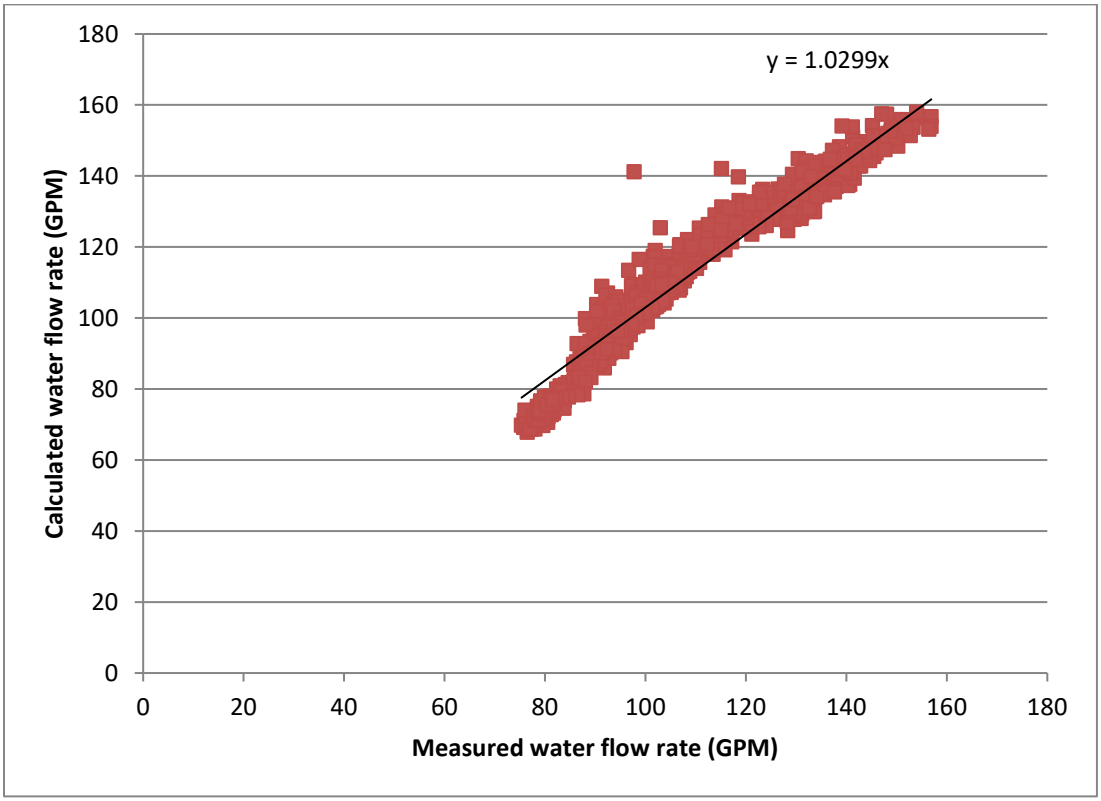

2. Validation chart

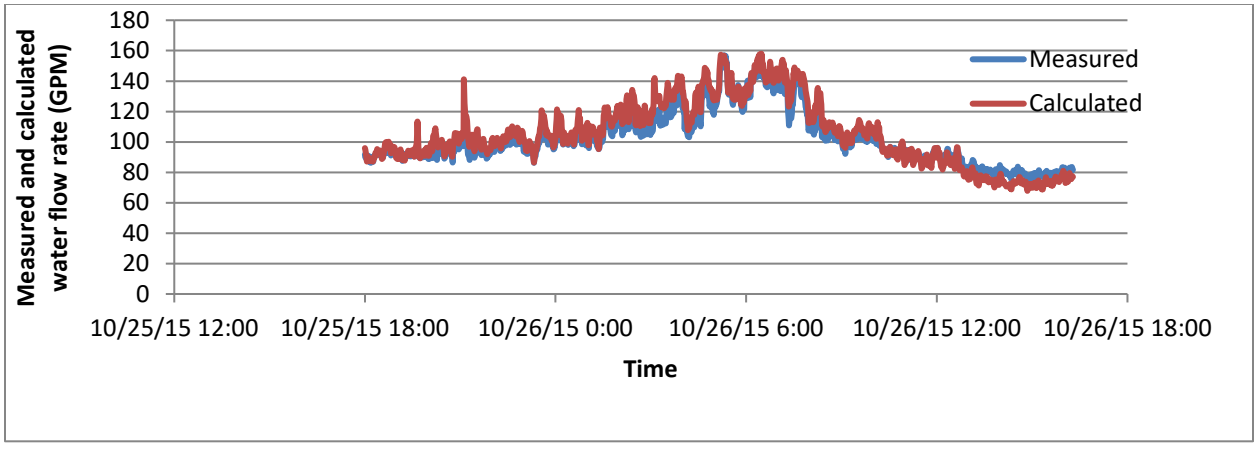

G.2. Primary Chilled water pumps

1. Flow validation comparison (measured v.s. calculated) chart

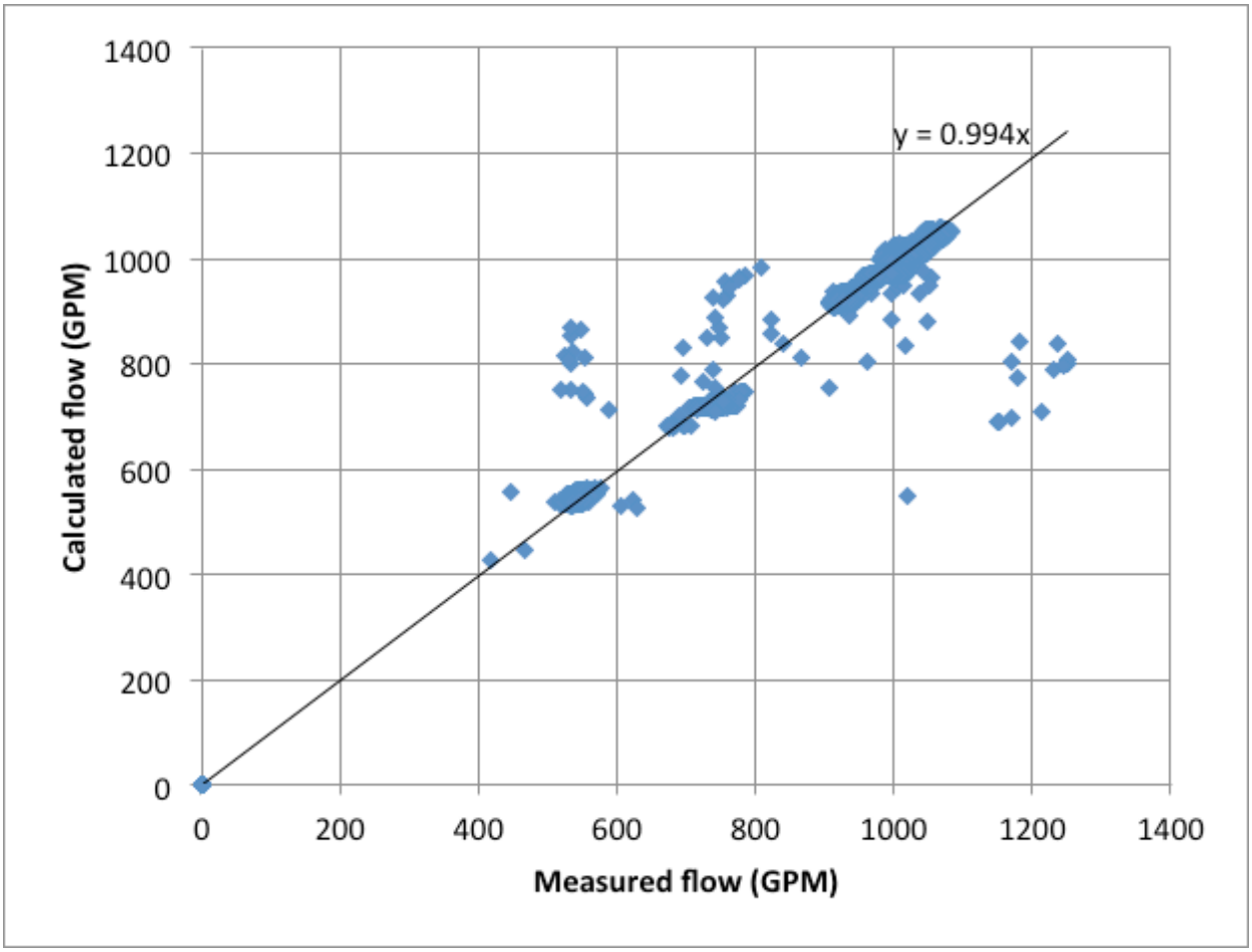

2. Validation chart

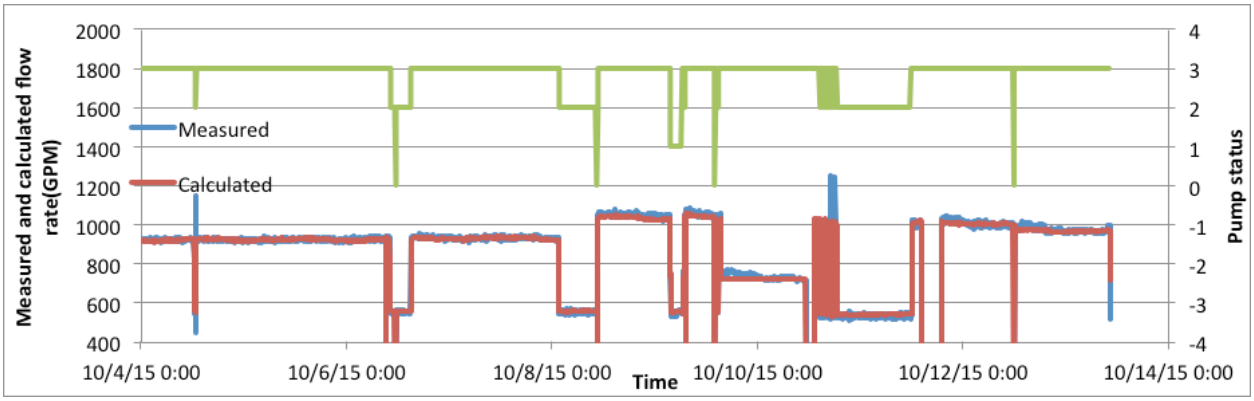

G.3. Secondary Chilled water pumps

1. Flow validation comparison (measured vs. calculated) chart

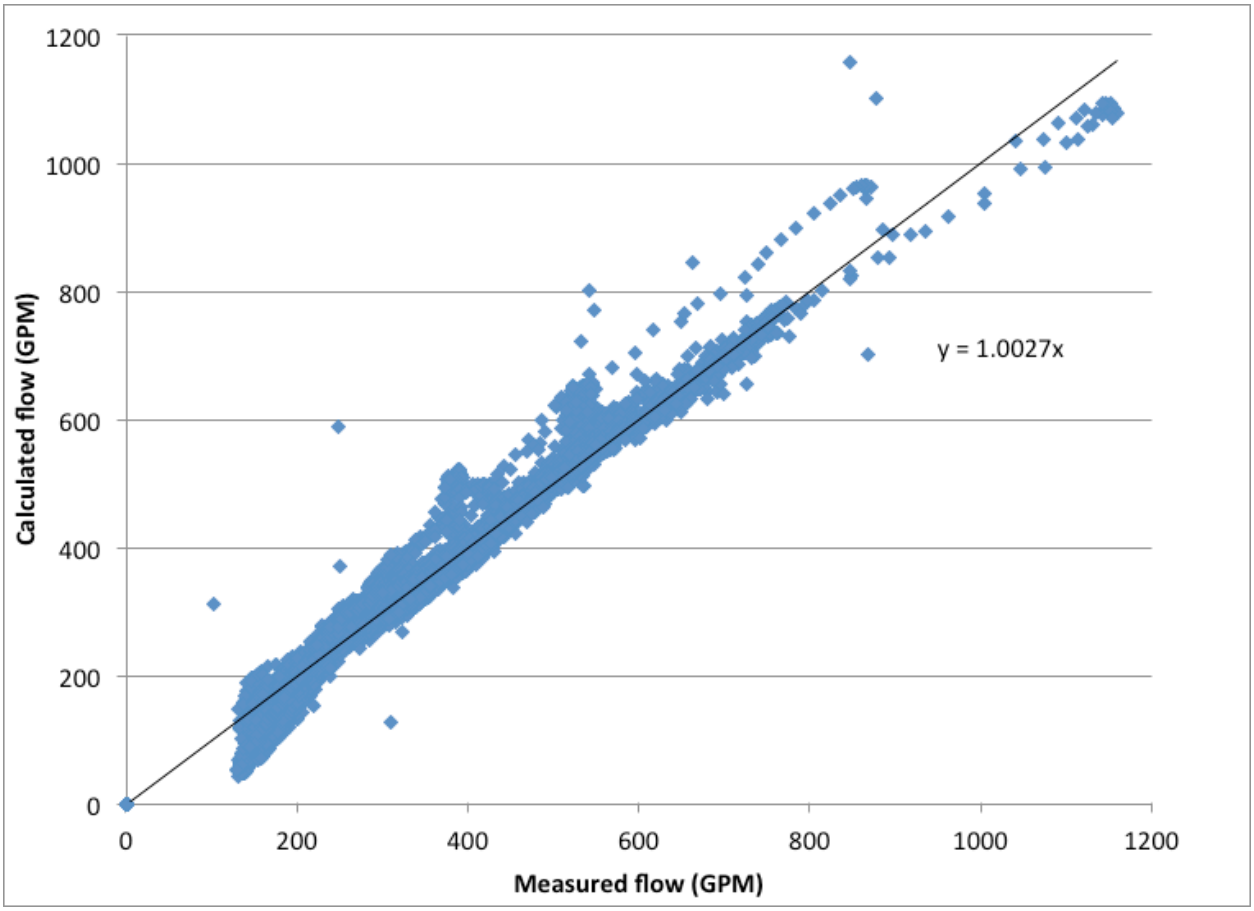

2. Validation chart

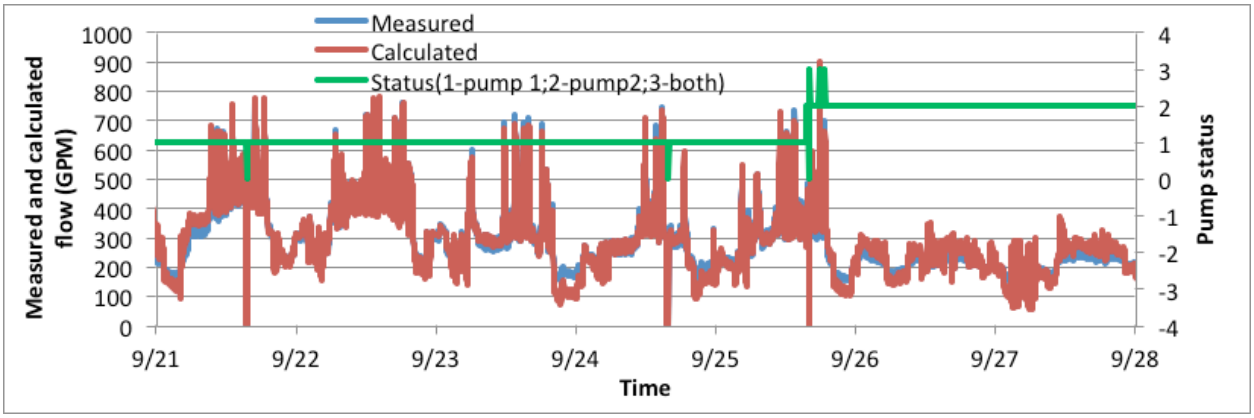

G.4. Condensing water pumps

1. Flow validation comparison (measured vs. calculated) chart

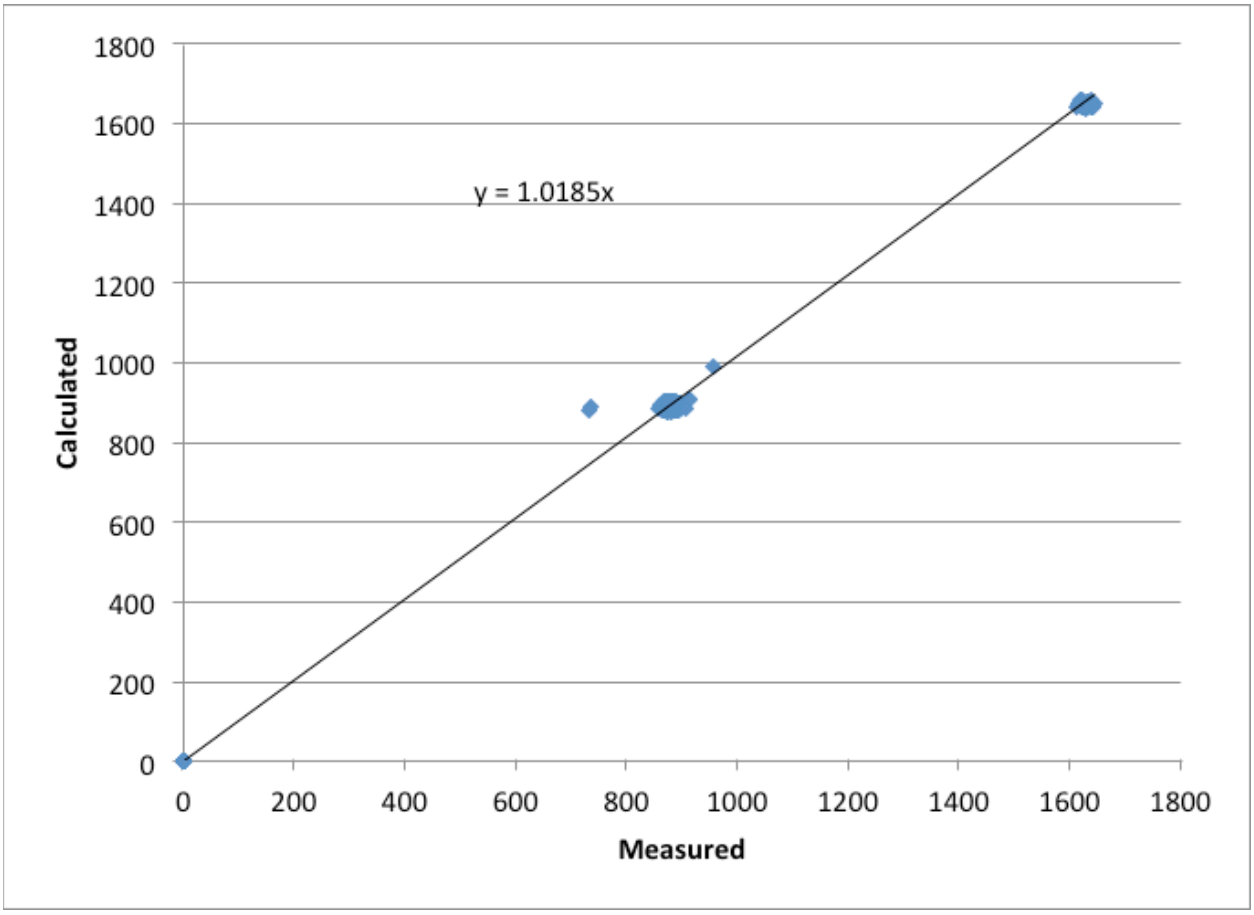

2. Validation chart